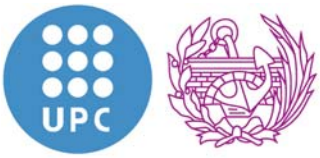

Escola Tècnica Superior d'Enginyers de Camins, Canals i Ports de Barcelona

UNIVERSITAT POLITÈCNICA DE CATALUNYA

PROJECTE O TESINA D'ESPECIALITAT

Títol

NEW METHODS TO MEASURE SUSPENDED SEDIMENT CONCENTRATION

Autor/a

Ma TERESA COSTA VILÀ

Tutor/a

VICENTE GRÀCIA GARCIA

IVAN CACERES RABIONET

Departament

ENGINYERIA HIDRÀULICA, MARÍTIMA I AMBIENTAL

Intensificació

ENGINYERIA MARÍTIMA

Data

3 JULIOL DE 2009

New methods to measure suspended sediment concentration

Author: MªTeresa Costa Vilà
Supervisors: Vicente Gràcia Garcia i Ivan Caceres Rabionet

Abstract

In order to understand Coaastal morphology processes many studies are focused on suspended sediment concentration or waves and currents forces or both.

In this study ADV sensors were tested front OBS sensors in order to get a reliable concentration mesure from ADV signals.

In order to get this goal mathematical and statistical tools were applied and although no reliable result was found, it was observed how indirect methods are more effectives than the direct ones. Moreover, notice how the better result was archieved when working with concentrations above 10g/l., contrary to many authors found in their work.

However this work is an aim to correlate ADV signals (a particle velocity sensor) to OBS outputs (a suspended sediment concentration sensor) in the coastal area, which means that measurement conditions are quite different to the standard ones.

Resum

Per tal d'entendre la morfologia de les costes molts estudis es centren en concentracions de sediment en suspensió o ones i corrents o fins i tot els dos junts.

En el present estudi sensors ADV van ser provats front sensors OBS per tal d'aconseguir una mesura de la concentració de sediment en suspensió de ocnfiança a partir de les senyals de l'ADV.

Per tal d'aconseguir-ho s'han aplicat eines matemàtiques i estadístiques i tot i que cap resultat de confiancça ha sigut trobat s'ha observat com els mètodes indirectes són més eficients que els directes. A més a més, cal notar com el millor resultat s'ha obtingut quan s'estava treballant amb concentracions per sobre els 10g/l, contrari al que molts autors diuen en els seus estudis.

De totes maneres, aquest treball és un intent de relacionar les senyals de ADV (un sensor de velocitats de partícules) amb els outputs dels OBS (un sensor de mesura de concentració de sediment en suspensió) a la zona de costa, el que significa que les condicions de mesura són lleugerament diferents a les standard.

Acknowledgements

I would like to thank for all the support and help on writing this minor thesis to my supervisors Vicenç Gràcia and Ivàn Caceres. Without their knowledge on coastal processes and experience with computational methods this work could not be done anymore.

Index

I. Introduction

Coastal morphology can be understood as the interaction between sediment and driving forces. Due to that all studies of this field are focussed in suspended sediment distribution or waves and current forces or both. The study is done theoretically but also measuring the system under different conditions.

Measurements techniques of suspended sediment concentration have experienced an important evolution in the last decades. At the very beginning measurements were taken by means of sediment traps at different levels, however such rudimentary techniques only give results at low frequency domain.

More recently the use of backscattering has offered the possibility of extend such measures at lower time measurements due to its high frequency response.

In parallel with the development of OBS an important effort has been done to measure the velocity field by the use of the Doppler Effect.

In the last 5 years there has been an important effort to simply use the different outputs of the ADV to directly obtain measures of the SSC in the water column.

The main aim of this minor thesis is to analyse the measurements of ADV obtained at the CIEM flume in order to measure SSC. SSC results are going to be compared with OBS data in order to check the reliability of these.

In order to obtain this goal ADV and OBS measurement devices were submitted to different wave conditions (erosive and accretive) along a period of time.

Later on, computational methods, i.e., least squared method, backscattered intensity method, multivariate analysis, etc. and more robust methods to predict suspended sediment concentration from ADV techniques as running average, are going to be applied to the obtained data in order to get secondary objectives.

These secondary objectives are the application of different adjusts like direct and indirect methods and also some existent results from different authors are applied to the data obtained by the ADV.

The structure of this minor thesis has been divided in 5 mean chapters:

- ✓ In chapter II, a detailed revision of the different measuring techniques of velocity and SSC is shown.
- ✓ In chapter III a description of the experiment environment and conditions have been done.
- ✓ In chapter IV works related to the same item and from different authors are exposed.
- ✓ In chapter V results obtained applying direct and indirect methods, i.e., least squared method, running average, multivariate analysis, etc., are presented.
- ✓ In chapter VI results of the application of existing methods to the data obtained from ADV, are shown.
- ✓ Chapter VII summarizes and concludes the results obtained in the previous chapters.

II. Sediment transport measurements

II.1 Introduction

The measurement of suspended sediment concentration (SSC) in the sea has always been a difficult task and nowadays there isn't any exact technique to measure it. A lot of researches have been measuring SSC in coastal and estuarine environments for more than forty years due to its importance in sediment transport. Among all this years numerous experiments have been done and some techniques to measure sediment concentration have been deployed.

As Jeffrey W. Gartner and John R. Gray said in their essay, traditional methods for characterizing suspended sediments in surface waters are increasingly being replaced in favour of accurate, continuously collected surrogate data that may be safer, and less expensive to obtain. Bulk optical properties of water such as turbidity and optical backscatterance are the most commonly used surrogates for suspended sediment, but the use of other techniques such as acoustic backscatter laser diffraction, digital photo-optic, and pressure difference technologies is increasing too (Gray et al., 2003). Some of these techniques also measure suspended- sediment size characteristics.

Therefore this essay is going to try to enumerate and describe some of these techniques but it is important to take into account that most of them require instrument calibration. In the following lines the methods for measuring suspended sediments concentration are going to be described.

II.2 Methods to measure suspended sediments

The following sections describe methods for measuring suspended sediment concentration and, in some cases, particle size distribution.

II.2.1 Bulk optics (Transmittance and Scatterance)

For a long time the suspended material in the surface waters has been characterized using optical methods based on attenuation (or transmittance) or scatterance.

Transmittance means that the source and detector are placed in an opposite direction of each other at a distance l. The sediment particles in the measuring volume reduce the beam intensity resulting in a reduced detector signal. The relationship between the detector signal (It) and the sediment concentration (c) is:

$$It = k1 * e^{-k2*c} \qquad (1)$$

in which:
k1 = calibration constant depending on instrument characteristics, fluid properties and travel distance (l),
k2 = calibration constant depending on particle properties (size, shape), wave length and travel distance (l).

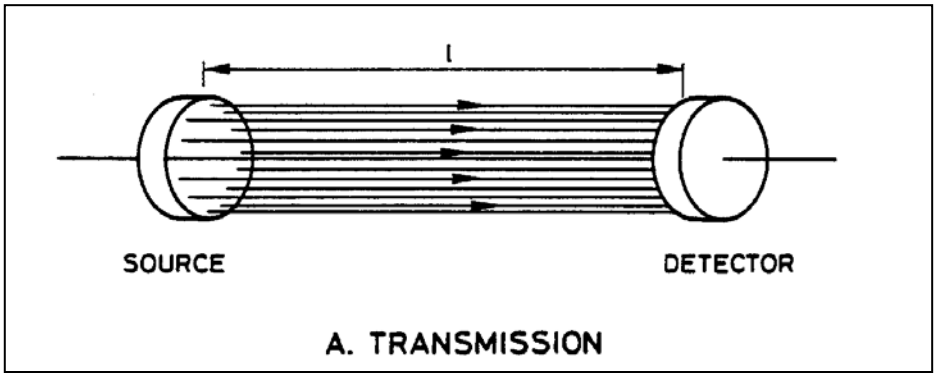

Figure 1: Transmitance (Manual Sediment Transport Measurements). February 2006. Pg. 5.113.

Scatterance means that the source and detector are placed at an angle (ϕ) relative to each other. The detector receives a part of the radiation scattered by the sediment particles in the measuring volume. The relationship between detector signal (Is) and sediment concentration (c) is:

$$Is=k3 * c * e^{-k2 * c} \qquad (2)$$

in which:

k3 = calibration constant depending on instrument characteristics, fluid and particle properties (size, shape), wave length and travel distance (l).

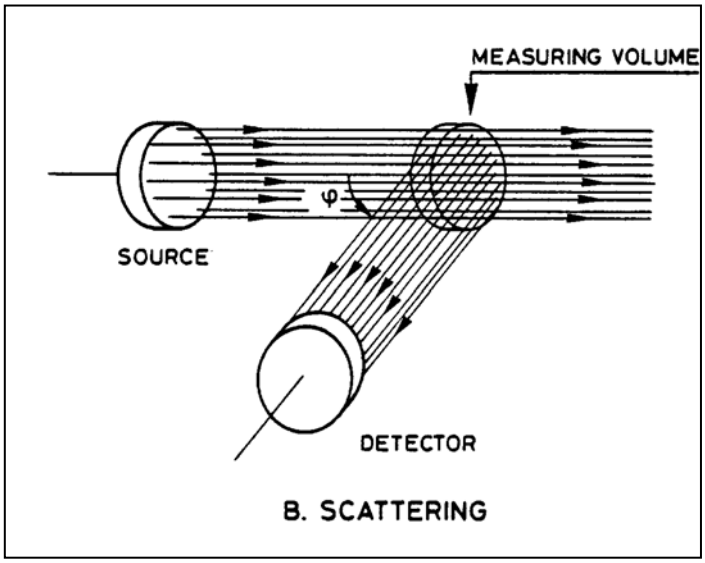

Figure 2: Scatterance (Manual Sediment Transport Measurements). February 2006. Pg. 5.113.

There are several difficulties associated with the use of optical instruments that include (Downing, 1996):

1) Limited standard for design
2) Instrument response varies with grain size, composition, shape and coating
3) Biological fouling or damage to optical windows
4) Nonlinear response sensors

It is known that the transmissometer is more sensitive at low concentrations but the OBS has superior linearity in turbidity water. Because of the relation between OBS gain and particle size, OBS is best suited for conditions of constant particle size distribution unless recalibrated (Jeffrey W. Gartner and John R. Gray (2002)).

Next, in the following paragraphs, there is a brief explanation focus on scatterance and transmittance systems.

II.2.1.1 Optical Backscatter (OBS)

The optical backscatterance sensor (OBS) was developed at the University of Washington for monitoring suspended sediment concentrations in the surf zone (Downing et al., 1981) and has proved and excellent tool for suspended sediment studies due to its high frequency response, relative insensitivity to bubbles, approximately linear response to concentration, and small size (causing minimal disruption to the transporting flow and allowing measurements within a few centimetres of the sea bed).

OBS devices have been used with some success (Hanes and Huntley, 1986) despite that they are intrusive (disturbing the aqueous suspension they are measuring) and give measurements at only one elevation.

The operating principle of this method

The OBS (Downing et al., 1981; Downing, 1983) is a type of nephelometer that measures scattering of infrared radiation by suspended particles in a small volume (on the order of a few cubic centimetres). Thus these instruments provide essentially a single point measurement.

The sensors consist of a high intensity infra-red emitting diode (IRED), a detector (four photodiodes), and a linear, solid state temperature transducer (Downing et al., 1981). The OBS sensor measures infra-red radiation scattered by particles in the water at angles ranging from 140º to 165º. Infra-red radiation from the sensor is strongly attenuated in clear water (D&A instruments, 1989).

The sensor head is 20mm in diameter by 11mm long. The optical components are encapsulated in the recessed face of the sensor head with crystal-clear epoxy (figure 3).

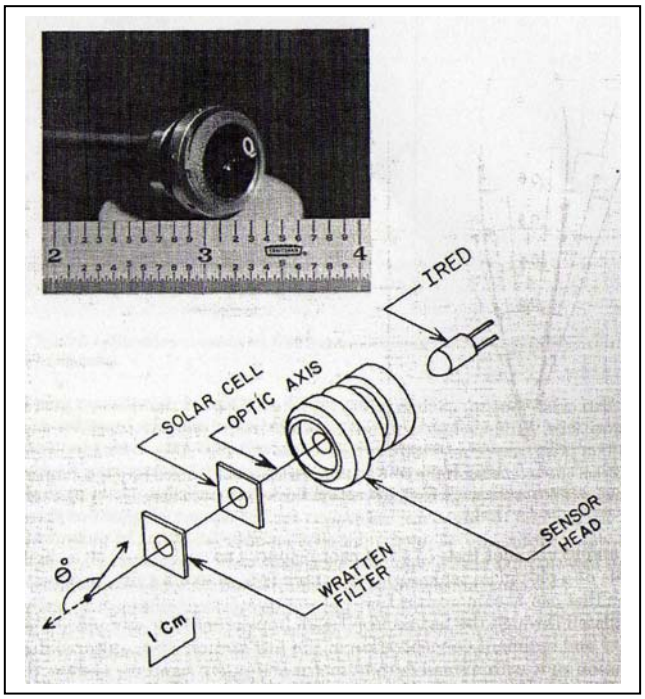

Figure 3: OBS (Downing, J.P, Sternberg, R.W. and Lister, C.R.B.). Marine Geology, 1981.

On one hand the IRED disadvantages are that they emit light in all directions and lenses and mirrors are required to produce a collimated, pencil-like beam (Manual sediment transport). On the other hand the IRED advantages are that the infrared radiation (IR) is strongly attenuated by sea water therefore IR attenuation minimizes interference between closely spaced sensors. Also, the complement of low surface IR and the low- pass optical filter suppresses the level of ambient solar radiation. Consequently, OBS sensors can be operated to within 25cm of the surface without significant degradation of signal- to noise ratio (Downing, J.P., Sternberg, R.W. and Lister, C.R.B., 1981)

Advantages

✓OBS response to varying concentrations of homogeneous sediments is nearly linear (Green and Boon (1993), Black and Rosenberg (1994), and others).

✓OBS sensors allow very good spatial and temporal resolution.

Disadvantages

✓ Particle size dependency (Ludwig and Hanes (1990), Conner and De Visser (1992), Kineke and Sternberg (1992), Green and Boon (1993), Black and Rosenberg (1994); Xu (1997).

✓ OBS sensors are more sensitive to smaller particles sizes. In environments with particle size < 100 μm, OBS gain is greatly affected. OBS performs well for measuring concentrations where particle size is constant or remains in the 200 – 400 μm range (Conner and De Visser (1992)).

✓OBS instrument intrude into the flow.

✓OBS can reach saturation if there is a high particle concentration.

✓When used to record field data over long periods of time, fouling of the sensor face is a problem.

II.2.1.2 Optical Transmission

The operating principle of this method

In optical transmission the light is directed into the sample volume where sediment present on it will absorb and/ or scatter a portion of the light. A sensor located opposite the light source measures the attenuation of the light beam. The sediment concentration is determined using empirical calibration information. The size of the measurement volume will vary according to the geometry of the device (Clifford et al. 1995)

Advantages

✓Optical transmission instruments have most of the same advantages as OBS instruments (Wren, D.G. et al. 2000).

✓Optical transmission sensors allow very good spatial and temporal resolution and generally are more sensitive to low particle concentrations (Wren, D.G. et al. 2000).

Disa*dvantages*

✓Optical transmission instruments show weaknesses similar to OBS devices, although the particle- size dependency is less severe than with OBS (Clifford et al. 1995).

✓The reflective index of the particles also affects transmission device (Baker and Lavelle 1984).

✓Optical transmission instruments show a nonlinear response to increasing particle concentrations. Large variations in sediment concentration will require multiple transmission instruments or a multiple path instrument (Instruction 1991).

✓These instruments are flow intrusive (Wren, D.G. et al. 2000).

II.2.2 Acoustic Method

As it is known accurate measurements of suspended sediment concentration are difficult to obtain due to suspended sediment is highly variable in time and space (Lapointe,1992, 1993 and 1996; Kostaschuk and Churxh, 1993; Hay and Bowen, 1994; Kostachuk and Villard, 1996; Thorne et al., 1996).

Single frequency acoustic backscatter measurements of suspended sediments in the ocean were made at least as early as the early 1980's (Young et al., 1982; Hay, 1983; Hess and Bedford, 1985; and Lynch, 1985).

Accurate single frequency acoustic measurements require detailed knowledge of the characteristics of the sediment in suspension or the sediment concentration at some known range from the acoustic transducer. This type of measurement system can be useful in situations where more information on the size distribution of sediment in suspension or the concentration at a point above the bed is available (Wren, D. et al., 2000)

The process of estimate suspended sediment concentration from acoustic backscatter is based on the sonar equation. In its exponential form, the equation is:

$$SSC_{(est)}=10^{(A+B*RB)} \quad (3)$$

The exponent of Eq. (3) contains a term for the measured relative acoustic backscatter, RB, as well as terms for an intercept, A, and slope, B, determined by regression of current ABS. (Thevenot et at., 1992).

In its simplified form for reverberation, the sonar equation (Urick, 1975) can be written as:

$$RL= SL – 2TL + TS \quad (4)$$

Where RL is reverberation level, SL is the source level, which is the intensity of emitted signal that is known or measurable, 2TL is the two-way transmission loss, and TS is the target strength which is dependent on the ratio of wavelength to particle diameter. All variables are measured in dB.

The operating principle of this method

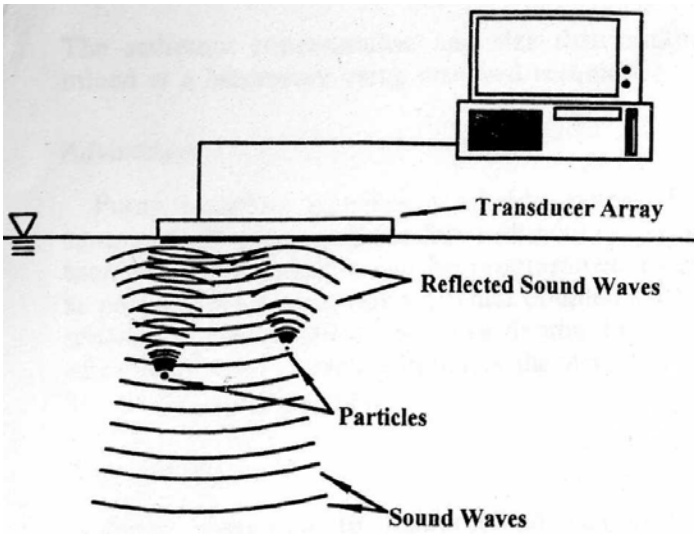

Figure 4: Acoustic Backscatter (Wren et al. 2000). Journal of Hydraulic Engineering.

A pulse (short bursts (≈10 μs)) of high frequency sound (1- 5MHz) is emitted from a sonar transducer. As the sound pulse spreads away from the transducer, it insonifies any suspended material in the water column. This scatters sound energy, reflecting some of it back towards the sonar transducer, which also acts as a sound receptor. With knowledge of the speed of

sound in water, the scattering strength of the suspended material and the sound propagation characteristics, a relationship may be develop between the intensity of the received echoes and the characteristics of the suspended material. With typical acoustic ranges in excess of 1 meter, the acoustic head remains outside the area of study, and therefore makes the instrument non-intrusive (Thorne et al. 1991).

When the sediment is of uniform size, the strength of the backscattered signal is dependent on particle size as well as concentration. At the high frequencies generally employed, backscatter devices have a range of 1-2m due to water and sediment attenuation of signal and the desire for high resolution measurements (Downing et al. 1995).

Measurements in water depths > 2m may be taken by submerging the transducer to the desire depth. The validity of the acoustic approach has been established by several researchers (Thorne et al. (1991, 1993, 1994, 1995), Thorne and Campbell (1992), Crawford and Hay (1993), Schat (1997), and others).

Advantages

✓ Acoustic suspended sediment measurement offers the ability to nonintrusive measure sediment parameters through a vertical range on the order of several meters. This claim is unique among suspended sediment measurements techniques (Thorne et al. 1995).

✓ The high degree of temporal (≈ 0.1 s) and spatial (≈ 1 cm) resolution offer the opportunity to study the mechanics of turbulent sediment transport (Thorne et al. 1994).

✓It allows the researchers to observe the behaviour of turbulent process acting on the sediment.

✓This technique is well suited for deployment over long periods of time.

Disadvantages

✓ Translation of acoustic backscatter data into sediment concentration and size is a difficult problem (Hanes et al. 1988).

✓ Difficulty to creating a calibration suitable for use in calibrating instruments.

✓Attenuation becomes a significant problem at high particle concentrations; therefore attenuation must be accounted to compute the conversion from backscattered signal to sediment parameters.

✓ It is assumed that the method leads to errors that increase in magnitude as distance from the sensor increases (Thorne et al. 1995).

II.2.2.1 Acoustical Backscatter sensor (ABS)

ABS system was developed at the UK Directorate of Fisheries Research, Ministry of Agriculture, Fisheries and Food (MAFF) in Lowestoft, UK.

ABS measurement is a non-intrusive technique for the monitoring of water-suspended sediment particle and changing sea bed characteristics.

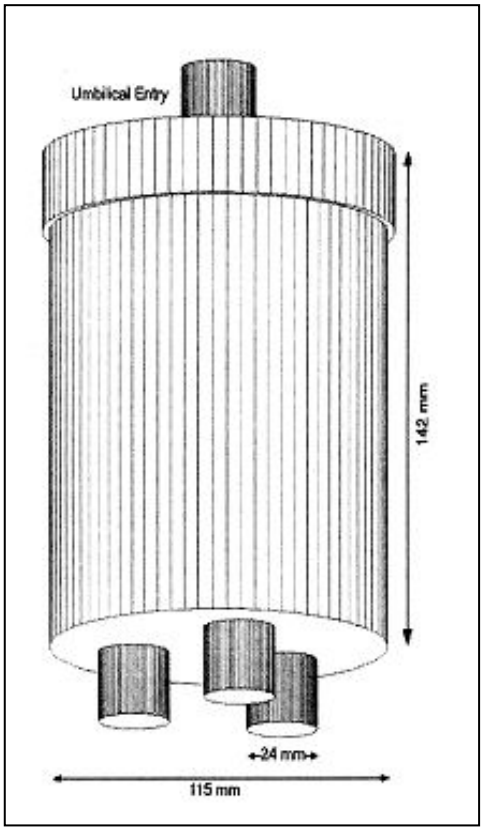

Figure 5: Acoustic Backscatter Sensor (Manual Sediment Transport Measurements). February 2006.

The sensor comprises three separate acoustic transducers, each turned to a different operating frequency, that emit pulses of sound, which are incident on the sea bed. They receive sound reflected by the sea bed and suspended sediment in the intervening water mass. The instrument records the amplitude of reflected sound at gated intervals, thus building a reflected profile.

The choice of frequencies and the transducer characteristics are essential in determining how the system will operate:

a) Higher frequencies are used to resolve smaller particles. To determine particle size, the choice of frequencies should be such that the particle sizes of interest span the region of variable response. But higher frequencies are attenuated more.

b) The dimensions and shape of the transducer affect the horizontal spatial resolution of the system, and the characteristics of the acoustic response.

c) Perpendicular incidence angles will yield information on sediment suspension between the sensor heat and sea bed, and on the erosion or accretion of the bed level (Smerdon, A.M., Rees, J.M., Vincent, C.E.).

Advantages

✓ Non- intrusive profiler covering the lowest 1meter of the water column where most of the suspended sediment transports takes place.

✓ Time- resolution of concentrations within wave cycle can be accurately determined.

✓ Particles sizes can be determined using multiple frequencies (calibration required).

✓ Usable in coastal environments.

✓ Almost no effects of biological fouling.

Disadvantages

✓ In-situ calibration is required for accurate results; in-situ calibration is problematic in coastal environments.
✓ Not suitable for upper concentrations range (>10g/l).

✓ Measurement of velocity requires multiple sensors (cross- correlation).

✓ Sensitive to air bubbles and organic materials in the water column; not suitable for breaking wave conditions (surf zone).

II.2.2.2 Acoustical Doppler Current Profile (ADCP)

The success of the acoustic Doppler current profiles, ADCP, which typically provide mean current profiles with decimetre spatial resolution, has simulated interest in using acoustics to measure nearbed velocity profiles. But also an ADCP anchored to the seafloor can measure current speed at equal intervals all the way up to the surface.

The objective is to use the same backscattered signal as used by the ABS, but process the data to obtain velocity profiles with comparable spatial and temporal resolution to the acoustic backscatter systems. It is known that sound waves that hit particles far from the profiler take longer to come back than waves that strike close by. Therefore by measuring the time it takes for the waves to bounce back and the Doppler shift, the profiler can measure current speed at many different depths with each series of pulses.

The ADCP works by transmitting pulse of sound at a constant frequency into the water. As the sound waves travel, they ricochet off particles suspended in the moving water, and reflect back to the instrument. Due to the Doppler effect, sound waves bounced back from a particle moving away from the profiler have a slightly lowered frequency when they return. Particles moving toward the instrument send back higher frequency waves. The difference in frequency between the waves the profiler sends out and the waves it receives is called the Doppler shift. The instrument uses this shift to calculate how fast the particle and the water around it are moving.

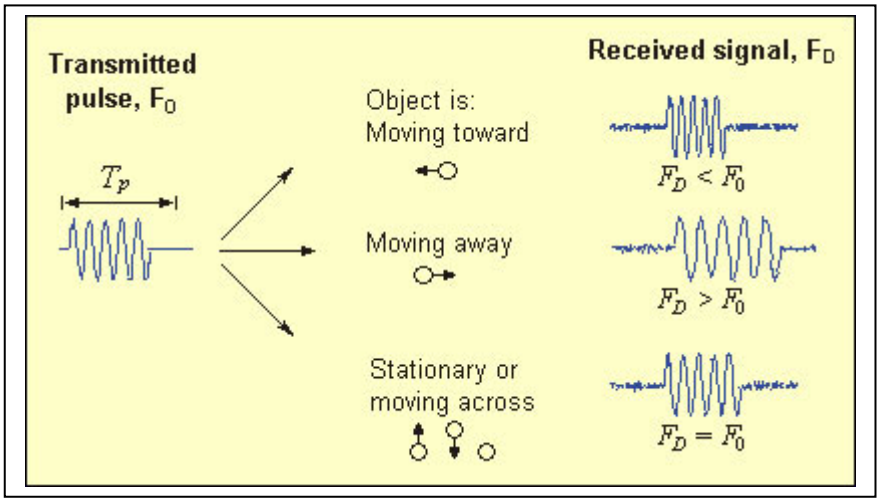

Figure 6: How the ADCP works: A Sontek figure showing what happens to the frequency of sound waves when they reflect off of moving objects. (Ocean instruments (web page)).

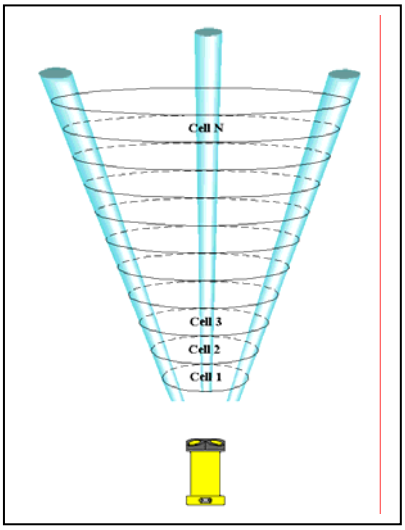

Figure 7: Acoustic Doppler Current Profile (Sontek manual, 1993)

Doppler profiles are instruments used to measure water motion using acoustic properties of sound transmitted at fixed frequency. The instrument measures phase or frequency change of sea bed echoes backscattered from suspended material in the water and converts the echoes to acoustic beam velocities. The ADCP then, converts the acoustic beam velocities to north/south, east/west and vertical velocity components. Therefore the ADP records nine values with each depth cell: three signal strength values (one for each acoustic beam), three velocity values (one for each velocity component), and three standard deviation values (one for each velocity component).

The ADCP backscatter of sound from an aqueous suspension containing sediment can be modelled by the sonar equation (Medwin and Clay, 1998), describing the balance

between the differences between emitted and received energy and the energy lost during the round trip of the acoustic pulse. A working version of the sonar equation in units of decibel is adopted (Deines, 1999):

$$Sv = 2\alpha R + Kc*(E - Er) + 10*\log_{10}(TT*R^2 / L*PT) + C \quad (5)$$

Here, Sv denotes the volume backscattering strength [dB], R is the slant range or range along the central beam axis [m], a is the attenuation coefficient [dB/m], E is the echo strength [counts], Er is received noise [counts], Kc is a scale factor [dB/count], TT is the transducer temperature [8C], L denotes transmit pulse length [m], PT is the transmit power [W], and C is a constant [dB].

The values of Er and Kc are beam-specific and may be determined from calibration. The ADCP records TT, PT, and E and computes R from the time span between emission and reception of the acoustic pings using a formula for the speed of sound (Medwin, 1975; Hitink, A.J.F. and Hoekstra, P., 2004).

However, there are two practical limitations to the method. The first one is the common limitation of any single- frequency instrument that they can not differentiate between changes in concentration level and changes in particle size distribution. The second limitation depends on instrument frequency and particle size of suspended material (A.J.F. and Hoekstra, P., 2004).

In general ADCP tends to underestimate SSC when size distribution becomes smaller (A.J.F. and Hoekstra, P., 2004).

The major advantage of estimating SSC from ADCP is the ability to estimate profiles of SSC.

Advantages:

✓In the past, measuring the current depth profile required the use of long strings of current meters. This is no longer needed.

✓Measures small scale currents.

✓Unlike previous technology, ADCPs measure the absolute speed of the water, not just how fast one water mass is moving in relation to another.

✓Measures a water column up to 1000m long

Disadvantages:

- ✓ High frequency pings yield more precise data, but low frequency pings travel farther in the water. So scientists must make a compromise between the distance that the profiler can measure and the precision of the measurements.
- ✓ ADCP set to "ping" rapidly also run out of batteries rapidly.
- ✓ If the water is very clear, as in the tropics, the pings may not hit enough particles to produce reliable data.
- ✓ Bubbles in turbulent water or schools of swimming marine life can cause the instrument to miscalculate the current.

✓ Users must take precautions to keep barnacles and algae from growing on the transducers.

II.2.2.3 Acoustical Doppler Velocimeter (ADV)

The Acoustic Doppler Velocimeter (ADV) was designed and developed several years ago by the U.S. Army Engineer Waterways Experimental Station and SonTek, San Diego, Calif., as a tool to measure all three components of the velocity vector in laboratory and field environment (Lohrmann et al., 1994; Kraus et al., 1994; SonTek ADV specifications).

Since their introduction in 1993, acoustic Doppler Velocity meters (ADV's) have quickly become valuable tools for laboratory and field investigations in flow rivers, canals, reservoirs, the oceans, and around hydraulic structures in laboratory scale models (Tony, L. Whahl, 2000).

The ADV's are widely used for laboratory and field measurements of 2D and 3D water velocities. These instruments are relatively rugged, easy to operate and can be readily mounted and manoeuvred.

The ADV conduct 3 component current measurements in a sampling volume below transmit- transducer. Its operation is based on the Doppler shift effect. It is implemented as a bistatic (focal point) acoustic Doppler system.

Sound bursts of known duration and frequency are emitted by the central transmitter and subsequently reflected back by suspended particles moving to the sampling volume. The three 10-MHz receivers are positioned in 120º increments on a circle around a 10-MHz transmitter. The probe is submerged in the flow and the receivers are slanted at 30º from the axis of the transmit transducer, focusing on a common sample volume that is located approximately 10.8cm from the probe, which ensures nonintrusive flow measurements (Fig. 8).

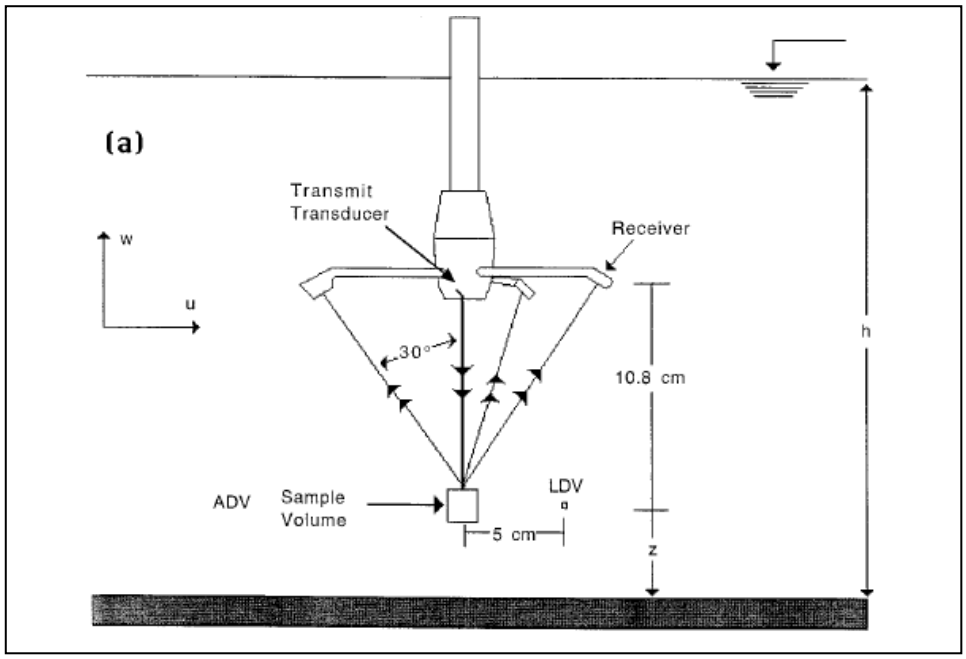

Figure 8: Schematic diagram showing the ADV transmit transducer/receiver layout and the principle of operation (Vollgaris, G. and Trowbridge J.H., 1998)

The size of the

sample volume is a function of the length of the transmit pulse, the width of the receive window, and the beam pattern of receive and transmit pulses. The first parameter defines the vertical extent of the sample volume, whereas the latter two parameters define its lateral extent.

The system operates by transmitting short acoustic pulses along the transmit beam. As the pulses propagate through the water column, a fraction of the acoustic energy is scattered back by small particles suspended in the water (Fig. 8). The phase data from successive coherent acoustic returns are converted into velocity estimates using a pulse-pair processing technique (Miller and Rochwarger 1972).

Advantages:

- ✓ ADV is non- invasive due to the measuring volume is located at some distance away from the actual probe.
- ✓ It measures the flow in a small sampling volume (≈0.25 cm^3) that is 5- 10 cm away from the sensing elements.
- ✓ No periodic recalibration is required.
- ✓ Acoustic pulses do not suffer the range of limitations of optical pulses in turbid water.

Disadvantages:

- ✓ The measured values may underestimate the actual flow velocities near the bottom.
- ✓ Doppler noise floor
- ✓ Spikes caused by aliasing of the Doppler- signal. The phase shift between the outgoing and incoming pulse lies outside the range between -180º and +180º and there is ambiguity, causing a spike in the record.

II.2.3 Laser Diffraction

Laser diffraction technology has been used and evaluated in various instruments to measure the size spectra of suspended particles (Bale et al., 1989; Bale, 1996; Agrawal and Pottsmith, 1994, 2000; Lynch et al., 1994; Phillips and Walling, 1998; Beuselinck et al., 1999; Traykovski et al., 1999).

In laser diffraction, a laser beam is directed into the sample volume where particles in suspension will scatter, absorb and reflect the beam.

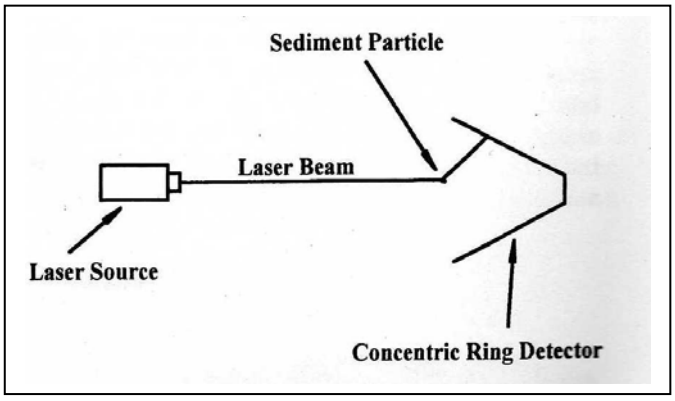

Figure 9: Laser Diffraction (Wren, D.G. et al., 2000)

Scattered laser is received by a multielement photodetector consisting of a series of ring shaped detectors of progressive diameters that allow measurement of the scattering angle of the beam. Particle size can be calculated from knowledge of this angle.

By basing concentration measurements on these measured particles size, particle- size dependency is eliminated (Swithenbank et al., 1976; Knight et al., 1991; Riley and Agrawal, 1991; Agrawal and Pottsmith 1994). However, in the absence of additional information, particle density must be assumed.

Advantages:

✓Particle – size dependency is not a factor because sediment concentration is calculated from size measurements.

✓Calculated sediment parameters can be output at a rate of about 1 Hz.

✓Particle composition does not affect readings.

✓Laser diffraction instruments readings are not affected by the refractive index of the particle (Agrawal and Pottsmith, 1996).

Disadvantages:

✓Laser diffraction devices are expensive.

✓The principle operation of the instrument limits the particle- size measurements to 250 μm and the concentration range to 5,00 mg/L (H.C. Pottsmith, personal communication, July 28, 1997).

✓Longer focal distances are necessary for measurement of larger particles (Witt and Rothele, 1996).

✓Instruments are flow intrusive because the measuring volume of laser diffraction devices is very close to the instrument.

✓They are complicated devices that may require specialized training for operation and data interpretation.

✓The statistical algorithms that translate the data do not arrive at unique concentration measurement. This process works better when the sediment has a smooth distribution. (C. Friedricks, personal communication, September 4, 1997)

II.2.3.1 Laser in situ scattering and transmissometry (LISST – 100)

The LISST 100 (laser in situ scattering and transmissometry) instrument developed by Sequoia Scientific Inc. measures volume concentrations and size spectra using laser diffraction as well as measuring beam transmission.

It works by measuring the intensity of scattered laser light at different angles with a series of concentric ring detectors. The intensities of light gathered by the ring detectors are inverted to estimate the particle area concentrations for eight multiple size categories ranging from 5 to 500 mm in the version of the model 100.

These estimates, along with an empirically determined volume calibration constant, then provide a volume concentration spectrum over this same size range. The LISSTs transmissometer detector is located in the center of the ring detectors and measures the light which is not scattered or absorbed (Agrawal and Pottsmith (1994, 2000).

The LISST works well in resolving unimodal silicate particle distributions (Traykovski et al., 1999; Agrawal and Pottsmith, 2000; Battisto, 2000). More recent tests by Agrawal and Pottsmith (2000) with an improved inversion algorithm have shown higher resolution of multimodal distributions of glass spheres.

The presence of particles finer and coarser than the measured size range also affects the estimated size distributions from the LISST (Traykovski et al., 1999; Mikkelson and Pejrup, 2000).

II.2.3.1.1The LISST – 100 devices and principle of laser scattering; diffraction

The LISST-100, with diameter of 13 cm and length of 81 cm, is a laser particle size analyser and consists of a diode laser operating at 670 μm which is collimated to form a parallel beam of light (figure 10). The beam passes through a 5 cm sample cell of water where particles produce scattering. The forward diffracted beam is collected by a set of 32 ring detectors that are logarithmically spaced and located in the focal plane of the laser receiving lens. Each ring detector measures scattering over a sub-range of angles. The ring radius and focal plane length of the receiving lens determine the range of the angles. A photo-diode is placed behind the ring detector which detects the main laser beam. This supplies the optical transmissometer function. The background scattering is recorded to account for the optical effect of the flow-through chamber.

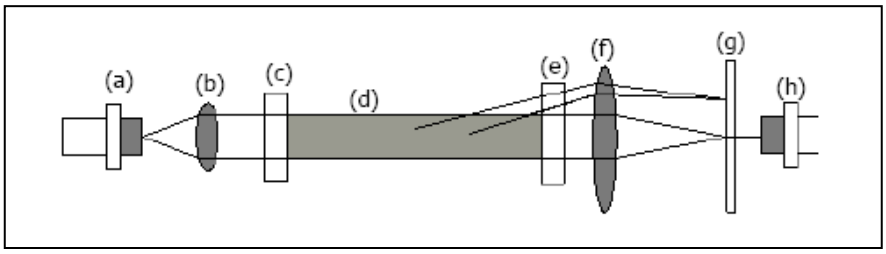

Figure 10: The LISST devices elements: (a) laser diode source, (b) companion focusing optics, (c) and (e) two pressure windows, (d) sample volume, (f) receiving lens, (g) concentric photodetector rings, (h) transmission detector (Ramazan Meral, February 2008)

Advantages:

✓simultaneous measurement of particle size, concentration and fall velocity.

✓simulataneous measurement of mud, silt and sand particles

✓instrument can measure in standalone Mode.

Disadvantages:

✓limited concentration range for silty and muddy sediments (up to 500 mg/l).

✓not close to bed (relatively large sampler size)

✓ fragile instrument in coastal conditions with surface waves

✓ calibration required for nonspherical particles

II.2.3.2 Laser Doppler Velocimetry (LDV); also known as Laser Doppler Anemometry (LDA)

Laser Doppler Anemometry (LDA) is an optical technique ideal for non-intrusive 1D, 2D and 3D point measurement of velocity and turbulence distribution in free flows and internal flows. It was invented by Yeh and Cummins in 1964.

LDA system consists of a laser (typically a continuous wave Ar-Ion-laser), fibers optics, frequency shifter, signal processor, traversing system and a computer to control the measurement and save the data. The velocity is measured in a point in which a typically a series of 10000 samples is measured after which the probe is moved to next position. By moving the prove spatial distributions can be created. The principle of velocity measurement can be explained with so called Fringe model.

In LDA the laser beam is first divided into two beams with equal intensities. The beams are then directed to optical fibers which deliver them to the probe optics. The focal length of the probes front lens determines both the size and position of the crossing point of the two beams. Optics is used to guide the two laser beams into the measurement point where the beams cross each other. Thus the measurement volume formed by the laser beams is an ellipsoid. The beams crossing with each other form interference fringes, so that there are high intensity planes of light and between them low intensity planes which are perpendicular to the laser beam plane. The spacing between the planes is determined purely by optical parameters of the setup, namely the laser light wavelength, and the angle between the beams.

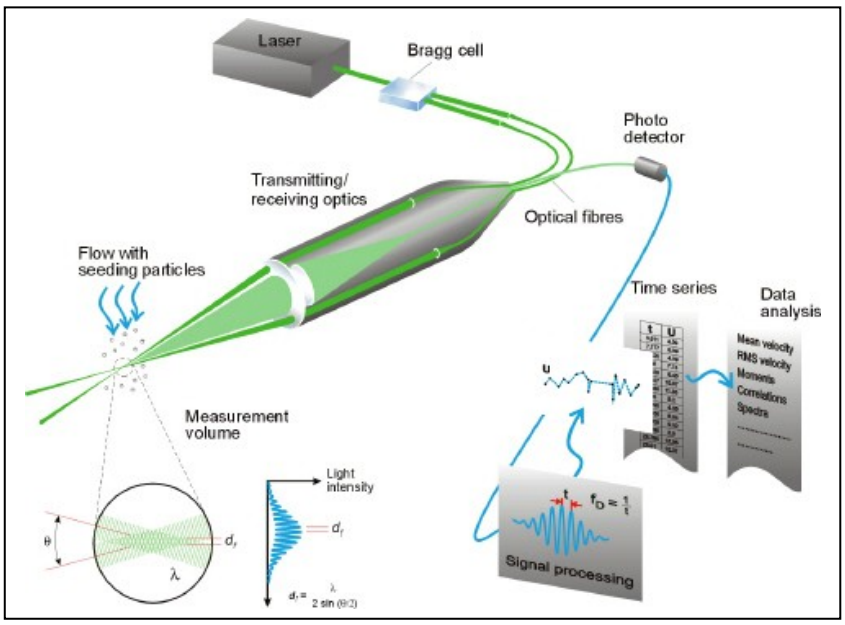

Figure 11: The principle of a laser Doppler anemometer. (Dantec Dynamics (web page)).

The flow is seeded with small particles, which can follow the turbulent motion of the fluid. When these particles pass by the measurement volume they scatter light according to the Mie-theory. The intensity fluctuation of the scattered light depends on the velocity of the particle (see figure 11). The time (dt) can relative easily be measured and then it is very simple to calculate the velocity of the particle by dividing the traveled distance d_f by the spent time dt.

The signal to noise ratio of the LDA signal depends directly on laser power, angle of the receiving optics and particle diameter, among other parameters. These three parameters can be adjusted by the user. The scattering intensity of particles depends strongly on the viewing angle. Usually, for practical reasons, the backscatter mode where receiving optics is combined with transmitting optics is used. The sampling frequency depends on the arrival frequency of the particles to the measurement volume.

Advantages:

✓ Velocity measurements in Fluid Dynamics.

✓ Up to 3 velocity components.

✓Non-intrusive measurements because is a single point optical measuring technique.

✓ Absolute measurement technique (no calibration required).

✓Very high accuracy.

✓ Very high spatial resolution due to small measurement volume.

Disadvantages:

✓ Expensive

✓Is necessary a transparent flow through which the Light beams can pass.

✓They do not give continuous velocity signals.

II.2.4 Turbidity Threshold Sampling

The Turbidity Threshold Sampling (TTS) method was developed by the U.S. Department of Agriculture, Forest Service to efficiently utilize continuous turbidity measurements in triggering suspended sediment samples from pumping samplers (Lewis 1996, Lewis and Eads 2001)

TTS was designed to permit accurate determination of suspended sediment loads by establishing a relation between SSC and turbidity for each sampling period with significant sediment transport.

Turbidity is an optical measure of the number, size, shape and colour of particles in suspension. The optical properties of sediment, mainly size and shape, have a large influence on the magnitude of the turbidity signal. TTS utilizes turbidity thresholds, points at which physical samples are collected, distributed across the entire range of expected rising and falling turbidities.

The design objectives of TTS are:

1) Facilitate accurate estimation of suspended sediment loads at a reasonable cost.
2) Provide an adequate number and distribution of physical samples to validate every significant rise in turbidity and calibrate turbidity against SSC for each period being estimated.
3) Provide a continuous estimate of sediment concentration and flux based upon turbidity.

The Turbidity Threshold automated method distributes sample collection using real-time over the range of rising and falling turbidity values and attempts to sample all significant turbidity episodes. It does so by collecting pumped suspended sediment samples at short intervals (5 to 15 minutes) when pre-selected turbidity conditions, or thresholds, are satisfied. By using in situ sensors and programmable data logger uses these measurements to make real- time determinations of whether a pumping sampler should be activated. During analysis the relations are applied to the nearly continuous turbidity data for the respective sampling periods to produce a continuous record of estimated SSC (Lewis, 2002). The product of discharge and estimated SSC is then integrated to obtain accurate suspended yields.

Additional benefits of TTS are:

a) It provides samples that can be used to determine whether turbidity spikes resulted from fouling or actual sediment transport.
b) The continuous record of turbidity is useful for revealing the timing of erosion events, assessing impacts on beneficial uses, and enforcing water quality regulations (Lewis and Eads, 2002).
c) Turbidity Threshold Sampling is not limited to sampling suspended sediment. Mercury, phosphorus, and fecal coliform bacteria are often adsorbed on sediment particles; therefore, sampling for these and other constituents could be improved by using TTS.
d) Total dissolved solids or specific Chemicals salts could also be sampled and estimated by modifying TTS to employ electrical conductivity as the surrogate variable.

II.2.5 Pump sampling

Pump sampling is an attractive method for concentration measurements in coastal conditions because a relatively long sampling period can be used which is of essential importance to obtain a reliable time-averaged value. The sampling period should be rather long (15 min) in irregular wave conditions (at least 100 waves). (Manual sediment transport measurements).

A problem of sampling in conditions with irregular waves is that the magnitude and direction of the fluid velocity is changing continuously. This complicates the principle of isokinetic sampling in the flow direction.

Operating principle

In pump sampling a vacuum is applied to a line submerged in the channel, and a fluid/sediment sample is taken and stored until retrieved for laboratory analysis. To avoid sample biasing, the intake velocity must be matched to the local stream velocity. The sediment concentration and size distribution are determined at a laboratory using standard techniques.

Advantages:

✓ Reliable method for collecting samples

✓ Works well for fine sediment (< 0.062mm).

✓ Pump samples tends to be automated which eliminates the need for personnel to be present to take samples.

✓ Automatic pump samplers can be programmed to take samples at predetermined intervals.

Disadvantages:

✓ Pump sampled has poor temporal resolution.

✓ The amount and size of sediment sampled are dependent on the pump's speed.

✓ Pump sampling is flow intrusive.

II.2. 6 Bottle sampling

Bottle sampling is commonly conducted by lowering a bottle attached to a sampling pole into the stream or by placing a bottle under the dropping flow exiting a pipe.

The operating principle consists on depth integrated samplers that are used to sample the water column in a vertical section by lowering the apparatus to the desired level, usually as close to the bed as possible, and then rising the sample back to the surface at the same rate. This technique is dependent on the speed of the sample as it moves through the water column. Point integrating samplers can sample sections of water depth by electronically opening a valve at the appropriate time (Interagency Committee, 1963).

In its simple form, bottle sampling involves extracting a water sample by dipping with a jar. If the velocity at the mouth of the jar differs from the local stream velocity then the amount of sand- size suspended sediment entering in the jar may not be representative of that in the steam that is the subject of measurement. Sediment concentration and size distribution are determined from the samples by laboratory analysis using standard techniques (Wren, D. G. et al., 2000).

Advantages:

✓ Well documented and widely use technique.

✓ Depth and point integrating samplers allow nearly the entire depth of the stream to be sampled.

✓Bottle samplers are generally considered the standard against which other types of samplers are calibrated.

Disadvantages:

✓ Bottle sampling has poor temporal resolution.

✓ Personal must be on hand to take samples.

✓ Most of the bottle samplers cannot sample the lowest 0.1 – 0.15 m of the water column.

✓Intrusion in the flow.

II.2. 7 Focused beam reflectance

In focused beam reflectance measurement a laser beam focus a very small spot (< 2 μm^2) in the sample volume and this is rotate very quickly. As it rotates, the beam encounters particles that reflect a portion of the beam. The time of this reflection event is used to determine the chord length of the particles in the path of the laser (Phillips and Walling, 1995; Law et. al, 1997 and Wren et al., 2000).

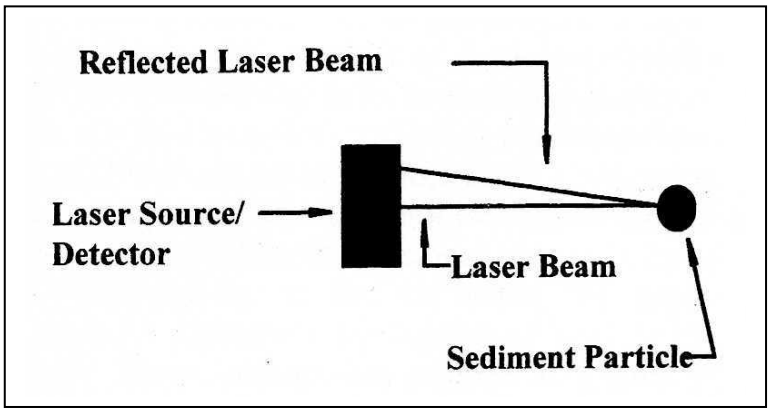

Figure 12: Focused Beam Reflectance (Wren et al., 2000)

Advantages:

✓ There is no particle dependency.

✓ The instrument has a wide particle measuring range of roughly 1- 1,000 μm, with measurements of over the range of 10 mg/L to 50 g/L (Wren et al., 2000)

Disadvantages:

✓ If particles have little or no reflectance the instrument will work poorly.

✓ At low particle concentrations (< 1 mg/L), long counting times are required.

✓ Assumption of spherical particles.

✓ Is flow intrusive.

II.2. 8 Nuclear measurement

In general, nuclear sediment measurement utilizes the attenuation or backscatter of radiation.

There are three basic types of nuclear sediment gauges:

1) Those that measure backscattered radiation from an artificial source
2) Those that measure transmission of radiation from and artificial source.
3) Those that measure radiation emitted naturally by sediments.

(McHenry et al., 1967; Welch and Allen, 1973; Tazioli,1981).

Operating principle

In backscatter gauges, radiation is directed into the measurement volume with the radioactive source isolated from the detector by lead. A sensor in the same plane as the emitter measures radiation backscattered from the sediment. In transmission gauges, the detector is opposed to the emitter, and the attenuation of the radiation caused by the sediment is measured and compared to the attenuation of the rays caused by passage through distiller water. The ratio between these measurements allows calculation of sediment concentration (McHenry et al., 1967, 1970; Rackoczi, 1973; Berke and Rakoczi, 1981).

Advantages:

- ✓ Continuous monitoring.
- ✓ Used over a wide range of sediment concentrations (500 – 12.000 mg/L).
- ✓ Not affected by the colour of water or suspended matter.

(Papadopulos and Ziegler, 1966; Berkle and Rakoczi 1981; Tazioli 1981).

Disadvantages:

- ✓ Changes on the chemical composition of sediments can affect reading.
- ✓ Licensing and training are requirements for the use of nuclear devices.
- ✓ Low sensivity.
- ✓ Field calibration is difficult.

II.2. 9 Spectral Reflectance

Spectral reflectance is based on the relationship between the amount of radiation reflected from a body of water and the properties of that water.

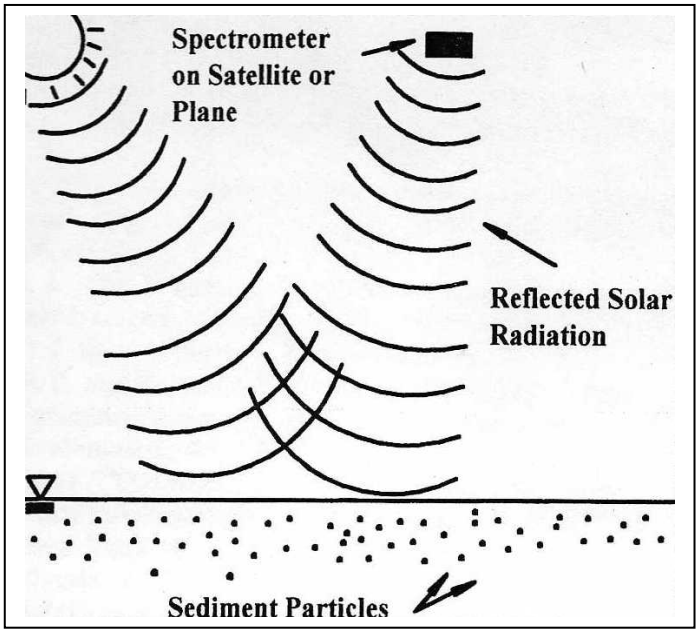

Figure 13: Remote Spectral Reflectance (Wren et al., 2000)

The radiation is measured by a handheld, airborne or satellitebased spectrometer.

The correlation between concentration of suspended sediment and the reflected radiation has been observed and validated by several researchers (Blanchard and Leamer 1973; Ritchie and Schiebe 1986; Novo et al. 1989; Bhargava and Mariam 1991; Choubey 1994). This relation ship is dependent on many parameters such as the optical properties of the sediment type, sensor observation angle, solar zenith angle and the spatial resolution of the measurements (Novo et al. 1989; Choubey 1994; Gao and O'Leary 1997).

Advantages:

- ✓ Ability to measure sediment over broad areas.
- ✓ Is used to identify water body with high suspended sediment concentrations.

Disadvantages:

- ✓ In higher sediment concentrations the measure range is limited.
- ✓ Larger errors in measured suspended sediment concentration readings may be introduced when the sediment type is unknown (Choubey, 1994).
- ✓ Particle size dependence (Novo et al., 1989).

II.2.10 Pressure Difference

The pressure difference technique employs dual pressure transducers to infer SSC from density of sediment bearing water at two locations in the water column. The pressure difference is converted to a water density value. Implicit assumptions in the method are that density of water and sediment are known and very sensitive pressure transducers are used.

The technique has been applied in laboratory with promising results of better than 3 percent accuracy for determining mass concentration of suspensions of glass microspheres (Lewis and Rasmussen,1999).

For field applications, laboratory analysis of water samples is used to convert the density values to determine average SSC between the two pressure transducer inlets at known distance apart.

The differential pressure method has been generally successful in the field at concentrations above about 50 g/L but needs additional evaluation in the range of 10-50 g/L. Therefore the technique may not be reliable at lower concentrations.

Application of this technique in the field is complicated by low signal to noise ratio, turbulence, dissolved solids concentration, and temperature variations (Larsen and others, 2001). Additionally, analysis may be complicated by density variations of suspended material.

III. Experiment set-up

As one could observe in the last section, nowadays there is no method that allows observing turbulent and intra wave fluid sediment interactions over the whole boundary layer. Most of the available techniques disturbs the water and sediment fluxes and therefore limited the accuracy and efficiency of the results. Moreover, mobile test are designed with scaling laws which are only valid for a part of the physical problem, for instance, the Froude scaling does not lead correctly scaled bed shear-stresses which distorts the test bottom boundary layer.

From 12/03/08 to 2/04/08 consecutive experiments based on measure SSC and velocities with OBS and ADV respectively, were conducted in CIEM wave flume (Barcelona). This experiments includes 47 tests with erosive waves conditions (H_s 0.53 m and T_p 4.14 s) and 35 tests with accretive wave conditions (H_s .32 m and T_p 5.44 s)

III.1 Environment description

The CIEM flume is one of the biggest research installations within the Universitat Politècnica de Catalunya. With 100 m length, 3 m width and 5 m depth the CIEM flume is an excellent tool for scaled test, allowing the larger scale ratios a reduction of scale effects inherent to all scaled experiments.

The flume original configuration for the experiments is depicted in the next figure considering the slope of the profile.

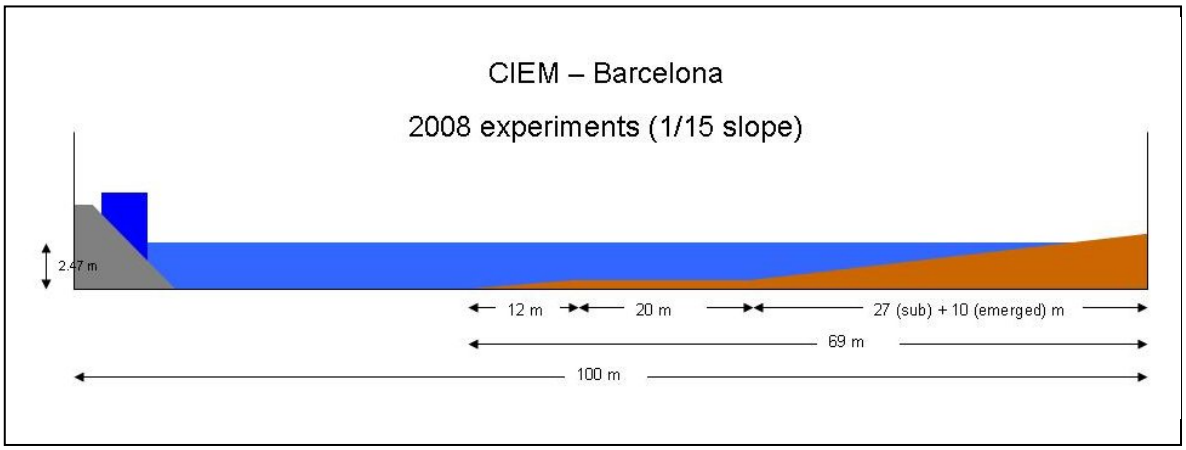

Figure 14: CIEM bottom profile during the SANDS experiments (March 2008). (Cáceres,I., Alsina, J.M. and Sánchez-Arcilla, A., 2009. "Mobile bed experiments focused to study the swash zone evolution". Journal of Coastal Research, SI 56 (Proceedings of the 10th International Coastal Symposium). Lisbon Portugal, ISBN).

III.2 Experiment Objectives

Among the objectives of the experiments done the next aims can be found:

- ✓ Improve the scaling and analysis procedures and achieve more "repeatable" and compatible movable bed tests (with known error bounds).
- ✓ Innovate data capture and analysis using advanced optical and acoustic non intrusive probes.
- ✓ Develop new protocols for the design and interpretation of the movable bed test results.

III.3 Experiment description

The experiments consist in velocities and sediment concentration measurements at the same flume position using ADV and OBS respectively. These two sensors were just moved vertically and one according to the other.

During the experiments, each morning the ADV and OBS vertical coordinates were changed and three different configurations were probed along the whole investigation. These three different configurations had the finality to acquire the better information for later on numerical model validation.

The first configuration was:

ADV	OBS	X	Z_{adv}	Z_{obs}
437	0	71,61	0,11	0,14
431	1	71,61	0,125	0,07
387	2	71,61	0,2	0,03
374	3	73,26	0,115	0,06
392	4	73,26	0,1	0,03
388	5	75,17	0,02	0,03
376		76,89	0,02	

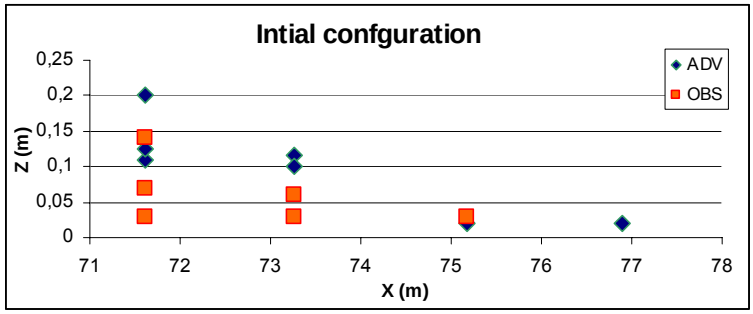

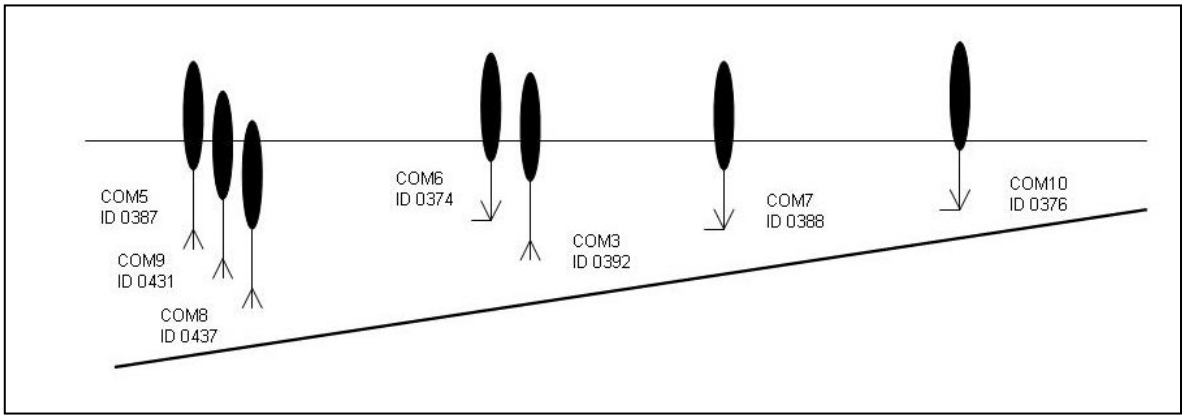

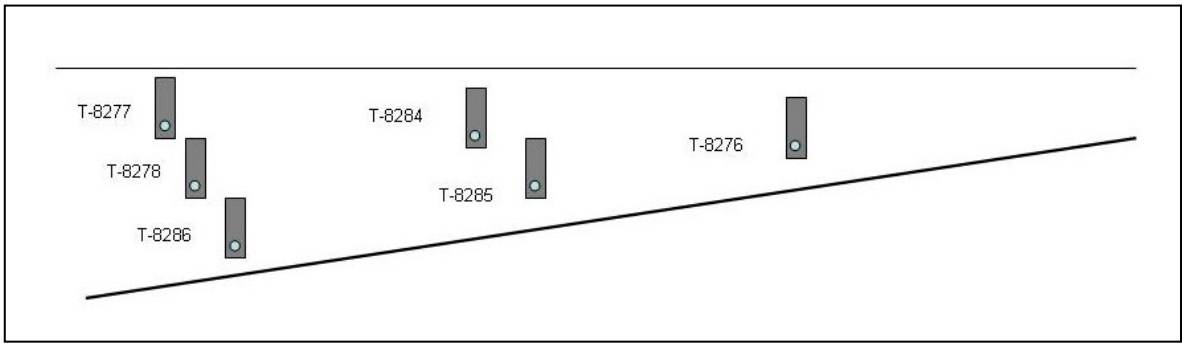

Figure 15: First OBS and ADV configuration used in the CIEM flume. *(*Cáceres,I., Alsina, J.M. and Sánchez-Arcilla, A., 2009. "Mobile bed experiments focused to study the swash zone evolution". Journal of Coastal Research, SI 56 (Proceedings of the 10th International Coastal Symposium). Lisbon Portugal, ISBN).

The specific instrumentation used in these experiments was:

- ✓ Up to 14 resistive waves gauges were used to measure wave height.
- ✓ Up to 11 acoustic gauges were distributed along the flume.
- ✓ Seven ADV were placed in the Swash Zone.
- ✓ At the beginning 6 OBS were placed but later on one more was added. The OBS distribution followed always the one previously seen for the ADV. Every OBS was placed in front of an ADV and using the same depth reference to allow later a correlation between the velocity and concentration acquired information.

Several of the acoustic gauges did not measure correctly during the initial tests. After several attempts to understand the nature of the problem it was understood that all the equipment measuring after the breaking or under breaking conditions should be closer to the water surface than the other equipment measuring under linear conditions. Due to these problems the initial configurations of the ADV was changed during the experiments, mainly for those in the swash zone that were placed in this positions in an attempt to catch the run-up excursion and the thickness of the water layer

Wave conditions

The wave conditions being tested reproduce erosive (Hs= 1 m and Tp= 5.7 s) and accretive (Hs= 0.6 m and Tp= 7.5 s) wave conditions (values at a prototype scale).

The time series were ran consecutively, first the erosive conditions and without reshaping the beach slope the accretive wave conditions. Every time series had 500 waves.

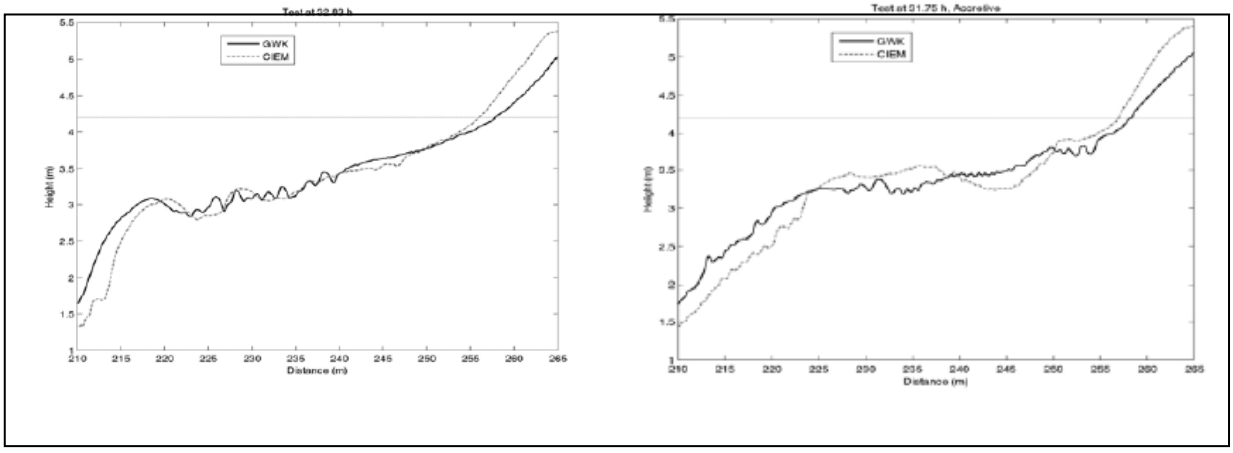

Figure 16: Profile evolution under erosive wave conditions to accretive wave conditions. *(*Cáceres,I., Alsina, J.M. and Sánchez-Arcilla, A., 2009. "Mobile bed experiments focused to study the swash zone evolution". Journal of Coastal Research, SI 56 (Proceedings of the 10th International Coastal Symposium). Lisbon Portugal, ISBN).

It was supposed a homogeneous flume due to there is no difference between right and left and waves were broken similar to both sides.

Sediment characteristics

The sand characteristics were controlled by measuring the sediment size (d_{50}), fall velocity, density and a core sample to analyze the sediment packing properties was taken at different locations.

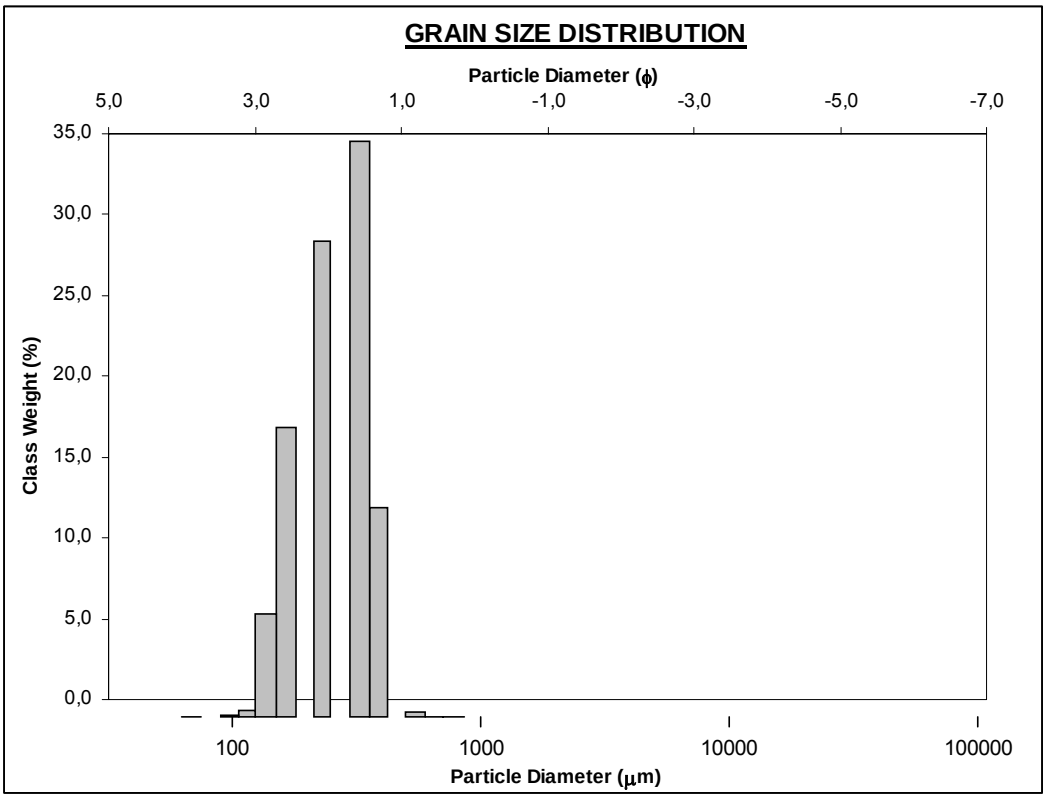

Figure 17: Grain size distribution. *(*Cáceres,I., Alsina, J.M. and Sánchez-Arcilla, A., 2009. "Mobile bed experiments focused to study the swash zone evolution". Journal of Coastal Research, SI 56 (Proceedings of the 10th International Coastal Symposium). Lisbon Portugal, ISBN).

IV. Use of ADV as SSS

Acoustic Doppler Velocimeter (ADV) works by measuring the reflection of an acoustic signal from particulate matter in water. While these instruments are primarily used to measure the velocity of particles, they can also provide information about Signal to noise ratio (SNR), correlation and signal amplitude.

For a long time many authors have been trying to relate the outputs from an ADV to suspended sediment concentration (SSC). Some of they results used as a point to start for our work are present below.

IV.1 Data control

Stuart J. MC Lelland and Andrew P. Nicholas[1] present in their study a new method for calculating the total measurements errors, including sampling errors, Doppler noise and errors due to velocity shear in the sampling volume associated with single point ADV measurements. This procedure incorporates both the effects of instrument configuration and the distribution errors between velocity components for any probe orientation. It is also shown that the ADV can characterize turbulent velocity fluctuations at frequencies up to the maximum sampling rate and that Reynolds shear stress errors are very small.

In the experiment they used a system that incorporates a non- standard configuration. The probe is mounted on a 0.007m, 0.15m long stem is attached by 0.8m flexible cable to the signal conditioning module. This module contains analogue electronics, which detect and amplify acoustic signals. A 15m shielded cable connects the signal-conditioning module to a digital signal processor, which controls the AD system. This paper describes data collected using an array of four identical ADVs that are operated simultaneously using a portable computer.

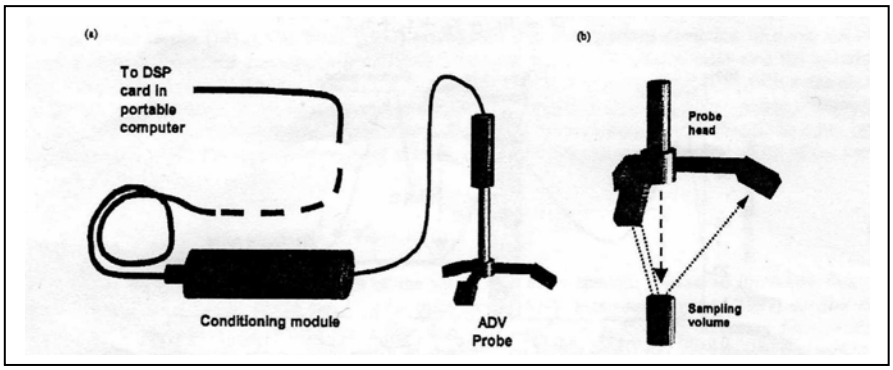

Figure 18: (a) Schematic diagram of showing ADV probe and signal conditioning module. (b) Exploded view showing ADV probe head geometry and the position of the sampling volume. Long- dashed line shows transmitted beam path and short-dashed lines show received beam paths (Stuart J.McLelland et al. (2000). Hydrological processes.

One part of the study was the ADV data validation. In that one they let us know that the spectral width of the covariance function is contaminated by signal to noise ratio due to the loss of signal coherence during its propagation through the fluid. This with noise cannot be removed by improving the acoustic qualities of the system, but different

[1] Note that this paper was used just a reference to know if our ADV were working correctly

pulse repetition rates permit the separation of variance due to the signal alone from that contributed by noise (Lhermitte and Serafin, 1984).

Hence, assuming a Gaussian distribution for the phase power spectrum, the correlation coefficient (R^2) can be related to the dimensionless spectral width (φr):

$$R^2=e^{-2*\pi\wedge2*\varphi r\wedge2} \quad (6)$$

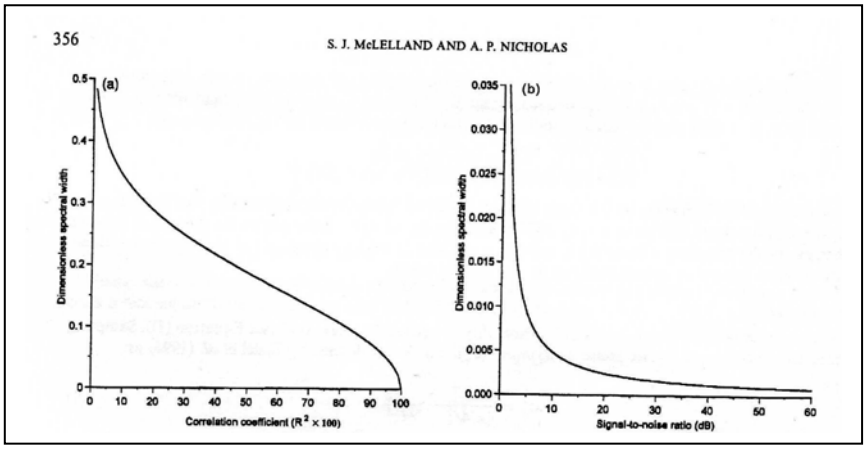

Figure 19: (a) Relationship between dimensionless spectral width and the correlation coefficient. Note that dimensionless spectral width is independent of the instrument velocity range. (b) Variation of dimensionless spectral width of the noise component of the received signal of the instrument velocity range. (Stuart J.McLelland et al. (2000). Hydrological processes.

One can appreciate that the dimensionless spectral width decreases as the correlation coefficient increases.

As described above, the acoustic signal will be contaminated with noise that is intrinsic to the propagation of acoustic waves and the Doppler detection system. This noise can obscure the real signal and the standard deviation of the mean velocity estimate increases as the signal-to-noise ratio decreases (Zrnic,1977). For a given instrument velocity range, the dimensionless spectral width of the signal noise (φn^2) is:

$$\varphi n^2= \ln(1+(1/SNR))/2*\pi^2 \quad (7)$$

As mentioned at the beginning, in this work they also show how to deal with measurement error in ADV data. This can be caused by sampling errors generated by ADV hardware, Doppler noise due to the motion of acoustic reflectors in the sampling volume and errors due to velocity shear in the sampling volume.

Sampling errors are characterized by the phase uncertainty ($\sigma\phi^2$). To estimate this one they mounted four ADV probes in a basin of still water seeded with a very high concentration of alluvial sediment in order to maximize the SNR as particles settled out of suspension. They plot the results and obtained that there is greater radial velocity variance as both the sampling rate and instrument velocity range increase.

Doppler noise is produced by the variance of scatterer velocities in the sampling volume, which broadens the received signal spectrum. Because the ADV operates in the acoustic near field, however, it can be assumed that the sampling volume is approximately cylindrical in shape and the beam strength is uniform throughout the sampling volume (Lohrmann et al., 1995).

Therefore one can see that this paper shows a robust method for evaluating total signal noise associated with single- point ADV measurements at any sampling frequency or instrument velocity range.

IV.2 Least squared method

IV.2.1 Least squared method – SNR[2]

Sebnem Elçi, Ramazan Aydn and Paul A. Work worked with ADV in rivers trying to measure suspended sediment concentration. Also soil samples were collected from all measuring stations and particle size analysis was conducted by mechanical means.

In order to investigate the reliability of an ADV for SSC measurements in different environments, flow velocities by ADV and SSC measurements by a water quality meter were carried out in different streams located in the Aegean region of Turkey having different soils types.

Simultaneous measurements were made using the turbidity sensor and the Flowtracker ADV at each river site, where SNR data were average over 20 seconds. Measured SNR and SSC data were subjected to statistical analysis to investigate the correlation of the SNR and SSC data.

Water quality meters used here measures turbidity by using the scattered light measurement method. Turbidity measurements provide a reading of the amount scattered light. In this study turbidity measurements were made using DKK-TOA's multiparameter water quality meter. The data accuracy for turbidity was $\pm$3%. The relationship between the suspended solids in the liquid and the light intensity due to particles scatter is determined by the factory calibration of the instrument. In the laboratory, the relationship between SSC and turbidity was tested and a linear relationship was found.

The relationship between SNR and SSC was primarily assessed using least square analysis. They obtained an R^2= 0.9 in one of the rivers and R^2= 0.8 and R^2= 0.7 in the others. The predicted SSC is given by the formula:

SSC (estimated)= 1.49 X SNR – 13.5 (8)

As can be seen on figure 20, SNR measurements followed closely the turbidity peaks observed in the river.

[2] Work from *S.A. Hosseini, A.Shamsai, B.Ataie-Ashtiani.* Estimation of suspended sediment concentration in rivers using acoustic methods.

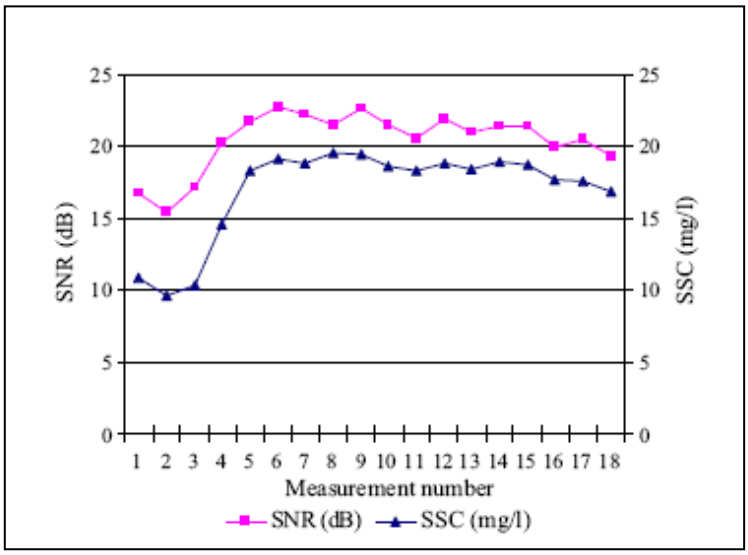

Figure 20: ADV and SSC measurements R^2= 0.9. (Sebnem Elçi et al. 2008). Environ. Monit. Assess.

Measurements showed that the ADV can be used to estimate SSC in low-turbid (SSC < 200 mg/l) water system.

IV.2.2 Least squared method – Amplitude

The ADV works by measuring the reflection of an acoustic signal from particulate matter in the water. This instrument is primarily used to measure the velocity of the particles but it can also provide information about the signal amplitude. Many authors have tried to relate this information with suspended sediment concentration.

For example *S.A. Hosseini, A.Shamsai, B.Ataie-Ashtiani* tried to relate signal amplitude with intensity and after with suspended sediment concentration. Another example is *Hubert Chanson, Maiko Takeuchi and Mark Trevethan* when they related signal amplitude with backscattered intensity and that one with suspended sediment concentration.

IV.2.2.1 Amplitude – Intensity[3]

Low density turbidity currents were investigated in a laboratory flume. An Acoustic Doppler Velocimeter (ADV) was used to measure the velocity. The dimensionless velocity profiles were compared with previous studies to check the accuracy of acoustic measuring techniques for turbidity currents.

[3] Work from *S.A. Hosseini, A.Shamsai, B.Ataie-Ashtiani.* Synchronous measurements of the velocity and concentration in lo density turbidity currents using an Acoustic Doppler Velocimeter.

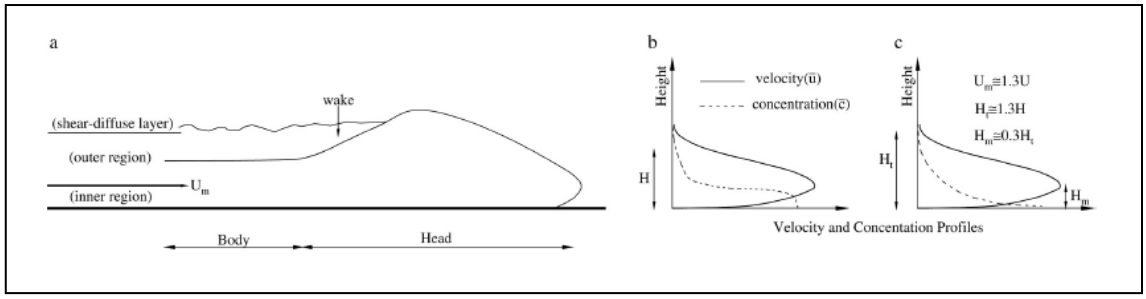

Figure 21: Sketch of defined regions in density currents and a typical profile of downstream velocity and mean concentration. (S.A. Hosseini et al., 2005). Flow measurement and instrumentation.

A 10MHz 5cm Nortek acoustic Doppler Velocimeter was used for measuring velocities in the experimental runs. It uses a technique known as pulse-to-pulse coherent Doppler sonar for measuring the velocity vector (Nortek As, ADV Specification User and Operation Manual, 1999). The mean downstream velocity (ū) was calculated by temporal averaging if the recorded time series at each point for all of the vertical profiles. The velocity maximum (u_m), as the characteristic velocity, and the height of the velocity maximum (H_m) and the depth- averaged thickness of the current (H) were used to obtain the non-dimensional form of the velocity profiles.

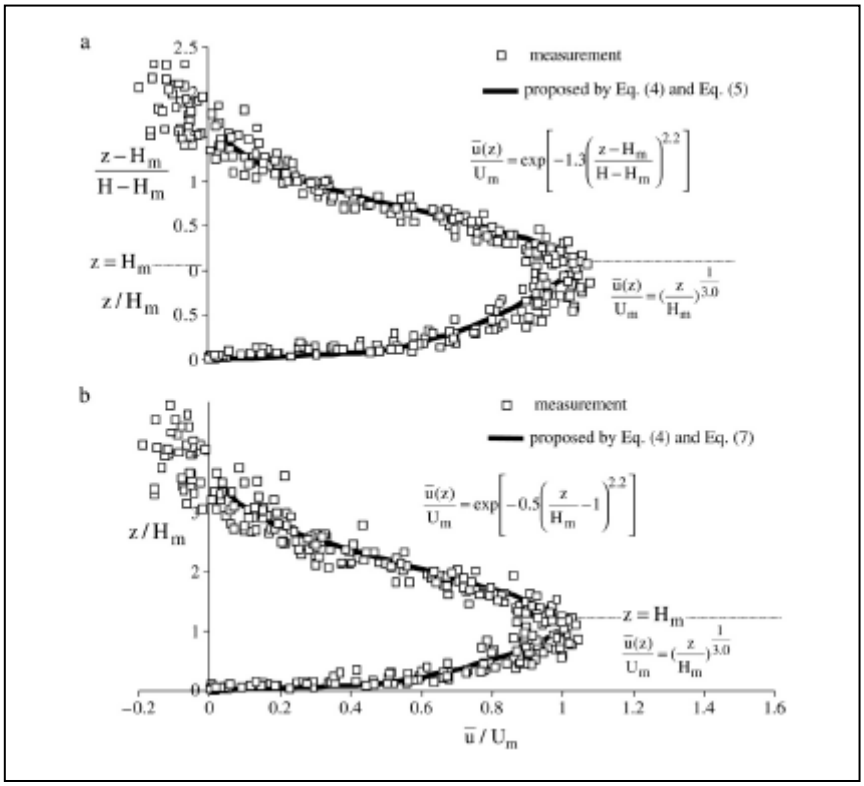

Figure 22: Dimensionless velocity profile. (S.A. Hosseini et al., 2005). Flow measurement and instrumentation.

They obtained that velocity distributions can be reasonably well represented by similarity profiles. The upper and lower parts of the profile had a different behaviour due to the effect of velocity gradient, boundary drag and shear; therefore the total profile was separated into two parts and the flow behaviour in each region was considered for the proposed profiles.

Within the inner region of current that is placed below the velocity maximum (U_m), the drag at the lower boundary is the main parameter and the expression for the velocity profile is a logarithmic relation that can be simplified to an empirical power relation as follows:

$$\frac{\overline{u}(z)}{u_*} = \frac{1}{k}\ln z + \text{Cons.} \longrightarrow \frac{\overline{u}(z)}{U_m} = \left(\frac{z}{H_m}\right)^{\alpha_v} \quad (9)$$

The effect of the upper drag boundary on the velocity profile was modelled by a density-stratified layer of finite thickness between two homogeneous fluids. The velocity distribution in the outer region was given by a near- Gaussian relation:

$$\frac{\overline{u}(z)}{U_m} = \exp\left[-\beta_v\left(\frac{z - H_m}{H - H_m}\right)^{\gamma_v}\right] \quad (10)$$

In order to estimate the mean sediment concentration in turbidity currents acoustic backscattering analyses were used. With this approach, the signal amplitude (SA) value obtained by the ADV is proportional to the logarithm of the intensity of the acoustic signal that is backscattered from small particles within the sampling volume. The intensity backscattered by particles within the sampling volume, I, is estimated using:

$$I \propto 10^{0.0434SA} \quad (11)$$

In this study the authors calculated I as the average if three intensities values obtained by three receivers. The backscattered intensity, but, is a function of the particle type, concentration and size of particles. The simplified relation between the intensity, I, and sediment concentration, c, can be expressed as:

$$I = \frac{I_0 c S_f S_a \exp\left[-2r(\alpha_w + \alpha_s)\right]}{r^2} \quad (12)$$

Where Io is the transmitted intensity, c is the mass sediment concentration, S_f contains all system specific parameters such as transducer size, efficiency, probe geometry, and receive se sensitivity, S_a holds all the particle specific parameters (size, elasticity, and density), α_w is the water absorption, α_s is the absorption due to particle scattering, and r is the acoustic propagation path.

The authors also took into account that for low concentration[4] particle attenuation can be neglected. Since their acoustic frequency was 10MHz, the water absorption coefficient (α_w) could be assumed as constant and therefore a nearly linear relationship between intensity, I, and concentration (c) appeared:

$$I_a \propto c \propto (10^{0.0434SA_1} + 10^{0.0434SA_2} + 10^{0.0434SA_3}) \quad (13)$$

Where SA_1, SA_2 and SA_3 are the signal amplitudes obtained by three receiving transducers and Ia is the average of three intensity values obtained by three receivers.

Figure 23 shows the relationship obtained between the mean of the averaged acoustic intensity (Ia) and the mean of the mass sediment concentration (c). As seen, the calibration curve was almost linear with zero offset, therefore:

$$\overline{c} = \lambda \overline{I}_a \quad (14)$$

Where λ is the calibration coefficient and is unique to each ADV.

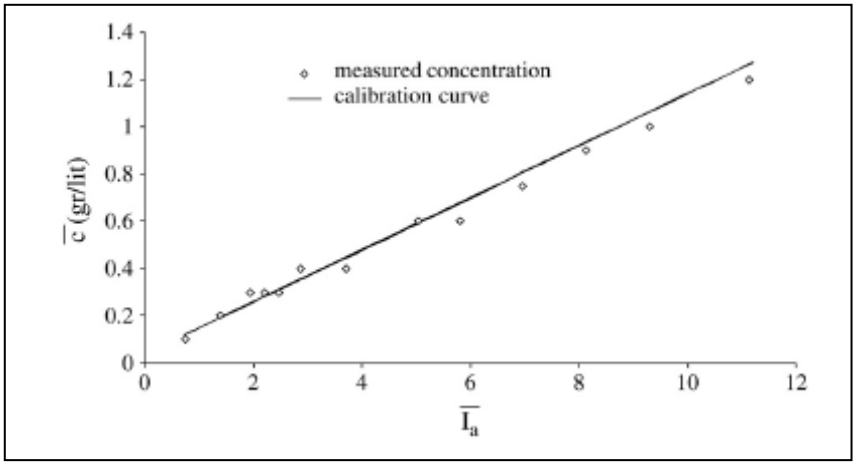

Figure 23: Relationship between acoustic backscattering intensity and mass sediment concentration (S.A. Hosseini et al., 2005). Flow measurement and instrumentation.

Also in this study, the height of the velocity maximum (H_m) and the concentration at this height (C_m) were used to obtain dimensionless forms of concentration profiles. They observed that concentration distribution can be represented by similarity profiles as well as the velocity.

[4] general experiences showed that low concentration corresponds at concentrations below 10 g/l

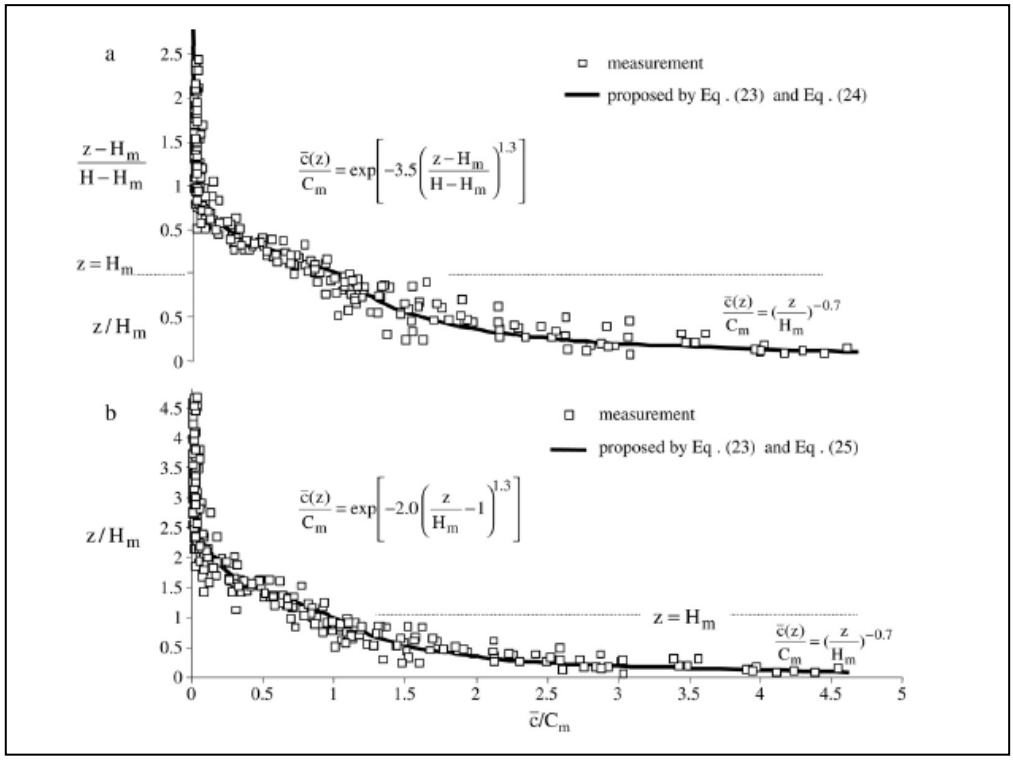

Figure 24: Dimensionless concentration profile (S.A. Hosseini et al., 2005). Flow measurement and instrumentation.

Similar to the velocity profile case, two expressions were suggested for concentration profiles in the inner and outer regions. Within the inner region of current that is placed below velocity maximum (U_m), the expression for the concentration is an empirical power relation as the velocity profile:

$$\frac{\bar{c}(z)}{C_m}=\left(\frac{z}{H_m}\right)^{-\alpha_c} \tag{15}$$

A Gaussian – type relation similar to the velocity profiles can approximate the concentration distribution in the outer region:

$$\frac{\bar{c}(z)}{C_m}=\exp\left[-\beta_c\left(\frac{z-H_m}{H-H_m}\right)^{\gamma_c}\right] \tag{16}$$

Successful estimation of the velocity and concentration, in the present experiments, indicated that this technique could be appropriate and useful for determining the flow structure in turbidity currents.

Therefore, observing these results, it is shown that the ADV provides an excellent opportunity to study the dynamics of sediment laden gravity currents. Velocity and concentration profiles from these experiments are in good agreement with other experimental research. Also it is observed that the measured velocity and concentration can be reasonably well represented by similarity profiles.

IV.2.2.2 Amplitude – Backscattered intensity- Turbidity[5]

The aim of the work from *Hubert Chanson, Maiko Takeuchi, Mark Trevethan* was to asses the ability of an ADV to measure instantaneous suspended sediment flux in a small subtropical system with fine cohesive sediment materials (mud and silt).

Hubert Chanson, Maiko Takeuchi and Mark Trevethan made a series of experiments, under controlled conditions, in laboratory. They used water and mud samples that had been collected in a small subtropical estuary of Eastern Australia and a microADV (16MHz) in order to measure the acoustic backscatter amplitude. The average amplitude measurements represented the average signal strength of the ADV receivers. The backscatter intensity (BSI) was related to the signal amplitude as:

$$BSI = 10^{-5} \times 10^{0.043 \times Ampl} \quad (17)$$

Where BSI is the acoustic backscatter intensity and Ampl is the average signal amplitude data measured in counts by the ADV system. The coefficient 10^{-5} was a value introduced in order to avoid large values of BSI (Nikora and Goring, 2002).

The relationship between suspended sediment concentration and turbidity exhibited a linear relationship (figure 24), while the relationship between suspended sediment concentration and acoustic backscatter intensity showed a monotonic increase (figure 25).

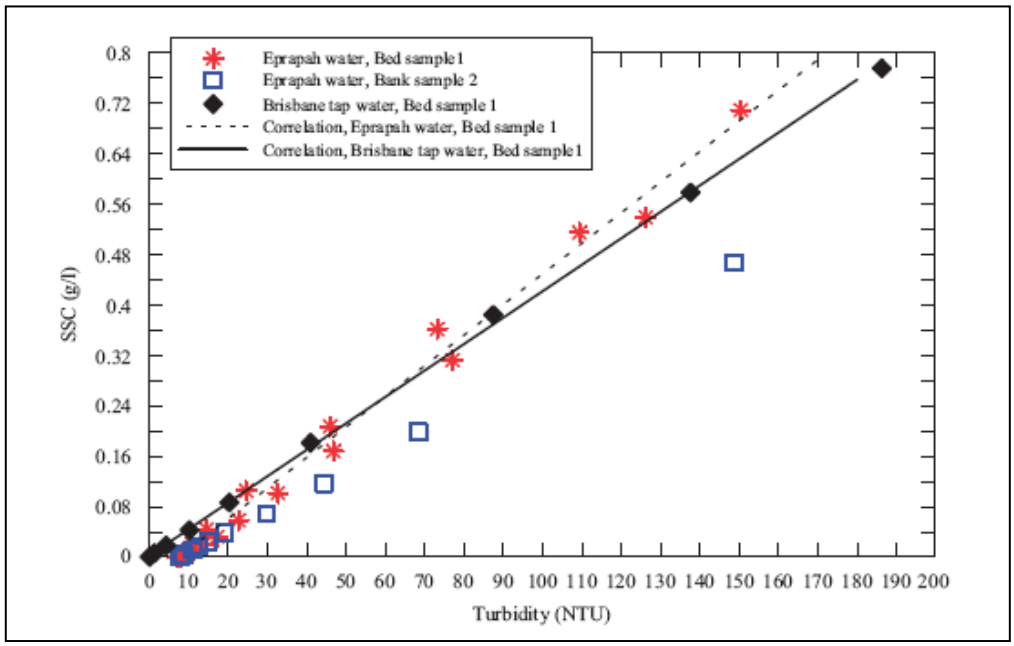

Figure 25: Relationship between SSC (g/l) and turbidity (NTU). (Hubert Chanson, Maiko Takeuchi and Mark Trevethan, 2008).

[5] Work from *Hubert Chanson, Maiko Takeuchi, Mark Trevethan. Using turbidity and acoustic backscatter intensity as surrogate measurements of suspended sediment concentration in a small subtropical estuary*

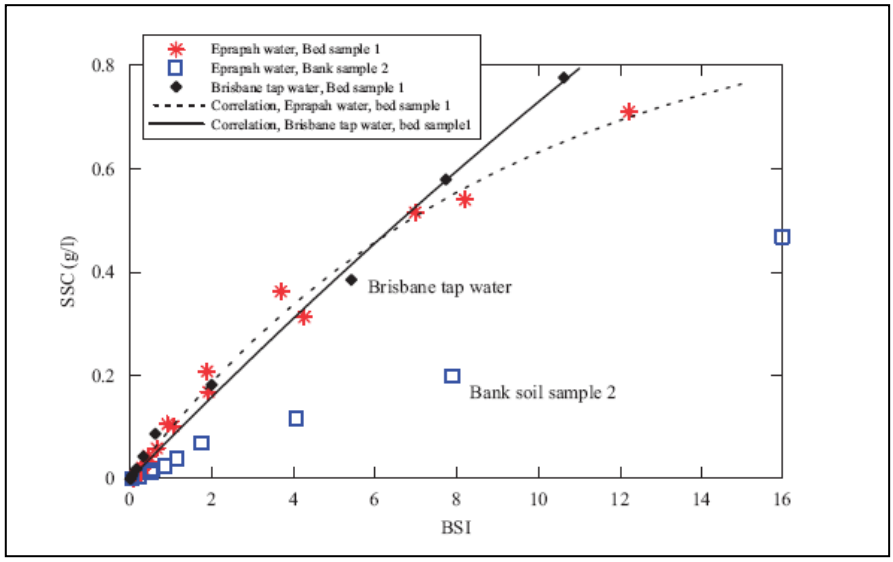

Figure 26: Relationship between SSC (g/l) and backscattered intensity (BSI). (Hubert Chanson, Maiko Takeuchi and Mark Trevethan, 2008).

For the laboratory tests the best fits for sample 1 (fine silt and mud material) were:

$$SSC = 0.9426 \text{ X } (1-\exp(-0.1109 \text{ X BSI})) \text{ with } R^2=0.9924 \quad (18)$$
$$SSC = 0.00485 \text{ x Turb} - 0.0350 \text{ with } R^2= 0.9922 \quad (19)$$
$$Turb= 171.06 \text{ x } (1-\exp(-0.1593 \text{ x BSI}) \text{ with } R^2= 0.9884 \quad (20)$$

The sample 2 was coarser than sample 1, and it consisted of a mix of mud and fine sand but the overall trends were similar with both soil samples.

The calibration curves were affected by both sediment material characteristics and water quality properties, implying that the calibration of an acoustic Doppler system must be performed with the waters and soil materials of the natural system.

The results were applied to some field studies in the estuary during which the acoustic Doppler velocimeter was sampled continuously at high frequency. The data yielded the instantaneous suspended sediment flux per unit area in the estuarine zone. This sediment flux per unit area was calculated as:

$$qs= SSC \text{ x } Vx \quad (21)$$

They showed some significant fluctuations in instantaneous suspended mass flux, with a net upstream suspended mass flux during flood tide and net downstream sediment flux during ebb tide. For each tidal cycle, the integration of the suspended sediment flux per unit area data with respect of time yielded some net upstream sediment flux in average.

It must be stressed that this work highlighted a number of limitations:

- Calibration relationships were based upon a 2-day-period study.
- Results might not be suitable for field studies with different water quality conditions.
- The calibration curves were also specific to the microADV unit.
- The present work was carried out for a subtropical estuary wuth relatively low turbidity levels.
- The present results are not applicable to turbid flows with high SSC.

IV.2.3 Multivariate analysis[6]

Multivariate analysis was utilized by *S.A. Hosseini, A.Shamsai, B.Ataie-Ashtiani* to investigate the effect of soil type and water temperature on the measurements. Statistical analysis indicates that SNR readings obtained from the ADV are affected by water temperature and particle size distribution of the soil, as expected, and a prediction model is presented relating SNR readings to SSC measurements where both water temperature and sediment characteristics type are incorporated into the model. The coefficients of the suggested model were obtained using the multivariate analysis.

Multivariate analysis was carried out on a data matrix of five variables including SSC, dimensionless mean diameter (d_{50}/d_{50b}), coefficient of gradation (Cg), and dimensionless absorption coefficient (α/α_c). Here, d_{50b} is the particle diameter corresponding to predicted maximum sensitivity for the ADV (d_{50b} = 0.025mm in this study), α_c is the absorption coefficient for the calibration temperature calculated using:

$$\alpha = 8.687 \times \frac{3.38*10^{-6}*f^2}{21.9*10^{6-(1520/T+273)}} \qquad (22)$$

Where 8.687 is the conversion factor from nepers to decibels, α is the absorption coefficient, f is the acoustic frequency, in kilocycles per second and T is the water temperature in ºC.

And finally Cg is the coefficient of gradation calculated as:

$$Cg = (D_{30})^2 / (D_{60} \times D_{10}) \qquad (23)$$

As dimensionless mean diameter and coefficient of gradation were both soil properties were combined by multiplication and PLS (Partial Least Squared) analysis was conducted using a data matrix of four variables (SSC, SNR, d_{50}/d_{50b} X Cg, α/α_c). The relation founded was:

$$SSC = -13.8 + 0.8 \text{ X SNR} + 21.04 \times (\alpha/\alpha_c) + 4.52 \times d_{50}/d_{50b} \text{ X Cg} \qquad (24)$$

Figure 26 gives the comparison of observed SSC values and the SSC values predicted by the model.

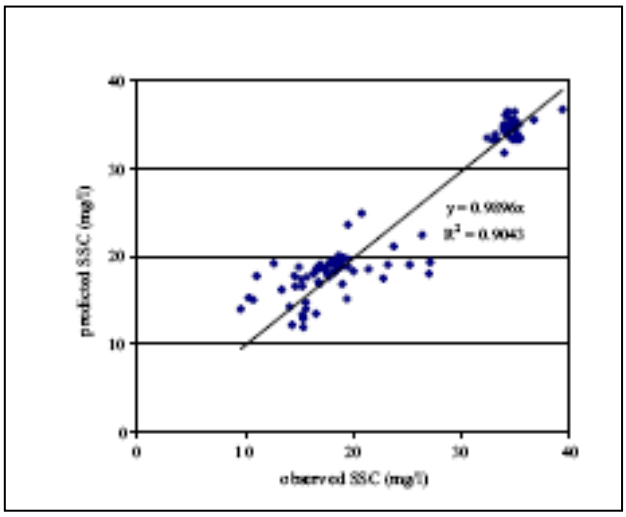

Figure 27: Comparison of observed SSC values and the SSC values predicted by the model. (Sebnem Elçi et al. 2008). Environ. Monit. Assess.

[6] Work from *S.A. Hosseini, A.Shamsai, B.Ataie-Ashtiani.* Estimation of suspended sediment concentration in rivers using acoustic methods

Effect of high turbidity conditions on ADV performance was also investigated during rain events. In these flood events the performance of the ADV for predicting the suspended sediment concentration failed due to the high turbidity conditions (SSC > 200 mg/l). As can be seen in the figure below the ADV could not resolve the changes in SSC, and the SNR values remained constant.

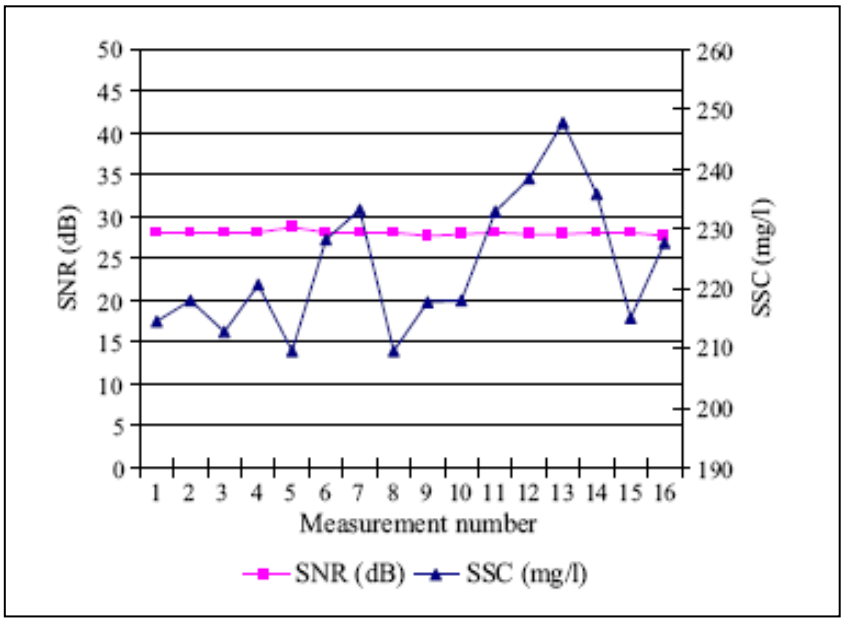

Figure 28: ADV and SSC measurements in flood conditions. (Sebnem Elçi et al. 2008). Environ. Monit. Assess.

Therefore in this study measurements showed that the ADV can be used to estimate SSC in low turbid (SSC< 200 mg/l) water systems. Also using a multivariate analysis they saw that reported SSC values depend on at least three parameters: water temperature, mean diameter of the soil and shape of the particle size distribution curve.

On the other hand, when turbidity exceeds a limit concentration (SSC>400 mg/l) was not possible to make predictions of SSC from ADV.

V. Results

The acoustic Doppler velocimeter (ADV) is widely used in water systems to measure flow velocities and velocity profile. This is a relatively new instrument that measures three-dimensional turbulent velocities at sampling frequencies up to 100Hz in a small, remote sampling volume (e.g. Kraus et al., 1984; Lorhmannn et al., 1995).

Despite the ADV's advantages some measurement errors are inherent to the system. There are three sources of measurement errors: (Stuart,J. and Andrew,P., 2000)

1. sampling errors that are Hardware controlled
2. Noise that is intrinsic to the Doppler measurement.
3. Errors due to velocity gradient in the sampling volume.

Although sampling errors may introduce bias to mean velocity measurements, Doppler noise does not affect mean velocity estimates because it is 'white noise' and is independent from velocity measurements (Lohrmann et al.,1995)

To ensure that ADV measurements provide an accurate representation on the flow velocity, one should evaluate two additional parameters provided in the ADV file, the signal-to-noise-ratio (SNR) and the correlation (COR) (Tony,L.Wahl). Also some authors (S.A. Hosseini, A.Shamsai,B.Ataie-Ashtiani) use the amplitude signal (SA).

Different parameters that affect the performance of an ADV for the prediction of SSC are investigated in this study. In order to investigate the reliability of and ADV for SSC measurements in the surf zone, different tests were carried out in CIEM- Barcelona flume.

V.1 Data control

The ADV emits a square-shaped $4.8*10^{-6}$ s acoustic pulse at a frequency of 100 Hz from an element at the centre of the probe head. As each pulse propagates through the fluid, acoustic energy is reflected back by air bubbles or small particles suspended in the fluid and three receive elements detect the resulting acoustic echo. Following the detection of strong acoustic reflections from the transmitted beam the signal amplitude decreases to a base level that represents the system noise, which typically is 23-28 dB (Nortek,1997).

The ADV uses a dual pulse-pair scheme with unequal pulse repetition rates (τ_1 and τ_2) separated by a dwell time (τ_d)

V.1.1 Spectral width

As Stuart J.McLelland and Andrew P.Nicholas let us know in their study[7] the correlation between dual pulse-pair velocity estimates is derived using the covariance method (e.g. Miller and Rochwarger, 1972; Zrnic, 1997). However, the spectral width (or spectral variance) of the covariance function is contaminated by signal noise due to the loss of signal coherence during its propagation through the fluid (Lhermitte and Serafin, 984). This white noise cannot be removed by improving the acoustic qualities of the system, but different pulse repetition rates permit the separation of variance due to signal alone from that contributed by noise (Lhermitte and Serafin, 1984). Hence, the dual pulse-pair scheme used by the ADV allows accurate prediction of the spectrum

[7] Study described in section IV.1

width by removing any noise bias from the velocity estimates. Assuming a Gaussian distribution for the phase power spectrum, the correlation coefficient (R^2) can be related to the dimensionless spectral width (φr):

$$R^2=e^{-2*\pi\wedge2*\varphi r\wedge2} \quad (25)$$

The dimensionless spectral width is the product of the received signal width and the sample time interval.

$$\varphi r= \sqrt{(-\ln(R^2)/2*\pi^2)} \quad (26)$$

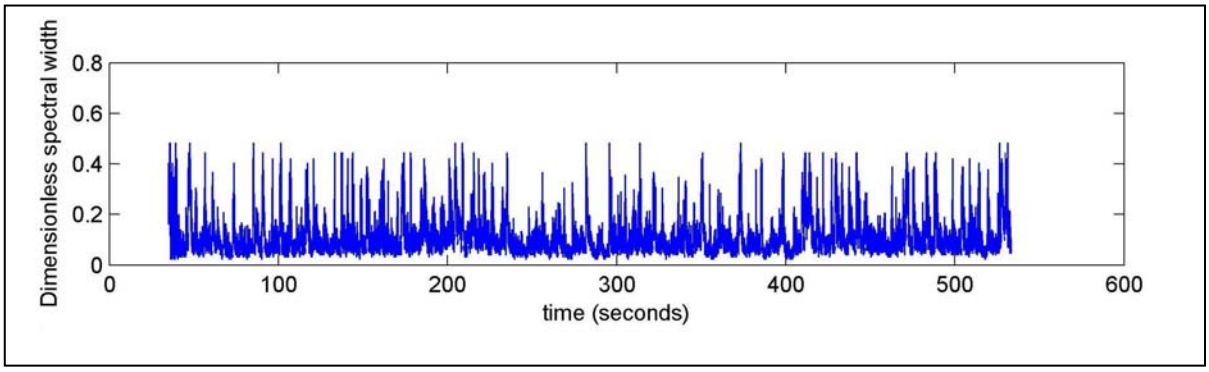

Figure 29: *Dimensionless spectral width versus time*

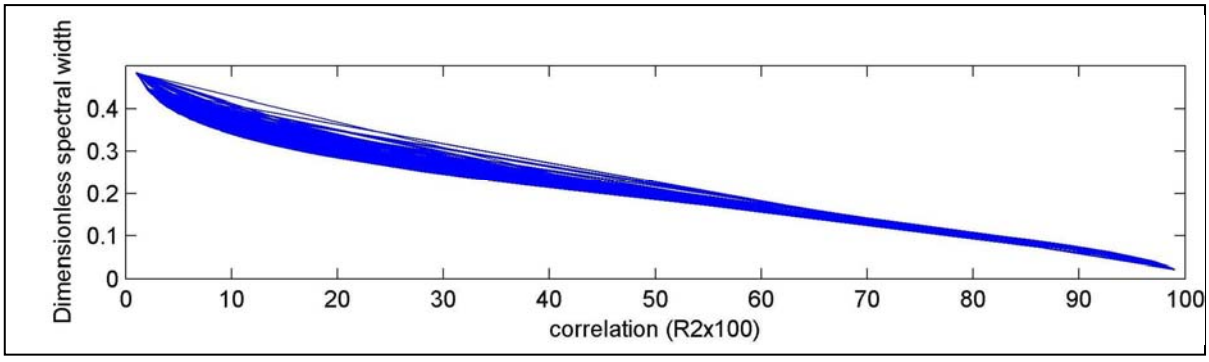

Figure 30: *Dimensionless spectral width versus correlation*

Hence, for a given correlation coefficient the variance of the received signal will increase for larger instrument velocity ranges because the sample interval decreases as the velocity range increases. Lhermitte and Serafin (1984) demonstrate that for a lower limit of $\varphi r<0.16$ the difference between the measured spectral variance and the variance for different spectral shapes is less than 8% (Stuart J. McLelland and Andrew P. Nicholas,2000).

Also the acoustic signal will be contaminated with noise that is intrinsic to the propagation of acoustic waves and the Doppler detection system. This noise can obscure the real signal and the standard deviation of the mean velocity estimate increases as the signal-to-noise ratio decreases (Zrnic,1977). For a given instrument velocity range, the dimensionless spectral width of the signal noise (φn^2) is:

$$\varphi n^2= \ln(1+(1/SNR))/2*\pi^2 \quad (27)$$

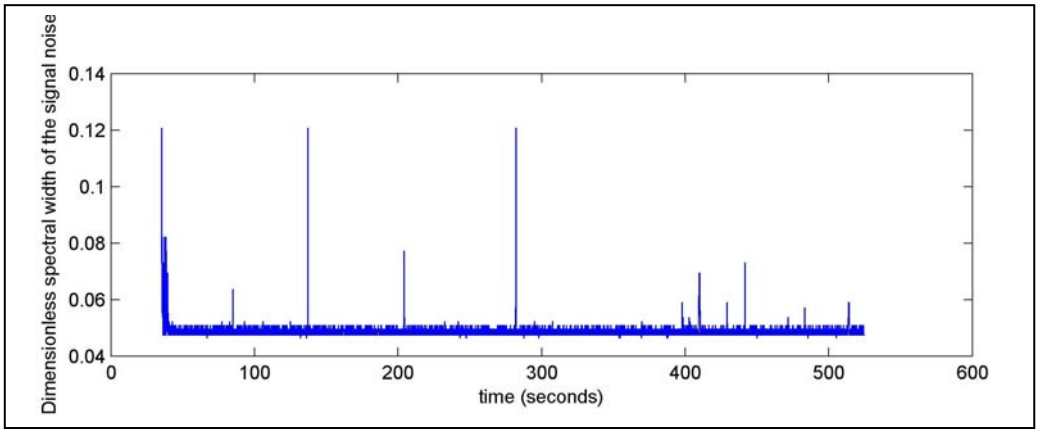

Figure 31: *Dimensionless spectral width of the SNR versus time*

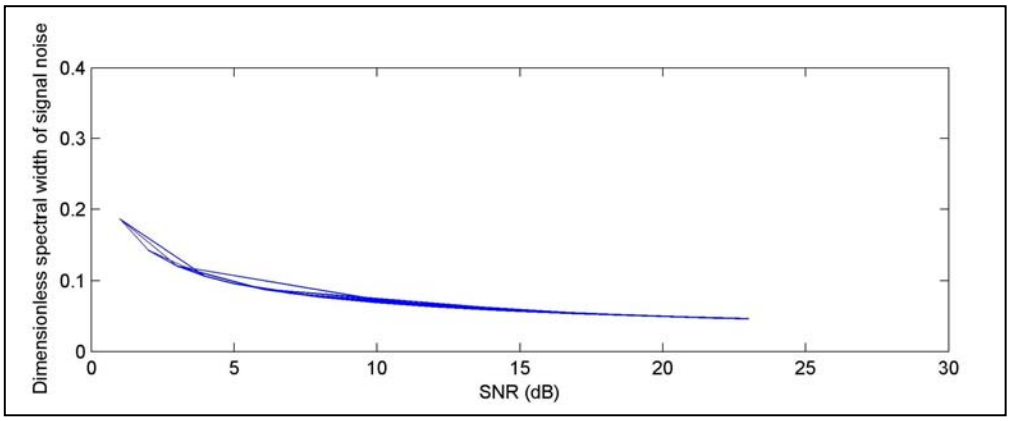

Figure 32: *Dimensionless spectral width of the SNR versus SNR*

Figure 32 illustrates that the dimensionless spectral width of the signal noise decreases as SNR increases. Nortek (1997) suggest that SNR>5 dB is required for collecting mean flow data and that SNR>15 dB is necessary for collecting instantaneous flow data. As the spectral width of the received signal increases, the relative magnitude of signal noise will increase, therefore the corollary of these theoretical and practical considerations is that the minimum correlation coefficient for any receiver should be at least 60% and the signal-to-noise ratio should be maximized during measurements.

One can appreciate that these figures showed a good agreement with the theoretical figure in the real study (fig. 21).

V.2 Time series

In this work two kinds of devices were used, OBS and ADV, and data were obtained from them along the time.

In one hand OBS is an excellent tool for suspended sediment studies dues to its high frequency response, relative insensitivity to bubbles, approximately linear response to concentration and small size.

On the other hand ADV are widely used for laboratory and field measurements of 2D and 3D water velocities.

V.2.1 OBS

During the tests carried out in CEM flume data from OBS were collected in two different configurations. The first configuration was with erosive wave conditions (47 tests) while the second was in accretive wave conditions (35 tests). The beach profile was not reshaped during the experiments; therefore the accretive conditions start after the last profile result of the erosive tested conditions.

V.2.1.1 Profile evolution

As it is known the slope of a beach is changing while different waves conditions are acting; therefore morphodynamics parameters have to be studied at every profile. These parameters include slopes (bar and foreshore), the position and height of the bar, the position and depth of the though, the sediment balance for different areas along the profile and for the whole profile.

Even if the aim of theses parameters is to quantify the bottom evolution for the different wave conditions tested, it is out of the scope of this study to enter in more detail on it. Just has to be notice how profile is changing and why we should study more than one case.

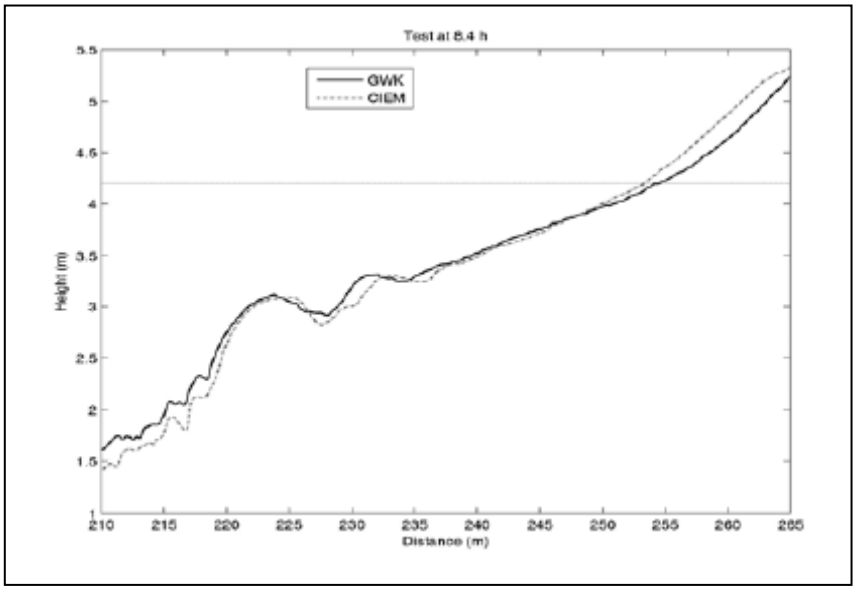

Figure 33: *Profile evolution in the flume after 8.4h of erosive wave conditions* (Cáceres,I., Alsina, J.M. and Sánchez-Arcilla, A., 2009. "Mobile bed experiments focused to study the swash zone evolution". Journal of Coastal Research, SI 56 (Proceedings of the 10th International Coastal Symposium). Lisbon Portugal, ISBN).

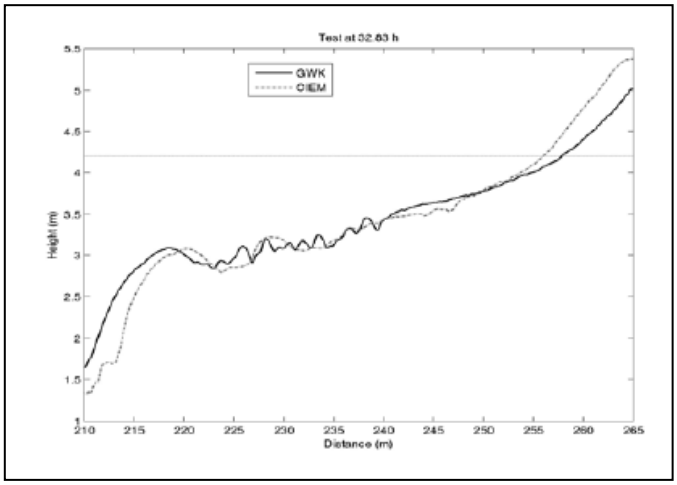

Figure 34: *Profile evolution in the flume after 32.83h of erosive wave conditions (*Cáceres,I., Alsina, J.M. and Sánchez-Arcilla, A., 2009. "Mobile bed experiments focused to study the swash zone evolution". Journal of Coastal Research, SI 56 (Proceedings of the 10th International Coastal Symposium). Lisbon Portugal, ISBN).

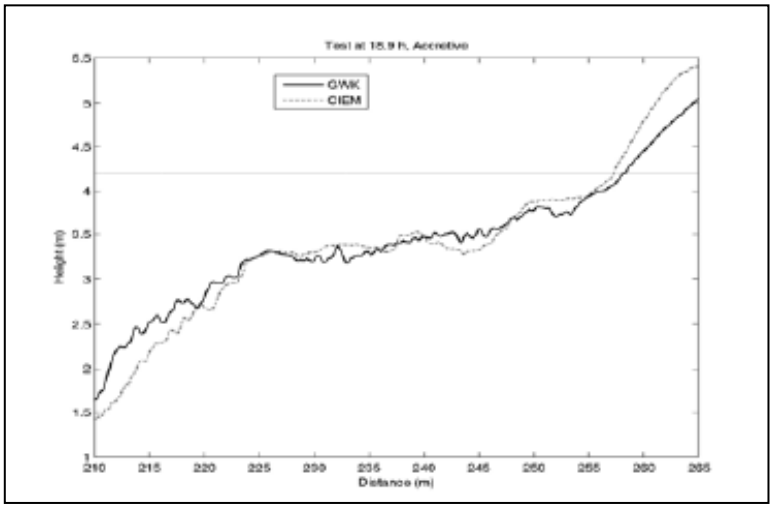

Figure 35: *Profile evolution in the flume after 18.9h of accretive wave conditions (*Cáceres,I., Alsina, J.M. and Sánchez-Arcilla, A., 2009. "Mobile bed experiments focused to study the swash zone evolution". Journal of Coastal Research, SI 56 (Proceedings of the 10th International Coastal Symposium). Lisbon Portugal, ISBN).

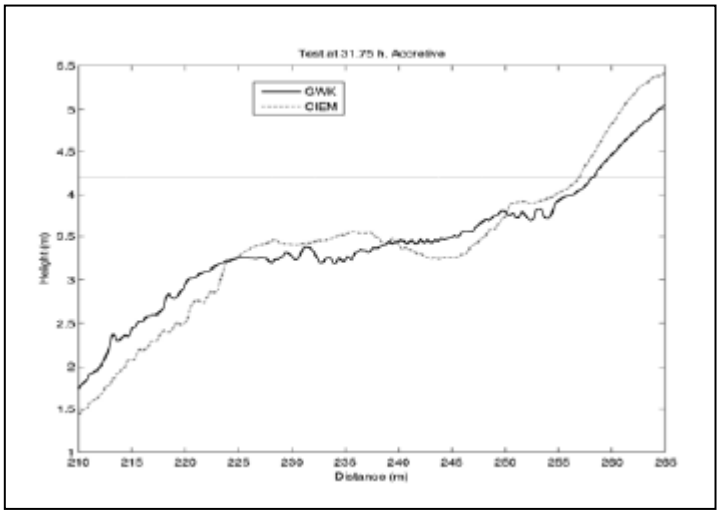

Figure 36: *Profile evolution in the flume after 31.75h of accretive wave conditions (*Cáceres,I., Alsina, J.M. and Sánchez-Arcilla, A., 2009. "Mobile bed experiments focused to study the swash zone evolution". Journal of Coastal Research, SI 56 (Proceedings of the 10th International Coastal Symposium). Lisbon Portugal, ISBN).

As one can appreciate from these figures and as has been explained before the beach slope is changing. Without going further one can see how littoral bars are moving far from the swash zone as the time in erosion series is running and how these bars are going on the opposite direction and smoothing its shape as the time is running in accretive conditions.

The sediment concentration data shows an important difference in suspended sediment concentration at the same position due to the existence of the submerged bar (the difference is one order of magnitude lower at the middle and end of the erosive wave conditions). The created bar filters the higher waves while allows the small ones to pass over the submerged barrier and break closer to the shoreline. Taking in account this effect and the profile evolution the study has firstly been divided in 2 cases: Erosive wave conditions and accretive wave conditions.

V.2.1.2 Erosive wave conditions

This situation occurs with waves period of Tp= 4.14 s and waves height in the order of Hs= 0.53m.

One should notice that the configuration is changing along the time while waves are acting. This means that the characteristics of the bottom, like slope, compaction of the sand, etc. are changing.

For example, at the beginning, when the firsts strong waves are approaching at the coast, due to the energy and the currents generated, sediment is bring into suspension. The quantity of sediment in suspension is bigger at the beginning than after a while because sediment is not compacted and it is easy to stir it up[8]. Also, some bars are formed along the time with the actions of these strong waves. The slope of the coast gets like a storm profile[9]. Therefore it is necessary to make a distinction between the firsts tests carried out in the erosive situation and the latest ones.

One can appreciate in figures 37 and 38 that a big difference in suspended sediment concentration exists. At the beginning of the erosive test suspended sediment concentration reaches values up to 60 – 80 g/l with some peaks reaching 100 – 120 and 180 g/l. At the end of this test suspended sediment concentration is up to values of 8-10 g/l. Therefore a big contrast is found and we should make a distinction between high concentration (above 10g/l) and low concentration (under 10 g/l).

Also, in figure 38 one can notice that the pulsating structure presents just one peak in the suspended sediment concentration distribution. One can think that it is a spike, but in fact it can not be consider as it because as many test you carry out you will found it peak, therefore it can not be assumed as a spike.

[8] Notice it in figures 37 and 38
[9] One can appreciate the bottom slope from figure 33 to figure 36

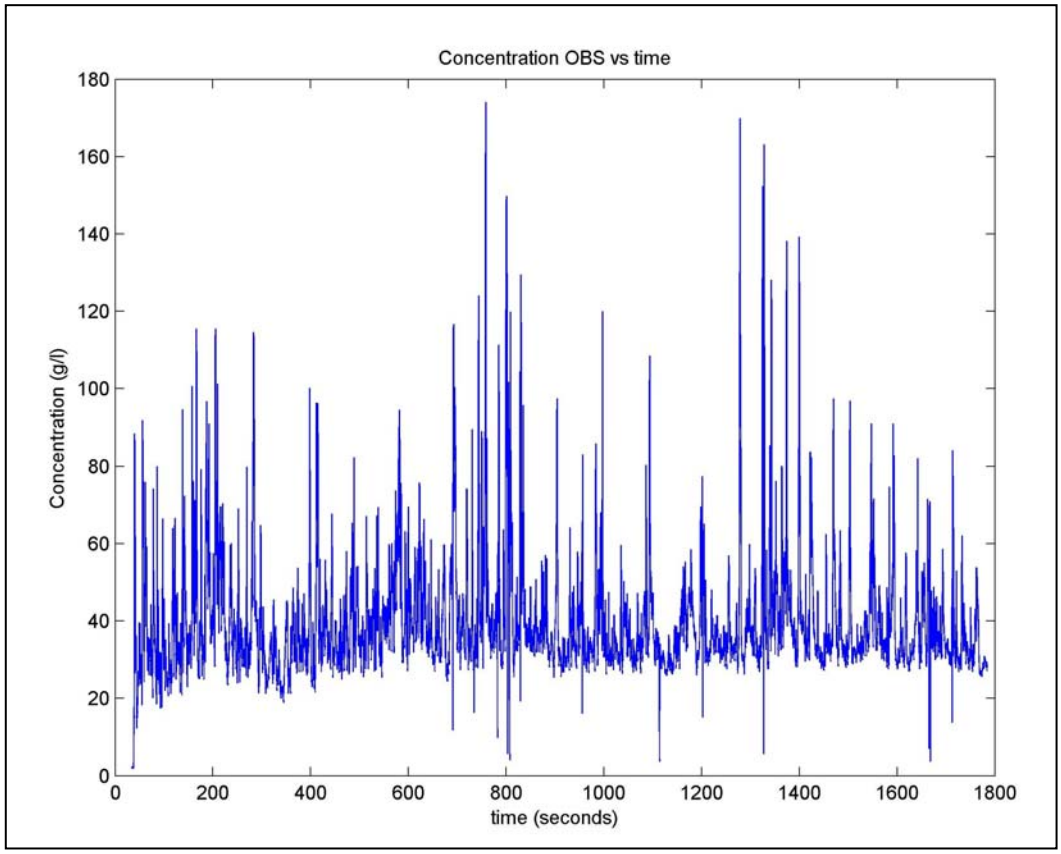

Figure 37: Concentration data at the beginning of the erosive test

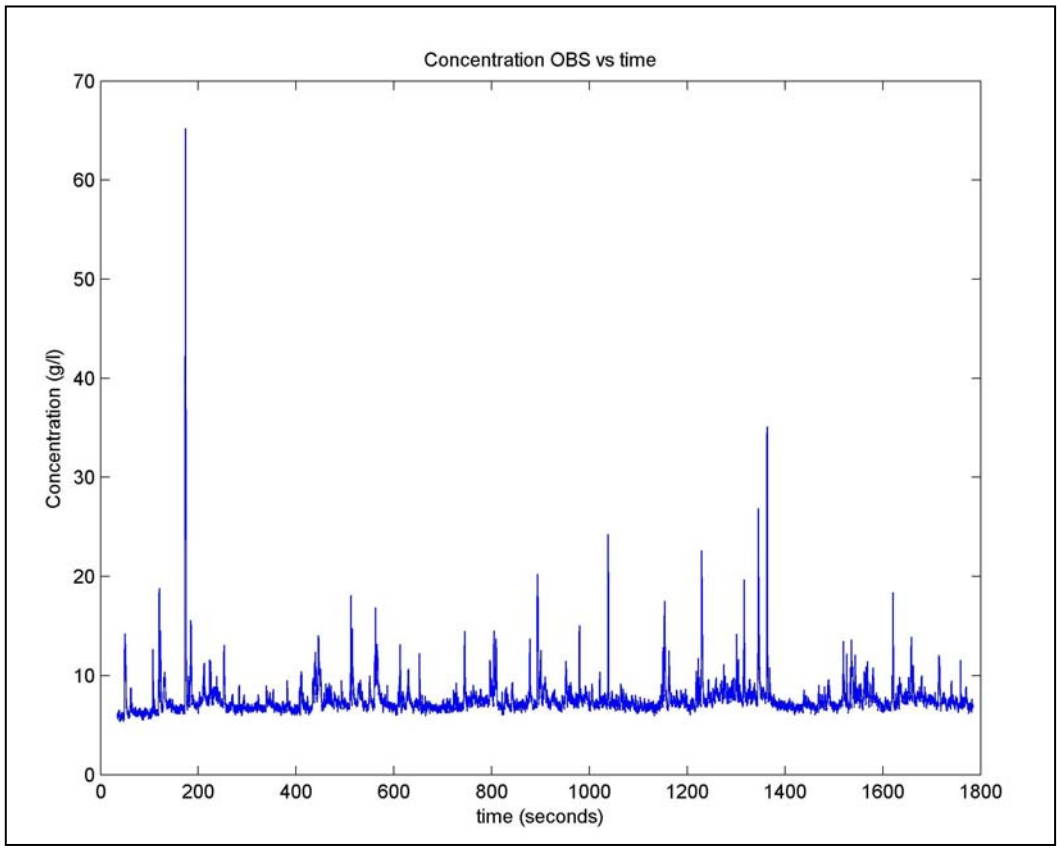

Figure 38: Concentration data at the end of the erosive test

V.2.1.3 Accretion wave condition

Another distinction needs to be made between erosion situation and accretion situation. The accretion configuration occurs with waves period of Tp=5.44 s and waves height in the order of Hs= 0.32m.

As it can be seen wave's characteristics are different from the previous case and therefore the profile effects are different too. Here sediment is not stir up and bring into suspension but is lying down due to the lower energy and currents.

When the SSC is analyzed a general pulsating behaviour can be observed. This general pattern is also present at low concentrations here considered below 5 g/l.

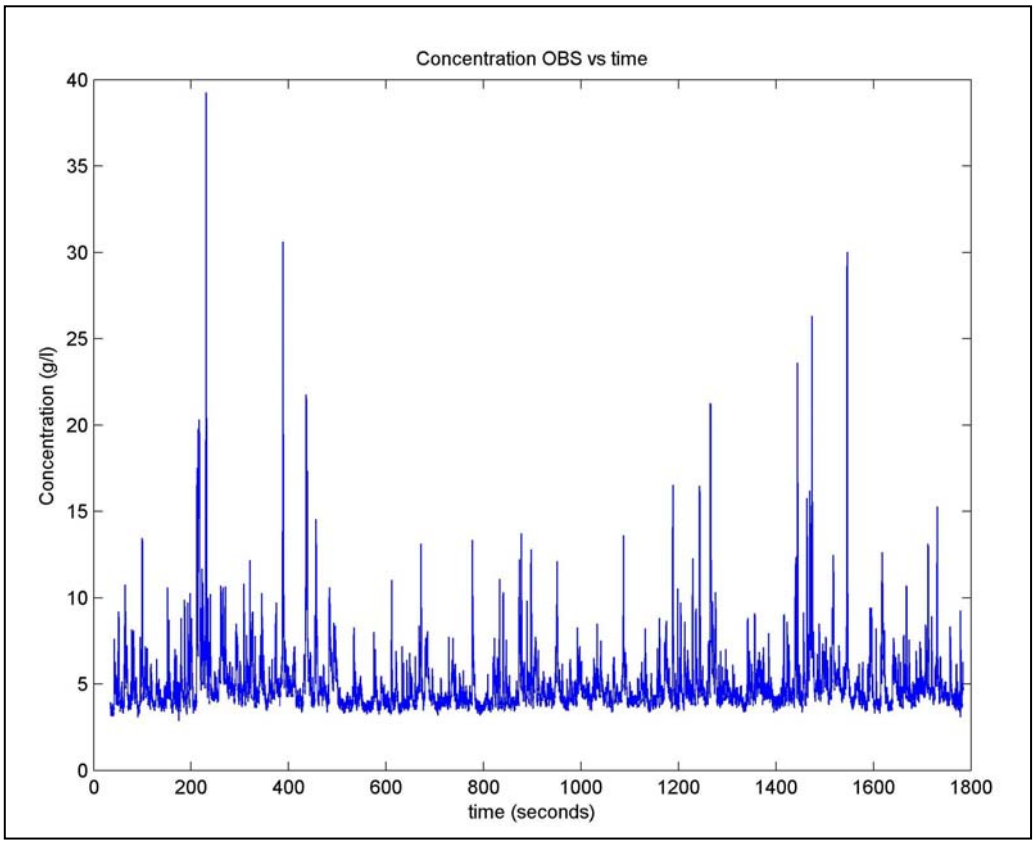

Figure 39: Concentration data from the accretive test

Therefore, comparing figures 37, 38 and 39 one can conclude that we need to differentiate three cases:

Case	Description	Hs (m)	Tp (s)
1	Erosive wave (beginning)	0.53	4.14
2	Erosive wave (ending)	0.53	4.14
3	Accreting wave	0.32	5.44

Table 1: *Cases and conditions of each study case*

V.2.2 ADV

An ADV can measure three- dimensional flow velocity at any depth within the water column. The magnitude of the acoustic reflection (signal strength) from the water is a function of the instrument used; influenced by sound frequency transmit power, receive sensitivity and range to measurement volume, and the conditions of the water, primarily the size and concentration of particle matter.

The ADV outputs, for each receiver:

1. signal amplitude (SA)
2. Signal-to-noise ratio (SNR)
3. correlation between successive radial velocities (R^2)

Several researches investigated the performance of ADVs for prediction of SSC. Formulations were derived by relating SNR (signal-to-noise ratio) and SSC of the water (Kostaschuk et al. 2004; Alvarez and Jones 2002; Gartner 2002; Hosseini et al. 2005; Creed et al. 2001; Rennie et al. 2002, Sebnem at al. 2007). However, these studies were site- specific (limited to a single river or water body).

One of the limitations using an ADV for SSC is that an ADV measures the velocity of solid particles rather than the fluid velocity. Therefore the sediment and the fluid are assumed to travel at the same velocity. This assumption is likely to be valid only when considering fine sediments, dominantly in suspension. Beyond this it is known that one can obtain concentration data and velocity data while the particles do not have to move at the same velocity as fluid.

Another limitation is that as the sediment concentration increases, acoustic waves are absorbed in sediment- laden flow and attenuated to the point where the ADV cannot operate properly in high sediment concentrations.

But, although these limitations are out of the scope of this work, the main goal of this study is to improve the methodology for predicting SSC using ADV backscatter data in the surf zone.

V.2.2.1 Signal to noise ratio (SNR)

SNR is a parameter that indicates the relative density of acoustic scatters in the flow and the resulting strength of the signal received compared to the noise level of the instrument. (Tony L.Whahl)

If one plots the signal- to- noise ratio versus time on the three cases exposed before, obtains:

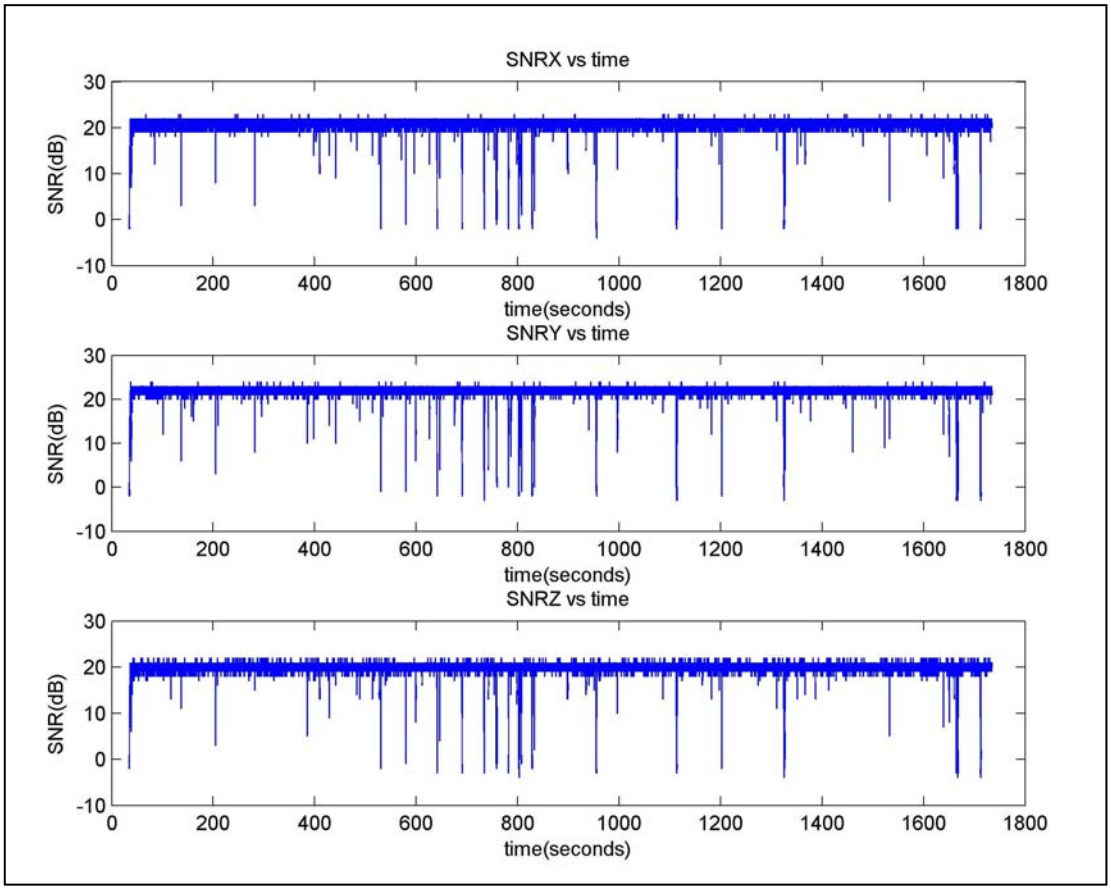

Figure 40: SNR versus time for case 1

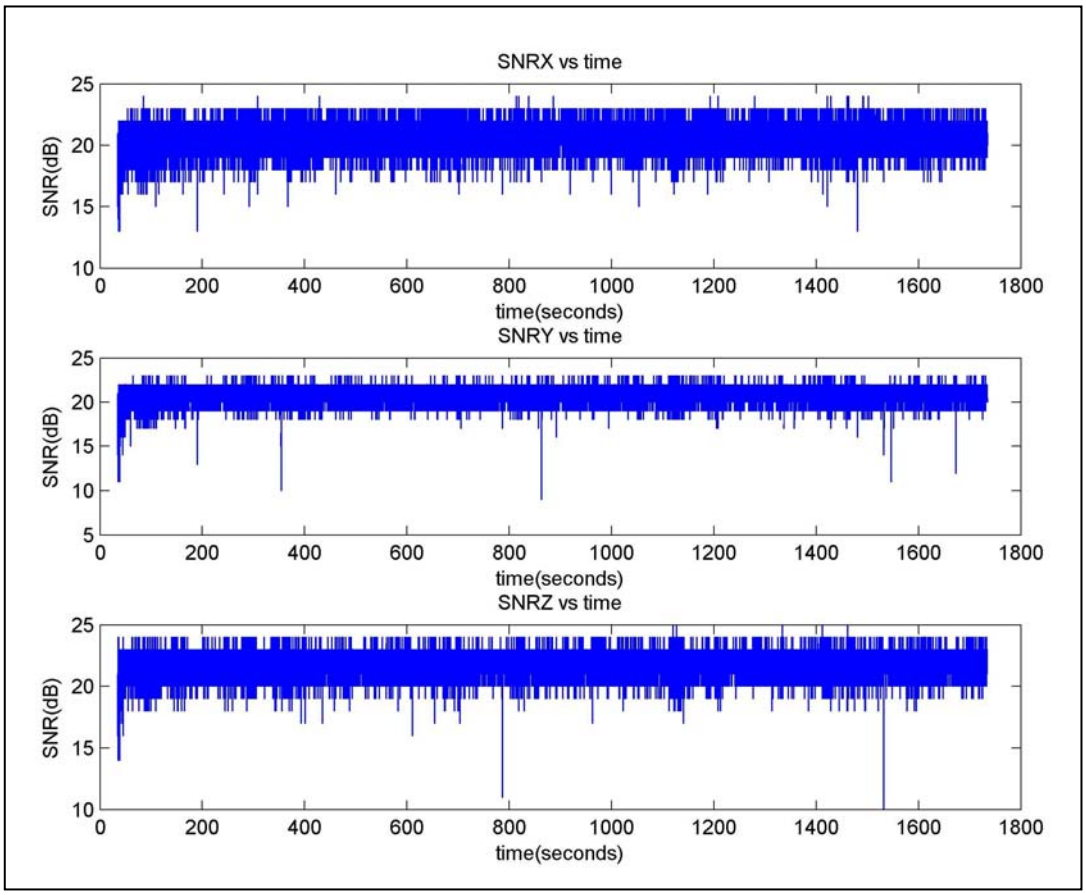

Figure 41: SNR versus time for case 2

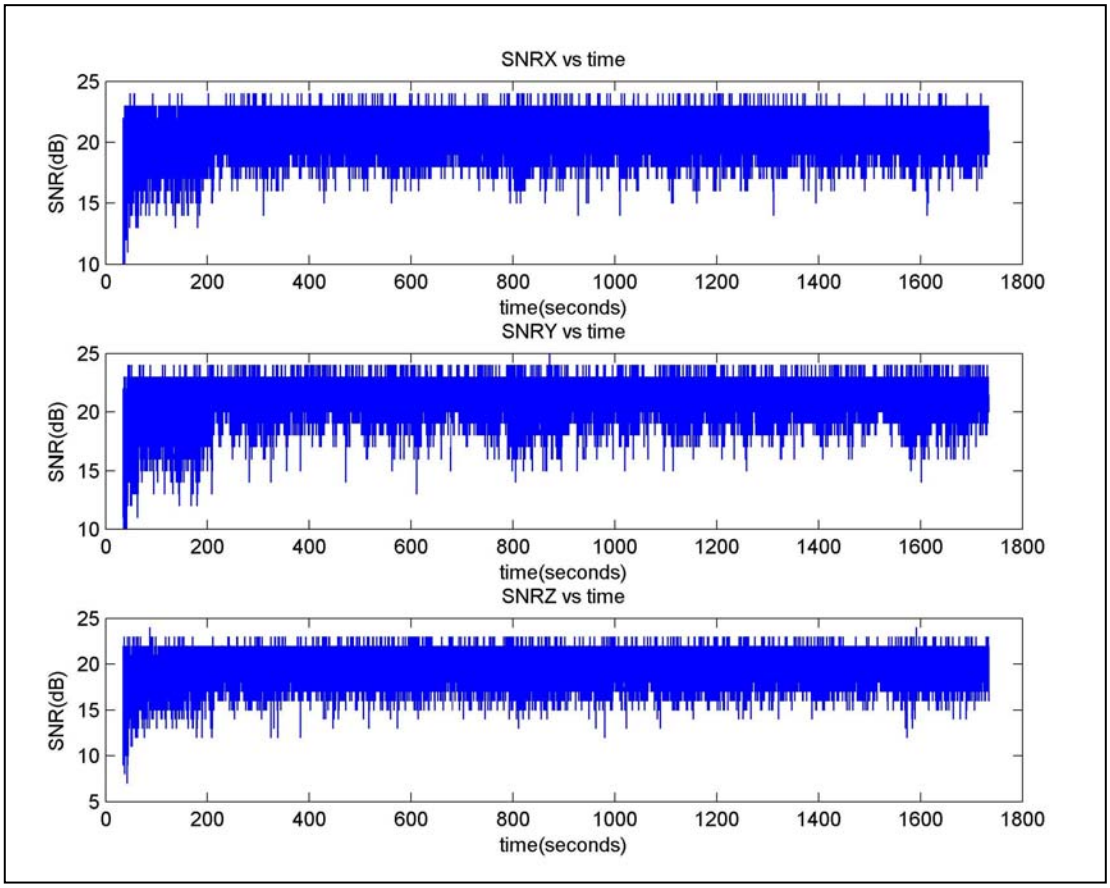

Figure 42: SNR versus time for case 3

From figures 40, 41 and 42 one can appreciate that SNR measured in the three directions (x, y, z) is not changing when focus in the same test. When one compares the SNR signal between the different cases exposed we can observe that is always oscillating around the same value (20 dB) but the distribution is widening as the concentration is lowering.

Another point to remark is that when one works with case 1 (high concentration) the distribution present some spikes which have been not removed because they contribute poorly to our work methods. As one works with lower suspended sediment concentration spikes disappeared due to the distribution widening (figure 38).

As one can appreciate SNR oscillates in a regular way between -3 dB and 23 dB in case 1, 13 dB to 25 dB in case 2 and 5 dB to 25 dB in case 3. ADV manufacturers (Nortek) recommend an SNR value of at least 5 dB when measuring average flow velocities and 15 dB or higher when measuring instantaneous velocities and turbulence quantities.

Also one can observed that from time 0 until 200 seconds SNR is not stabilized in all three cases; due to that and according to Nortek, in this study results dependents on SNR are starting after time 200 seconds.

V.2.2.2 Signal Amplitude (SA)

The ADV works by measuring the reflection of an acoustic signal from particle matter in water. While this instrument is primarily used to measure the velocity of the particles, it can also provide information about the quantity of sediment present. This information is measured in form of the intensity of the reflections received, also referred to as the backscattering strength or signal amplitude (Nortek, technical note).

An ADV system provides the signal amplitude as part of its output record. This is measured with the same frequency and in the same sampling volume as the velocities.

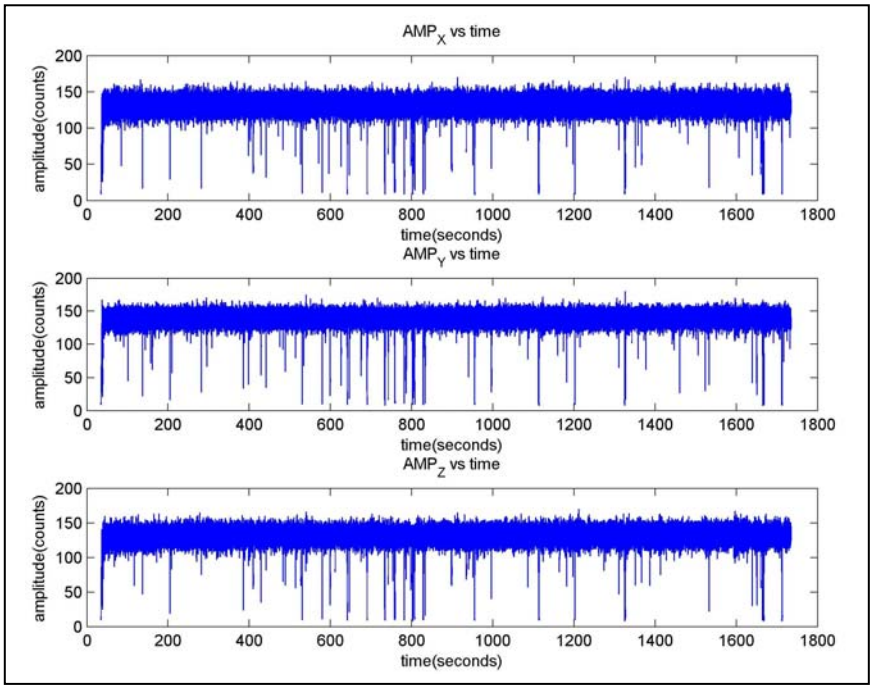

Figure 43: Amplitude versus time for case 1

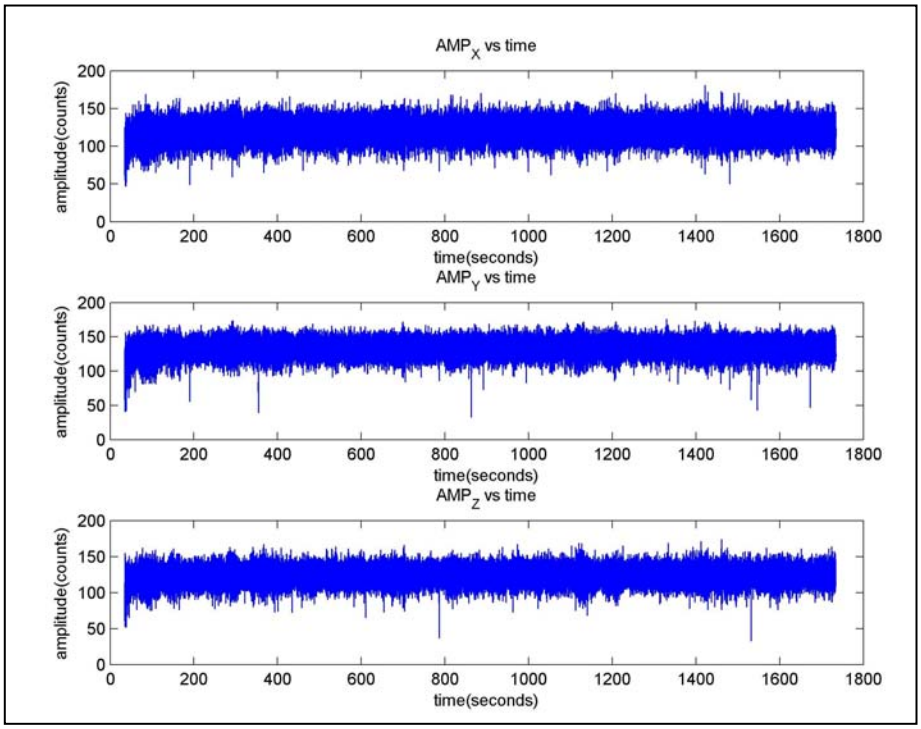

Figure 44: Amplitude versus time for case 2

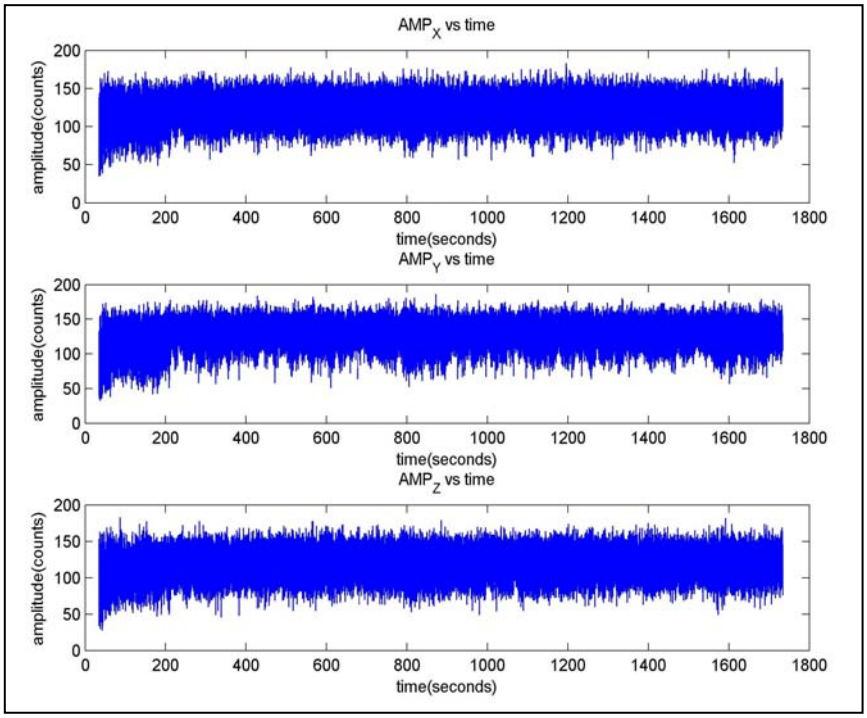

Figure 45: Amplitude versus time for case 3

As one can appreciate amplitude distribution shows a similar form than SNR. Here, in figure 43 one can see that amplitude oscillates between 100 counts and 150 counts. For case 3, figure 45, amplitude oscillates between 80 counts and 150 counts. Therefore one can affirm that the signal amplitude function is widening as suspended sediment concentration is decreasing as happens in SNR output.

Also, one can appreciate that signal amplitude distribution in case 1 (high concentration), figure 43, present a lot of spikes and how these spikes are absorbed by the same function as suspended sediment concentration is lowering and therefore signal amplitude distribution widening.

Another fact to take into account is that amplitude is independent on the direction we measure. In all three directions no shifts are present in signal amplitude distribution. Then if one wants to simplify calculations and work with just one direction (x, y, z) it doesn't mind in which direction chooses, results must be very similar.

The last point to notice here is that on the first 200 seconds records are not stabilized. Therefore results dependents on Signal Amplitude are starting after 200 seconds.

V.2.2.3 Correlation

Correlation is another of the outputs that ADV gives. This is an indicator of the relative consistency of the behaviour of the scatterers in the sampling volume during the sampling period. ADV's collect data at a higher sampling rate than the sampling reporting period, and the COR parameter indicates the consistency of the multiple measurements that take place within each sampling period. The value varies from 0 to 100.

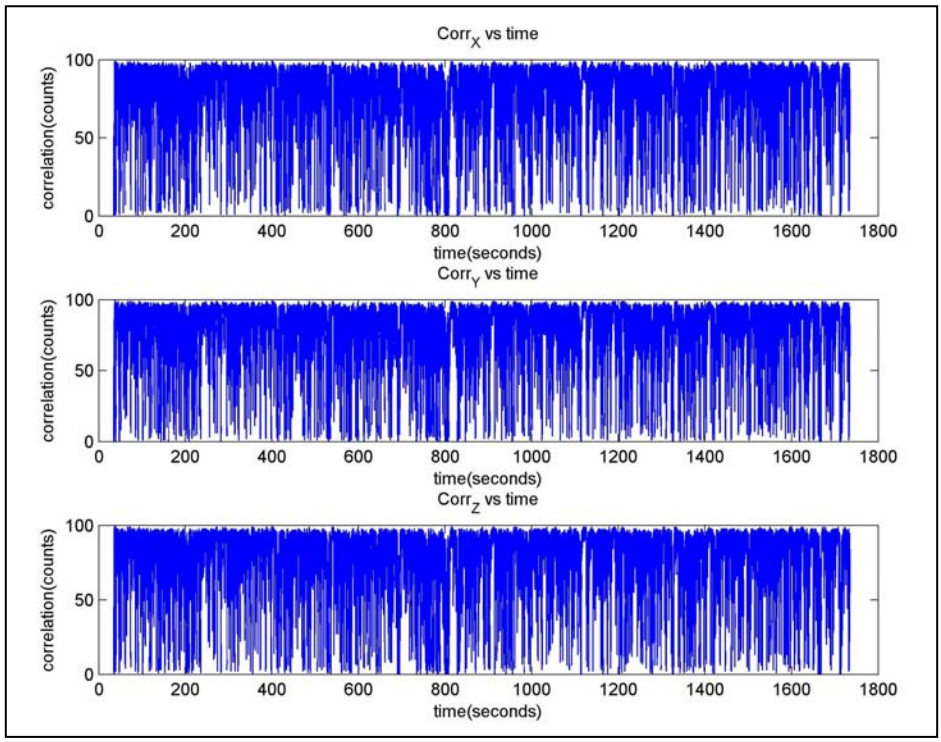

Figure 46: Correlation versus time for case 1

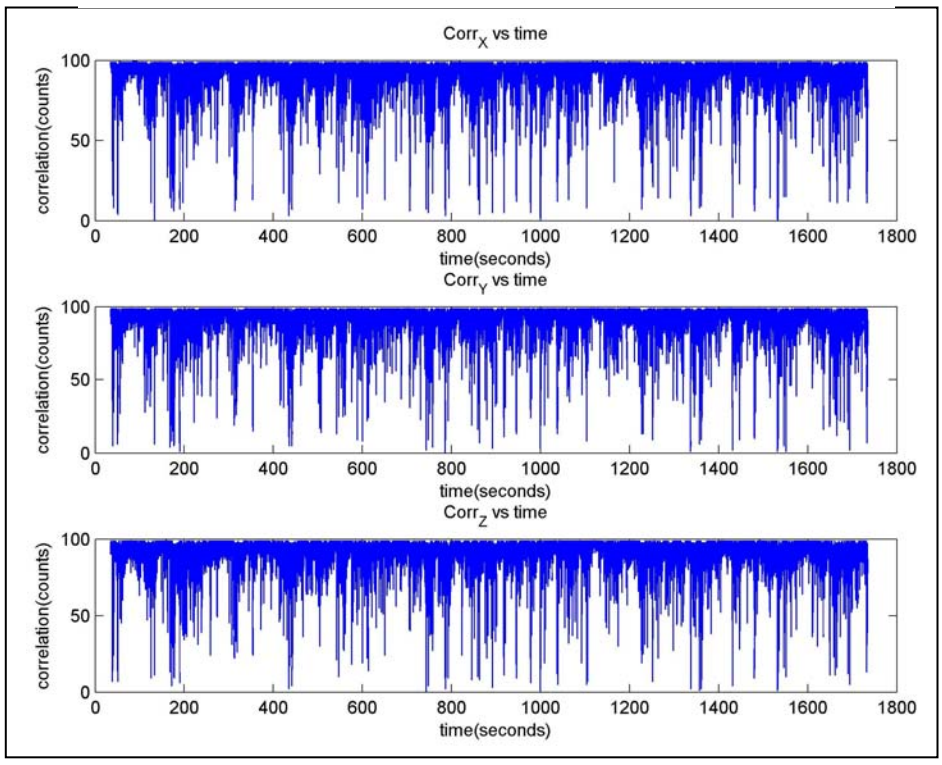

Figure 47: Correlation versus time for case 2

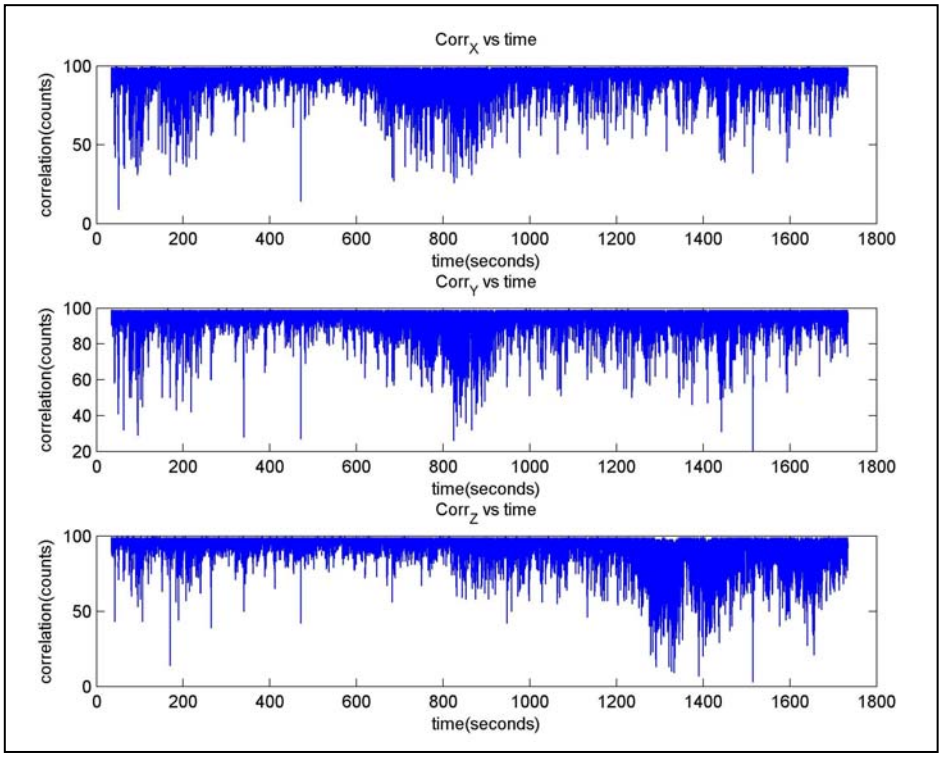

Figure 48: Correlation versus time for case 3

When one observes figures 46, 47 and 48 one can appreciate how correlation function is getting thinner as suspended sediment concentration decreases contrary to what happened with SNR and Signal amplitude.

Here one can found some spikes in case 3 where the distribution function is thinner. In case 1, where usually the spikes were one can not appreciate anything due to the wideness of the correlation function.

V.3 ADV versus OBS data correlation

As some authors have done before, this section shows an attempt to found a relation between ADV outputs and OBS outputs using different methods.

First of all a distinction between direct methods and indirect methods is needed, and later on, each method used is enumerated in its respective group.

V.3.1 Direct methods

V.3.1.1 Least squared method

In this section a least squared method is applied to the different ADV outputs. The section is composed in subsections of SNR, SA and correlation studies. In each of these subsections a distinction between the cases exposed in section V.2.1 is going to be made.

V.3.1.1.1 SSC versus SNR

As seen in section V.2.2.1, SNR revels a similar pattern in the three directions (x, y, z). Therefore and by simplicity here we work with just one direction.

When one plot suspended sediment concentration from the OBS versus SNR from the ADV obtains, for each of the cases mentioned before:

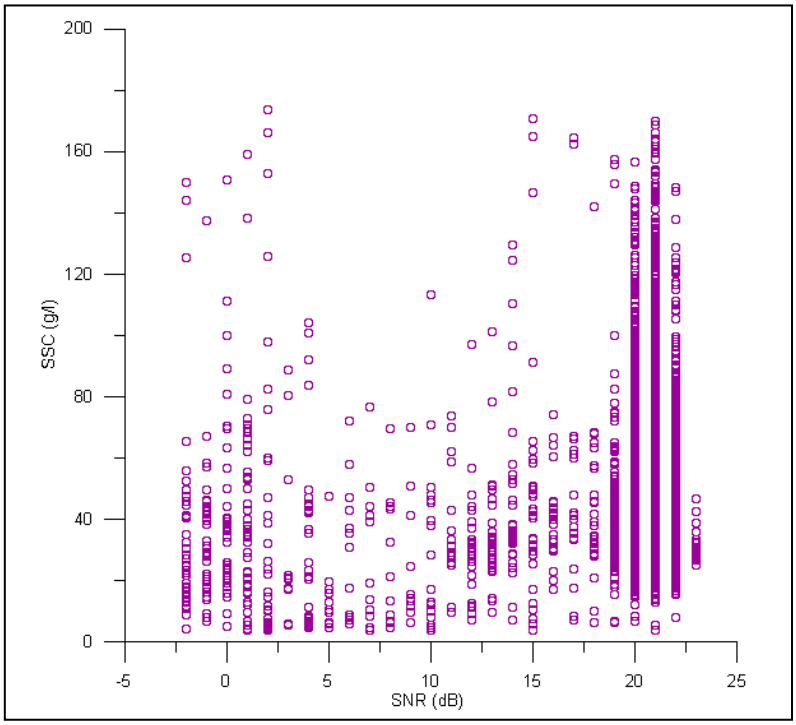

Figure 49: Concentration vs SNR in case 1

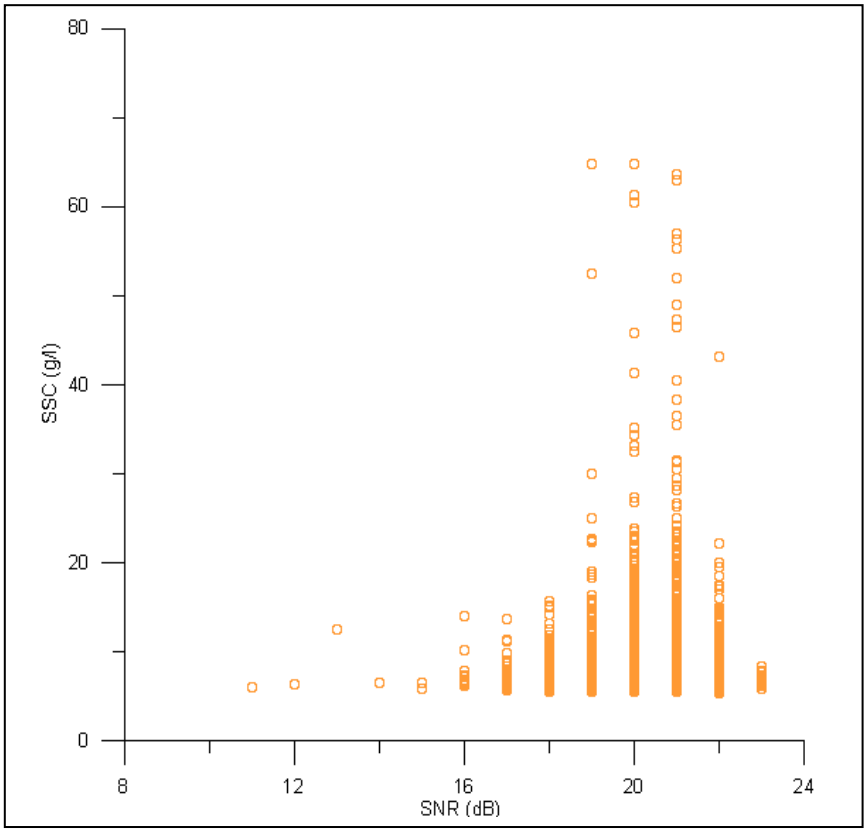

Figure 50: Concentration vs SNR in case 2

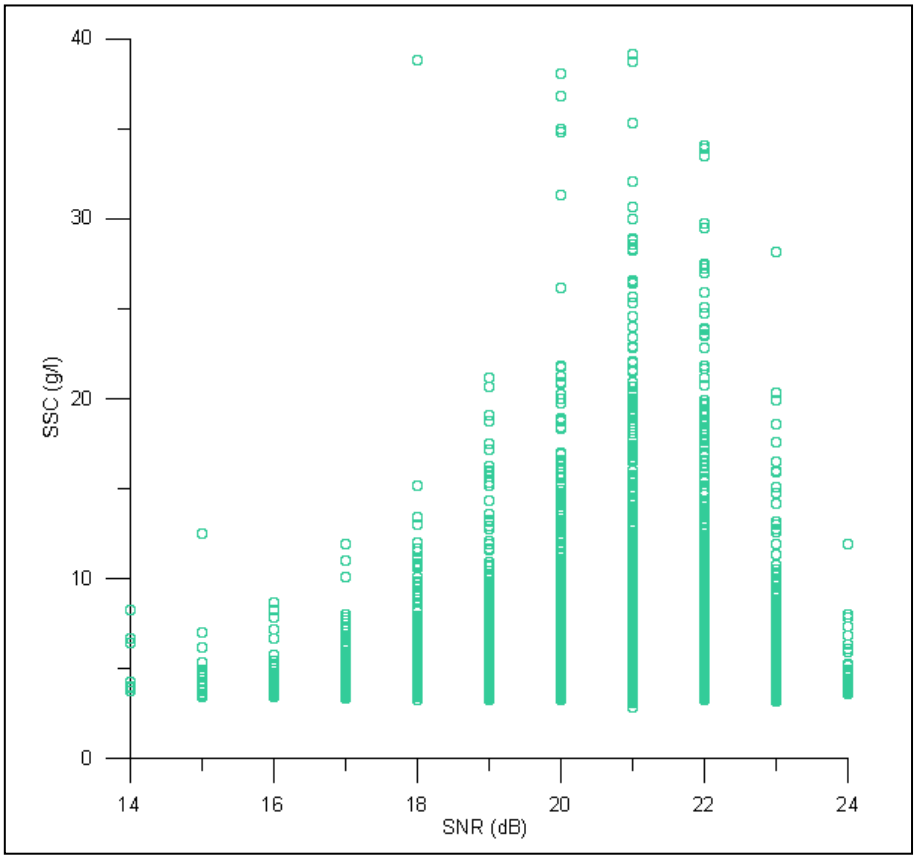

Figure 51: Concentration vs SNR in case 3

Paying attention at these figures one can see that there is no correlation between SNR and suspended sediment concentration.

Also one can notice that in all three cases the relation between concentration and SNR show the same behaviour (just straight lines).

If one focus on the SNR values can observe that in case 1, all SNR values are located between -5 dB and 25 dB, in case 2 SNR values are situated between 8 dB and 24 dB and in case 3 between 14 dB and 24 dB. Observing these rates one can notice that the SNR interval decreases as SSC decreases too. Therefore and according to Nortek the best cases to work with are case 2 and case 3, both cases of low concentration.

In figures 52, 53 and 54 a bubble plot has been used in order to know where is located the higher number of observations. Results show a major occurrence of observations between 20db to 22db in all cases, which in agreement with Nortek recommendations (1997), this happens when measuring instantaneous velocities and turbulence quantities which is the scope of our cases.

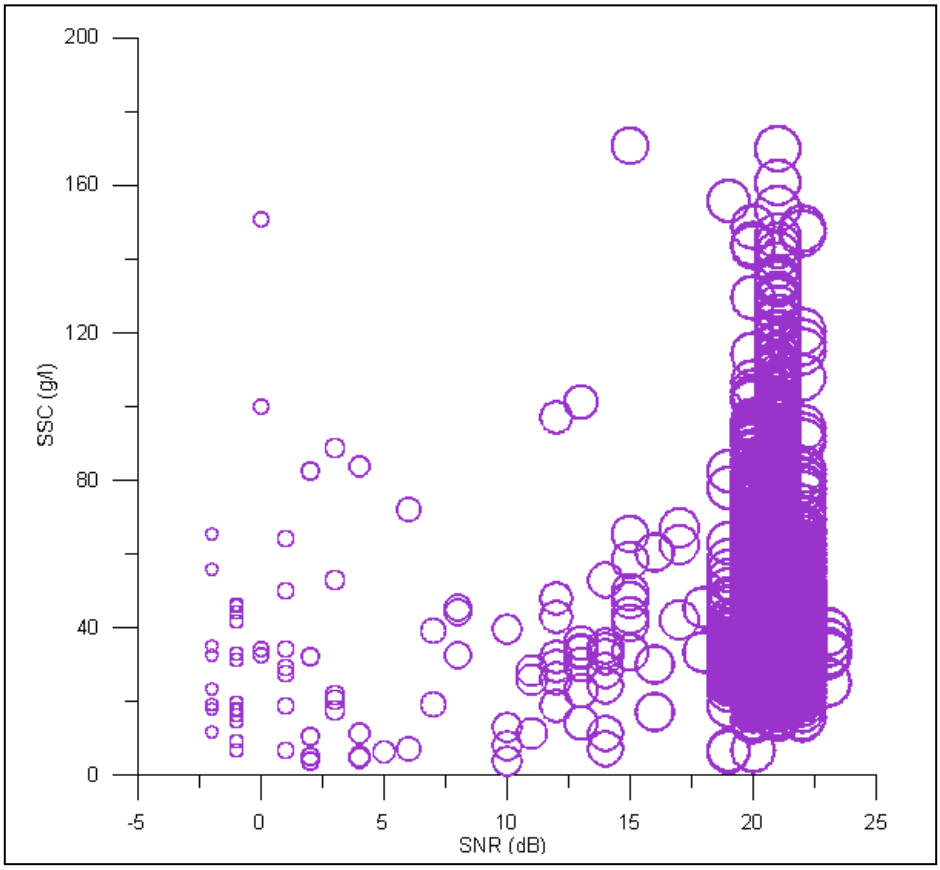

Figure 52: bubble plot for case 1

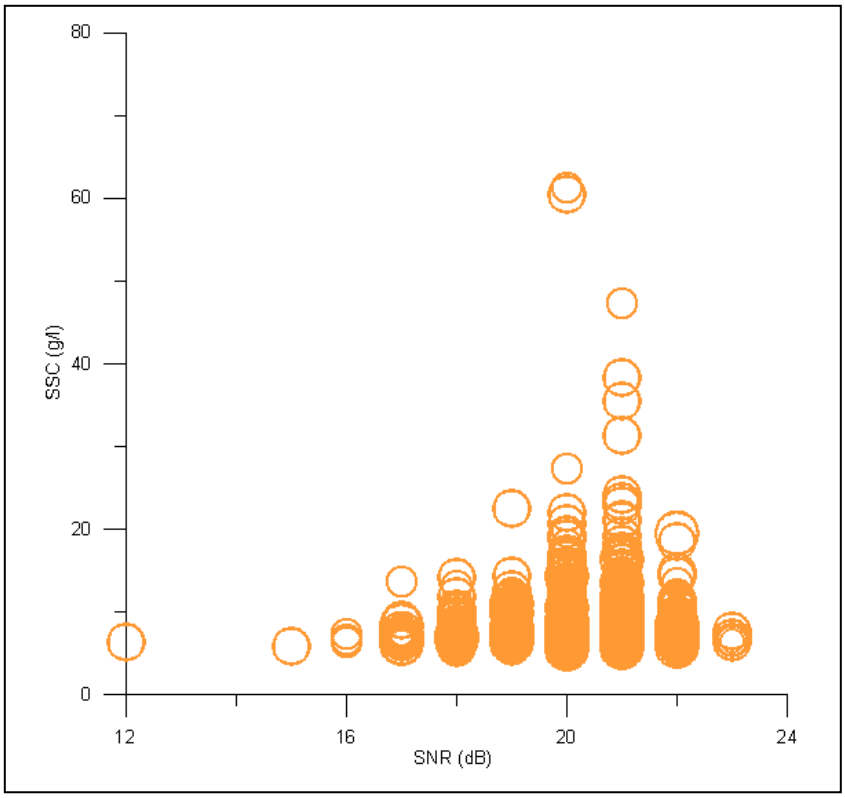

Figure 53: bubble plot for case 2

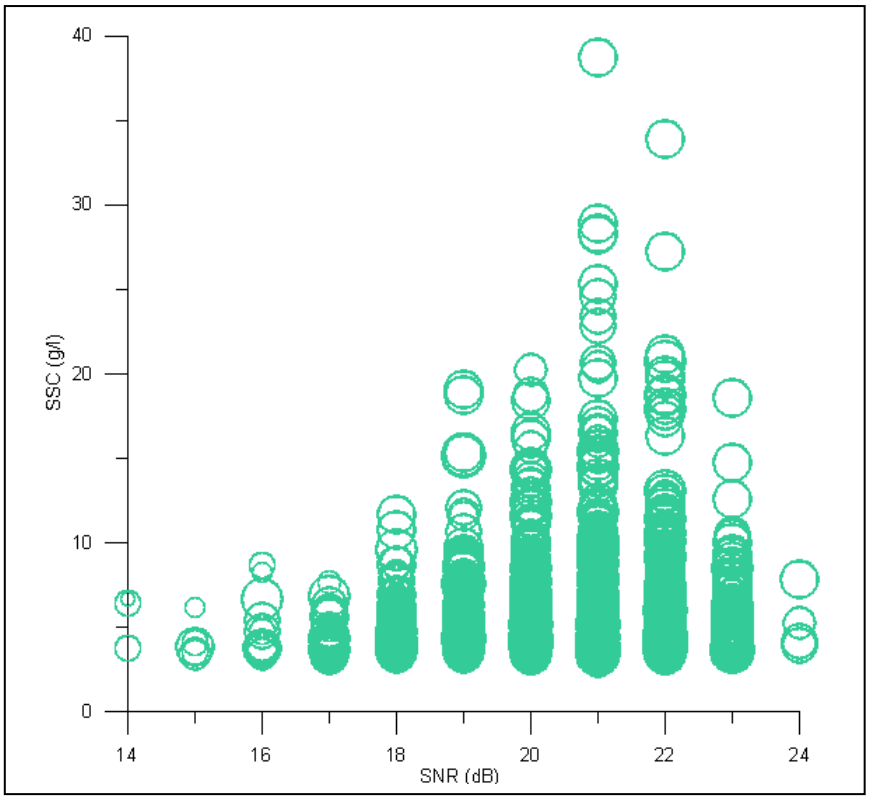

Figure 54: bubble plot for case 3

V.3.1.1.2 SSC versus Amplitude

An ADV system provides the signal amplitude as part of its output record. This is measured with the same frequency and in the same sampling volume as the velocities.

Remembering section V.2.2.2 and figures 43, 44 and 45 one has seen that signal amplitude distribution is similar in the three directions measured (x, y, z). Therefore, here a plot of suspended sediment concentration versus signal amplitude in one direction and for all three cases exposed before can be observed.

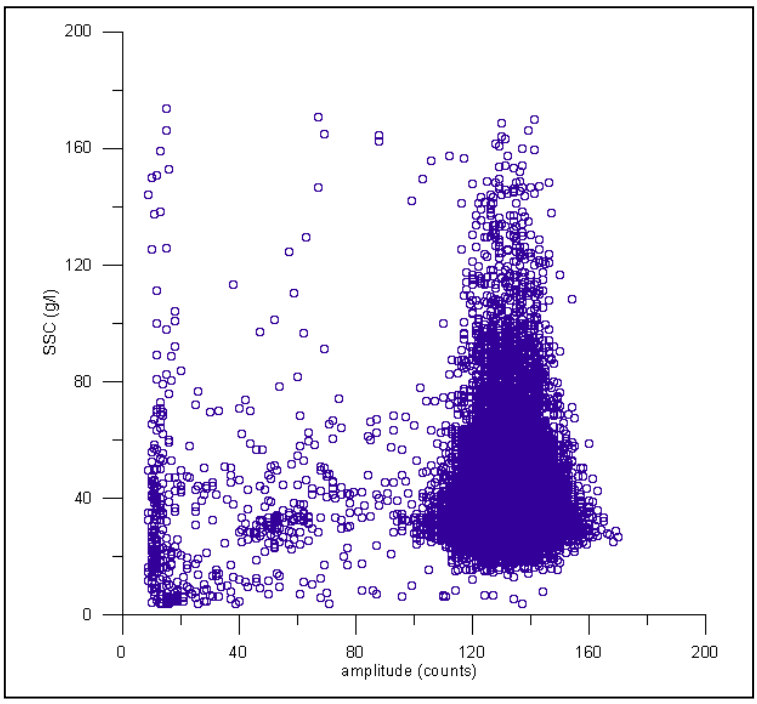

Figure 55: Concentration vs amplitude in case 1

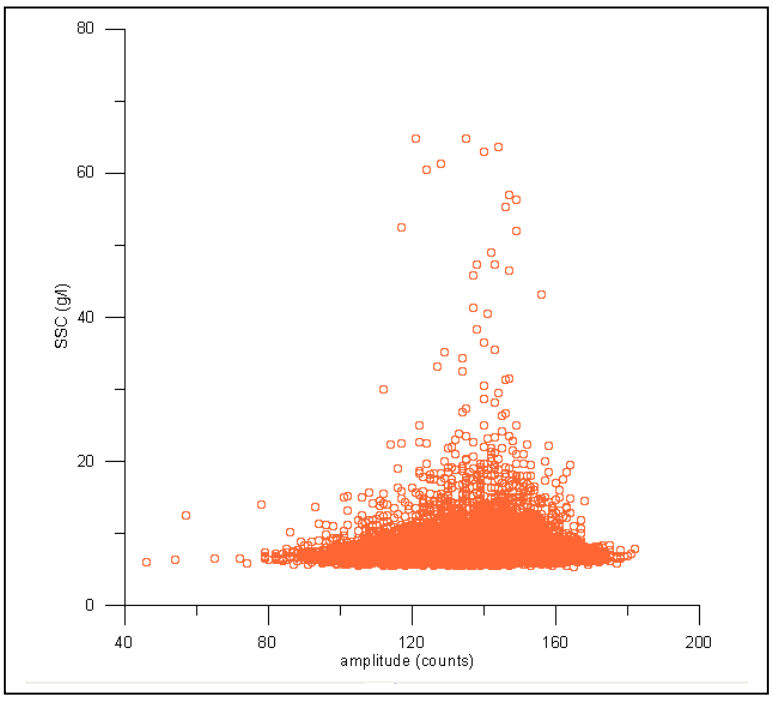

Figure 56: Concentration vs amplitude in case 2

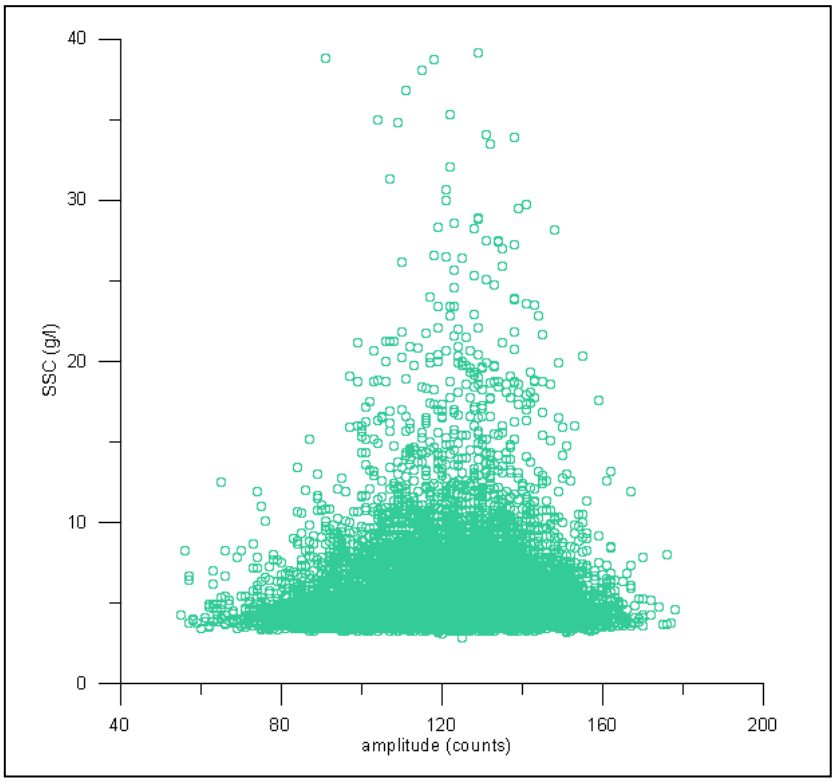

Figure 57: Concentration vs amplitude in case 3

First of all it is clear that these three graphs are very different.

In figure 55 one can observe that in low concentration of SSC (0- 10 g/l) amplitudes between 10 counts to 20 counts are mostly common. When SSC is in the order of 10 g/l to 150 g/l a wide range of amplitudes is present while at high concentrations (above 150 g/l) amplitudes of 10counts or from 120 to 140 counts are possible.

In contrast in figures 56 and 57 one can observe that at low concentrations (5 to 10 g/l) a wide range of amplitudes is present while when suspended sediment concentration reaches 30g/l to 40g/l this range is thinner (140 counts fro case 2 and 120 counts for case 3).

In fact a common effect in all cases is that when one tends to the maximum suspended sediment concentration in the case that is studied at that moment the amplitude range is thinner and tending around 130 counts always.

The last point to remark is that in cases 2 and 3 (low concentrations) the distribution of these amplitudes seems to follow a normal curve.

V.3.1.1.3 SSC versus *Correlation*

An ADV system provides the correlation as part of its output record. This is measured with the same frequency and in the same sampling volume as the velocities.

Going back to section V.2.2.3 and figures 46, 47 and 48, one can appreciate how correlation has the same distribution in all three measured directions (x, y, z). Therefore we just plot the concentration versus the correlation in one direction for all the three cases presented in section V.2.1.

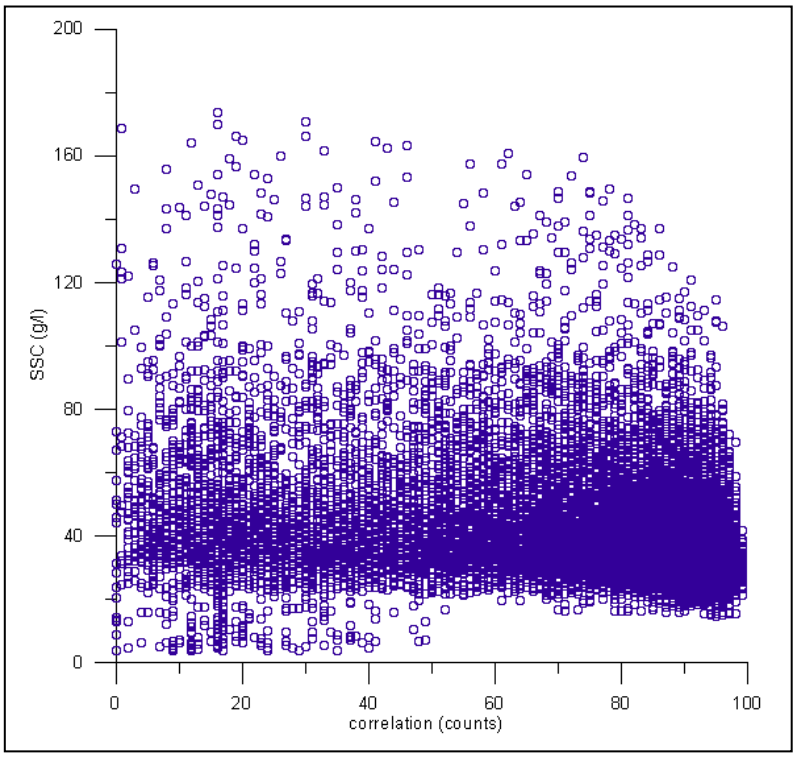

Figure 58: Concentration vs correlation in case 1

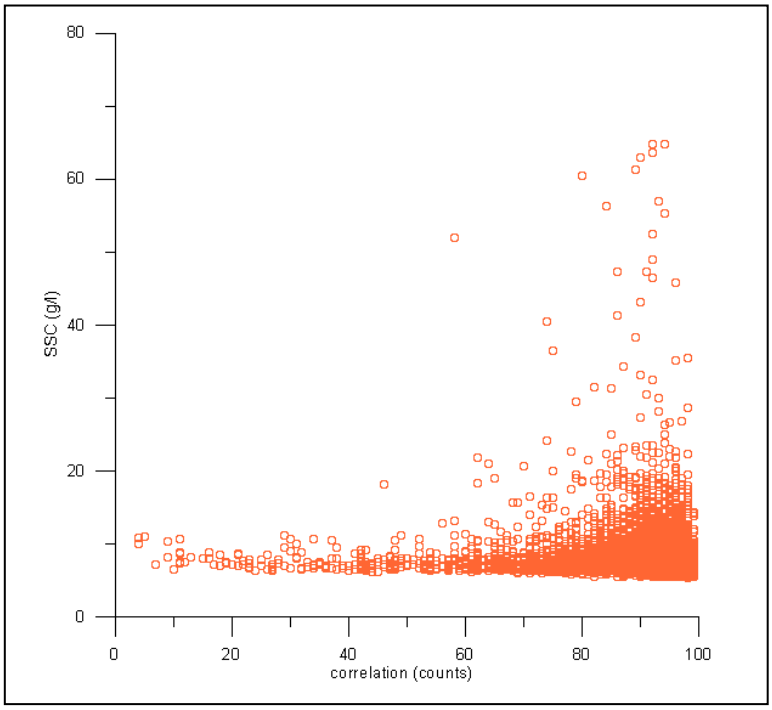

Figure 59: Concentration vs correlation in case 2

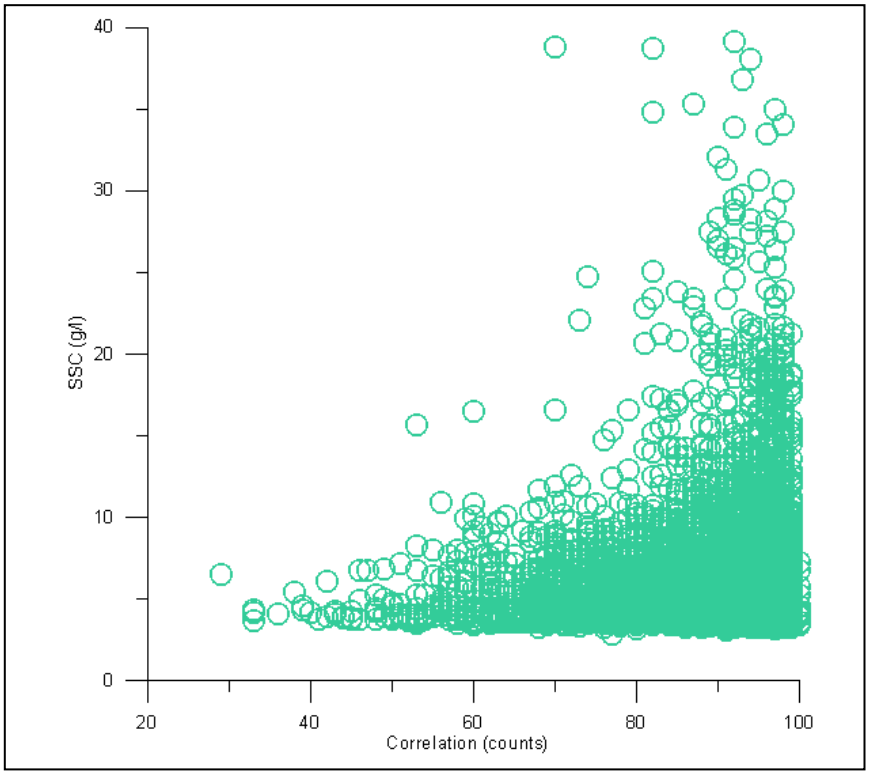

Figure 60: Concentration vs correlation in case 2

From figures 58, 59 and 60 one can expect no relation because the distribution is formed just for straight lines.

Also can be noticed that in case 1 (erosion wave conditions), a big cloud of points is distributed along all correlation values while in the other cases the amount of points is situated at maximum values of correlation (100 counts). Anyway, one can expect no relation.

V.3.1.2 Running average

In order to test a better fit a low pass filter has been applied to the time series with a time window of 50 inputs that corresponds to 1.25 seconds.

As it has been seen in section V.2.1 a differentiation between case 1, case 2 and case 3 is needed due to their different nature.

Also, as it was explained in section V.2.2.1, we are going to plot results only versus ADV outputs in one direction due to the similarity of the ADV outputs in all three directions.

V.3.1.2.1 SSC versus SNR

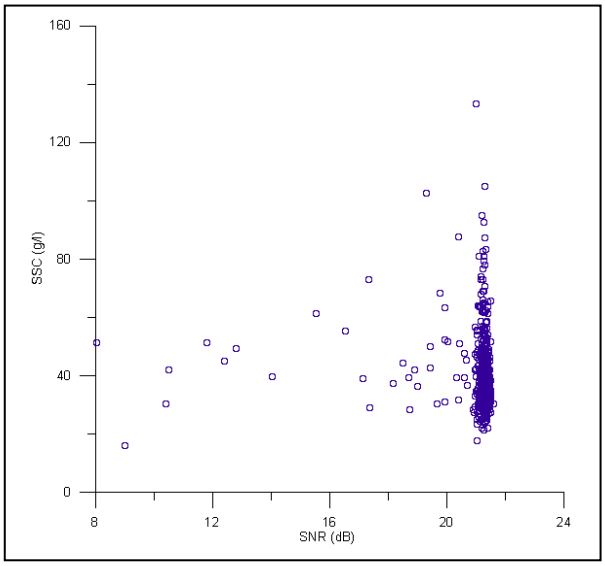

Figure 61: *SSC vs SNR in case 1*

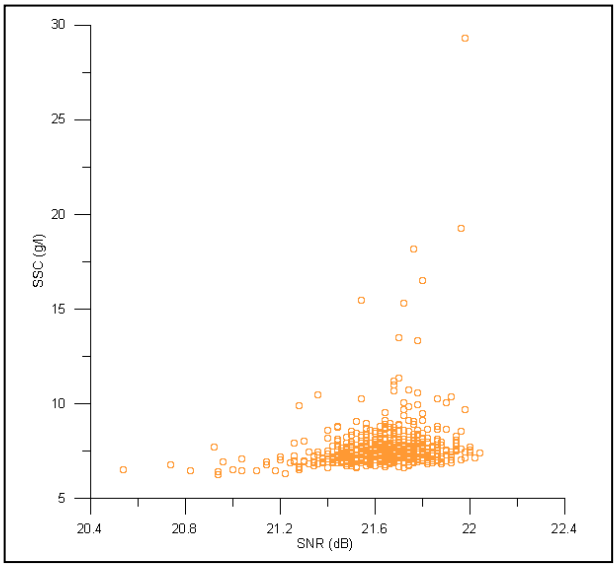

Figure 62: *SSC vs SNR in case 2*

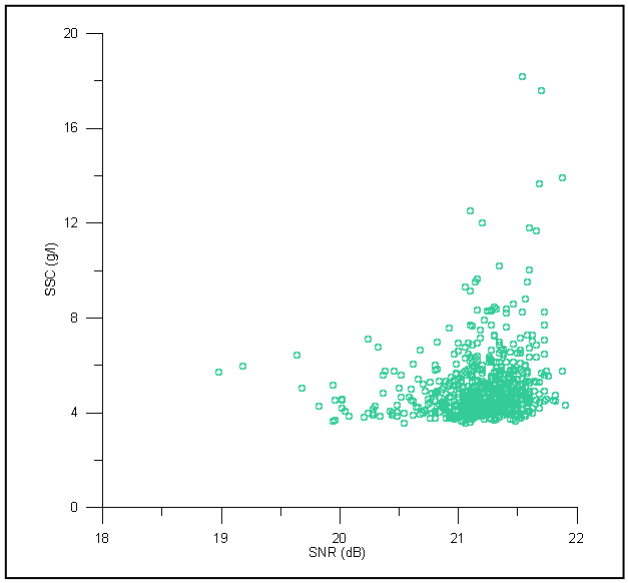

Figure 63: *SSC vs SNR in case 3*

Paying attention to figure 61, one can appreciate a thinner range of values of SNR (near 21.5 dB, too) while SSC is increasing. This causes a distribution like a vertical line where no relation can be expected.

On the other hand, one can see a similarity between case 2 and case 3. In these two cases the distribution presents a wide range of SNR values for low suspended sediment concentration values (5 g/l to 8 g/l). As concentration is increasing the value of SNR is tending to 21.5dB in both cases. Therefore one can think that a relation can be found.

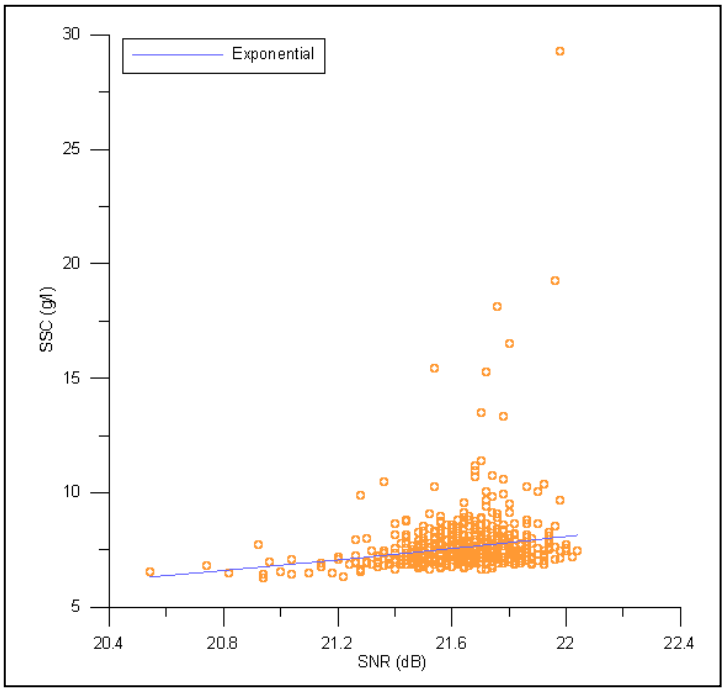

In figure 64 a plot of the relation between suspended sediment concentration and SNR can be observed. One can appreciate how an exponential fit is the best approximation; therefore it is drawn here. The respective equation is:

$$SSC = 0.193377 * e^{(0.16969*SNR)} \quad (28)$$

With a determination coefficient of:

$R^2 = 0.0585$

Figure 64: Relation between *SSC and SNR in case 2*

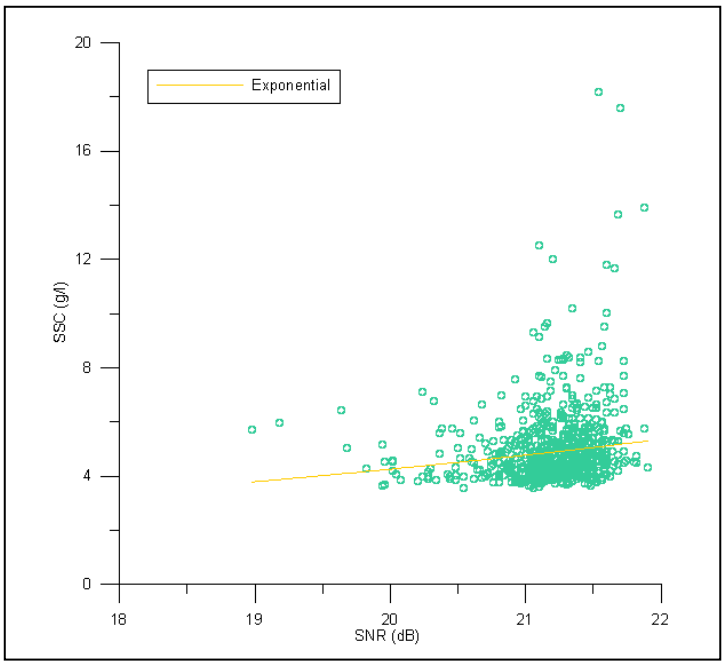

In figure 65 one can appreciate a big cloud of points between 20 dB and 21.5 dB. When one tries to find a relation inside this cloud can notice how the exponential fit is the best. Therefore this has been drawn to the distribution and the fitting equation is presented below:

$$SSC = 0.4285 * e^{(0.11484*SNR)} \quad (29)$$

The determination coefficient was:

$R^2 = 0.03157$

Figure 65: Relation between *SSC and SNR in case 3*

As one can appreciate differences between these two adjustments are present. One is the cloud of points that is denser in case 3 than in case 2, therefore a worst relation, as the determination coefficient shows, could be expected.

When one pay attention to the determination coefficients can appreciate that they are vey low so that indicates bad correlations.

However it can be noticed that compared to figures 50 and 51 here one can appreciate a small but not sufficient relation while in those figures no relation can be found (just straight lines).

V.3.1.2.2 SSC versus Amplitude

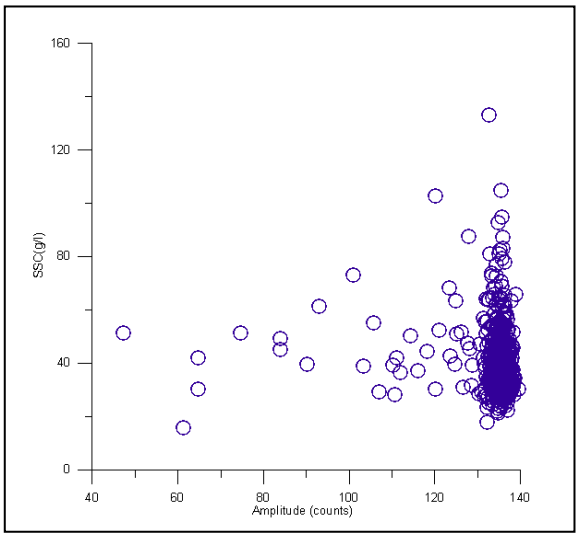

Figure 66: *SSC vs Amp in case 1*

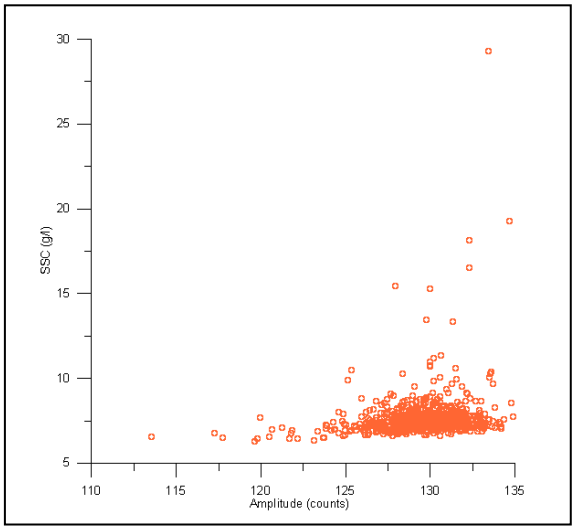

Figure 67: *SSC vs Amp in case 2*

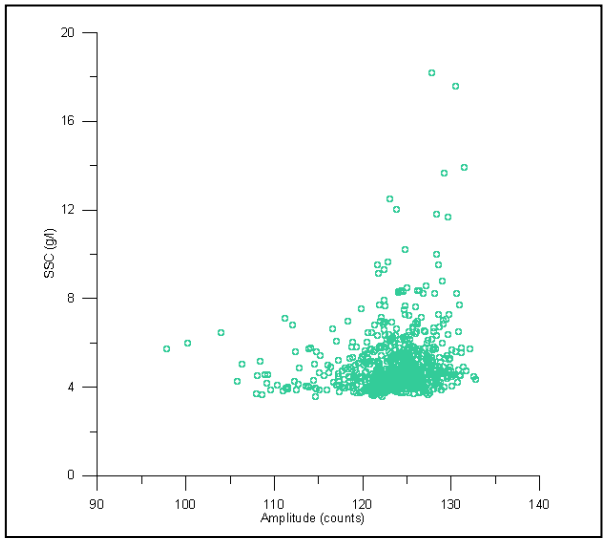

Figure 68: *SSC vs Amp in case 3*

Observing these figures one can notice that the behaviour of the distribution between suspended sediment concentration and amplitude is similar to the distribution behaviour between suspended sediment concentration and SNR.

Here one also can appreciate that figure 66 show a vertical line of data which indicates that a long amount of SSC values have the same amplitude value. In that case no relation between the two outputs can be found.

Even though one can notice that figure 67 and 68 show a small relation between outputs, just the case of figure 67 is going to be studied because, as has been seen before with SNR, the cloud of points is less denser in case 2 than in case 3 that implies a better relation between outputs.

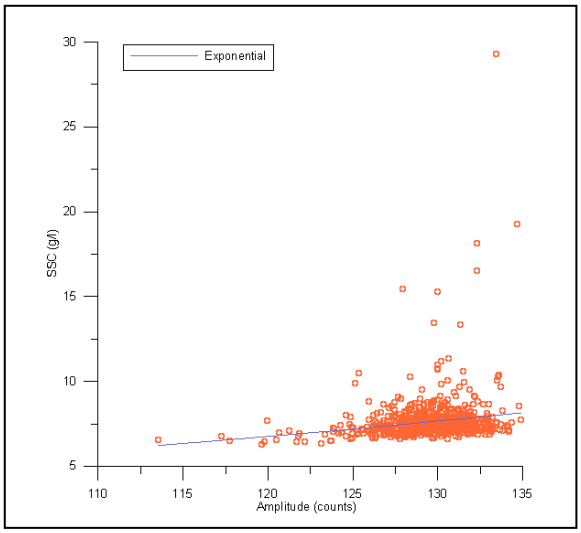

Figure 69: Relation between *SSC and amplitude in case 2*

As can be seen in figure 69 we have drawn an exponential fit to the distribution. This kind of fit has been chosen because it has been the best one that adjusts the distribution. The fitting equation is:

$$SSC = 1.4886 * e^{(0.0126011*Amplitude)} \quad (30)$$

With a determination coefficient of:

$$R^2 = 0.0659$$

Although this is not a very high determination coefficient and doesn't indicate a good correlation, one has to notice that is the best determination coefficient, and therefore fitting, found until this moment.

Furthermore one should notice that compared to figure 56, where no relation was possible, here at least we found a small relation. That indicates that running average is smoothing our data but not enough to get reliable relations.

V.3.1.2.3 SSC versus correlation

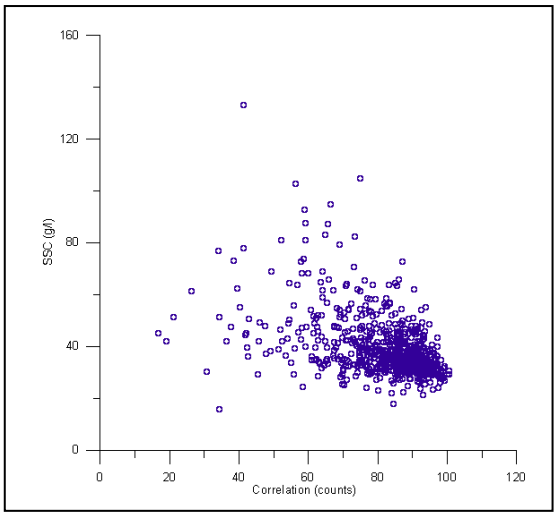

Figure 70: *SSC vs Correlation in case 1*

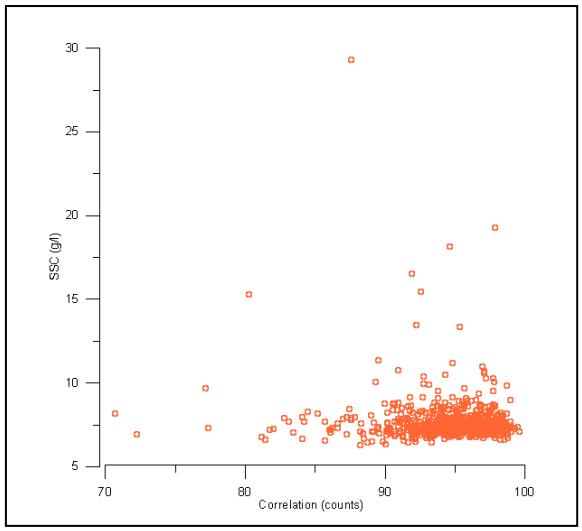

Figure 71: *SSC vs Correlation in case 2*

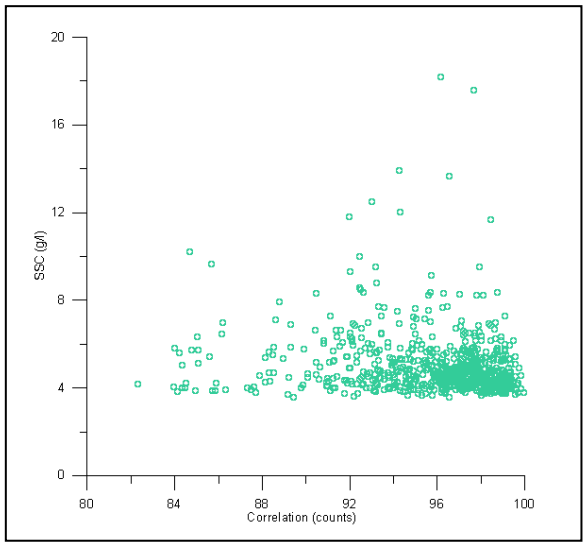

Figure 72: *SSC vs Correlation in case 3*

Back to figures 46, 47 and 48 where correlation was plotted versus time, one had noticed that as suspended sediment concentration was lowering the distribution function was getting thinner contrary what was happening with the two other outputs (SNR and amplitude).

Due to this effect here we notice that in case 1 is where the best fitting can be found while in case 2 and 3 the fittings are worst.

Moreover has to be remarked that in SNR and amplitude the best fit was for case 2 whereas here case 2 has the worst fit. So that case 2 is not going to be exposed here.

Below, in figures 73 and 74, one can appreciate the fittings for case 1 and case 3 with their expression and determination coefficients.

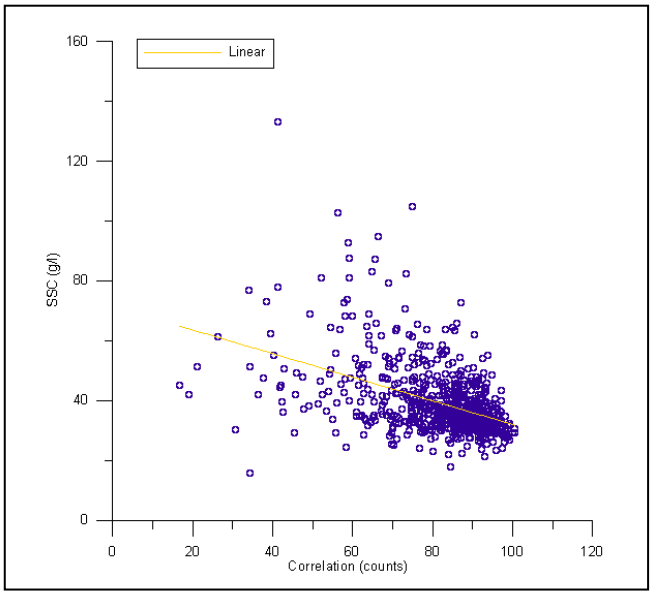

Figure 73: Relation between *SSC and Correlation in case 1*

In figure 73 it can be noticed that in the order of 60 counts to 100 counts, one can found a big cloud of points where a small linear relation can be made. Out of that just some points that we can not consider as representative can bee seen.

The linear equation is:

SSC= -0.3941* corr + 71.4619 (31)

And its determination coefficient:

R^2= 0.2

Although it is the higher determination coefficient found until now we can not take the adjustment as a reliable fit.

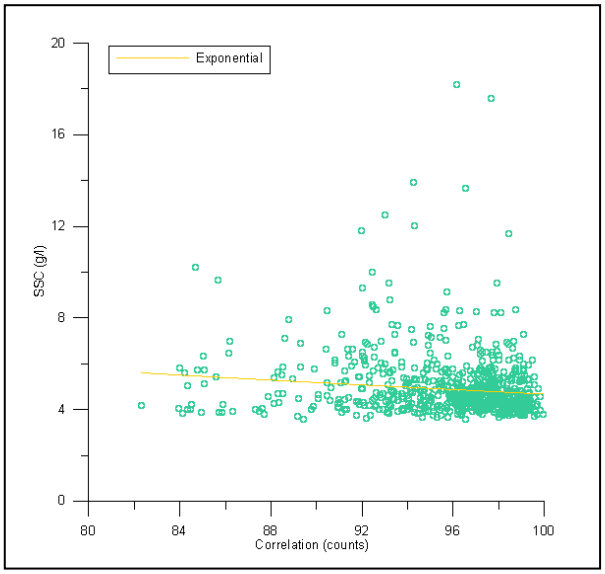

Figure 74: Relation between *SSC and Correlation in case 3*

In figure 74 a vast cloud of points can be observed in which one can appreciate that a value of concentration of 4 g/l corresponds to more than one correlation value.

Nevertheless when it was tried to fit it was found that the exponential adjustment is the better fitter. Its equation is:

$$SSC = 13.1915 * e^{(-0.01038*Correlation)} \quad (32)$$

With a determination coefficient of:

$$R^2 = 0.0236$$

As was expected the determination coefficient is lower in case 3 than in case 1.

Even though has to be remarked that both fittings have a negative slope which means that when suspended sediment concentration decreases correlation increases. In fact that can be expected because correlation is an indicator of the relative consistency of the multiple measurements that take place within each sampling period.

Besides this comparing this results to the ones obtained with least squared method one can observe that here a relation can be found while before was impossible to make a data relation.

V.3.2 Indirect methods

After applying some direct methods and achieving no reliable result some indirect methods are used in this section in order to try to improve the results obtained before.

The goal of this section is to try to found a useful method to obtain SSC from ADV outputs when these are near high concentration rates.

Some studies have been carried out with the finality to obtain a formulae or relation between SSC from ADCP, OBS, LISST, etc. and ADV outputs as well. Despite most of these studies where made in rivers or flumes and therefore they were working with low SSC, good results were obtained so that these methods are going to be the bases of our different applied methodologies.

V.3.2.1 Weighted least squared method

To start looking for a indirect correlation a weighted least squared method is applied. In that the matrix of dependence [Y] is formed by SSC data obtained from OBS and the matrix of independent coefficients [X] is composed for the data of the different outputs from the ADV.

$$[Y]=b*[X] \quad (16)$$

Where b is the vector where the weights of the difference variables composing X matrix (independent data) are stored.

V.3.2.1.1 Weighted least squared method with all outputs

One of the goals of this part is to observe how important the contribution of each output in the concentration relation is. The second main point is to try to get a relation between ADV outputs and OBS concentration.

As it has been seen in the last section one has to work separately in three cases: erosion waves- beginning (case 1), erosion waves-ending (case 2) and accretion waves (case 3).

Processing this data, vector b, the vector of the different weights in each case shows:

Output	Case 1 → Weight	Case 2 → Weight	Case 3 → Weight
SNR X	1.6571	0.2039	0.1954
SNR Y	1.4300	0.2367	0.1586
SNR Z	-1.4334	0.2156	0.1829
Amp X	-0.0236	-0.0092	-0.0091
Amp Y	0.0043	-0.0127	0.0003
Amp Z	0.1858	-0.0090	-0.0115
Corr X	-0.1037	-0.0023	-0.0083
Corr Y	-0.0533	-0.0048	-0.0350
Corr Z	-0.0991	-0.0138	0.0042

Table 2: Relation of weight coefficients in each study case

As one can observe the most important weight, in all three cases, is for SNR. Also one can observe that this weight is less important as the suspended sediment concentration is decreasing.

Therefore if we calculate the concentration with these outputs and these weights we obtain:

CASE 1: *ADV concentration= 1.6571*SNRX +1.4300*SNRY -1.4334*SNRZ - 0.0236*AmpX +0.0043*AmpY +0.1858*AmpZ -0.1037*CorrX -0.0533*CorrY - 0.0991*CorrZ* (17)

CASE 2*: ADV concentration= 0.2039*SNRX +0.2367*SNRY +0.2156*SNRZ - 0.0092*AmpX -0.0127*AmpY -0.0009*AmpZ -0.0023*CorrX -0.0048*CorrY - 0.0138*CorrZ* (20)

CASE 3*: ADV concentration= 0.1954*SNRX +0.1586*SNRY +0.1829*SNRZ - 0.0091*AmpX +0.0003*AmpY -0.0115*AmpZ -0.0083*CorrX -0.0350*CorrY +0.0042*CorrZ*

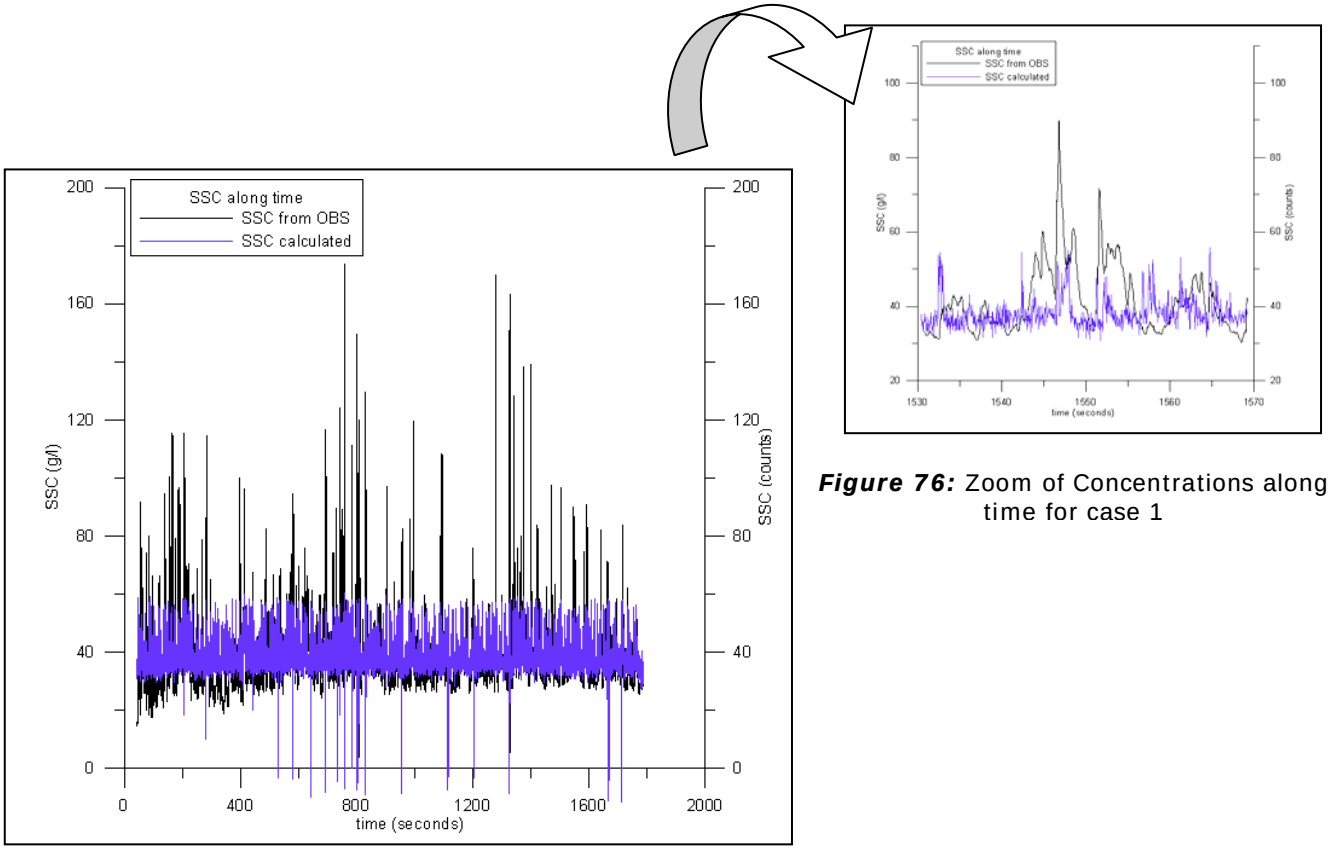

Figure 75: Concentrations along time for case 1

Figure 76: Zoom of Concentrations along time for case 1

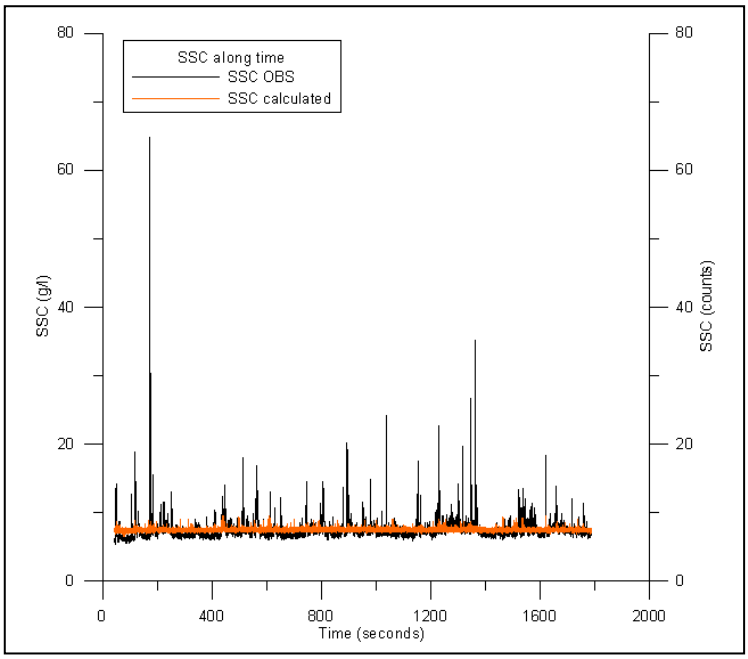

Figure 77: Concentrations along time for case 2

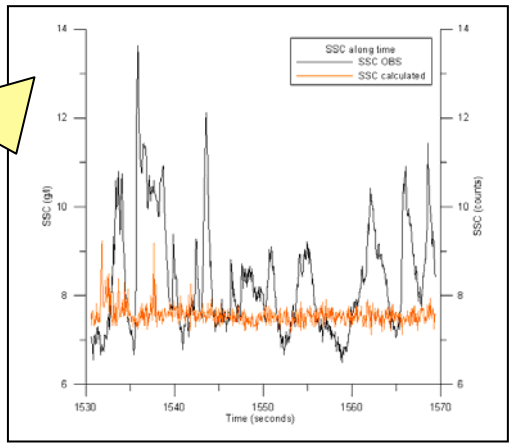

Figure 78: Zoom of Concentrations along time for case 2

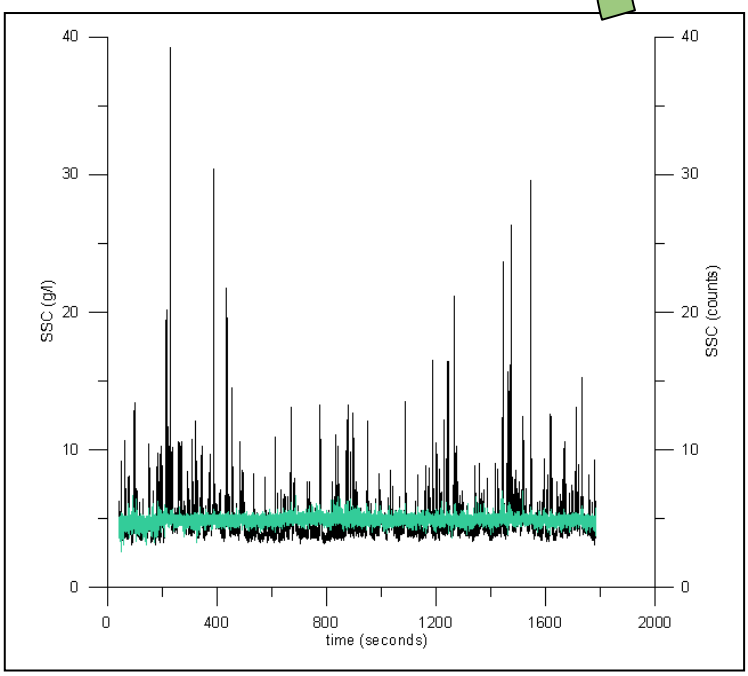

Figure 79: Concentrations along time for case 3

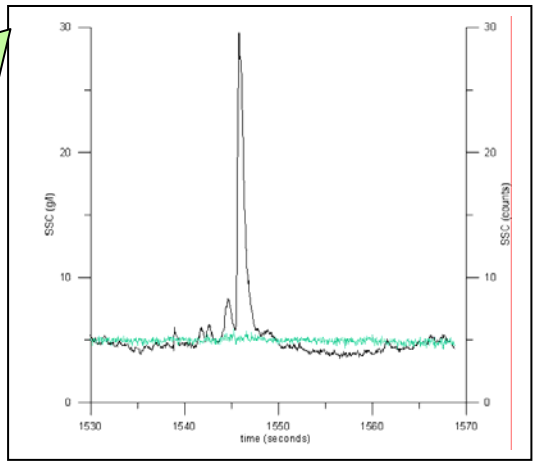

Figure 80: Zoom of Concentrations along time for case 3

As these figures show as lower the concentration the fitting gets worst. For instance, if one pays attention to figure 75 we can appreciate that the approximation is fitting the concentration in most of the points except in the peaks. Figure 76 agrees with figure 75 although in this later one some doubts about the approximation are appearing.

As one lows the concentration the fitting gets worst as figures 77, 78, 79 and 80 shows. In figure 78 we still can notice that calculated concentration follow the peaks with some differences but in figure 80 no relation can be found.

To corroborate this, a plot of relation between SSC from OBS and SSC calculated is shown below. Here just case 1 and case 2 are plotted because from figure 80 one can appreciate that no relation can be found in case 3.

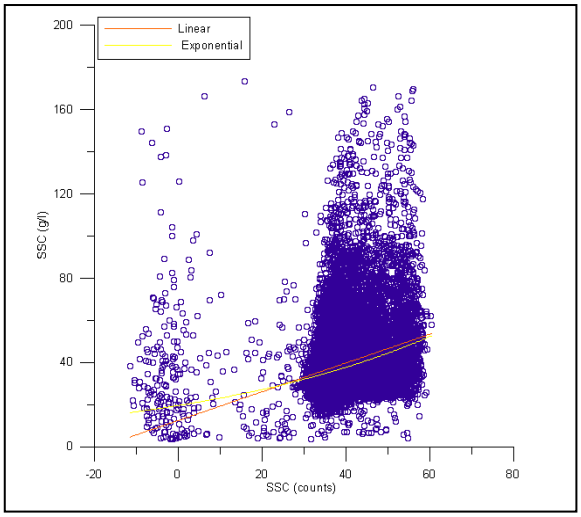

Figure 81: SSC real versus SSC calculated in case 1

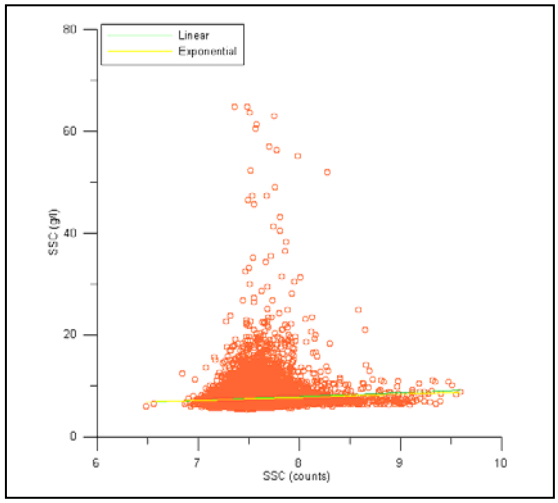

Figure 82: SSC real versus SSC calculated in case 2

In figure 81 one can see two lines trying to adjust the concentrations.

The orange adjust is a lineal fitting with equation:
SSC OBS= 0.7398*SSC all outputs + 10.519 with R^2= 0.0818 (33)

The yellow adjust is an exponential fitting with equation:
SSC OBS= $16.624*e^{0.0206*SSC\ all\ outputs}$ with R^2=0.1277 (34)

On figure 82 one can also see two fittings:

The green adjust is a lineal fitting with equation:
SSC OBS= 0.8146*SSC all outputs + 1.3733 with R^2= 0.0068 (35)

The yellow adjust is an exponential fitting with equation:
SSC OBS= $3.9344*e^{0.0837*SSC\ all\ outputs}$ with R^2=0.0103 (36)

As the determination coefficients show the better adjustment is the exponential fitting in case 1. But this is not enough closer to R^2=0.9 to confirm a reliable relation. Also one can notice that in case 2 the determination coefficients are very low meaning that no fit is going to work as we can deduce from figure 78.

Although results indicate a non sensitive dependence between signals these results are extended to obtain a weight for the full outputs obtained.

V.3.2.1.2 Weighted least squared method with SNR

Applying LS method with SNR implies that the dependence matrix Y is composed by SSC data from OBS and the independence matrix X is compose with SNR components (SNR_X, SNR_Y, SNR_Z).

As it has been seen in the last section one has to work separately in three cases: erosion waves- beginning (case 1), erosion waves-ending (case 2) and accretion waves (case 3).

Processing this data, vector b, the vector of the different weights in each case shows:

Output	Case 1 → Weight	Case 2 → Weight	Case 3 → Weight
SNR X	0.9923	0.1007	0.0759
SNR Y	1.0828	0.1252	0.1159
SNR Z	-0.2964	0.1313	0.0456

Table 3: Relation of weight coefficients in each study case

As one can observe the most important weight is for SNR Y in all the cases. Notice also, that the weight of SNR is lowering its value as SSC is lowering too.

Therefore if we calculate the concentration with these outputs and these weights we obtain:

CASE 1: *ADV concentration= 0.9923*SNRX +1.0828*SNRY -0.2964*SNRZ* (37)

CASE 2: *ADV concentration= 0.1007*SNRX +0.1252*SNRY +0.1313*SNRZ* (38)

CASE 3: *ADV concentration= 0.0759*SNRX +0.1159*SNRY -0.0456*SNRZ* (39)

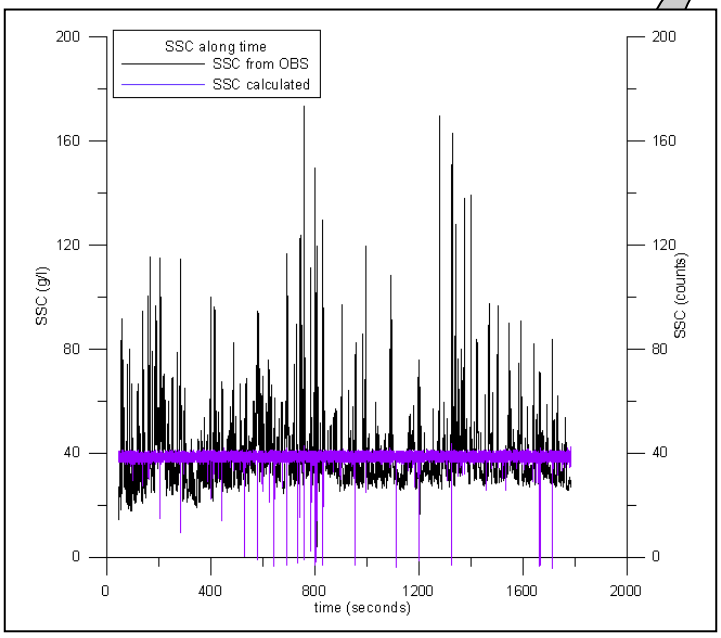

Figure 83: Concentrations along time for case 1

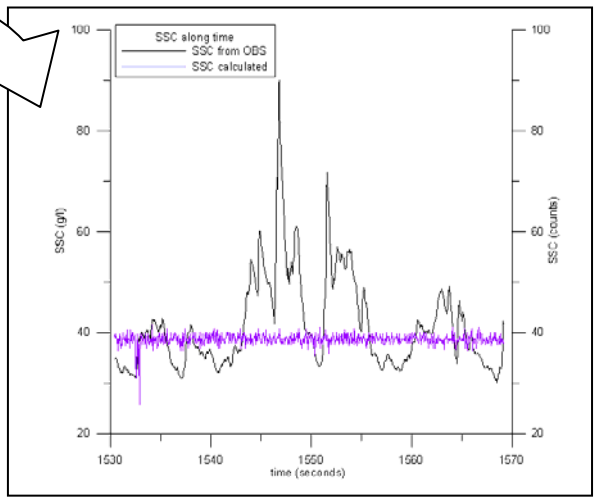

Figure 84: Zoom of Concentrations along time for case 1

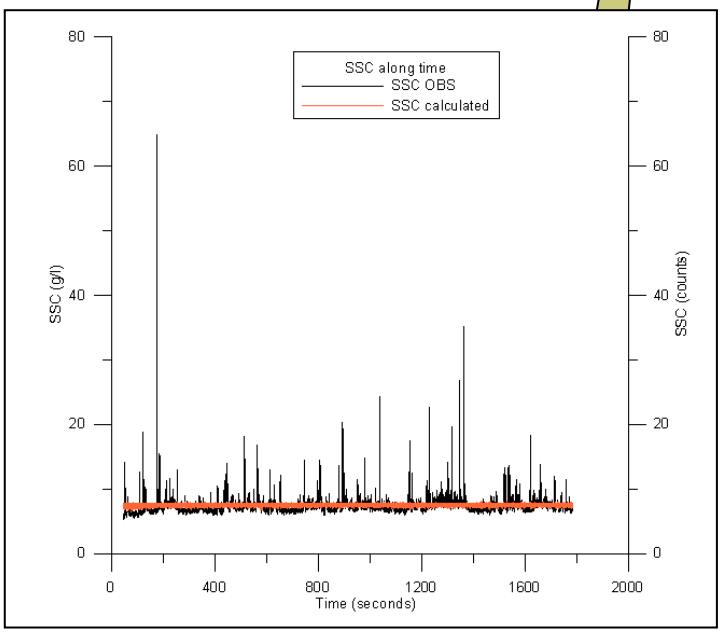

Figure 85: Concentrations along time for case 2

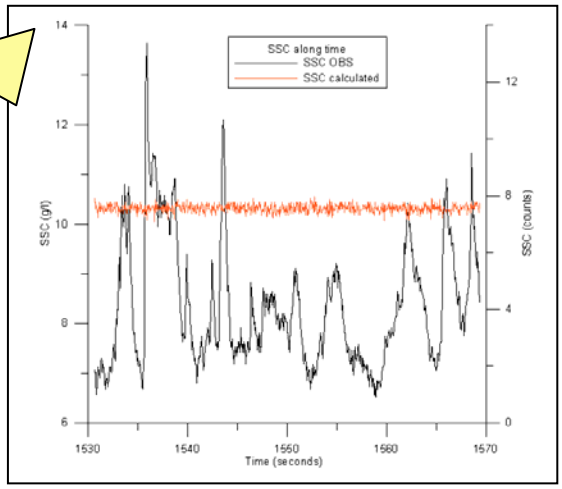

Figure 86: Zoom of Concentrations along time for case 2

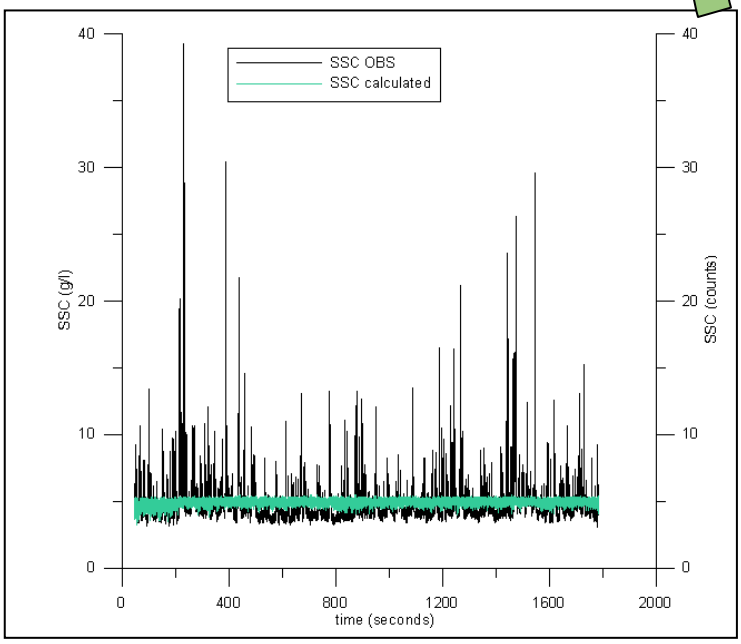

Figure 87: Concentrations along time for case 3

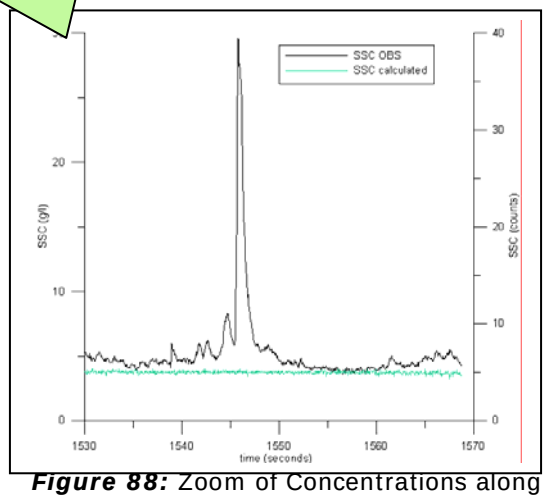

Figure 88: Zoom of Concentrations along time for case 2

Observing these figures one can appreciate that the fittings are not adjusting in a good way the distributions. ADV concentration calculated seems to not adjust in a good way the real concentration. ADV calculated has a very oscillating behaviour and in the peaks and downs is not adjusting well.

However one should notice how calculated suspended sediment concentration varies in dependence on the case. For instance, in case 1 SSC calculated is around 40counts along the time, in case 2 around 8counts whereas in case 3 is around 5counts. This indicates that some relation exists although not fitting correctly.

Anyway if one want to demonstrate it has to calculate the better fittings in case 1 and 2. Here case 3 was skipped because as figure 88 shows there is no way we can fit it.

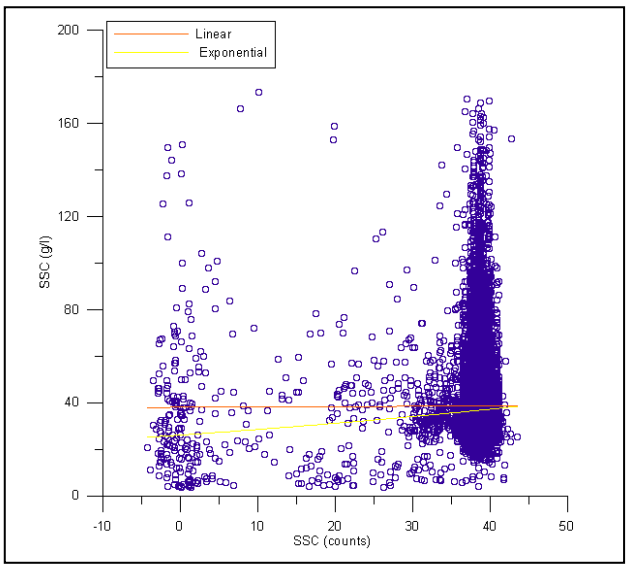

Figure 89: SSC real versus SSC calculated in case 1

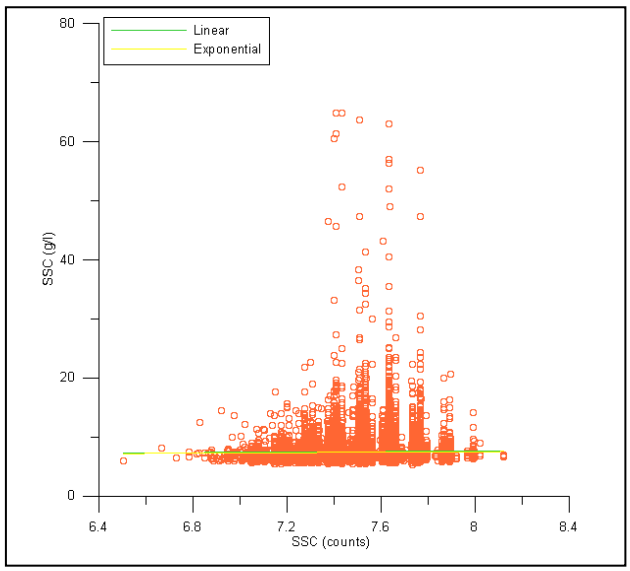

Figure 90: SSC real versus SSC calculated in case 2

In figure 89 one can see two lines trying to adjust these outputs.

The orange adjust is a lineal line with equation:
SSC OBS= 0.1254*SSC all outputs + 34.147 with R^2= 0.0008 (40)

The yellow adjust is a exponential tendency line with equation:
SSC OBS= $17.226*e^{0.0198*SSC\ all\ outputs}$ with R^2=0.0379 (41)

In figure 90 one can see three lines trying to adjust these outputs.

The green adjust is a lineal line with equation:
SSC OBS= 0.3429*SSC all outputs + 4.9328 with R^2= 0.0008 (42)

The yellow adjust is a exponential tendency line with equation:
SSC OBS= $5.2285*e^{0.0461*SSC\ all\ outputs}$ with R^2=0.0020 (43)

Paying attention to the determination coefficients one can conclude that all of them are very low. The best fit here is the exponential fit for case one as before, but now so far away from the adjustment with all outputs. Therefore one can not approve any of these fittings as reliable results to apply.

V.3.2.1.3 Weighted least squared method with Signal Amplitude

Applying LS method with amplitude implies that the dependence matrix Y is composed by SSC data from OBS and the independence matrix X is compose with amplitude components (AMP_X, AMP_Y, AMP_Z).

As it has been seen in the last section one has to work separately in three cases: erosion waves- beginning (case 1), erosion waves-ending (case 2) and accretion waves (case 3).

Processing this data, vector b, the vector of the different weights in each case show:

Output	Case 1 → Weight	Case 2 → Weight	Case 3 → Weight
AMP X	0.0956	0.0130	0.0137
AMP Y	0.1311	0.0207	0.0165
AMP Z	0.0571	0.0200	0.0097

Table 4: Relation of weight coefficients in each study case

As one can observe the most important weight is for AMP Y in all the cases. Notice also, that the weight of Signal Amplitude is lowering its value as SSC is lowering too.

Therefore if we calculate the concentration with these outputs and these weights we obtain:

CASE 1: *ADV concentration= 0.0956*AMPX +0.1311*AMPY +0.0571*AMPZ* (44)

CASE 2: *ADV concentration= 0.0130*AMPX +0.0207*AMPY +0.0200*AMPZ* (45)

CASE 3: ADV concentration= *0.0137*AMPX +0.0165*AMPY +0.0097*AMPZ* (46)

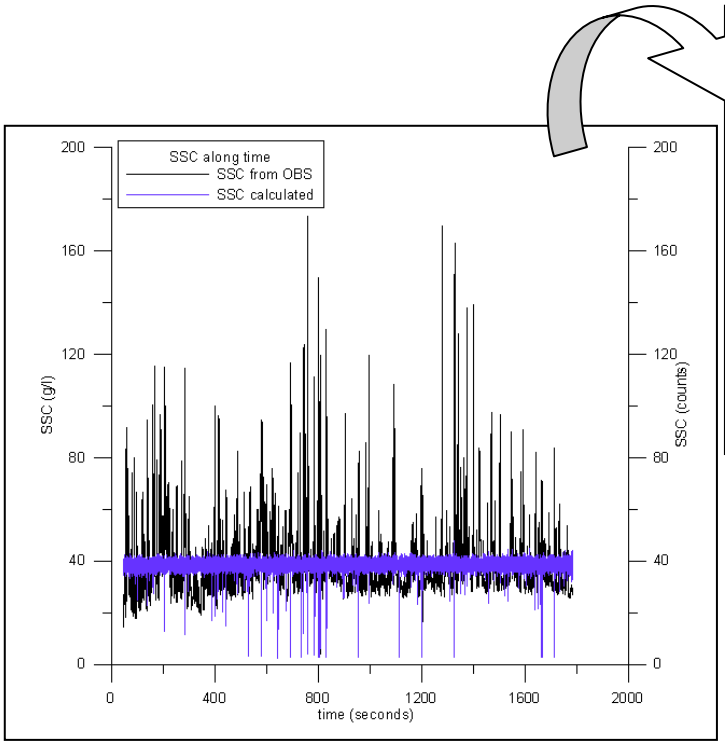

Figure 91: Concentrations along time for case 1

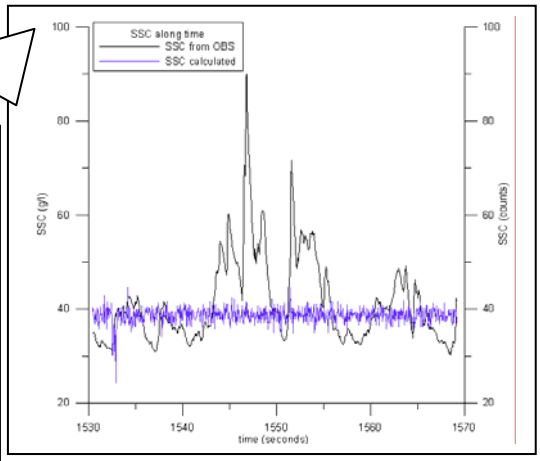

Figure 92: Zoom of Concentrations along time for case 1

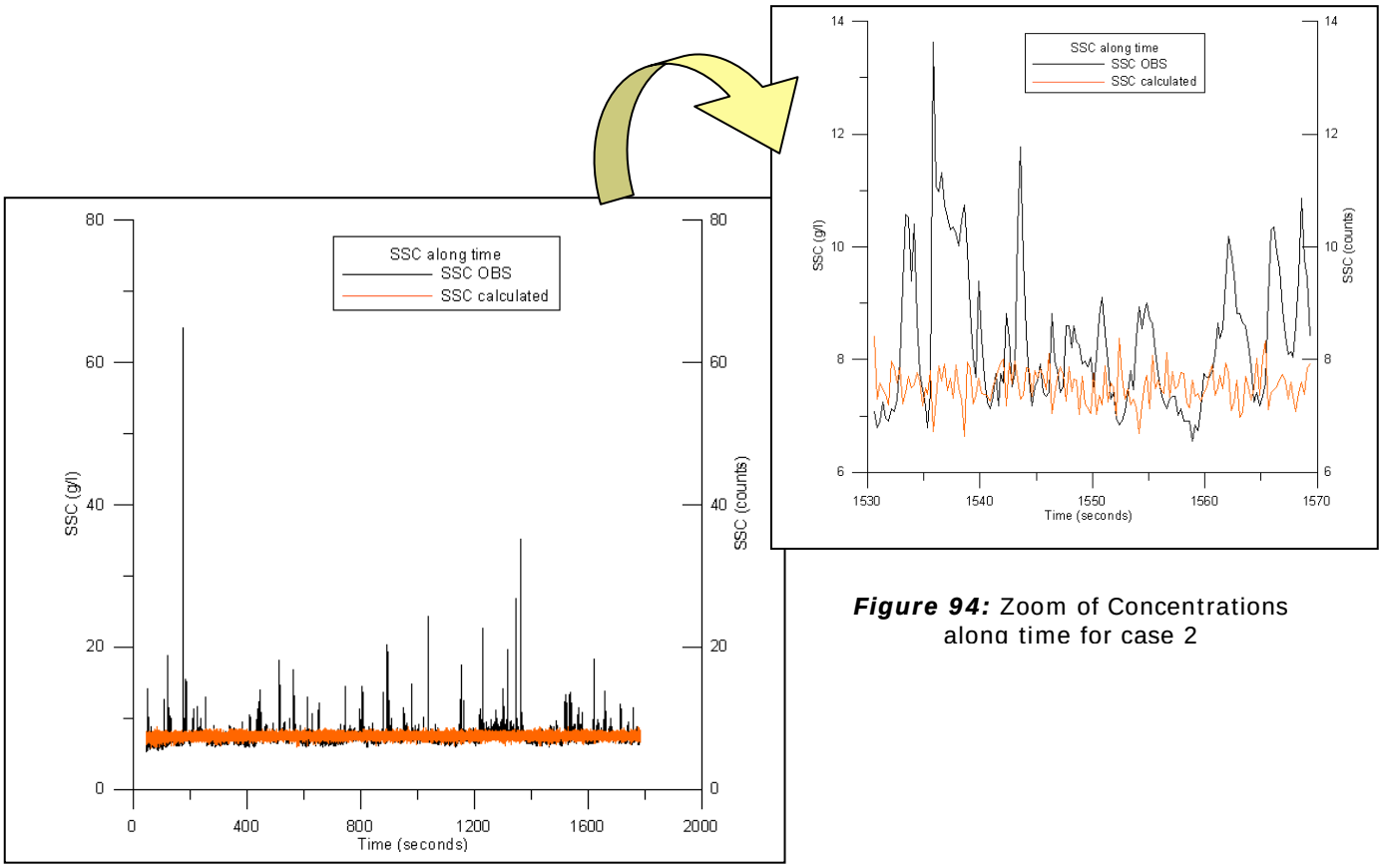

Figure 94: Zoom of Concentrations along time for case 2

Figure 94: Concentrations along time for case 2

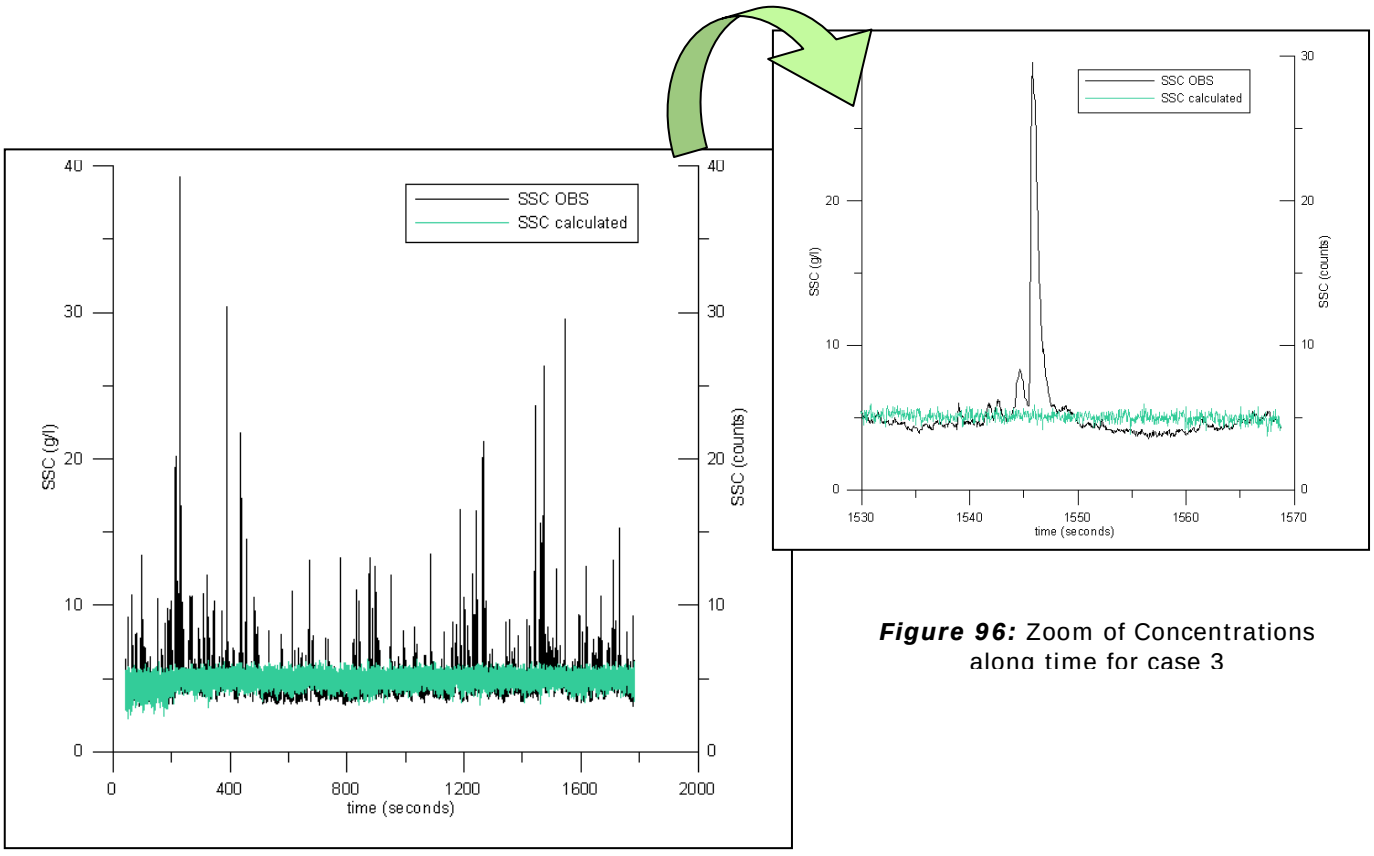

Figure 96: Zoom of Concentrations along time for case 3

Figure 95: Concentrations along time for case 3

Observing these figures one can appreciate that amplitude is not a good output to fit the concentration. Anyway some treats can be commented.

First of all, in case 1, figure 91, one can appreciate that SSC obtained from OBS has peaks in upward direction whereas SSC calculated from amplitude has peaks in downward direction. Moreover, in figure 92 one can appreciate that suspended sediment concentration calculated from amplitude presents more oscillations than suspended sediment concentration obtained by OBS. Also one can notice how calculated SSC is just moving on the range of 38 counts to 40 counts while OBS SSC has a bigger range of oscillation.

In figure 94, case 2, one can appreciate how calculated suspended sediment concentration from amplitude is oscillating more than in the first case but not as much to fit the SSC obtained from OBS.

On the other hand, on figure 96, one can appreciate how calculated suspended sediment concentration from amplitude seems to follow precisely the suspended sediment concentration obtained from OBS except on the peaks.

However, everything explained above are just suppositions therefore we need to check it.

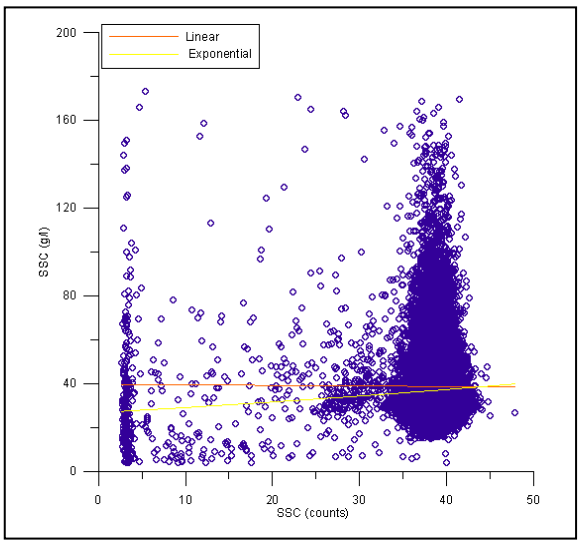

Figure 97: SSC real versus SSC calculated in case 1

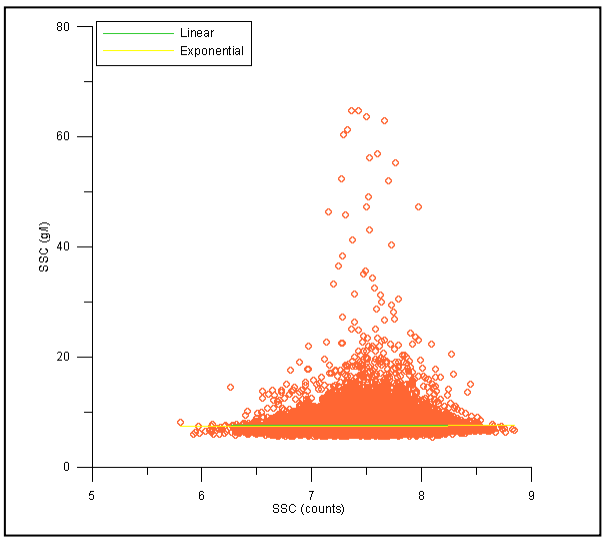

Figure 98: SSC real versus SSC calculated in case 2

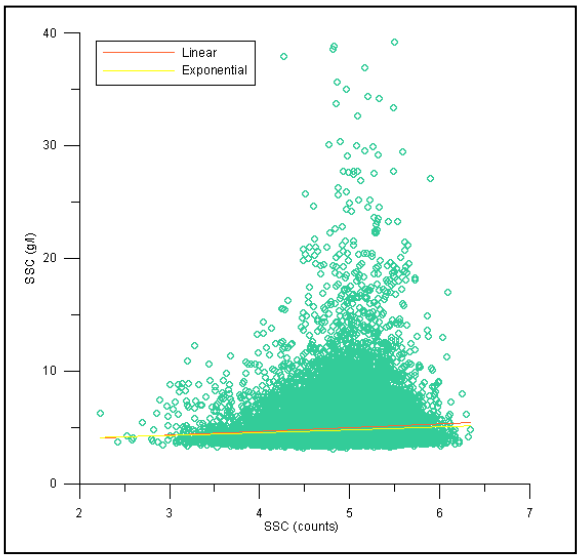

Figure 99: SSC real versus SSC calculated in case 3

In figure 97 one can see two lines trying to adjust these outputs.

The orange adjust is a lineal line with equation:
SSC OBS= 0.0813*SSC all outputs + 35.841 with R^2= 0.0004 (47)

The yellow adjust is a exponential tendency line with equation:
SSC OBS= $26.7232*e^{0.008325*SSC\ all\ outputs}$ with R^2=0.009558 (48)

In figure 98 one can see three lines trying to adjust these outputs.

The green adjust is a lineal line with equation:
SSC OBS= 0.1072*SSC all outputs + 6.7111 with R^2= 0.0003 (49)

The yellow adjust is a exponential tendency line with equation:
SSC OBS= $6.5252*e^{0.0167*SSC\ all\ outputs}$ with R^2=0.0012 (50)

In figure 99 one can see three lines trying to adjust these outputs.

The orange adjust is a lineal line with equation:
SSC OBS= 0.33116*SSC all outputs + 3.3145 with R^2= 0.00571 (49)

The yellow adjust is a exponential tendency line with equation:
SSC OBS= $3.6292*e^{0.0545*SSC\ all\ outputs}$ with R^2=0.00754 (50)

Then observing these results one observes that the best fitting is for the exponential fit in case 1 but very closed to the exponential fit in case 3. Therefore in contrast to the first results seen, the best fit is for case 1 but one can not validate it due to the distance of our determination coefficient with the accepted determination coefficient (R^2=0.9).

V.3.2.1.4 Weighted least squared method with Correlation

Applying LS method with correlation implies that the dependence matrix Y is composed by SSC data from OBS and the independence matrix X is compose with correlation components (Corr_X, Corr_Y, Corr_Z).

As it has been seen in the last section one has to work separately in three cases: erosion waves- beginning (case 1), erosion waves-ending (case 2) and accretion waves (case 3).

Processing this data, vector b, the vector of the different weights in each case show:

Output	Case 1 → Weight	Case 2 → Weight	Case 3 → Weight
Corr X	0.1258	0.0315	0.0142
Corr Y	0.1601	0.0353	0.0181
Corr Z	0.1539	0.0136	0.0202

Table 5: Relation of weight coefficients in each study case

As one can observe the most important weight is in case 1 and case 2 for Corr Y while in case 3 is for Corr Z.

Therefore if one calculates the concentration with these outputs and these weights obtains:

CASE 1: *ADV concentration= 0.1258*CorrX +0.1601*CorrY +0.1539*CorrZ* (51)

CASE 2: *ADV concentration= 0.0315*CorrX +0.0353*CorrY +0.0136*CorrZ* (52)

CASE 3: ADV concentration= 0.0142*CorrX +0.0181*CorrY +0.0202*CorrZ (53)

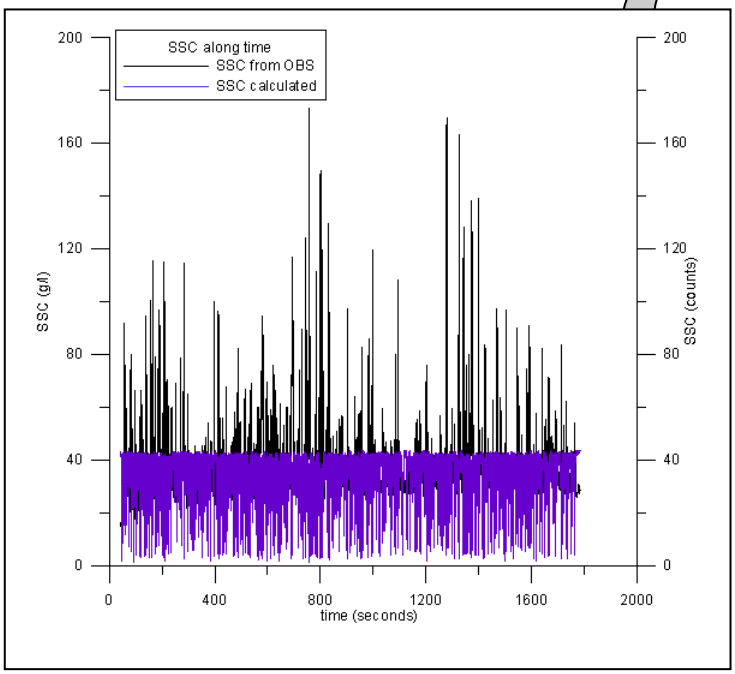

Figure 100: Concentrations along time for case 1

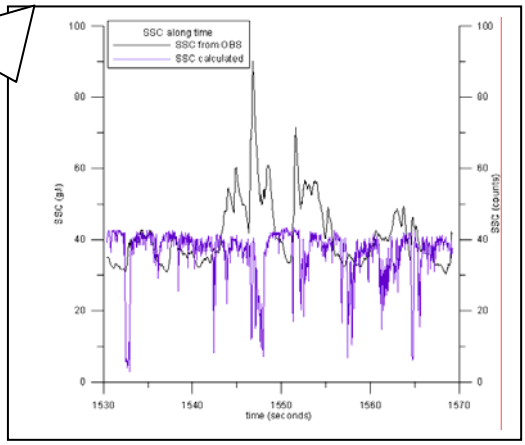

Figure 101: Zoom of Concentrations along time for case 1

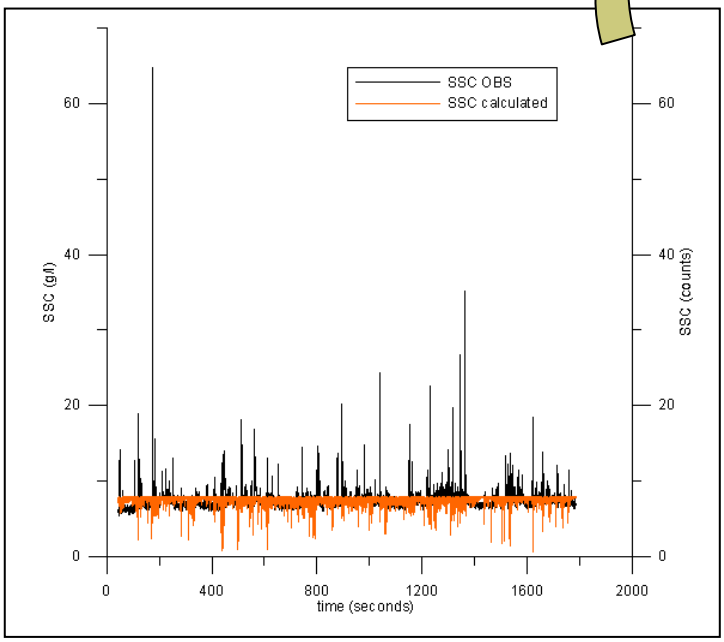

Figure 102: Concentrations along time for case 2

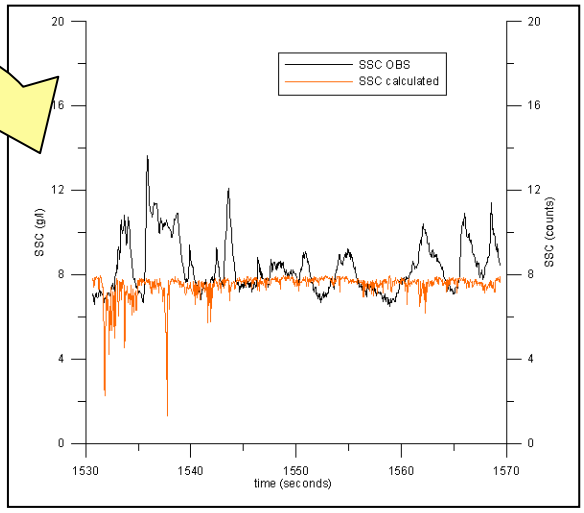

Figure 103: Zoom of Concentrations along time for case 2

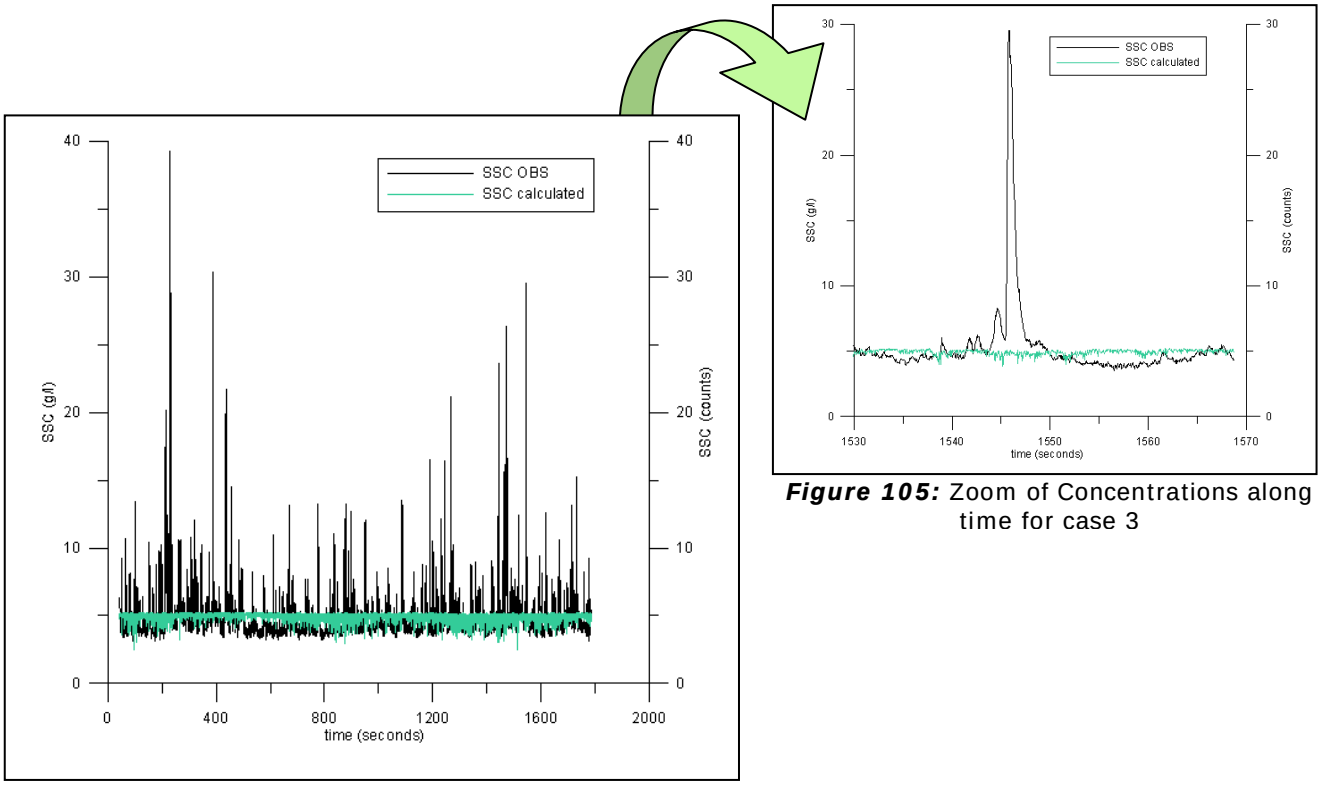

Figure 105: Zoom of Concentrations along time for case 3

Figure 104: Concentrations along time for case 3

Observing these figures one can found a big similarity with the one obtained by amplitude. As low is the suspended sediment concentration in the study case bigger is the similarity, this implies that case 3 is more similar than case 1. However, it has to be said, that correlation is not a good output to fit the concentration. Anyway some treats can be commented.

First of all, in case 1, figure 100, one can appreciate that SSC obtained from OBS has peaks in upward direction whereas SSC calculated from amplitude has peaks in downward direction. Moreover, in figure 101 we can appreciate that suspended sediment concentration calculated from amplitude presents more oscillations than suspended sediment concentration obtained by OBS. Also one can notice how calculated SSC is just moving around 40counts like in signal amplitude, while OBS SSC has a bigger range of oscillation.

In figure 103, case 2, one can appreciate how calculated suspended sediment concentration from amplitude is oscillating less than in the first case even if is not fitting in a good way the SSC.

In contrast, in figure 105, one can appreciate how calculated suspended sediment concentration from amplitude seems to follow precisely the suspended sediment concentration obtained from OBS except on the peaks.

However, everything explained above are just suppositions therefore we need to check it.

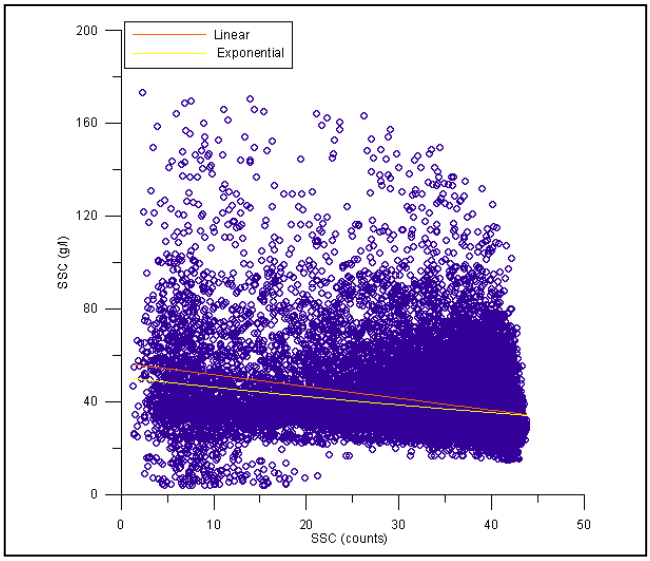

Figure 106: SSC real versus SSC calculated in case 1

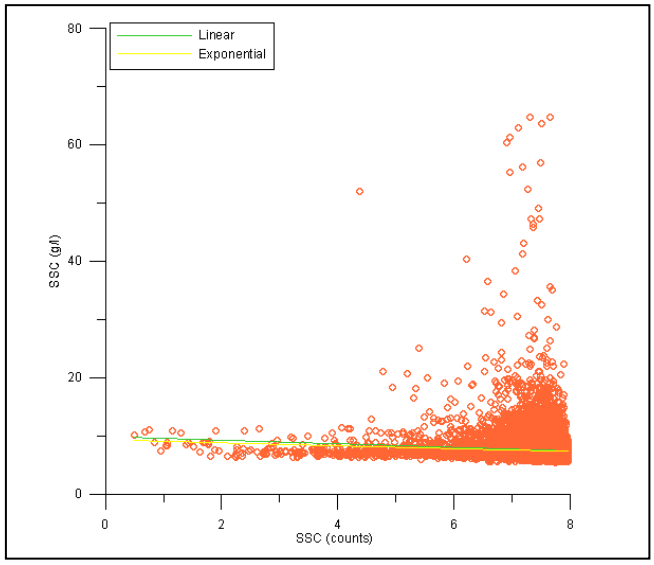

Figure 107: SSC real versus SSC calculated in case 2

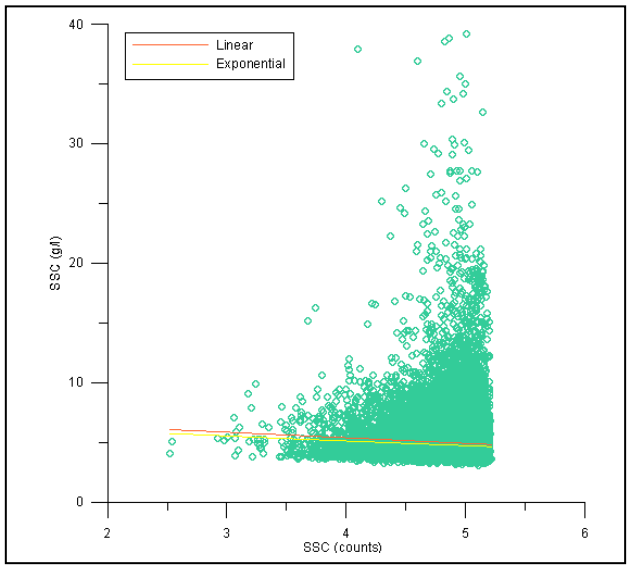

Figure 108: SSC real versus SSC calculated in case 3

In figure 106 one can see two lines trying to adjust these outputs.

The orange adjust is a lineal line with equation:
SSC OBS= -0.50923*SSC all outputs + 56.663 with R^2= 0.09615 (54)

The yellow adjust is an exponential tendency line with equation:
SSC OBS= $50.528*e^{-0.009*SSC\ all\ outputs}$ with R^2=0.0685 (55)

In figure 107 one can see two fittings with equations:

The green adjust is a lineal line with equation:
SSC OBS= -0.30875*SSC all outputs + 9.8695 with R^2= 0.007 (56)

The yellow adjust is an exponential tendency line with equation:
SSC OBS= $9.3367*e^{-0.0302*SSC\ all\ outputs}$ with R^2=0.00094 (57)

In figure 108 one can see two lines trying to adjust these outputs.

The orange adjust is a lineal line with equation:
SSC OBS= -0.46626*SSC all outputs + 7.24485 with R^2= 0.0036 (58)

The yellow adjust is an exponential tendency line with equation:
SSC OBS= $7.0109*e^{-0.07906*SSC\ all\ outputs}$ with R^2=0.0056 (59)

Paying attention to these fits it can be concluded that the best fit here is for the linear adjustment in case one. It has to be noticed that this is the first time that a linear fit adjust better than an exponential.

Also has to be mentioned that the slope in all the adjustments is negative meaning that SSC from OBS and SSC calculated are on an indirect relation as was happening before in the running average method applied to correlation.

To sum up no one of this results is enough reliable to be applied for future works. Therefore correlation is not a good output which to approximate suspended sediment concentration.

V.3.2.2 Weighted least squared method in dimensionless value

As the results shown before for the least squared method are compared with different units, now we work with dimensionless parameters. Also is in order to smooth the data and try to get a better correlation.

V.3.2.2.1 Weighted least squared method in dimensionless value with all outputs

The goal of this part is to observe how important the contribution of each output in the concentration relation is.

As it has been seen in the last section one has to work separately in three cases: erosion waves- beginning (case 1), erosion waves-ending (case 2) and accretion waves (case 3).

Processing this data, vector b, the vector of the different weights show:

Output	Case 1 → Weight	Case 2 → Weight	Case 3 → Weight
SNR X	0.2197	0.0723	0.1194
SNR Y	0.1978	0.0876	0.1010
SNR Z	-0.1900	0.0765	0.1119
Amp X	-0.0239	-0.0259	-0.0411
Amp Y	0.0043	-0.0351	0.0013
Amp Z	0.1863	-0.0245	-0.0534
Corr X	-0.0592	-0.0035	-0.0212
Corr Y	-0.0307	-0.0073	-0.0891
Corr Z	-0.0571	-0.0211	0.0107

Table 6: Relation of weight coefficients in each study case

As one can observe the most important weight, in all three cases, is for SNR. Also one can observe that this weight is less important in case 2.

Therefore if one calculates the concentration with these outputs and these weights we obtain:

CASE 1: *ADV concentration= 0.2197*SNRX +0.1978*SNRY -0.1900*SNRZ - 0.0239*AmpX +0.0043*AmpY +0.1863*AmpZ -0.0592*CorrX -0.0307*CorrY - 0.0571*CorrZ* (60)

CASE 2: *ADV concentration= 0.0723*SNRX +0.0876*SNRY +0.0765*SNRZ - 0.0259*AmpX -0.0351*AmpY -0.0245*AmpZ -0.0035*CorrX -0.0073*CorrY - 0.0211*CorrZ* (61)

CASE 3: ADV concentration= 0.1194*SNRX +0.1010*SNRY +0.1119*SNRZ - 0.0411*AmpX +0.0013*AmpY -0.0534*AmpZ -0.0212*CorrX -0.0891*CorrY +0.0107*CorrZ (62)

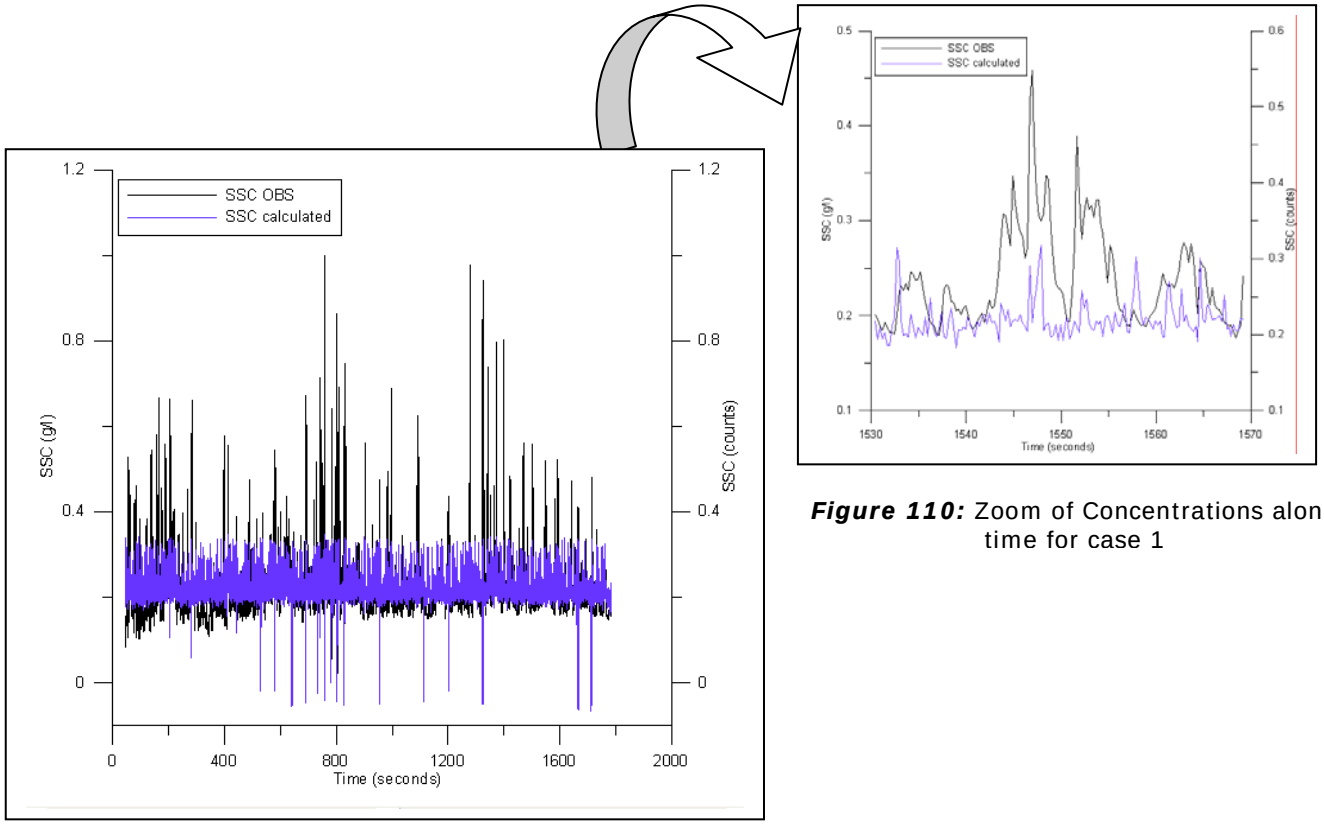

Figure 110: Zoom of Concentrations along time for case 1

Figure 109: Concentrations along time for case 1

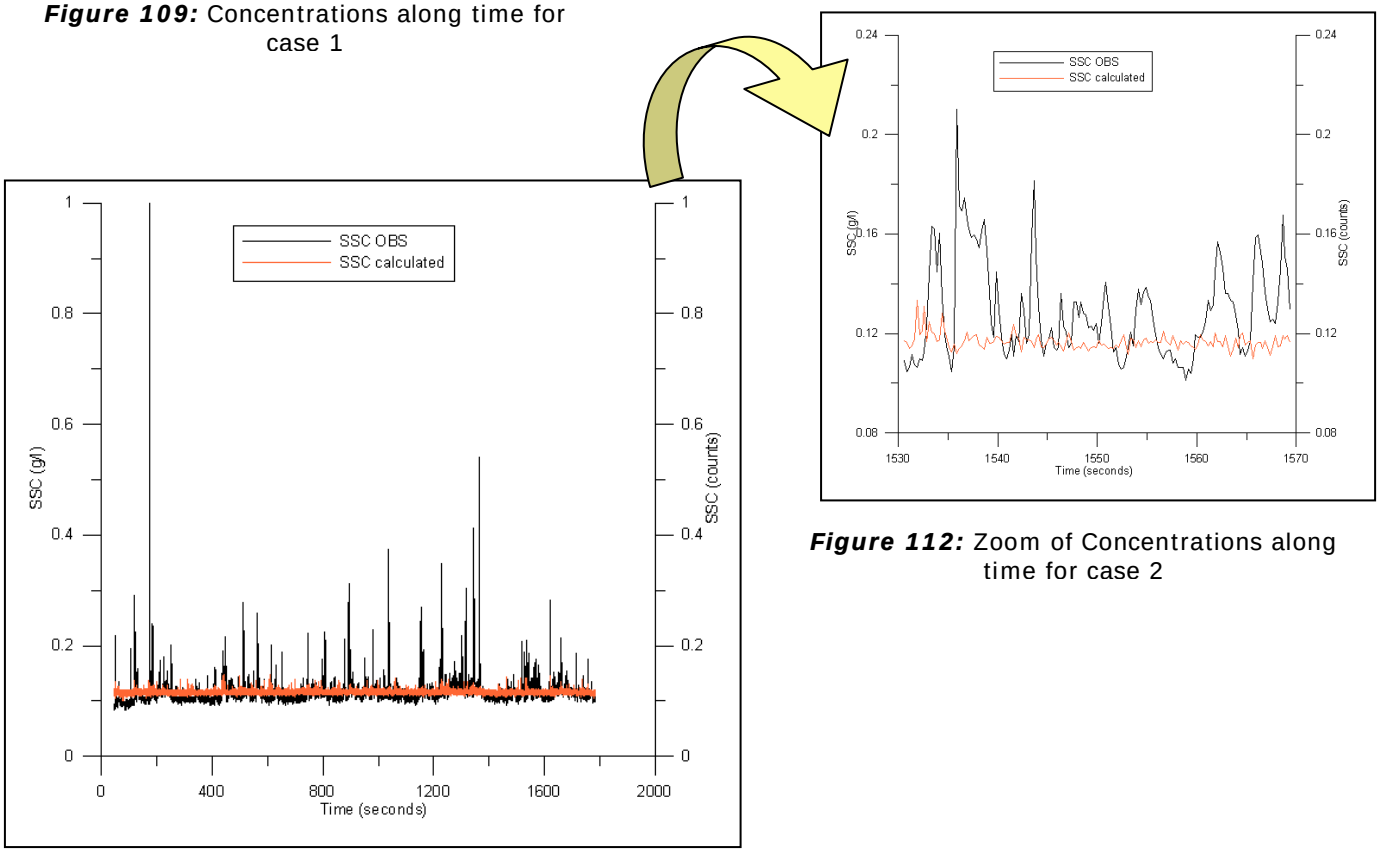

Figure 112: Zoom of Concentrations along time for case 2

Figure 111: Concentrations along time for case 2

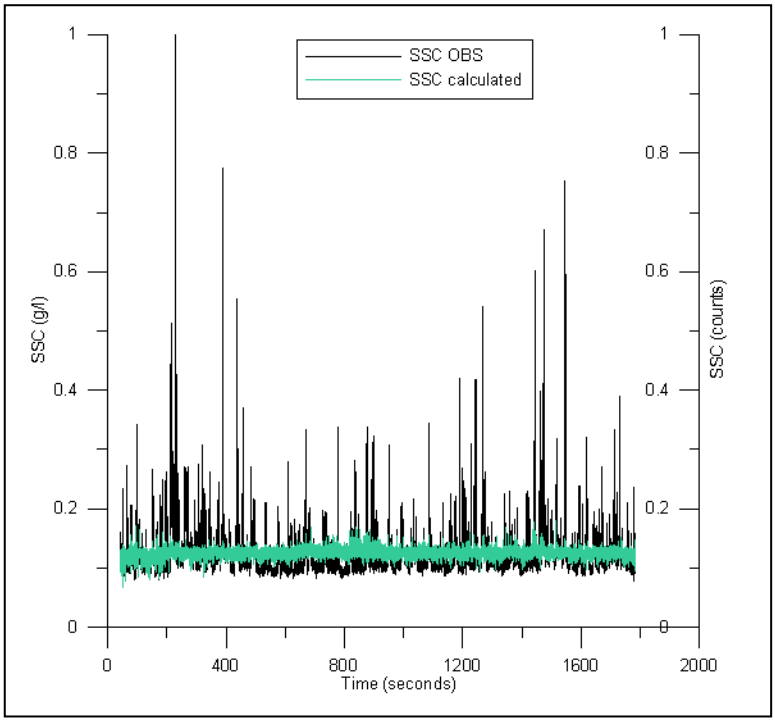

Figure 113: Concentrations along time for case 3

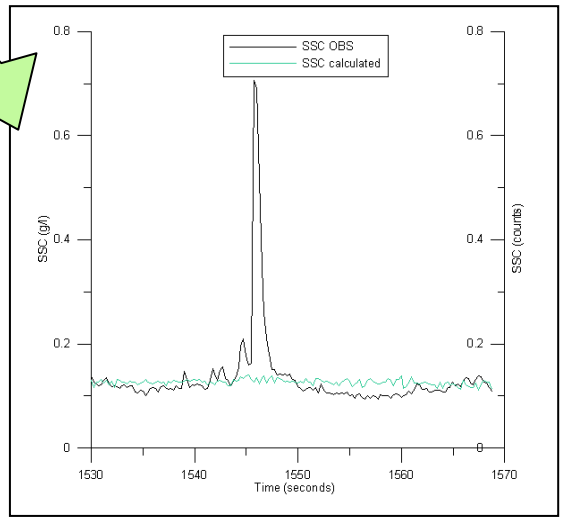

Figure 114: Zoom of Concentrations along time for case 3

Notice that it has been tried to smooth the result working in dimensionless value but as these figures show and in comparison to section V.3.2.1.1.1, weighted least squared method, no difference in the distributions shape can be appreciated. However, to corroborate it we are going to find the best fits and compare them with the ones obtained in section V.3.2.1.1.

Moreover, as we have seen in weighted least squared method with all outputs, case 3 can be omitted due to its badly approximation as figures 113 and 114 shows.

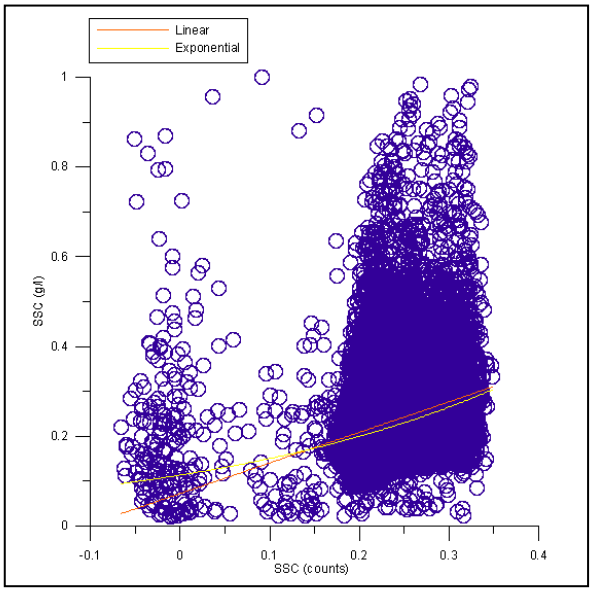

Figure 115: SSC real versus SSC calculated in case 1

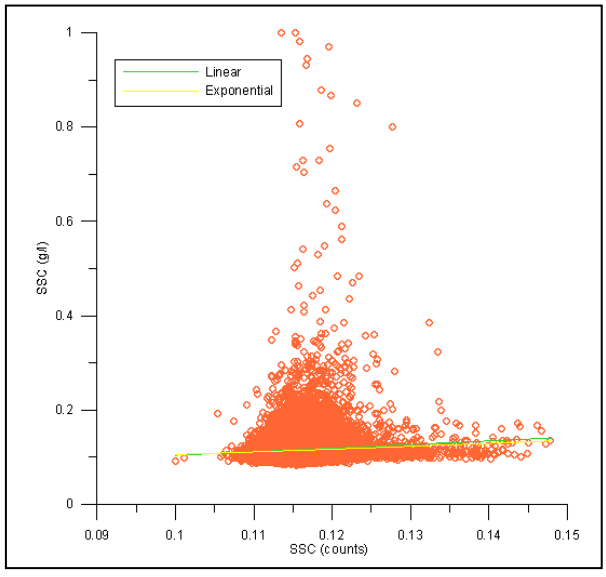

Figure 116: SSC real versus SSC calculated in case 2

In figure 115 one can see two lines trying to adjust the concentrations.

The orange adjust is a lineal fitting with equation:
SSC OBS= 0.7398*SSC all outputs + 10.519 with R^2= 0.0818 (63)

The yellow adjust is an exponential fitting with equation:
SSC OBS= $16.624*e^{0.0206*SSC\ all\ outputs}$ with R^2=0.1277 (64)

On figure 116 one can also see two fittings:

The green adjust is a lineal fitting with equation:
SSC OBS= 0.8146*SSC all outputs + 1.3733 with R^2= 0.0068 (65)

The yellow adjust is an exponential fitting with equation:
SSC OBS= $3.9344*e^{0.0837*SSC\ all\ outputs}$ with R^2=0.0103 (66)

In comparison with the results obtained in section V.3.2.1.1 one can appreciate that these are the same, as one can expect from figures 109 to 114. The reason of this phenomenon is because applying dimensionless value one just takes the data and move it between values of null to one but the data is always the same. Therefore when we try to correlate the fittings and the determination coefficients are always the same.

As a result of this section we are not going to explain here in detail all the outputs from ADV because all the results that one is going to obtain are going to be the same with the weighted least squared method. One can affirm this because, out of the scope of this section, this method has been probed and studied with all outputs like in the different sections of weighted least squared method.

V.3.2.3 Weighted running average least squared method

Observing the results obtained until this moment and noticing that running average and weighted least squared method have given the best results, here a weight least squared method is going to be applied to the data averaged with the running average method. Another time the data is going to be grouped in groups of 50 and average it. After weigh least squared method is going to be applied.

V.3.2.3.1 Weighted running average least squared method with all outputs

One of the goals of this part is to observe how important the contribution of each output in the concentration relation is. The second main point is to try to get a relation between ADV outputs and OBS concentration.

As it has been seen in the last section one has to work separately in three cases: erosion waves- beginning (case 1), erosion waves-ending (case 2) and accretion waves (case 3).

Processing this data, vector b, the vector of the different weights in each case shows:

Output	Case 1 → Weight	Case 2 → Weight	Case 3 → Weight
SNR X	4.3525	0.6960	-0.0388
SNR Y	6.3448	1.7482	-0.1409
SNR Z	-10.3086	-0.8775	0.3226
Amp X	-0.0764	-0.0275	0.0053
Amp Y	-0.3997	-0.2526	0.0633
Amp Z	0.9440	0.1444	-0.0307
Corr X	-0.1744	0.0356	0.0107
Corr Y	0.2277	0.0284	-0.0521
Corr Z	-0.5881	-0.1174	0.0007

Table 7: Relation of weight coefficients in each study case

Paying attention to the values presents in the table one can notice how SNR has a high weight in case 1 whereas in the other cases is less important. Also notice how correlation is in the same order of importance as amplitude in contrast with the weight least squared method.

Therefore if one calculates the concentration with these outputs and these weights one obtains:

CASE 1: *ADV concentration= 4.3525*SNRX +6.334*SNRY -10.3086*SNRZ -0.0764*AmpX -0.3997*AmpY +0.944*AmpZ -0.1744*CorrX +0.2277*CorrY -0.5881*CorrZ* (67)

CASE 2: *ADV concentration= 0.6960*SNRX +1.7482*SNRY -0.8775*SNRZ -0.0275*AmpX -0.02526*AmpY +0.1444*AmpZ +0.0356*CorrX +0.0284*CorrY -0.1174*CorrZ* (68)

CASE 3: ADV concentration= -0.0388*SNRX -0.1409*SNRY +0.3226*SNRZ +0.0053*AmpX +0.0633*AmpY -0.0307*AmpZ +0.0107*CorrX -0.0521*CorrY +0.0007*CorrZ (69)

(69)

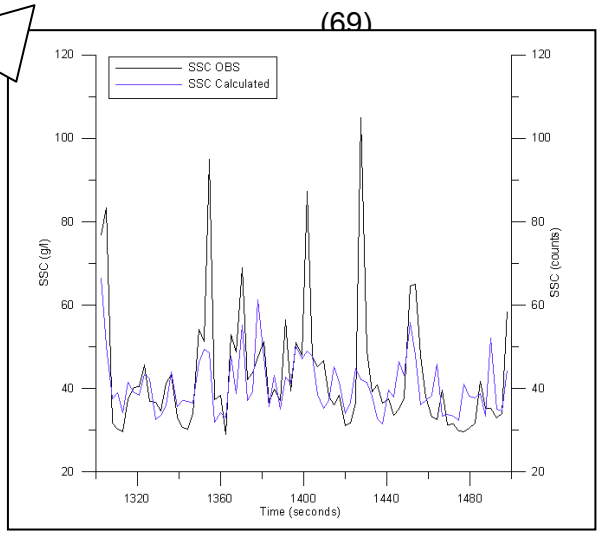

Figure 118: Zoom of Concentrations along time for case 1

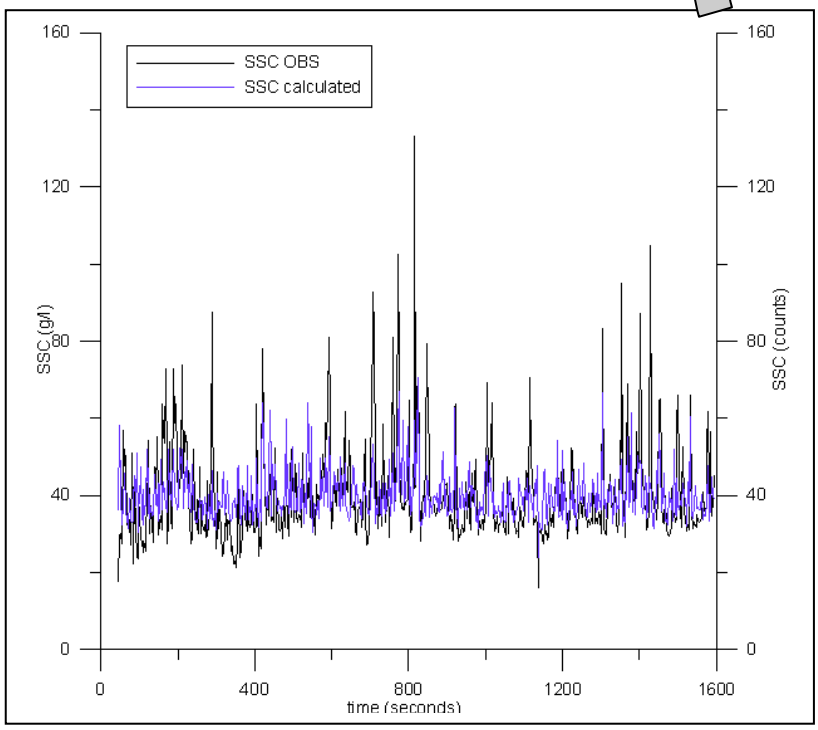

Figure 117: Concentrations along time for case 1

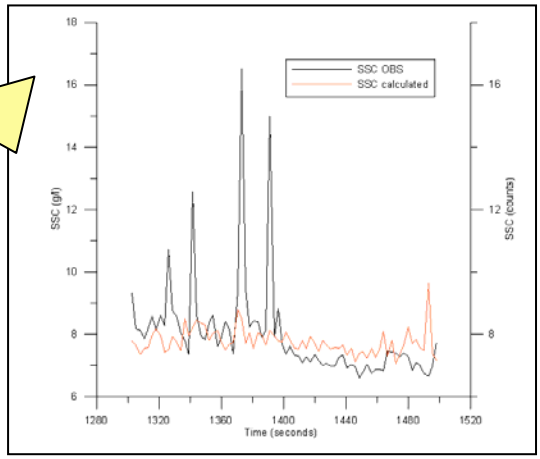

Figure 120: Zoom of Concentrations along time for case 2

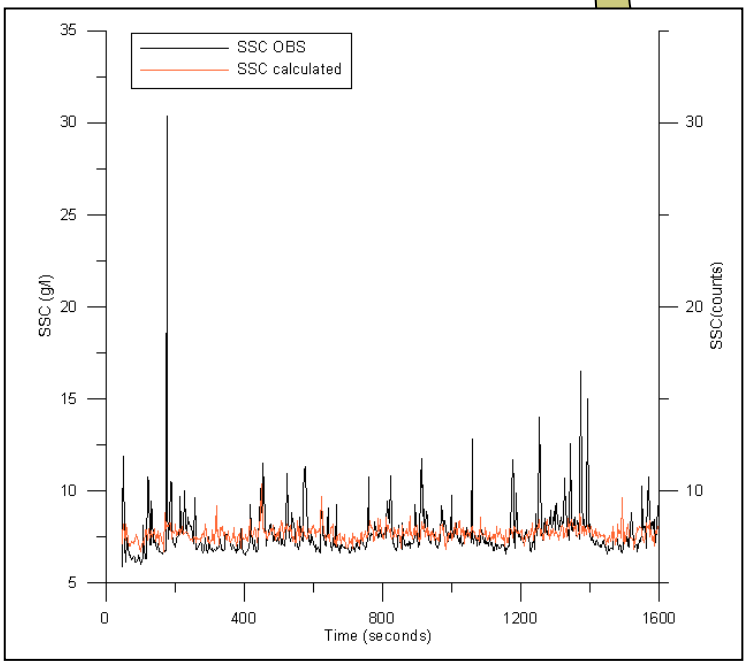

Figure 119: Concentrations along time for case 2

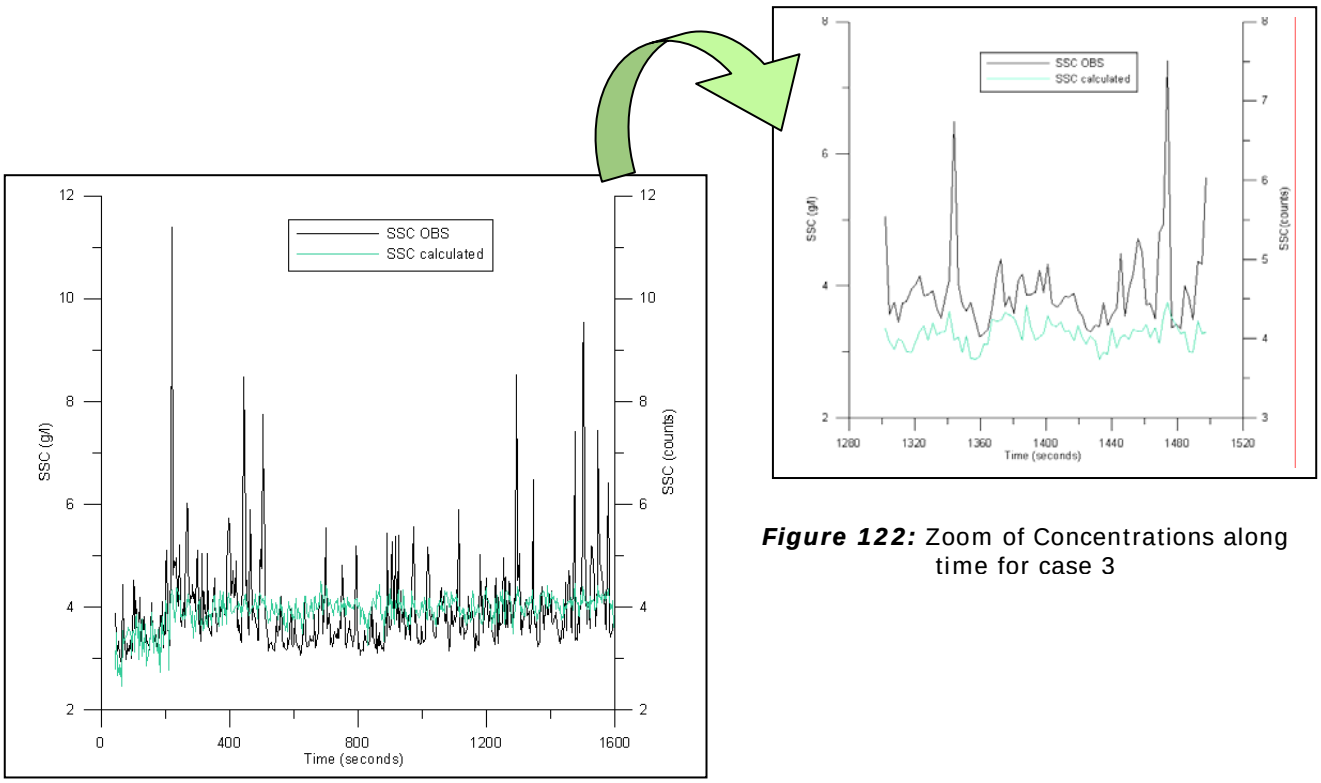

Figure 121: Concentrations along time for case 3

Figure 122: Zoom of Concentrations along time for case 3

Observing these figures seems that the method that has been applied is working in order to adjust the suspended sediment concentration.

Despite one can not confirm that is working in all the cases, one can appreciate how in case 1 seems that SSC from OBS is well adjusted by the SSC calculated, although in the peaks where suspended sediment concentration from OBS is over 60g/l some differences between both distributions can be appreciated.

Moreover in case 3, figure 122, one can appreciate how SSC calculated distribution follows the SSC obtained from OBS distribution, however with a few units below.

In contrast, on case 2, figure 120, one can appreciate how both distributions show quite a different behaviour. SSC calculated in always around 8 counts varying not too much, while SSC from OBS present big oscillations.

Nevertheless comparing with weighted least squared method; figure 76, case one presents here less oscillations and doesn't have big peaks in downward direction as in figure 75.

Furthermore figure 79, case 3, shows suspended sediment calculated as a big band and on figure 80 we can appreciate how the adjustment is not good. It is also happening in case 2, figures 77 and 78.

Consequently and noticing that these results seems to be better than the ones found before, we are going to search the respective fittings.

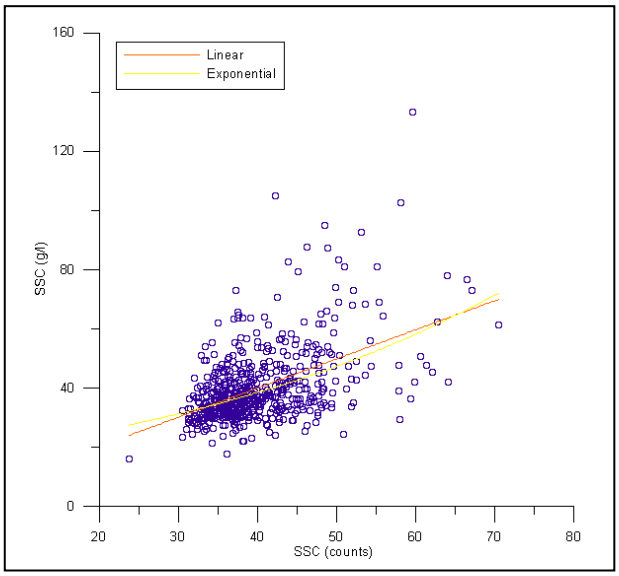

Figure 123: SSC real versus SSC calculated in case 1

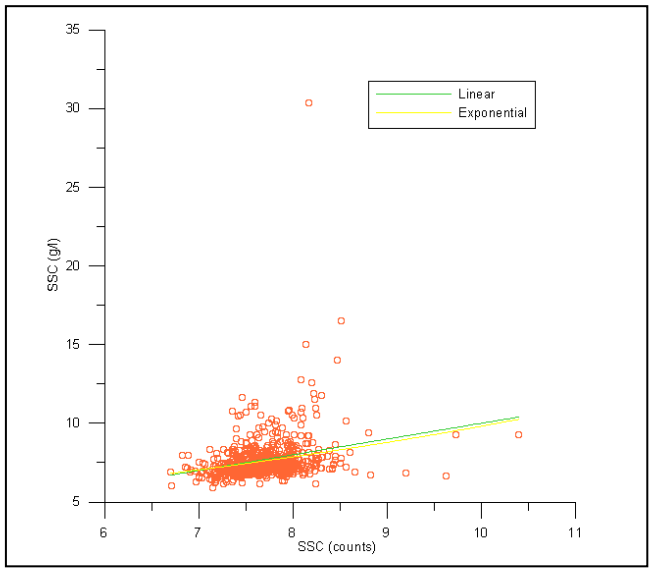

Figure 124: SSC real versus SSC calculated in case 2

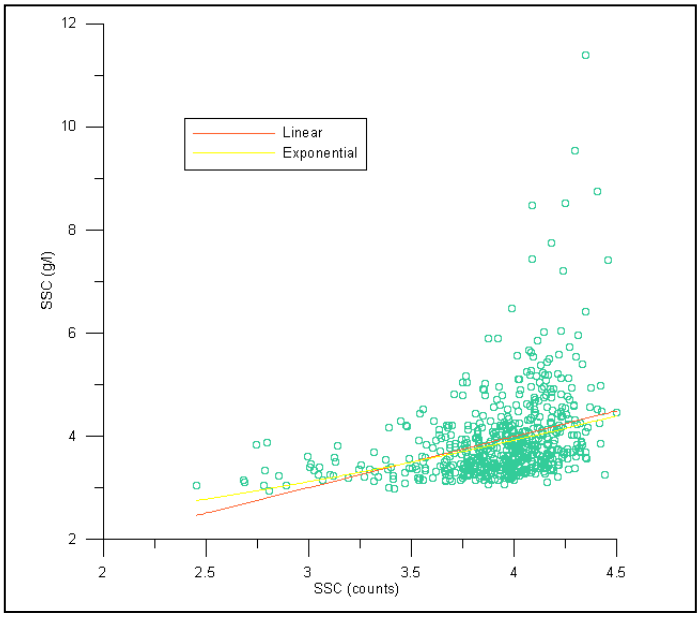

Figure 125: SSC real versus SSC calculated in case 3

In figure 123 one can see two lines trying to adjust the concentrations.

The orange adjust is a lineal fitting with equation:
SSC OBS= 0.985*SSC all outputs + 0.6188 with R^2= 0.25 (70)

The yellow adjust is an exponential fitting with equation:
SSC OBS= $16.8558*e^{0.02066*SSC\ all\ outputs}$ with R^2=0.25 (71)

On figure 124 one can also see two fittings:

The green adjust is a lineal fitting with equation:
SSC OBS=1.000524*SSC all outputs + 0.00404 with R^2= 0.0685 (72)

The yellow adjust is an exponential fitting with equation:
SSC OBS= $3.24929*e^{0.1105*SSC\ all\ outputs}$ with R^2=0.0906 (73)

On figure 125 one can also see two fittings:

The orange adjust is a lineal fitting with equation:
SSC OBS= 0.9929*SSC all outputs + 0.02789 with R^2= 0.1264 (74)

The yellow adjust is an exponential fitting with equation:
SSC OBS= $1.56953*e^{0.229142*SSC\ all\ outputs}$ with R^2=0.155378 (75)

Observing the results obtained one can sum up saying that the bests fits are obtained for case 1 with a determination coefficient of R^2= 0.25. Although these are the bests fits founded until this moment one can not consider them enough good because of the big difference with the validating determination coefficient (R^2= 0.9).

V.3.2.3.2 Weighted running average least squared method with SNR

One of the goals of this part is to observe how important the contribution of each output in the concentration relation is. The second main point is to try to get a relation between ADV outputs and OBS concentration.

As it has been seen in the last section one has to work separately in three cases: erosion waves- beginning (case 1), erosion waves-ending (case 2) and accretion waves (case 3).

Processing this data, vector b, the vector of the different weights in each case shows:

Output	Case 1 → Weight	Case 2 → Weight	Case 3 → Weight
SNR X	5.1003	0.4871	-0.3202
SNR Y	5.2900	-1.2653	0.7425
SNR Z	-9.1285	1.1929	-0.2677

Table 8: Relation of weight coefficients in each study case

As one can observe the most important weight is for SNR Y in all the cases. Notice also, that the weight of SNR is lowering its value as SSC is lowering too.

Therefore if one calculates the concentration with these outputs and these weights one obtains:

CASE 1: *ADV concentration= 5.1003*SNRX +5.2900*SNRY -9.1285*SNRZ* (76)

CASE 2: *ADV concentration= 0.4871*SNRX -1.2653*SNRY +0.7425*SNRZ* (77)

CASE 3: *ADV concentration= -9.1285*SNRX +1.1929*SNRY -0.2677*SNRZ* (78)

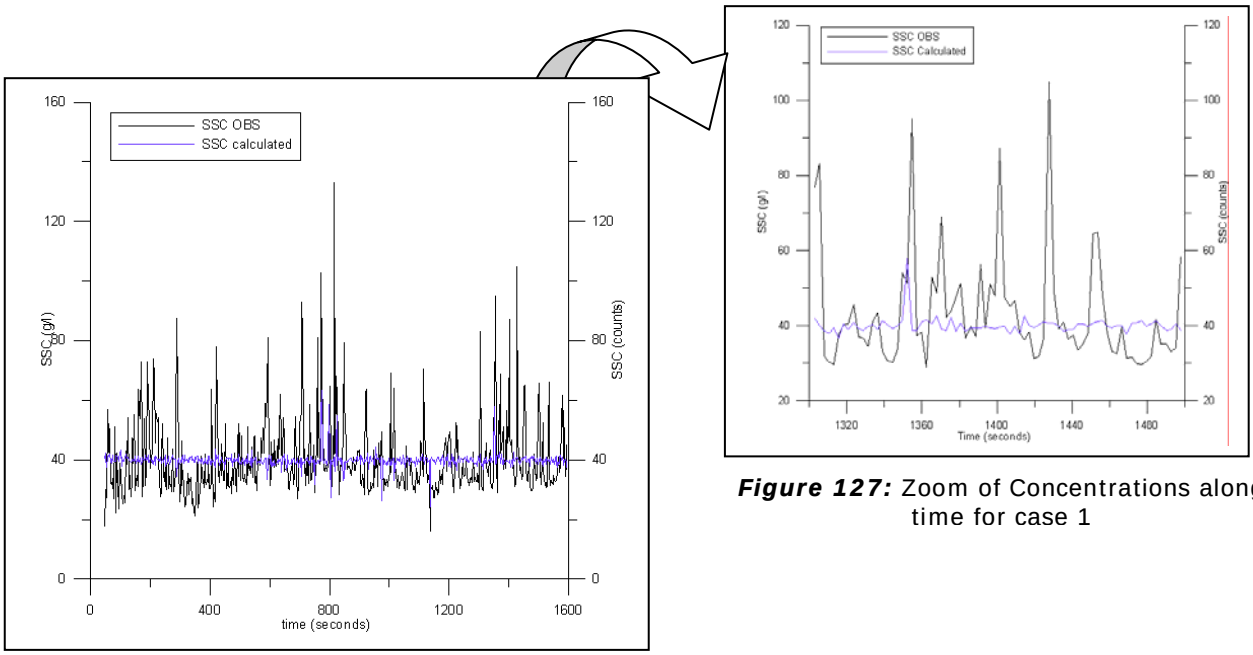

Figure 126: Concentrations along time for case 1

Figure 127: Zoom of Concentrations along time for case 1

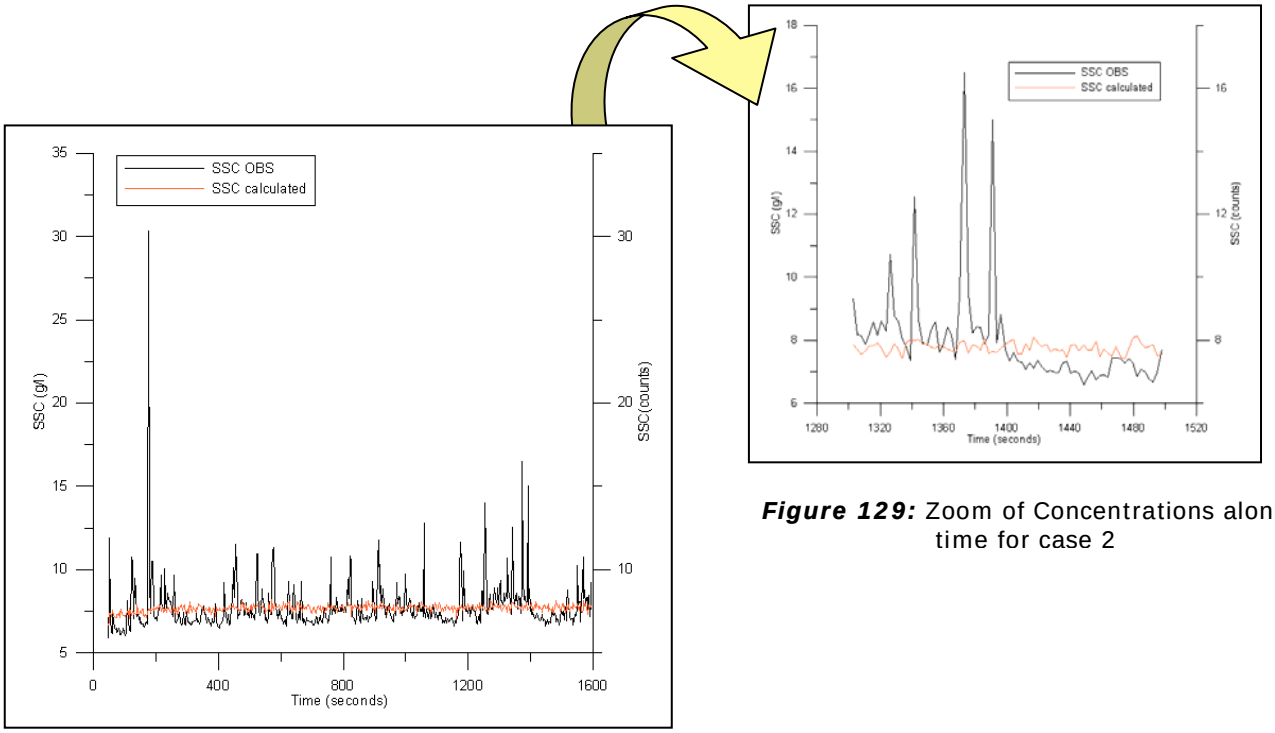

Figure 128: Concentrations along time for case 2

Figure 129: Zoom of Concentrations along time for case 2

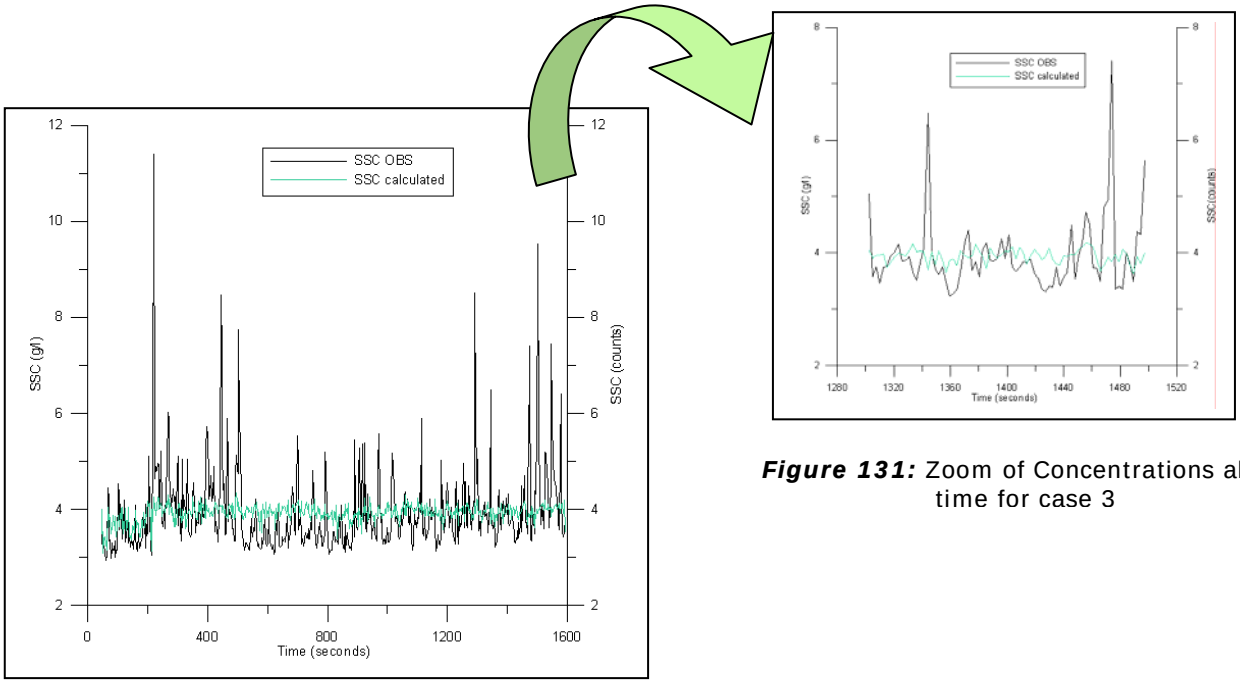

Figure 131: Zoom of Concentrations along time for case 3

Figure 130: Concentrations along time for case 3

Observing these figures seems that SSC calculated from SNR is not adjusting quite well the SSC obtained from OBS. In all the plots one can appreciate how in any case the distribution of calculated SSC is adjusting SSC from OBS in the peaks.

Moreover one can appreciate how in figure 127, case 1, the SSC calculated presents a big variation from SSC obtained by the OBS, like was the case in figure 84 for the weighted least squared method. Therefore we are not going to look for a relation in this case.

If now one compares figure 129 with figure 86 one can appreciate how in figure 129 the adjustment is better. Here, in figure 129, the distribution of suspended sediment concentration calculated is varying in a wider range than in figure 86 for the case of weighted least squared method. Therefore here one should obtain a better fit.

Furthermore, comparing figures 131 and 88 one can appreciate that here the adjustment is better, too. In figure 88 one has seen that calculated SSC presented a little variation under the value of the SSC obtained from OBS. Therefore one can expect a better fit using this new method.

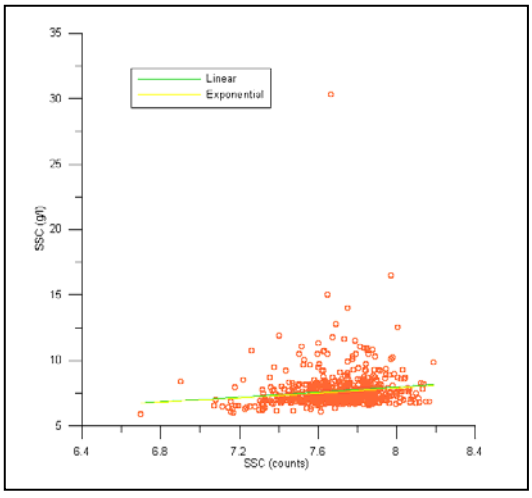

Figure 132: SSC real versus SSC calculated in case 2

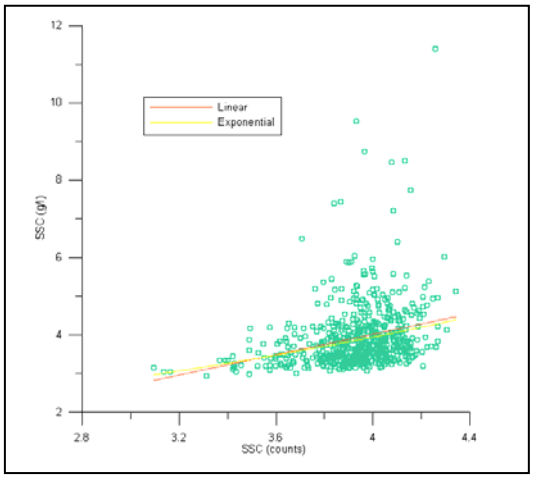

Figure 133: SSC real versus SSC calculated in case 3

On figure 132 one can see two fittings:

The green adjust is a lineal fitting with equation:
SSC OBS=0.9406*SSC all outputs + 0.04572 with R^2= 0.0168 (79)

The yellow adjust is an exponential fitting with equation:
SSC OBS= $2.948*e^{0.12316*SSC\ all\ outputs}$ with R^2=0.0314 (80)

On figure 133 one can also see two fittings:

The orange adjust is a lineal fitting with equation:
SSC OBS= 1.3172*SSC all outputs – 1.2493 with R^2= 0.0743 (81)

The yellow adjust is an exponential fitting with equation:
SSC OBS= $1.1268*e^{0.31327*SSC\ all\ outputs}$ with R^2=0.097 (82)

As can be appreciated from this fittings, and as the figures 129 and 131 revealed, when one adjusts the SSC from OBS using this method one obtains better results than before. However, these results can not be considered as reliable results because the determination coefficient is still too low.

V.3.2.3.3 Weighted running average least squared method with Signal Amplitude

Applying LS method with amplitude implies that the dependence matrix Y is composed by SSC data from OBS and the independence matrix X is compose with amplitude components (AMP_X, AMP_Y, AMP_Z).

As it has been seen in the last section one has to work separately in three cases: erosion waves- beginning (case 1), erosion waves-ending (case 2) and accretion waves (case 3).

Processing this data, vector b, the vector of the different weights in each case show:

Output	Case 1 → Weight	Case 2 → Weight	Case 3 → Weight
AMP X	0.4690	0.0268	-0.0094
AMP Y	0.6539	-0.0969	0.0521
AMP Z	-0.8643	0.1335	-0.0143

Table 9: Relation of weight coefficients in each study case

As one can observe the most important weight is for AMP Y in all the cases. Notice also, that the weight of Signal Amplitude is lowering its value as SSC is lowering too.

Therefore if one calculates the concentration with these outputs and these weights one obtains:

CASE 1: *ADV concentration= 0.4690*AMPX +0.6539*AMPY -0.8643*AMPZ* (83)

CASE 2: *ADV concentration= 0.0130*AMPX +0.0207*AMPY +0.0200*AMPZ* (84)

CASE 3: ADV concentration= *-0.0094*AMPX +0.0521*AMPY -0.0143*AMPZ* (85)

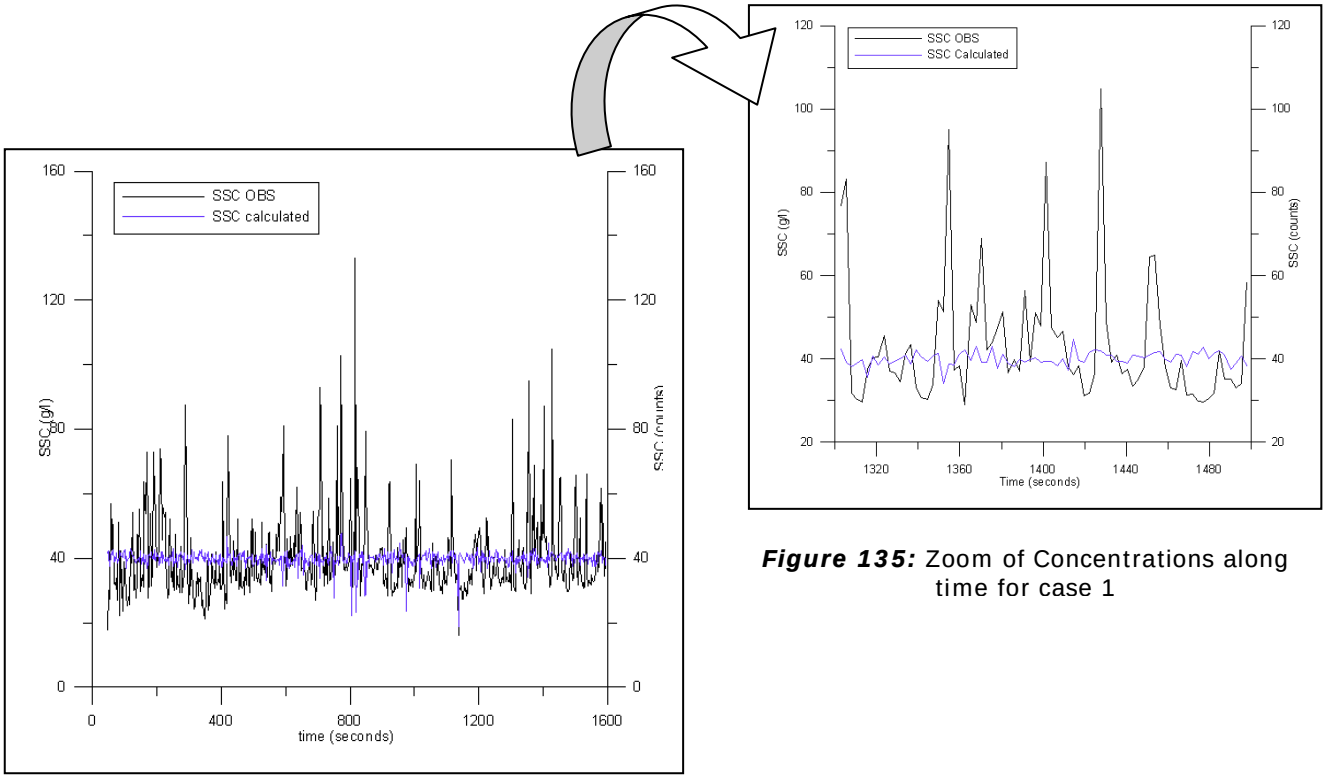

Figure 134: Concentrations along time for case 1

Figure 135: Zoom of Concentrations along time for case 1

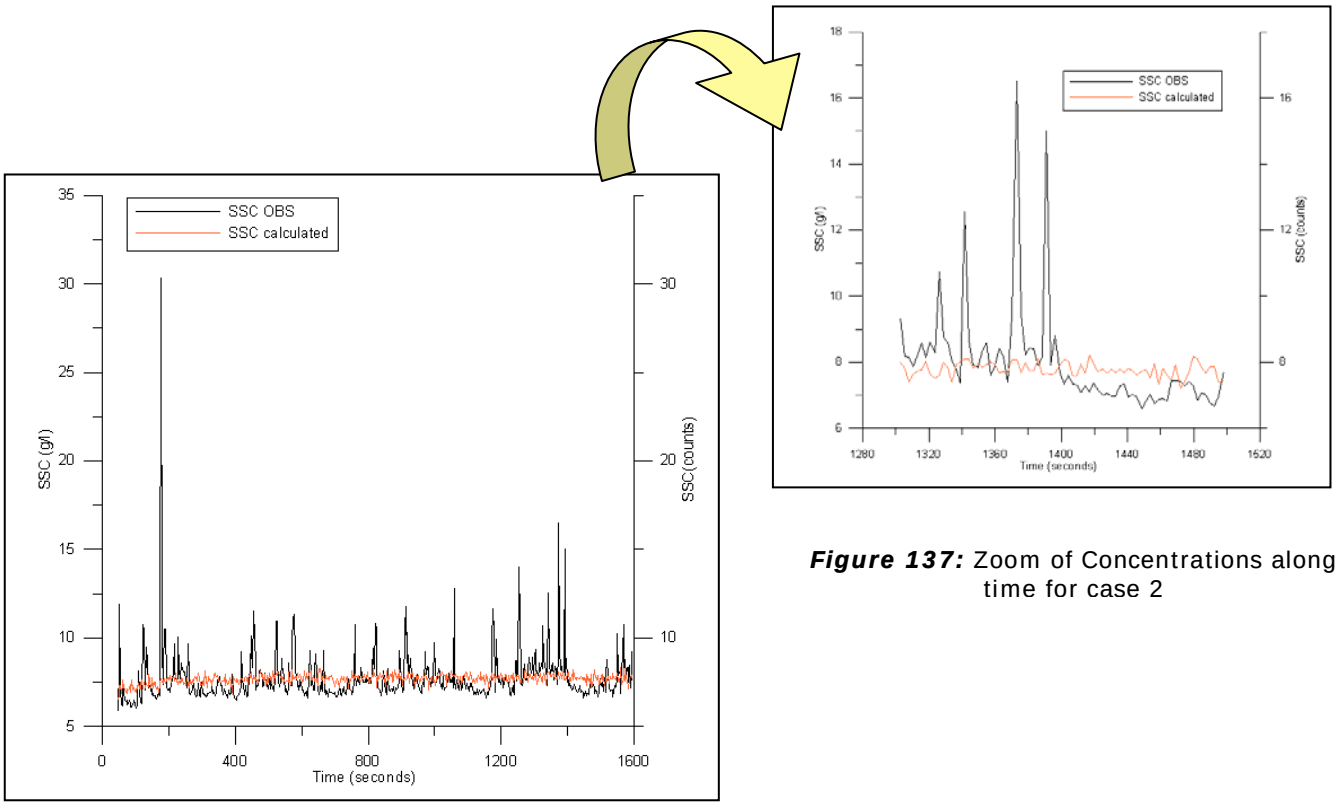

Figure 136: Concentrations along time for case 2

Figure 137: Zoom of Concentrations along time for case 2

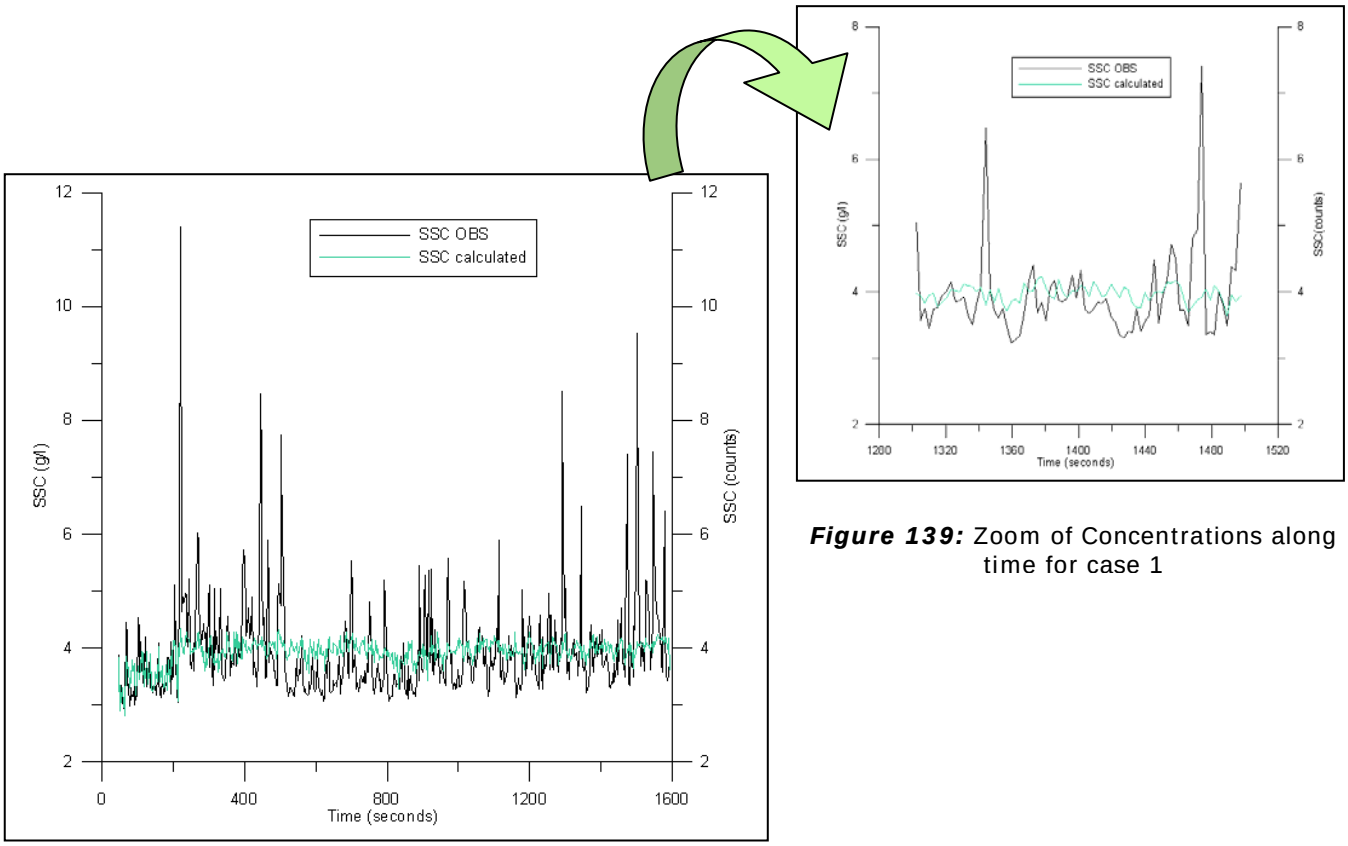

Figure 139: Zoom of Concentrations along time for case 1

Figure 138: Concentrations along time for case 3

Observing these figures one can appreciate how in case 1, figures 134 and 135, the calculated SSC is not adjusting in a good way the SSC from OBS. One can see how the calculated SSC is more or less an oscillation around 40 counts while SSC from OBS has not a constant value. As well as this, figures 91 and 93 for the case of weighted least squared method are also showing the same behaviour. Therefore when trying to look for the best fit one has to skip this case.

Besides this figures 137 and 138 shows how SSC calculated distribution follows more or less the distribution of SSC from OBS, in exception of the peaks. But it has to be notice from figures 93 and 94 that maybe the relation found here is not going to be as good as that one.

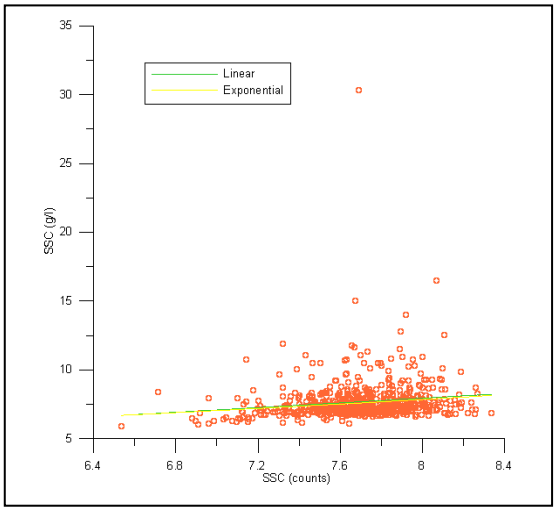

Figure 140: SSC real versus SSC calculated in case 2

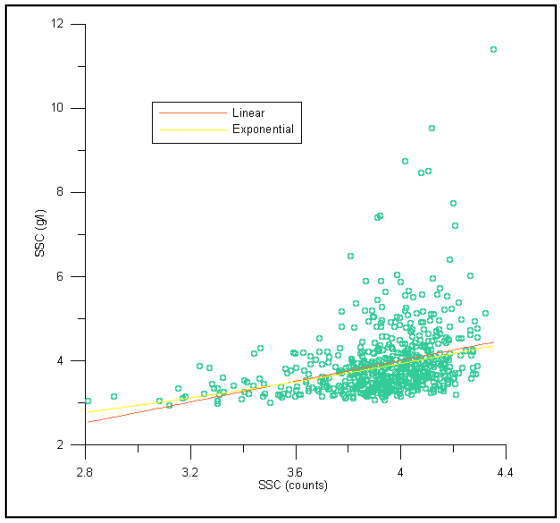

Figure 141: SSC real versus SSC calculated in case 3

On figure 140 one can see two fittings:

The green adjust is a lineal fitting with equation:
SSC OBS=0.8525*SSC all outputs + 1.13586 with R^2= 0.02322 (86)

The yellow adjust is an exponential fitting with equation:
SSC OBS= $3.300*e^{0.1085*SSC\ all\ outputs}$ with R^2=0.0408 (87)

On figure 141 one can also see two fittings:

The orange adjust is a lineal fitting with equation:
SSC OBS= 1.2348*SSC all outputs – 0.926 with R^2= 0.1013 (88)

The yellow adjust is an exponential fitting with equation:
SSC OBS= $1.12312*e^{0.2907*SSC\ all\ outputs}$ with R^2=0.129 (89)

As one can see if compares these results with the ones obtained in section V.3.2.1.3 the determination coefficients are more elevated which indicates better fits. However, this fits can not be used to approximate SSC calculated from ADV outputs because their determination coefficients are not higher enough (R^2=0.9).

V.3.2.3.4 Weighted running average least squared method with Correlation

Applying LS method with correlation implies that the dependence matrix Y is composed by SSC data from OBS and the independence matrix X is compose with correlation components (Corr_X, Corr_Y, Corr_Z).

As it has been seen in the last section one has to work separately in three cases: erosion waves- beginning (case 1), erosion waves-ending (case 2) and accretion waves (case 3).

Processing this data, vector b, the vector of the different weights in each case show:

Output	Case 1 → Weight	Case 2 → Weight	Case 3 → Weight
Corr X	-0.4991	0.0885	0.0529
Corr Y	0.9400	0.2083	-0.0184
Corr Z	0.0220	-0.2166	0.0067

Table 10: Relation of weight coefficients in each study case

As one can observe the most important weight is in case 1 for Corr Y, in case 2 for Corr Z whereas in case 3 is for Corr X.

Therefore if one calculates the concentration with these outputs and these weights one obtains:

CASE 1: *ADV concentration= -0.4991*CorrX +0.9400*CorrY +0.0220*CorrZ* (90)

CASE 2: *ADV concentration= 0.0885*CorrX +0.2083*CorrY -0.2166*CorrZ* (91)

CASE 3: ADV concentration= 0.0529*CorrX -0.0184*CorrY +0.0067*CorrZ (92)

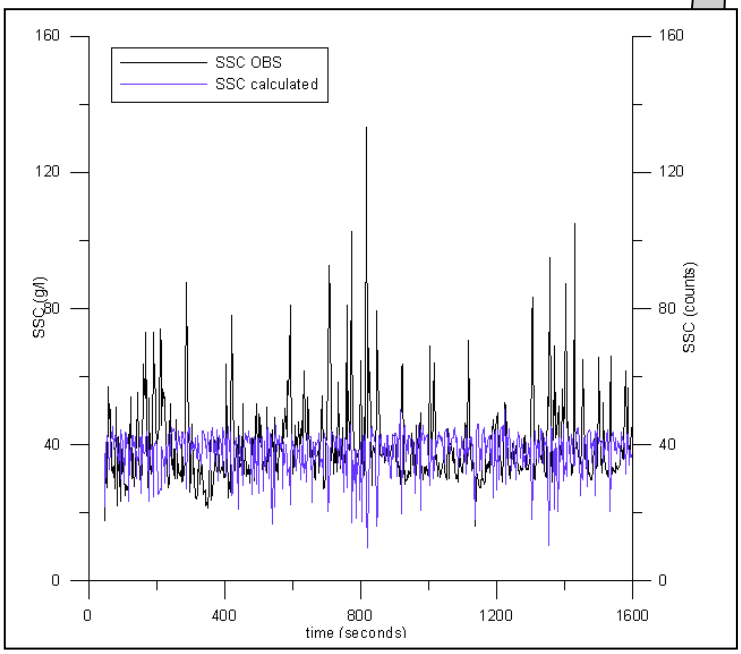

Figure 142: Concentrations along time for case 1

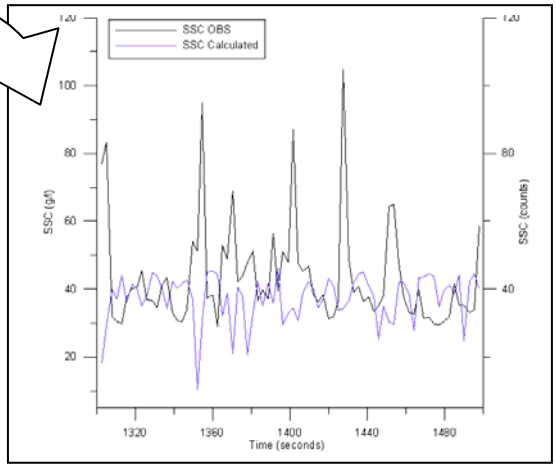

Figure 143: Zoom of Concentrations along time for case 1

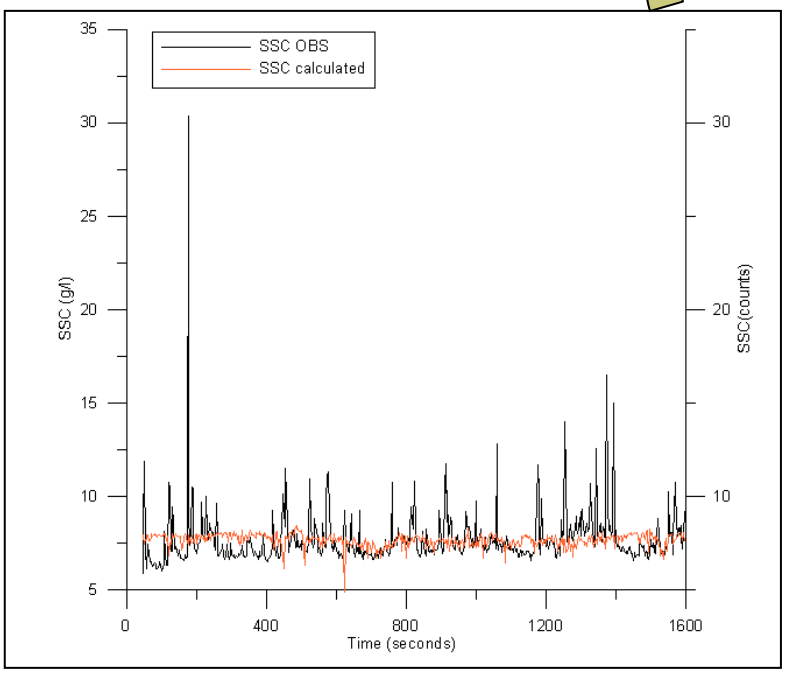

Figure 144: Concentrations along time for case 2

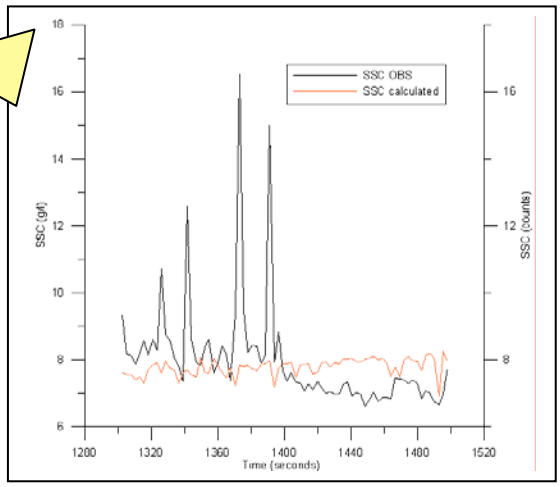

Figure 145: Zoom of Concentrations along time for case 2

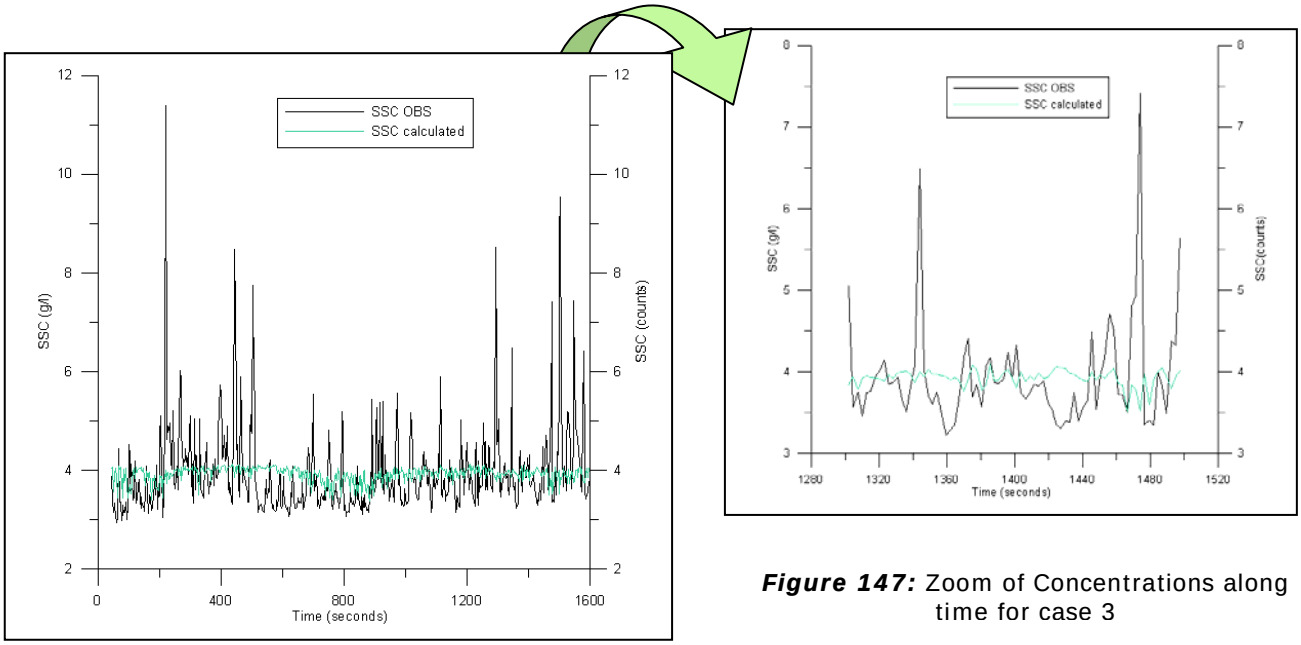

Figure 146: Concentrations along time for case 3

Figure 147: Zoom of Concentrations along time for case 3

Observing these plots one can notice that for instance, in figures 142 and 143 calculated SSC has peaks in downward direction when SSC from OBS has peaks in upward direction. Agreeing with that one has also seen figures 100 and 101, in section V.3.2.1.4, where these differences where bigger due to the non smoothness of the applied data.

As well as this, in figure 144 and 145 we can also notice this peaks in downward direction and how in figures 102 and 103, in section V.3.2.1.4, these are more signifier.

In contrast in case three, figures 146 and 147, one can not appreciate these big peaks in downward direction. Here, the SSC calculated is like a smooth line with small oscillations around 5 counts, making non sense if there is a peak or a valley.

Therefore, observing these results, one should to try to find a fitting in all cases but not expecting too much.

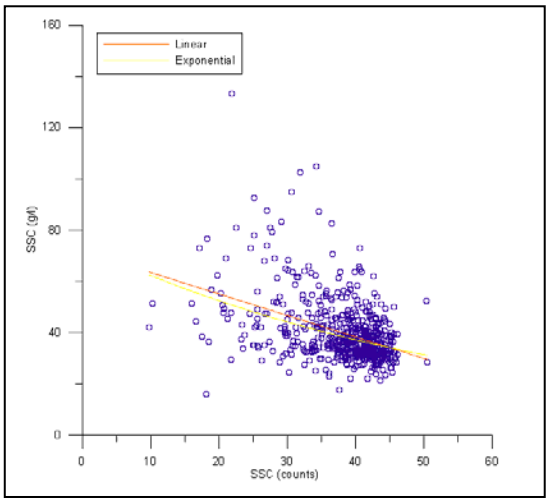

Figure 148: SSC real versus SSC calculated in case 2

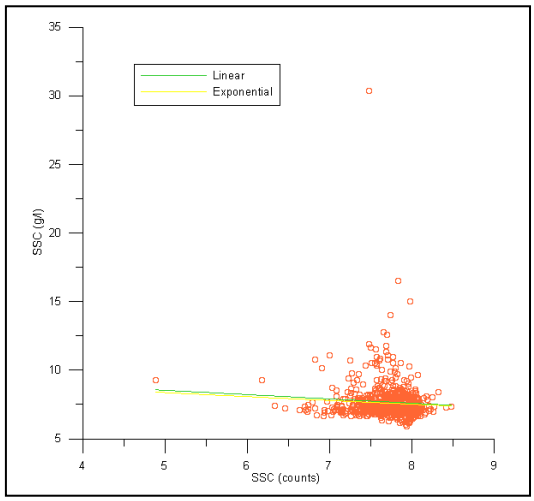

Figure 149: SSC real versus SSC calculated in case 2

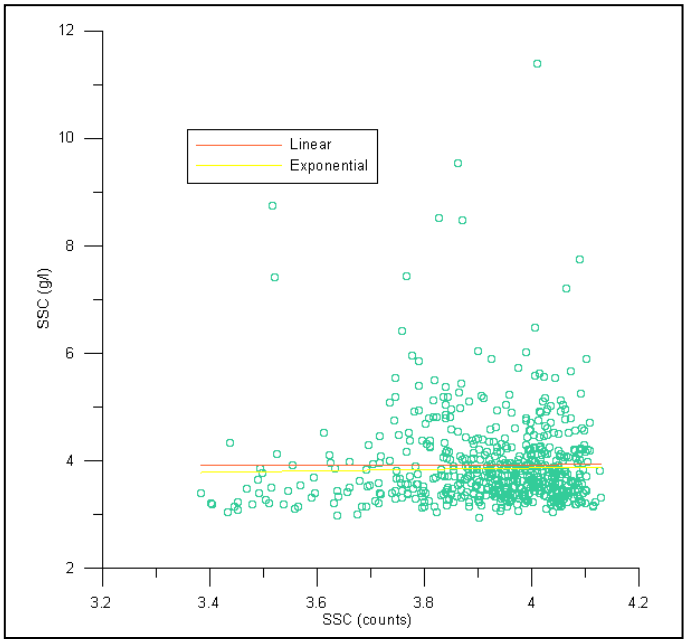

Figure 150: SSC real versus SSC calculated in case 3

On figure 148 one also sees two fittings:

The orange adjust is a lineal fitting with equation:
SSC OBS= -0.8401*SSC all outputs + 71.873 with R^2= 0.176 (93)

The yellow adjust is an exponential fitting with equation:
SSC OBS= $74.0097*e^{-0.01723*SSC\ all\ outputs}$ with R^2=0.166 (94)

On figure 149 one can see two fittings:

The green adjust is a lineal fitting with equation:
SSC OBS=-0.031309*SSC all outputs + 10.097 with R^2= 0.0051 (95)

The yellow adjust is an exponential fitting with equation:
SSC OBS= $9.986*e^{-0.03549*SSC\ all\ outputs}$ with R^2=0.0072 (96)

On figure 150 one can also see two fittings:

The orange adjust is a lineal fitting with equation:
SSC OBS= 0.03225*SSC all outputs +3.8091 with R^2= 3.0788E-05 (97)

The yellow adjust is an exponential fitting with equation:
SSC OBS= $3.3546*e^{0.0358*SSC\ all\ outputs}$ with R^2=0.016 (98)

Notice how all the figures 148, 149 and 150 show a negative slope in the fitting. That indicates that SSC from OBS and SSC calculated are negatively correlated. Pay attention to the fact that the best fit is in case 1 which from one would wait for the worst fit at the beginning (figure 143).

V.3.2.4 Multivariate analysis

Multivariate analysis is carried out on a data matrix of five variables including SSC, SNR, dimensionless mean sediment diameter (d_{50}/d_{50b}), coefficient of gradation (C_g), and dimensionless absorption coefficient (α/α_c). Here, d_{50b} is the particle diameter corresponding to predicted maximum sensitivity for the ADV (d_{50b}= 0.025mm), α_c is the absorption coefficient for the calibration temperature calculated using:

$$\alpha = 8.687 \times \frac{3.38*10^{-6}*f^2}{21.9*10^{6-(1520/T+273)}} \quad (99)$$

Where 8.687 is the conversion factor from nepers to decibels, α is the absorption coefficient, f is the acoustic frequency, in kilocycles per second and T is the water temperature in ºC.

And finally Cg is the coefficient of gradation calculated as:

$$Cg = (D_{30})^2 / (D_{60} \times D_{10}) \quad (100)$$

Therefore:

T=14ºC, f= 100Hz= 0.1 kilocycles per second, α = 2.6516E-08, Cg= 7.49E-01, d_{50b} = 2.46E-01.

T=4ºC, f= 100Hz= 0.1 kilocycles per second, αc = 0.05, Cg= 7.49E-01, d_{50b} = 2.46E-01.

(Sebnem Elçi, Ramazan Aydm· Paul A. Work)

Results from multivariate analysis in the different study cases shows:

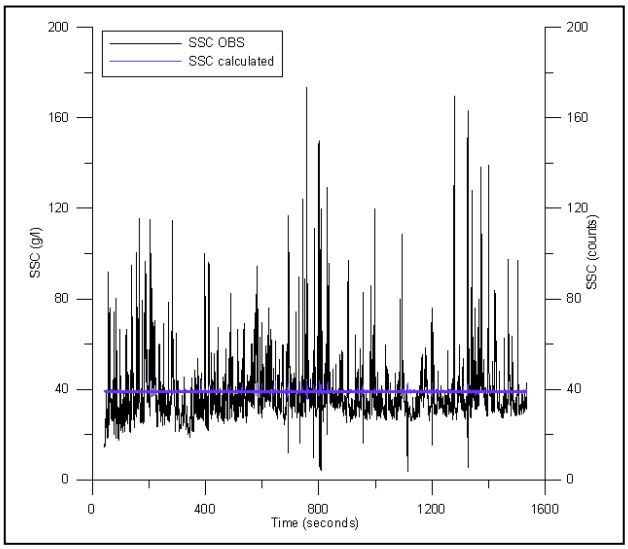

Figure 151: Concentrations along time for case 1

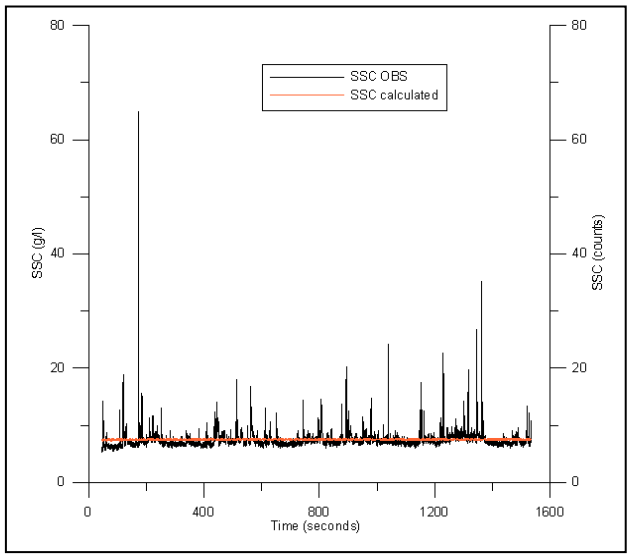

Figure 152: Concentrations along time for case 2

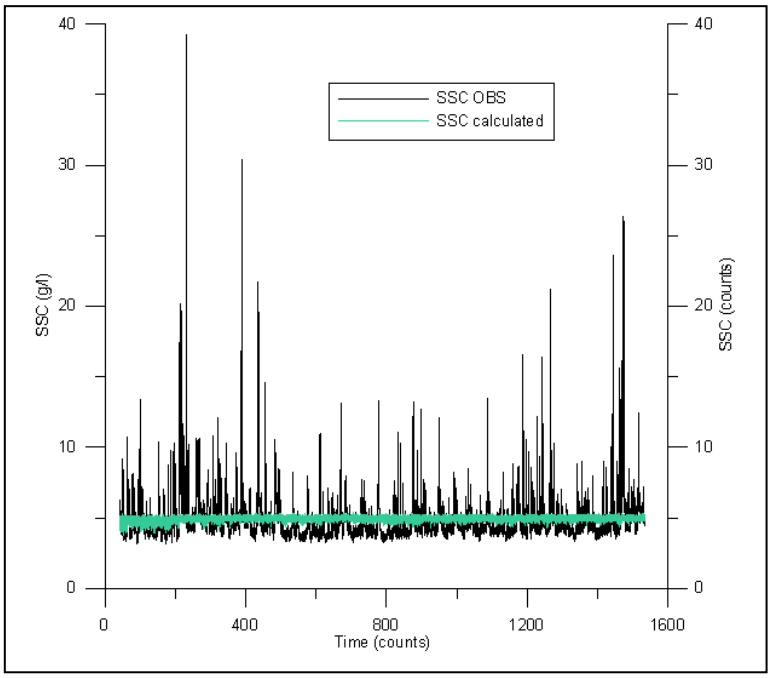

Figure 153: Concentrations along time for case 3

As one can appreciate in these figures concentration calculated differs from real concentration. We can appreciate that real concentration oscillates a lot compared to the one obtained with the multivariate analysis.

If one tries to correlate the variables one obtains figures 154, 155 and 156 where no relation can be expected.

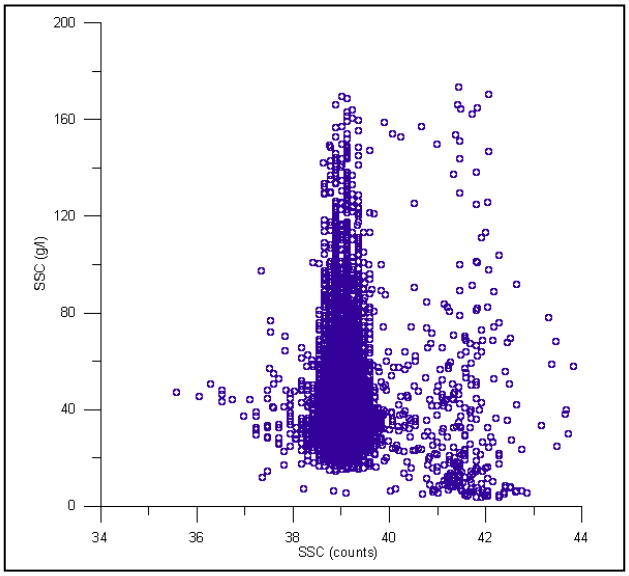

Figure 154: SSC real versus SSC calculated in case 1

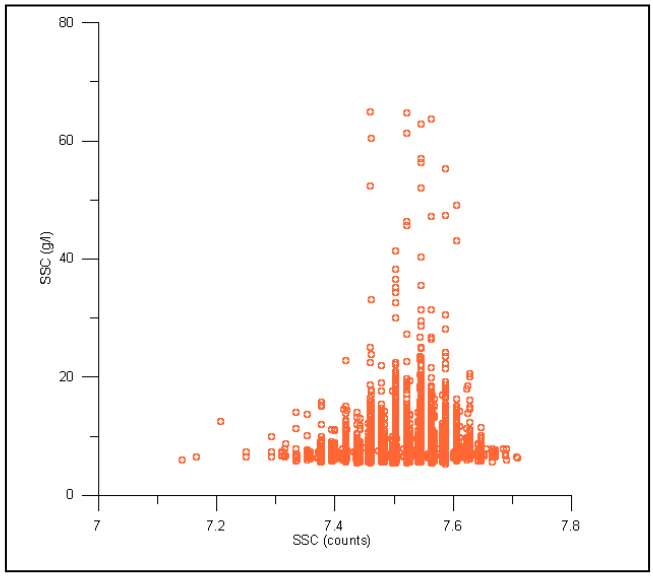

Figure 155: SSC real versus SSC calculated in case 2

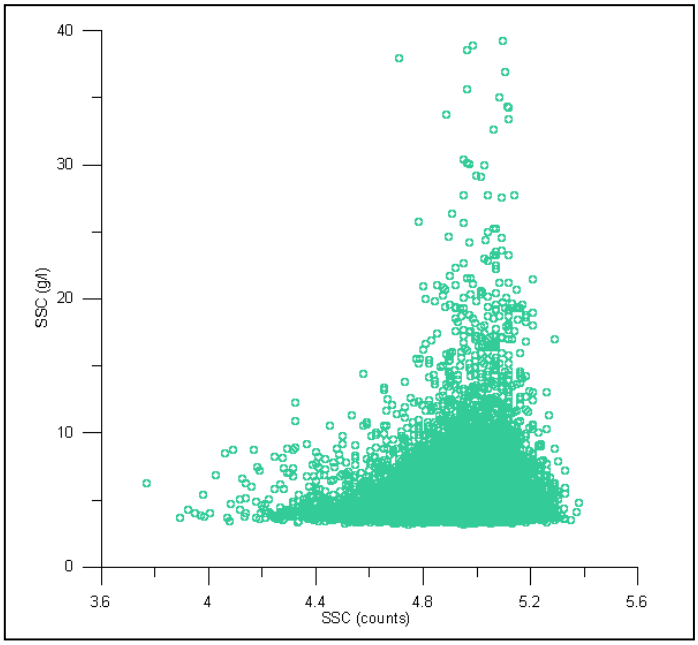

Figure 156: SSC real versus SSC calculated in case 3

As it has been seen before and now one can appreciate no relation between suspended sediment concentrations obtained by OBS and suspended sediment concentration obtained trough multivariate analysis can be found if we work with all data.

The authors, in they work, say that some relation can be expected if we work with concentration below 10 g/l. It has to be on mind but, that they were working on a river where there is less sediment in suspension than in the surf zone where we work.

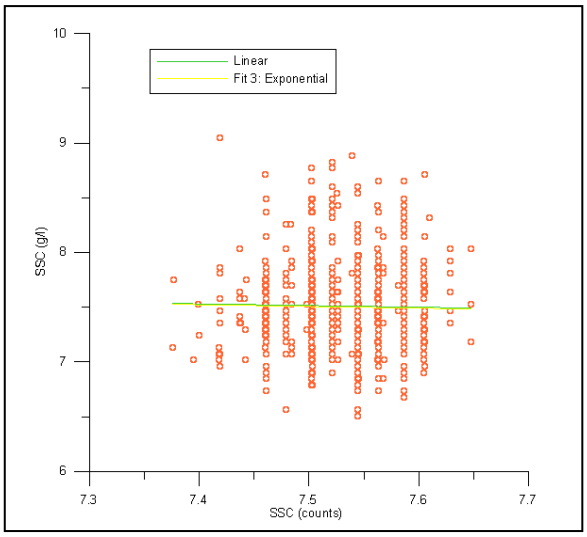

Figure 157: SSC real versus SSC calculated in case 2

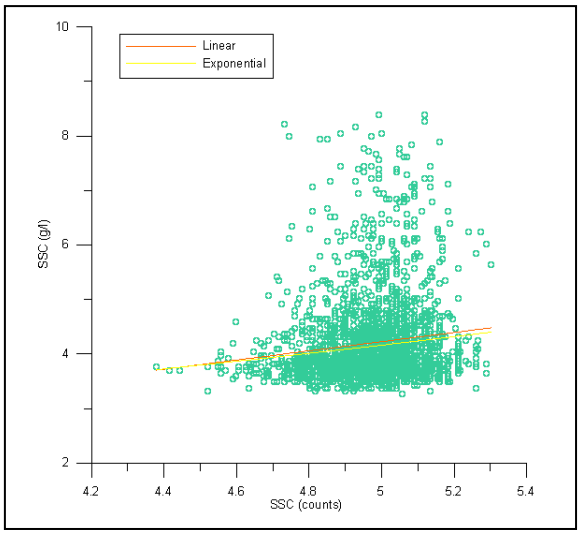

Figure 158: SSC real versus SSC calculated in case 3

The equations and determinations coefficients of these fittings are:

On figure 157 one can see two fittings:

The green adjust is a lineal fitting with equation:
SSC OBS=-0.151173*SSC all outputs + 8.64941 with R^2= 0.0003152 (101)

The yellow adjust is an exponential fitting with equation:
SSC OBS= $8.773*e^{-0.0207*SSC\ all\ outputs}$ with R^2=0.0003452 (102)

On figure 158 one can also see two fittings:

The orange adjust is a lineal fitting with equation:
SSC OBS= 0.84316*SSC all outputs +0.0102 with R^2= 0.0157 (103)

The yellow adjust is an exponential fitting with equation:
SSC OBS= $1.6598*e^{0.1839*SSC\ all\ outputs}$ with R^2=0.018 (104)

As one can observe from figures 157 and 158 both are under SSC< 10 g/l but the distributions are very different and also, in one the fits are better than in the other. This could be for the case on which we are working (erosion or accreting), like happened to the authors of the work. In flooding conditions (here should be erosion conditions) this method was not working, as we can appreciate.

Also one should notice that in case 3 where the fits are better, these have not high enough determination coefficient to validate them. This could be for the different environment in which we are working or due to the difference frequency at which the ADV was working (100 Hz in our case versus 10MHz in the author's case).

V.3.2.5 Intensity method

A standard ADV system provides signal amplitude as part of its output record, which is measured with the same frequency and in the same sampling volume as velocities.

The signal amplitude (SA) value obtained by the ADV is proportional to the logarithm of the intensity of the acoustic signal that is backscattered from small particles within the sampling volume. Lohrmann et al. (1994) calculated the backscatter intensity (I) from ADV signal to noise ratio (SNR):

$$SNR = 10 * \log (I/NL) \quad (105)$$

Sontek (1997) recommended against calculating backscatter intensity from signal to noise ratio. This can be calculated from signal amplitude by substituting SNR= 0.43(SL-NL) into equation (105). (SL= signal amplitude and NL=noise level). Kawanisi and Yokosi (1997) present a relationship between backscatter intensity and signal amplitude:

$$I = 10^{0.043SL} - 10^{0.043NL} \quad (106)$$

If ADVs operate at high frequencies (upper 10 MHz) the noise level is small compared to signal amplitude (Kawanisi and Yokosi (1997). Kawanisi and Yokosi (1997) deduced the backscatter intensity from the averaged intensity of the three receivers. Nikora and Goring (2002) neglected the effect of noise level (NL) and used:

$$I \alpha 10^{0.0434*SA} \quad (107)$$

The backscattered intensity, I, is a function of the particle type, concentration and size of particles. The simplified relation between the intensity, I, and sediment concentration, c, can be expressed as:

$$I = \frac{I_o * c * S_f * S_a * \exp[-2r(\alpha_w + \alpha_s)]}{r^2} \quad (108)$$

Where Io is the transmitted intensity, c is the mass sediment concentration, S_f contains all system specific parameters such as transducer size, efficiency, probe geometry, and receive se sensitivity, S_a holds all the particle specific parameters (size, elasticity, and density), α_w is the water absorption, α_s is the absorption due to particle scattering, and r is the acoustic propagation path.

For low concentration, the particle attenuation is negligible. Since the acoustic frequency if the ADV is quite high (100Hz), α_w is constant, approximately. Therefore, there should be a nearly linear relationship between concentration, c, and intensity, I. Outside the linear range, the intensity is a non – linear function of the concentration and the values should not be used for sediment analysis. General experience indicates that the linear region corresponds to a sediment concentration of about 10g/l. (S.A. Hosseini, A. Shamsai, B. Ataie-Ashtiani).

In this study, I is given as the average of three intensity values obtained by three receivers. Then, for low concentration eq.75 is simplified as:

$$Ia \alpha c \alpha (10^{0.0434\,SA1} + 10^{0.0434\,SA2} + 10^{0.0434\,SA3}) - (10^{0.0434\,NL1} + 10^{0.0434\,NL2} + 10^{0.0434\,NL3}) \quad (109)$$

Where SA_1, SA_2 and SA_3 are the signal amplitudes obtained by three receiving transducers, NL_1, NL_2 and NL_3 are the noise level in the three directions and Ia is the average of three intensity values obtained by three receivers.

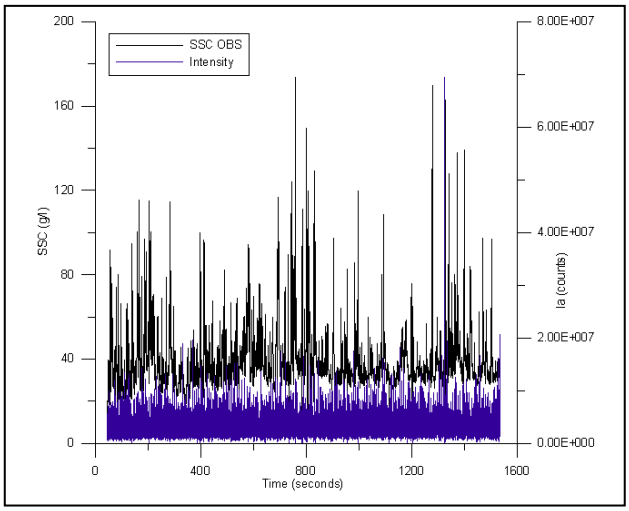

Figure 159: SSC and intensity versus time in case 1

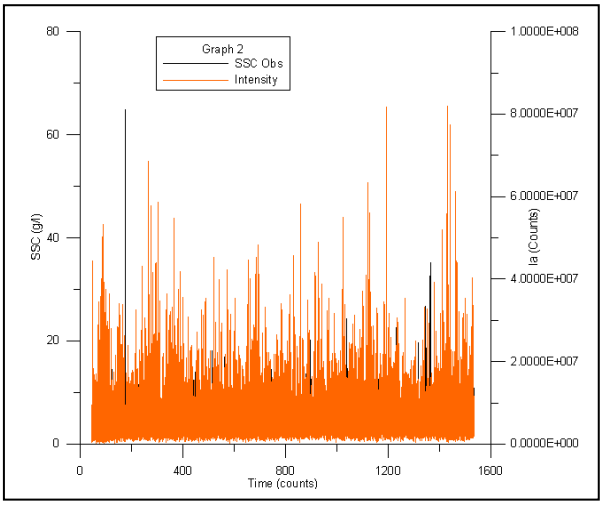

Figure 160: SSC and intensity versus time in case 2

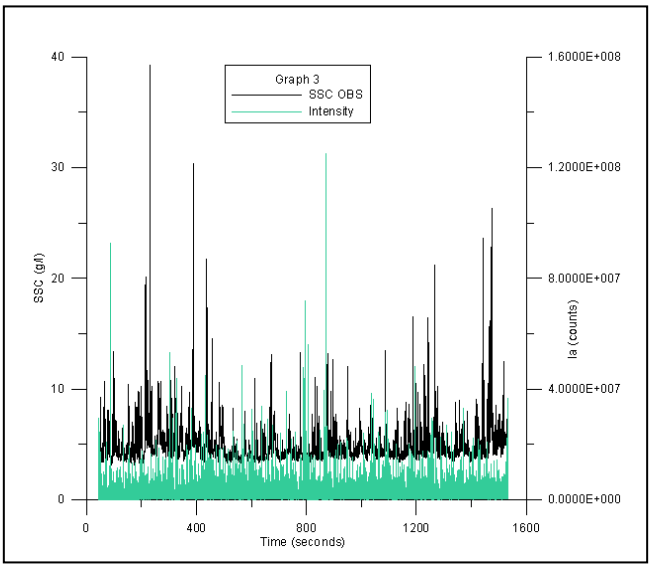

Figure 161: SSC and intensity versus time in case 3

From these figures seems that intensity is a good method to adjust the suspended sediment concentration. Therefore we are going to try to find a correlation between both variables using a least squared method.

Before but, notice how figures 159 and 161 seems to adjust better than figure 160, where suspended sediment concentration measured with OBS seems to be embedded by intensity.

Even if in figure 159, case 1, intensity seems to follow better SSC from OBS that in figure 161 for case 3, also in the peaks.

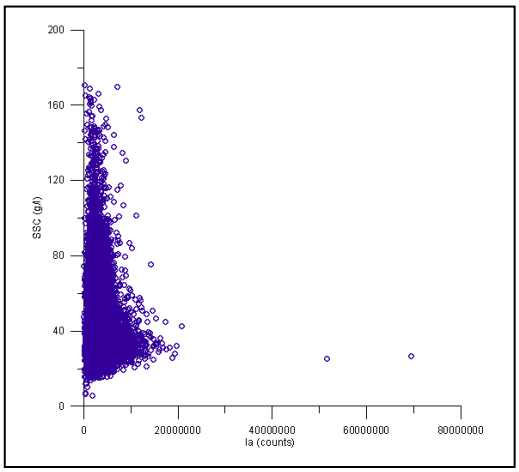

Figure 162: SSC versus intensity in case 1

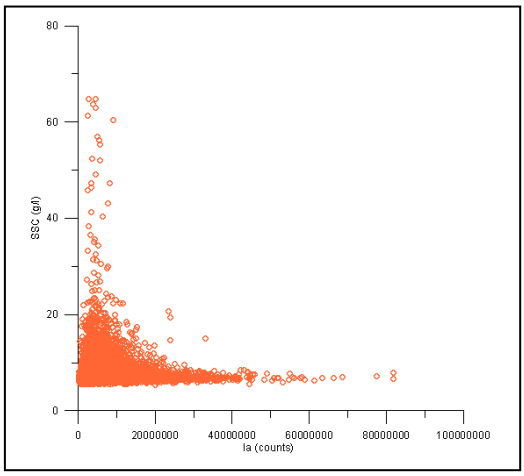

Figure 163: SSC versus intensity in case 2

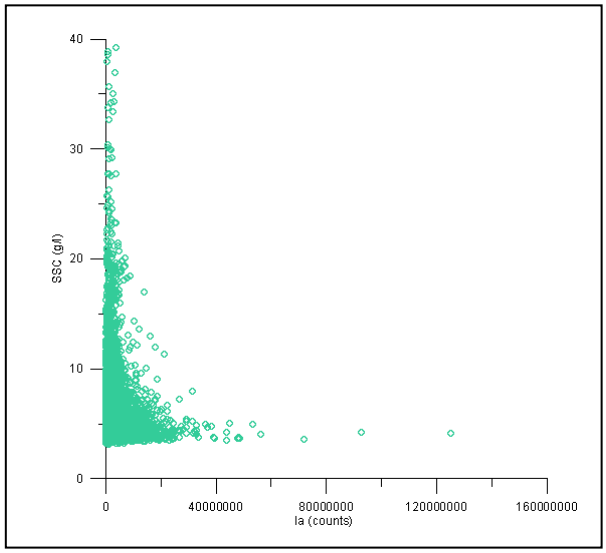

Figure 164: SSC versus intensity in case 3

Observing these plots one can appreciate that no correlation between suspended sediment concentration and intensity can exist, at least without working with the data. Although in figures 160 and 161 a good agreement seemed to be between SSC from OBS and intensity.

In figures 162, 163 and 164 one observes concentrations above 10 mg/l. All concentrations over this 0 to 10g/l are in the same vertical line and no relation can be found. When one observes values under 10g/l seems that some relation could be found.

In case 2, where concentration is higher than in case 3 we can work with 951 points, while in case 3 we can work with 2341 points. In case 1 a few points can be useful therefore we just skip this case. Anyway we don't expect too much relation.

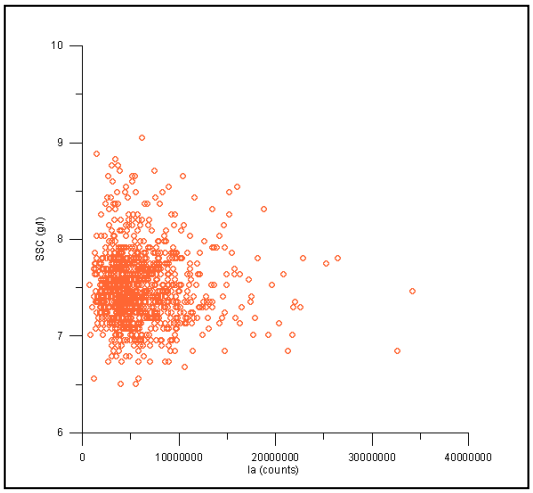

Figure 165: SSC versus intensity in case 2

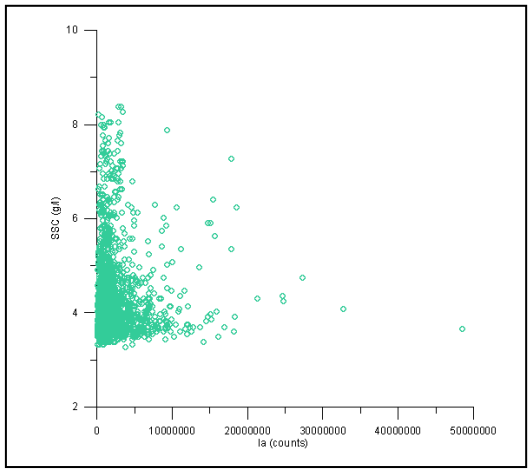

Figure 166: SSC versus intensity in case 3

As it can be expected no correlation can be found even if we are under SSC<10 g/l. This contradiction with what the authors tell can be due to the different working amplitude of the ADV (10MHz versus 100 HZ) or due to the environment where the experiments were carried out (tank laboratory versus channel laboratory).

As no results are obtained with a direct method we tried to apply a weighted least squared method which we can obtain an SSC from intensity and try to correlate it with SSC from obtained from OBS. The result obtained is:

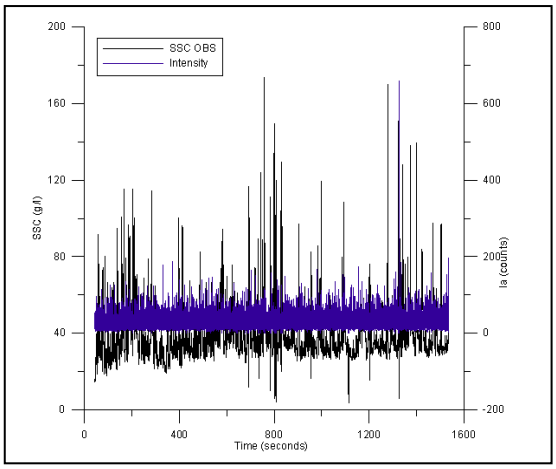

Figure 167: SSC and SSC from intensity versus time in case 1

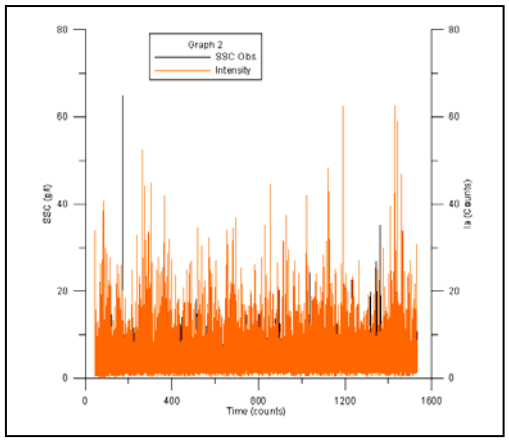

Figure 168: SSC and SSC from intensity versus time in case 2

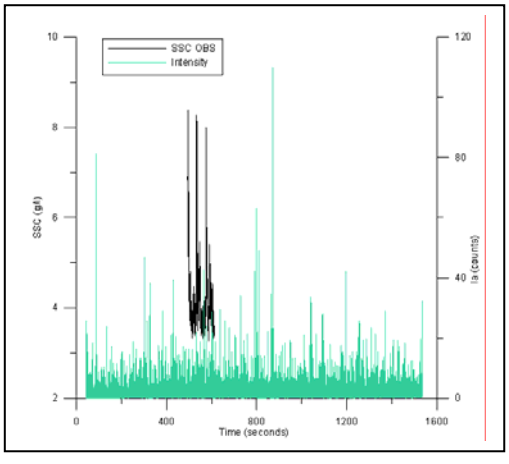

Figure 169: SSC and SSC from intensity versus time in case 3

From these figures one can observe that seems that no relation can be found. Also these figures seem to show a worst adjustment than before with least squared method. Anyway we are going to try to correlate both variables.

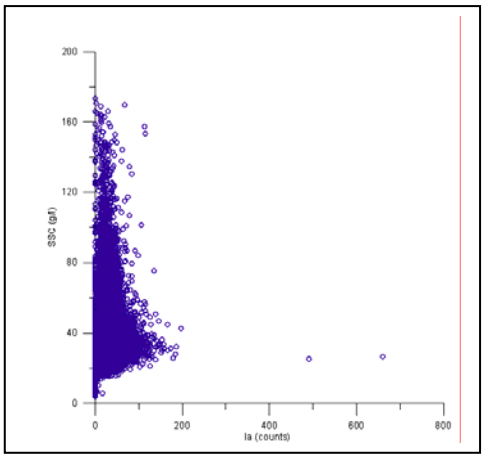

Figure 170: SSC versus intensity in case 1

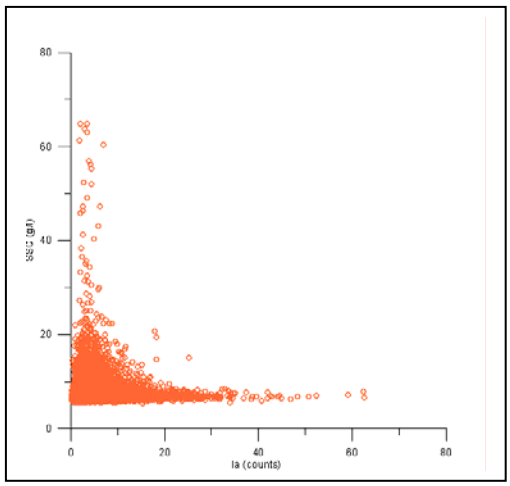

Figure 171: SSC versus intensity in case 2

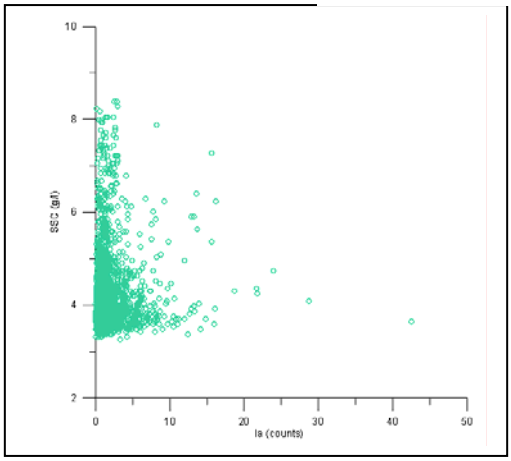

Figure 172: SSC versus intensity in case 3

As one can see in these figures no relation can be found, as was expected. As explained before this could be due to the different working amplitude of the ADV (10MHz versus 100 HZ) or due to the environment where the experiments were carried out (tank laboratory versus channel laboratory).

V.3.2.6 Backscatter intensity and turbidity

As Hubert Chanson, Maiko Takeuchi and Mark Trevethan did in their study we also have tried to work with backscattered intensity and turbidity.

Applying their method we have calculated the backscattered intensity from the average amplitude like:

$$BSI = 10^{-5} \times 10^{0.043*Ampl} \quad (110)$$

And turbidity like :

$$Turb = 171.6 \times (1-\exp(-0.1593 \times BSI)) \quad (111)$$

The evolution of these two variables along the time is:

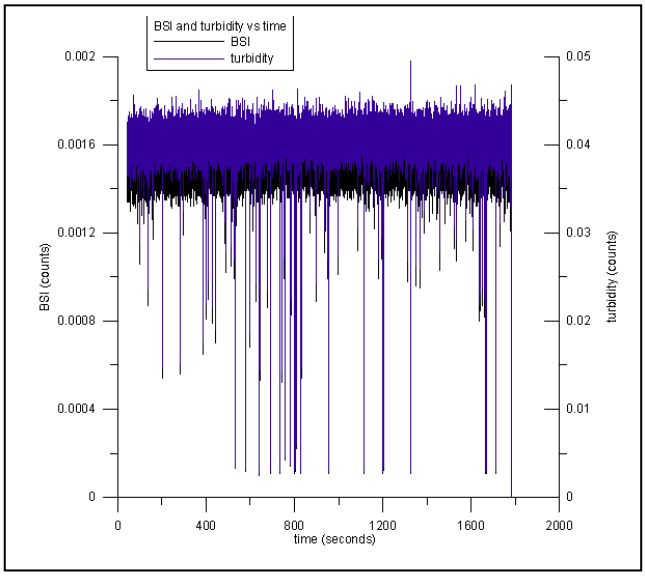

Figure 173: BSI and turbidity along the time in case 1

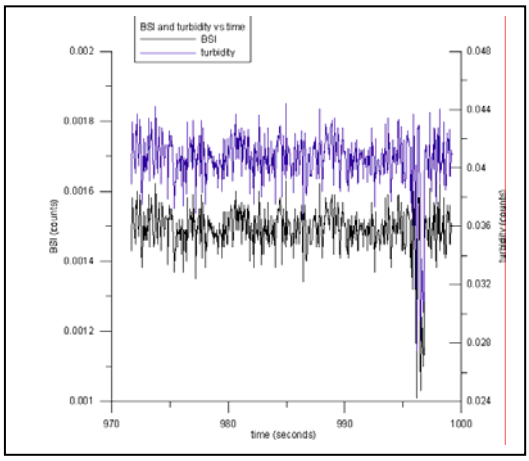

Figure 174: Zoom of BSI and turbidity along the time in case 1

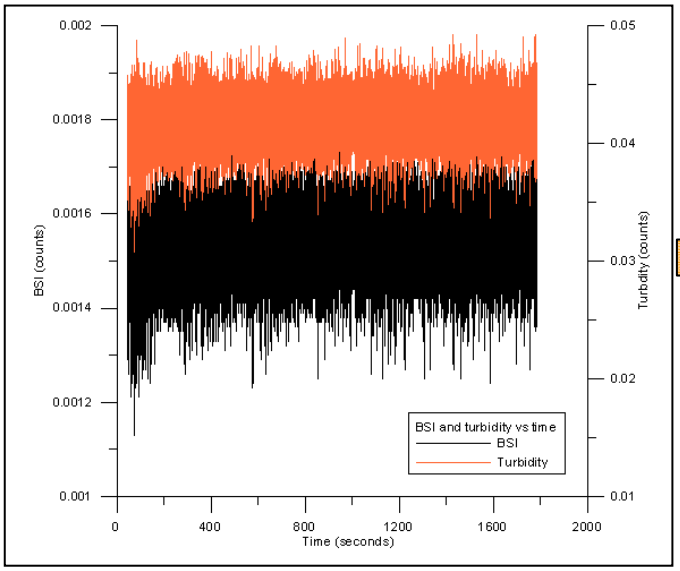

Figure 175: BSI and turbidity along the time in case 2

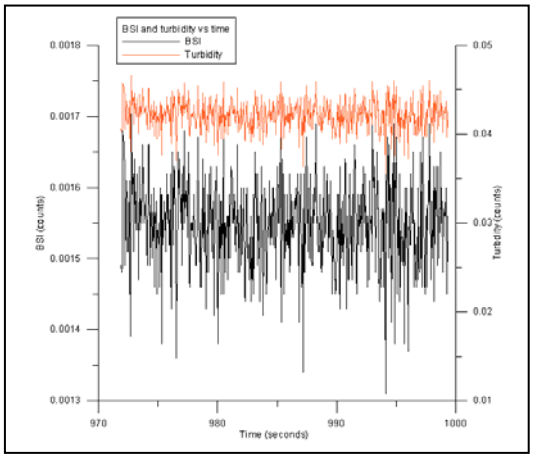

Figure 176: Zoom of BSI and turbidity along the time in case 2

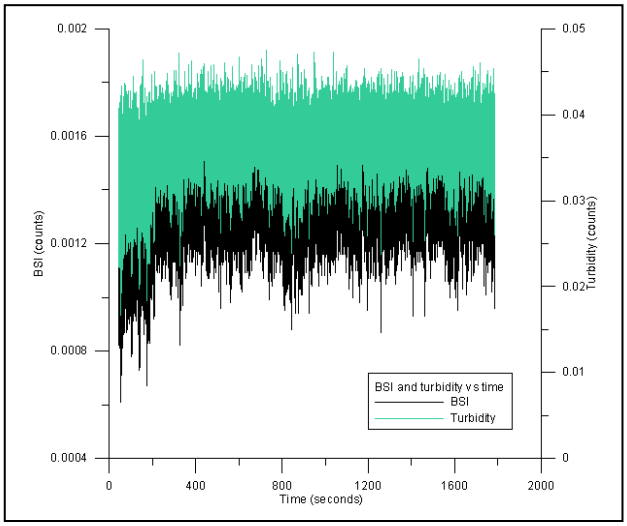

Figure 177: BSI and turbidity along the time in case 3

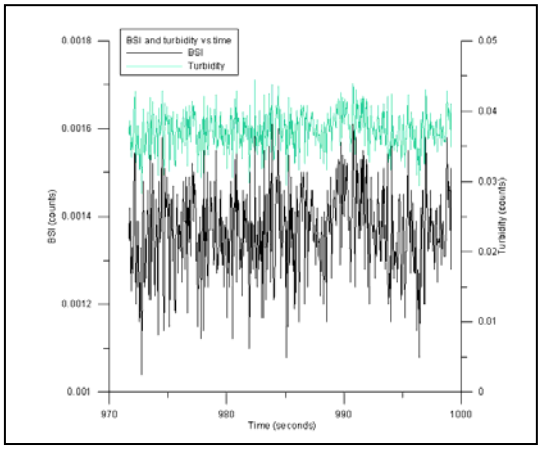

Figure 178: Zoom of BSI and turbidity along the time in case 3

From figure 173 to figure 178 we can appreciate the evolution along time of BSI and turbidity for all three study cases. In all figures one can appreciate how the distributions are quite similar. But notice that in case 1, figure 174 is where the evolutions seems to be more closers.

V.3.2.6.1 SSC versus BSI

When one tries to get a relation between SSC obtained by OBS and BSI we deal, like always, that we should separate take into account the three study cases: erosion waves- beginning (case 1), erosion waves-ending (case 2) and accretion waves (case 3).

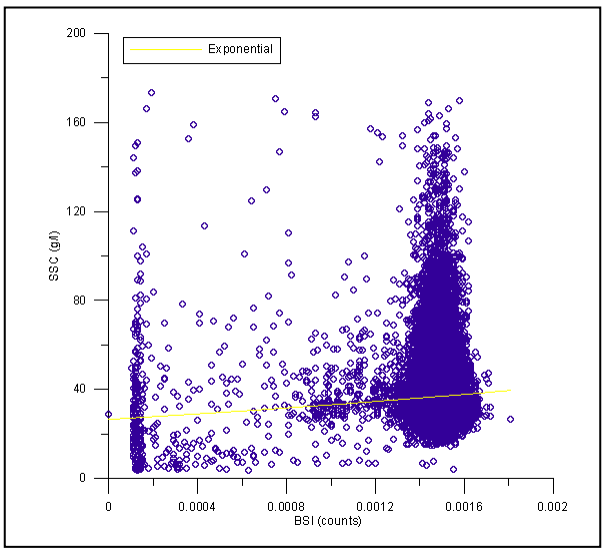

Figure 179: SSC versus intensity in case 1

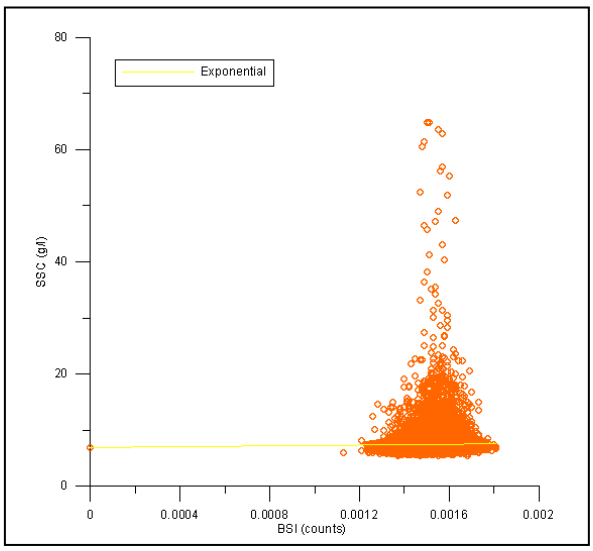

Figure 180: SSC versus intensity in case 2

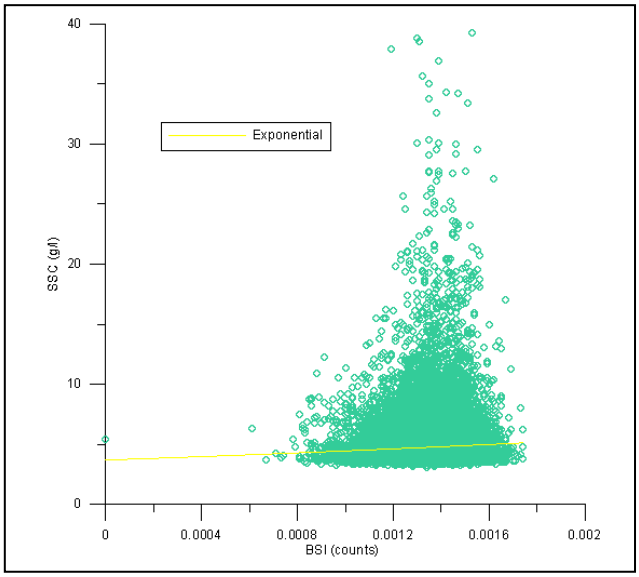

Figure 181: SSC versus intensity in case 3

In figure 179 we have drown one possible adjustment, just the one that fits in the best way. This is an exponential fit which equation and determination coefficients are:

$$SSC = 26.5386 \times \exp(220.4397 \times BSI) \quad \text{with } R^2 = 0.0102 \qquad (112)$$

In figure 180 we have drown one possible adjustment, just the one that fits in the best way. This is an exponential fit which equation and determination coefficients are:

$$SSC = 6.8879 \times \exp(49.982 \times BSI) \quad \text{with } R^2 = 0.000512 \qquad (113)$$

In figure 181 we have drown one possible adjustment, just the one that fits in the best way. This is an exponential fit which equation and determination coefficients are:

$$SSC = 3.6783 \times \exp(188.774 \times BSI) \quad \text{with } R^2 = 0.00678 \qquad (114)$$

Although this fits have a low determination coefficient that indicates that are not so good, notice how case 1 has the best fit, as we have already noticed in figure 174. Therefore one can sum up that we can not found any viable adjustment in difference to the original study.

V.3.2.6.1 SSC versus turbidity

Observing that we have found no result until now working with backscattered intensity, in this section we will try to find a relation between suspended sediment concentration obtained from OBS and turbidity calculated as a function of backscattered intensity.

$$Turb = 171.6 \times (1-\exp(-0.1593 \times BSI)) \qquad (115)$$

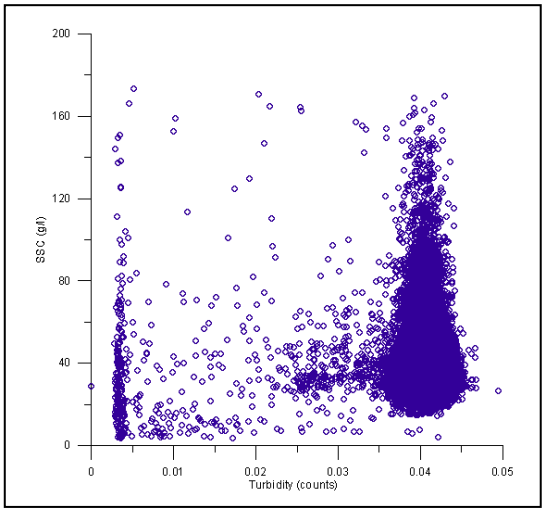

Figure 182: SSC versus intensity in case 3

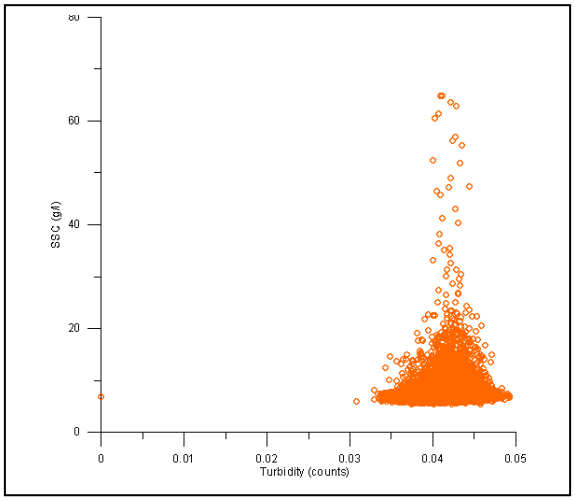

Figure 183: SSC versus intensity in case 3

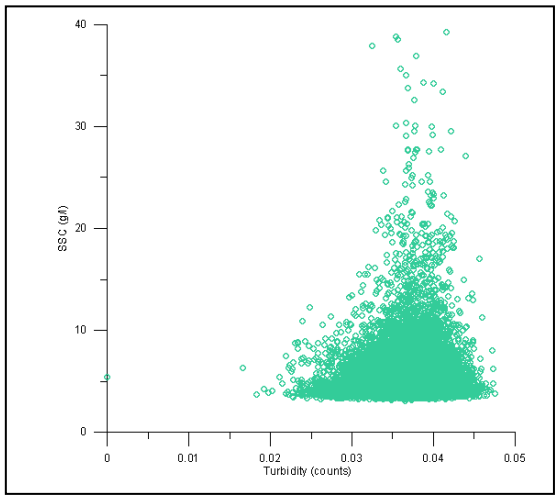

Figure 184: SSC versus intensity in case 3

Observing these figures one can appreciate that the distribution that they show is the same that in the case of the suspended sediment concentration from OBS versus backscattered intensity (BSI), as one can expect because turbidity is a function of BSI. Therefore, seeing these plots we have looked for no correlation because we already know that this doesn't exist.

Therefore, suspended sediment concentration can not be approximated by turbidity and BSI.

V.3.3 Conclusions

In this part of the study we have analysed several methods in order to try to estimate suspended sediment concentration from different outputs given by the ADV sensor.

In general it can be concluded that indirect methods approximations adjust better the real concentration to the calculated concentration than direct methods. Notice how in weighted least squared method (WLSM, indirect) seems that the approximations adjust better the real concentration to the calculated concentration than the least squared method (LS, direct); in fact in WLSM we can find a relation while in LS is impossible.

Paying attention to the running average method (RAM) in direct way and weighted running average least squared method (WRALSM) in indirect way, we should remark that in both cases applying RAM we get smoother results, but that the maximum determination coefficient was found with WRALSM (R^2= 0.25).

When the multivariate analysis is applied to the obtained data a change of the coefficients on the independence matrix of WLSM was done in order to find a better relation but, contrary to our expectations no reliable correlation could be found.

Moreover another method has been attempted, the intensity method. That one, and following authors that had worked with it, should have given us, for low concentration (under 10g/l), a linear relation, but contrary to that we could not found any relation.

On the other hand, in the last method applied (backscattered intensity and turbidity) some relation stronger for case 1 than for case 2 and 3 has been found, although this is not enough to get a reliable approximation.

Observing the results obtained one is able to notice that the better relations were obtained when working with case 1 where concentrations are above 10g/l in disagreement to that many authors expose in their works.

Knowing the conditions in which ADV was working (very high concentrations in general) and getting no reliable relation, one can think that these sensors were reaching high rates of suspended sediment concentration (near saturation).

VI. Applying existing methods

In the last section of this work we have tried to found a method to correlate the suspended sediment concentration from an OBS with the outputs of an ADV. As has been seen, after applying several statistical and mathematics tools, no method with enough reliability could be found.

Due to that in this section the equations that other authors found are applied to data obtained from the experiments carried out in CIEM flume in order to know the reliability of their results and if their relations work on well with this data got it from the outputs of the sensors used.

VI.1 Least squared method and multivariate analysis

If one follows the indications that Sebnem Elçi, Ramazan Aydn and Paul A. Work gave in their work one can try to get a relation between SSC and SNR on a first step and later on improve it by means of absorption coefficient, particle diameter and gradation coefficient.

When that information is used one should take care about the results obtained because of the difference environment in which sensors are working[10]. Also one should separate the different study cases because not all of them have the same concentration and in their work they affirm that their results are just applicable to low suspended sediment concentration (under 10 g/l).

Therefore one should just work with case 2 (erosion wave) and case 3 (accretion wave) and with concentration under 10 g/l, although maybe this is in a small interval of time.

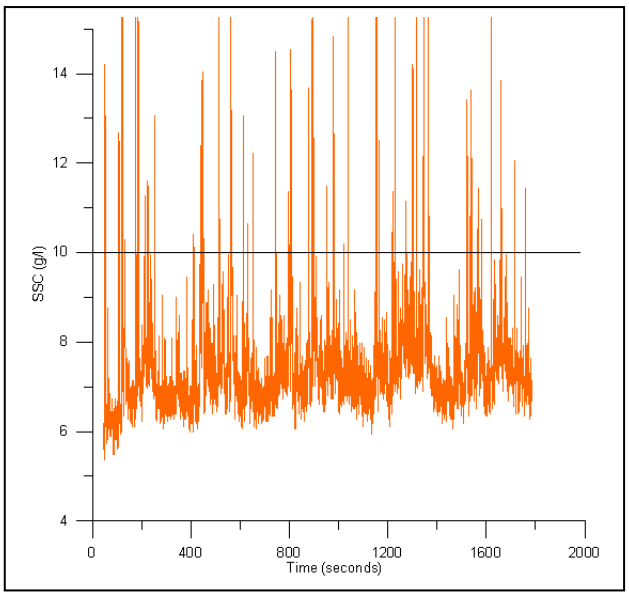

Figure 185: SSC versus time in case 2

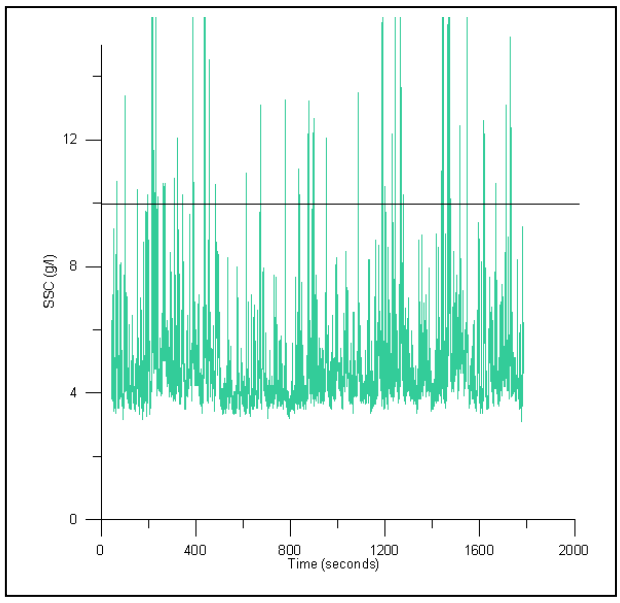

Figure 186: SSC versus time in case 3

[10] We work with data from a surf zone while they were working with data from a river. Sediment characteristics are going to be different.

As one can appreciate from figures 185 and 186 the intervals where one can find suspended sediment concentration under 10 g/l are small in both cases.

For case 2 this interval is composed by 2996 points while for case 3 the interval is composed by 3271 points.

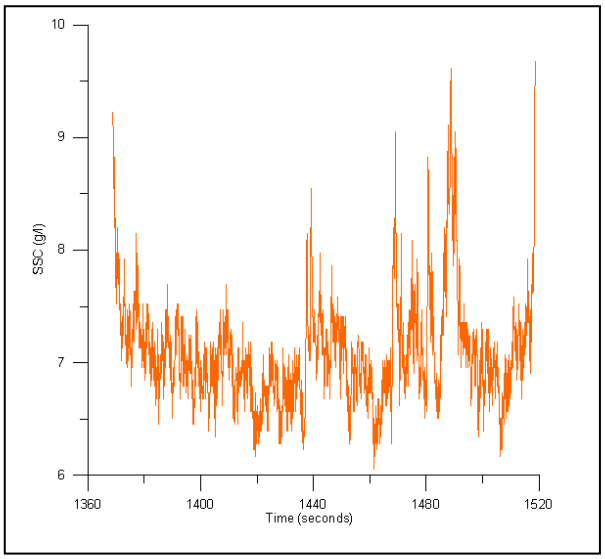

Figure 187: SSC under 10 g/l along a time interval in case 2

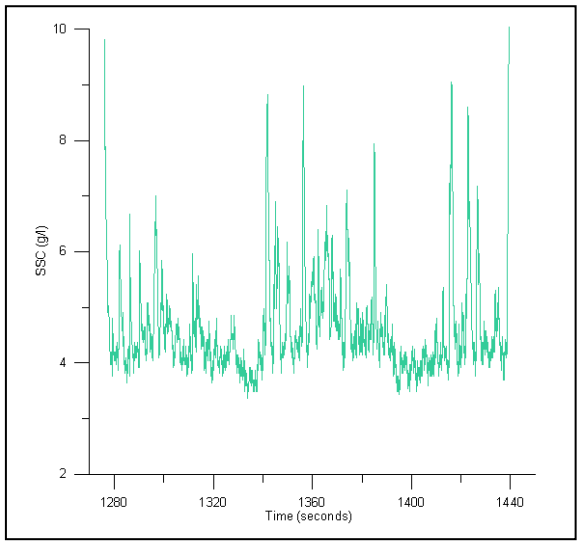

Figure 188: SSC under 10 g/l along a time interval in case 3

As can be expected we have more data points in case 3 than in case 2, but anyway the difference is very small. Also notice that the intervals taken are both around 1400 seconds.

Taking in account all the notions exposed before we can start with the first relation:

SSC = 1.49 x SNR – 13.5 (116)

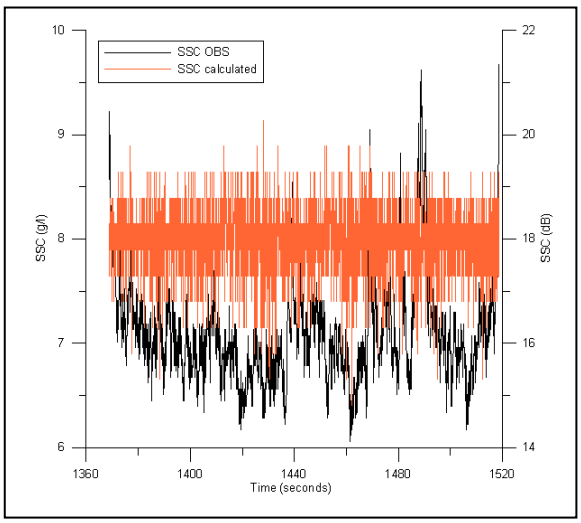

Figure 189: SSC from OBS and SSC calculated along the time in case 2

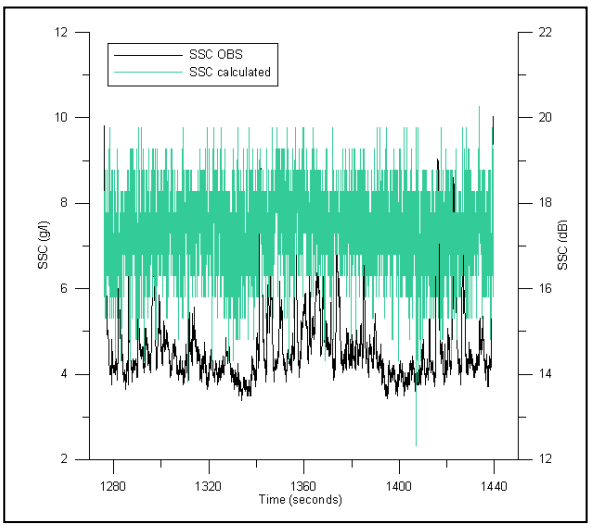

Figure 190: SSC from OBS and SSC calculated along the time in case 3

As one can observe in these figures suspended sediment concentration calculated from SNR follows the shape of SNR along the time (figure 41 and 42) and therefore presents a pulsating structure with a lot of pulses for moment measured.

When one tries to correlate these data, obtains:

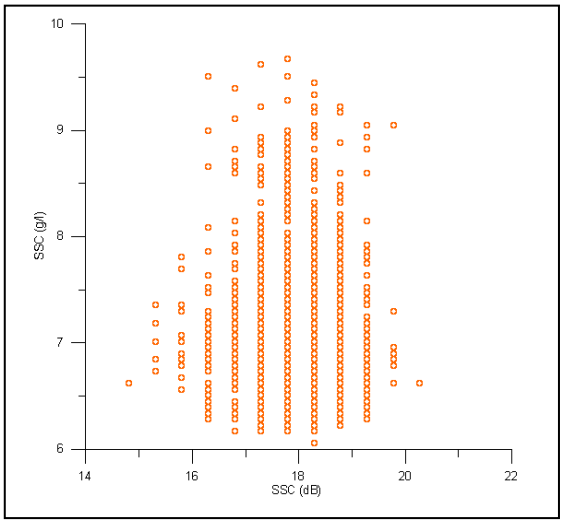

Figure 191: SSC from OBS versus SSC calculated in case 2

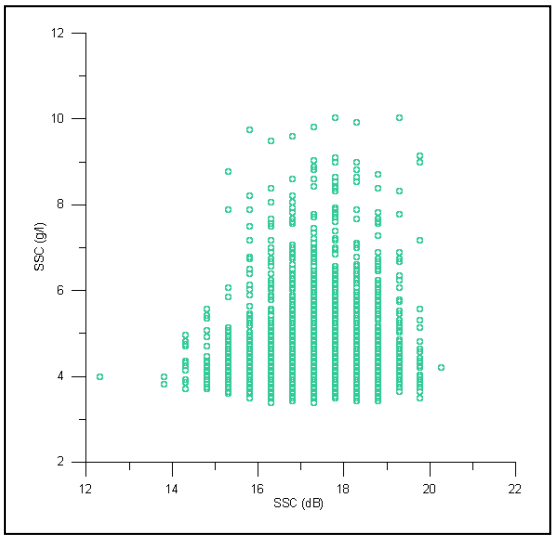

Figure 192: SSC from OBS versus SSC calculated in case 3

Observing these plots one can appreciate how no relation can be found. They are quite similar to the ones obtained with the least squared method (figures 50 and 51).

Therefore, contrary what to the authors affirm, this method is not working for our case possibly due to the different working environment and frequency of ADV.

Working with the second relation present in this work in which the authors combine SNR, absorption coefficient, particle diameter and gradation coefficient in order to smooth the SSC calculated from just SNR we get:

$$SSC = -13.8 + 0.8 \times SNR + 21.04 \times \alpha/\alpha_c + 4.52\ d_{50}/d_{50b} \times Cg \qquad (117)$$

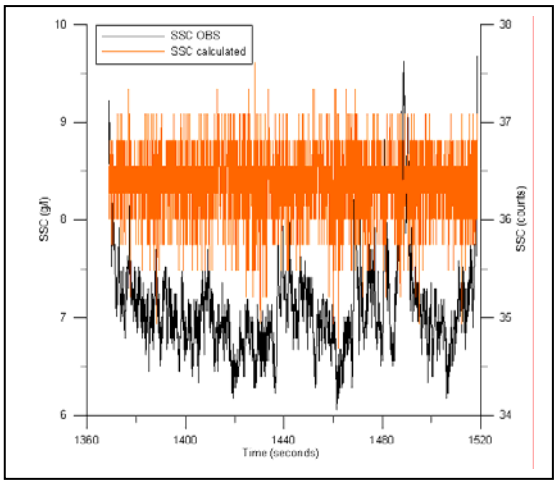

Figure 193: SSC from OBS and SSC calculated along the time in case 2

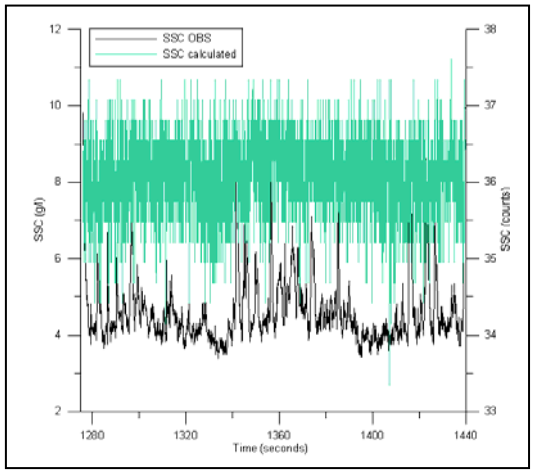

Figure 194: SSC from OBS and SSC calculated along the time in case 3

Observing figures 193 and 194 one still can appreciate how SSC calculated has the shape of SNR (figures 41 and 42). This is due to the weight of SNR in the equation.

Trying to correlate these data, one obtains:

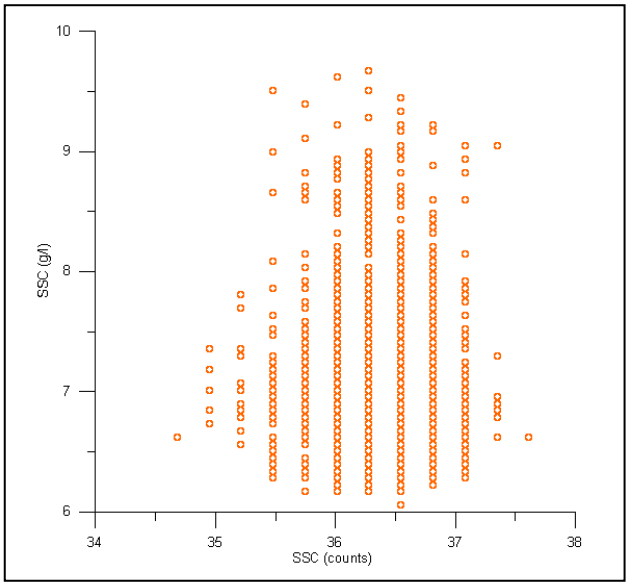

Figure 195: SSC from OBS versus SSC calculated in case 2

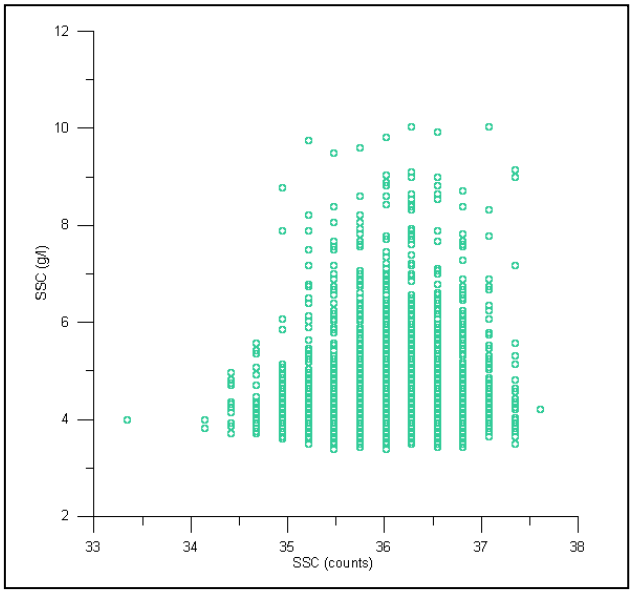

Figure 196: SSC from OBS versus SSC calculated in case 3

As happening before and observing these plots one can appreciate how no relation can be found. They are quite similar to the ones obtained with the least squared method (figures 50 and 51).

Therefore, contrary what to the authors affirm, this method is not working for our case possibly due to the different working environment and frequency of ADV.

VI.2 Backscattered intensity and turbidity

Hubert Chanson, Maiko Takeuchi and Mark Trevethan carried out a work in a laboratory with soil samples from Eprapah Creek close to Brisbane City, Australia. The aim of their work was to investigate the relationship between turbidity; ADV backscattered intensity and suspended sediment concentration assessing the ability of an ADV to measure accurately instantaneous suspended sediment flux in a small subtropical system with fine cohesive sediment materials (mud and silt).

The acoustic backscatter amplitude measurements were conducted with the microADV (16 MHz) system. The average amplitude measurements represented the average signal strength of the ADV receivers. The backscatter intensity (BSI) was related to the signal amplitude as:

$$BSI = 10^{-5} \times 10^{0.043*Ampl} \quad (118)$$

Where BSI is the acoustic backscatter amplitude and Ampl is the average signal amplitude data measured in counts by the ADV system. The coefficient 10_5 was a value introduced to avoid large values of BSI (Nikora and Goring, 2002).

The relations for SSC and turbidity with backscattered intensity that they found were:

SSC = 0.9426 x (1-exp (-0.1109 x BSI)) with R^2= 0.9924 (19 points) (119)

SSC= 0.00485 x Turb – 0.0350 with R^2= 0.9922 (19 points) (120)

Turb=171.06 x (1-exp(-0.1593 x BSI)) with R^2= 0.9884 (19 points) (121)

Where SSC is in g/l, the turbidity Turb is in NTU and the BSI is defined using Eq. (118). R^2 is the square of the normalised coefficient of correlation

When one applies these equations to data obtained in the experiments, obtains:

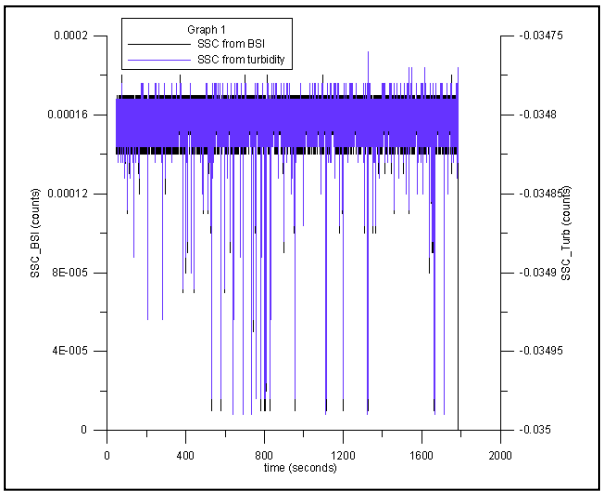

Figure 197: SSC from BSI and SSC from turbidity along time in case 1

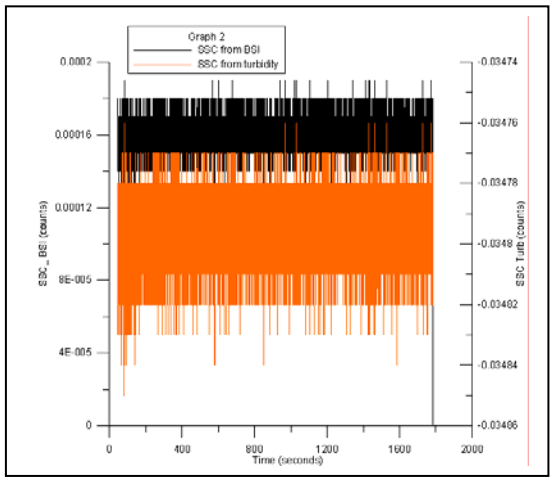

Figure 198: SSC from BSI and SSC from turbidity along time in case 2

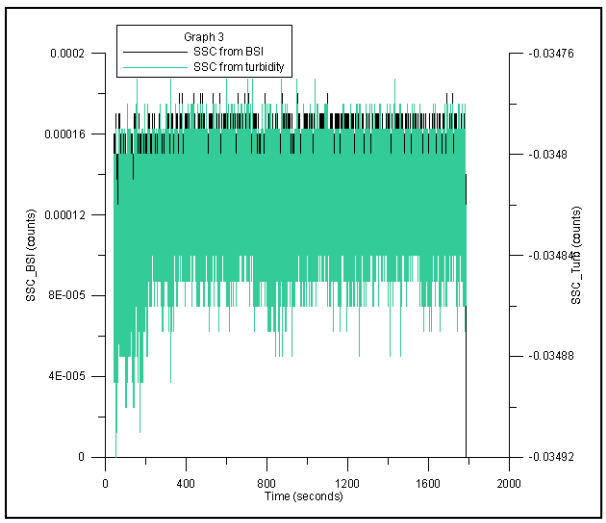

Figure 199: SSC from BSI and SSC from turbidity along time in case 3

As one can appreciate in these plots as SSC is lowering SSC calculated from turbidity is widening its shape. Moreover, compared to figures 173 to 178 one can appreciate how SSC calculated from backscattered intensity (BSI) and SSC calculated from turbidity follows the same model as the original variables, BSI and turbidity.

If one tries to correlate the SSC obtained with these two variables with the SSC measured from the OBS, obtains the results presents in the next sections.

VI.2.1 SSC versus BSI

VI.2.1.1 Case 1

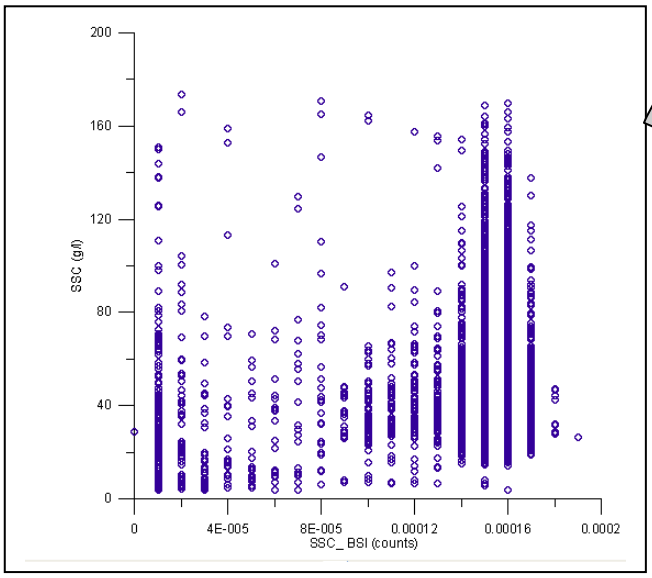

Figure 200: SSC from OBS versus SSC from BSI in case 1

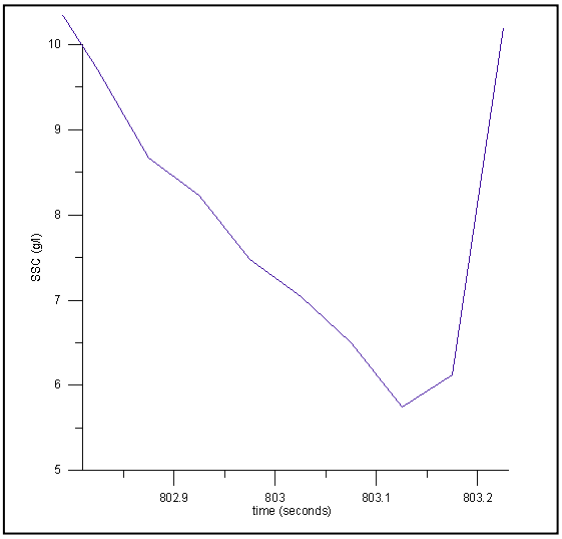

Figure 201: SSC from OBS, zoom in a time where SSC < 10 g/l. Case1

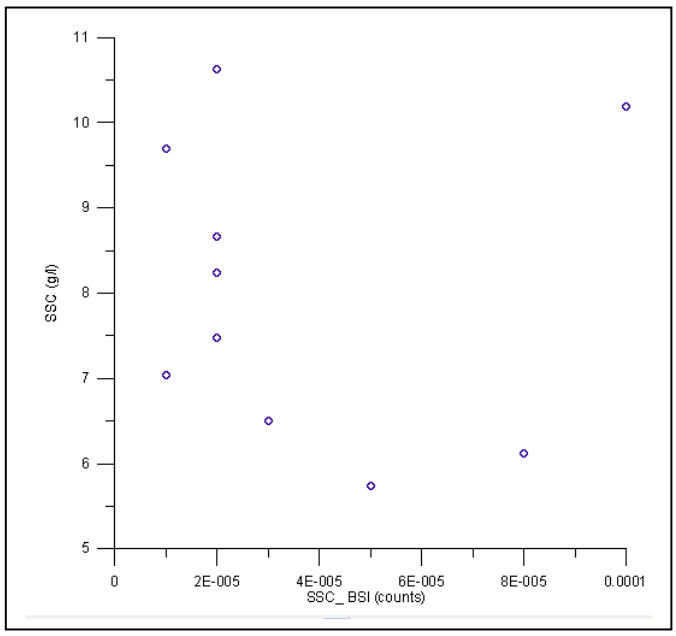

Figure 202: SSC from OBS versus SSC from BSI in case 1

This group of pictures wants to show how no relation can be found when one try to correlate SSC from OBS with SSC calculated from backscattered intensity (figure 200). As many authors affirm that this kind of correlations has to be found when SSC is under 10 g/l in figure 201 we had plot a piece of time where this occurs (10 data points fulfils that requirement).

Finally in figure 202 a correlation between these 10 data points has been tried to be found, but no good solution has been obtained. Notice that according to the authors, even if one is working with a low number of points no relation can be found. This can be due to the different environment in which we are working or due to the difference ADV working frequency (here one works at 100Hz while in many studies authors works at 10MHz).

VI.2.1.2 Case 2

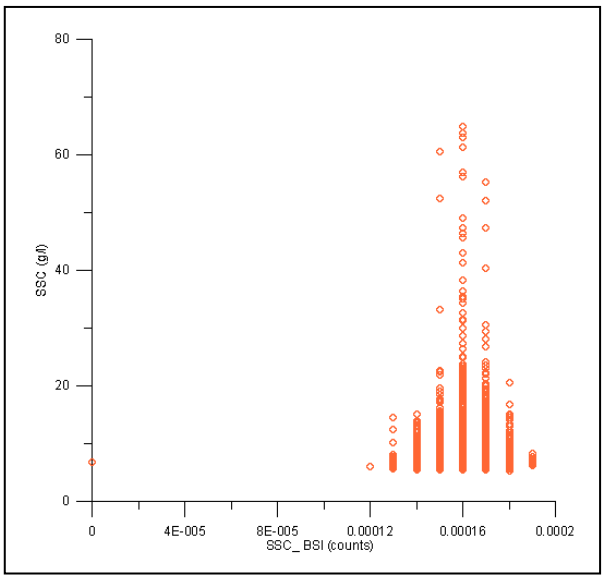

Figure 203: SSC from OBS versus SSC from BSI in case 2

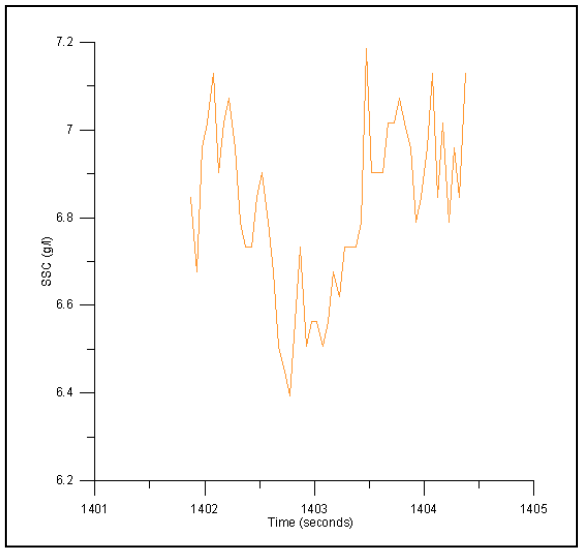

Figure 204: SSC from OBS, zoom in a time where SSC < 10 g/l. Case2

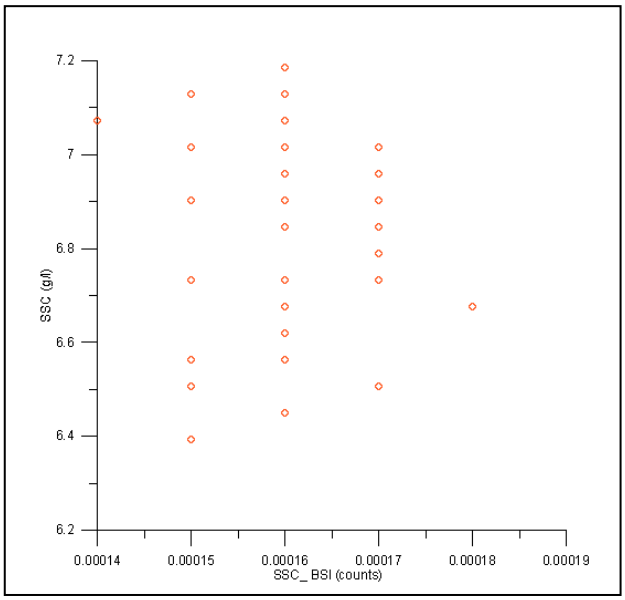

Figure 205: SSC from OBS versus SSC from BSI in case 2

In these plots one can observe, as before that no relation can be found between SSC from OBS and SSC calculated from backscattered intensity (figure 203). Moreover, when one reduces the number of data points which we are working with, we can see more clearly how figure 205 is composed by just straight lines. Here no relation can be appreciated.

VI.2.1.3 Case 3

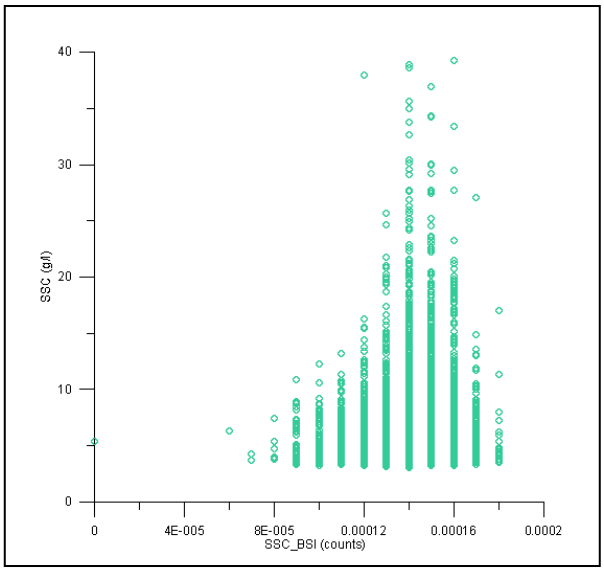

Figure 206: SSC from OBS versus SSC from BSI in case 3

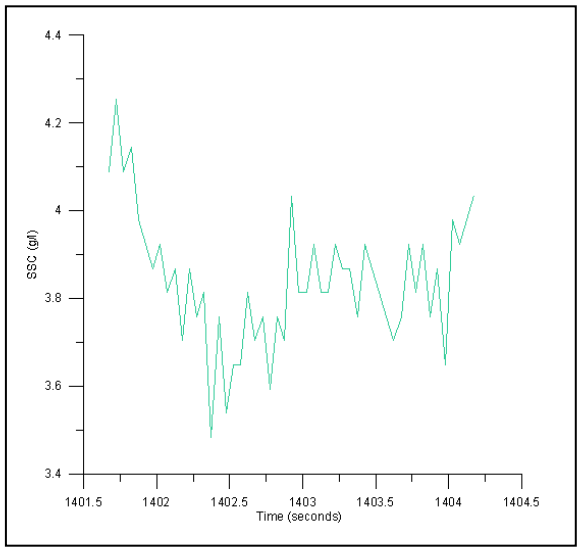

Figure 207: SSC from OBS, zoom in a time where SSC < 10 g/l. Case 3

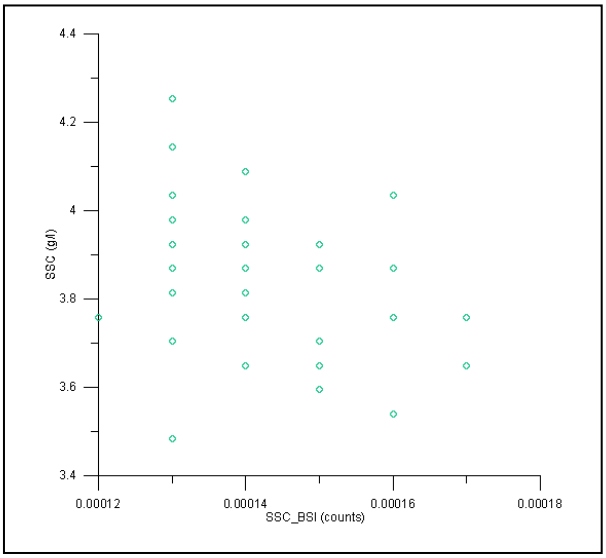

Figure 208: SSC from OBS versus SSC from BSI in case 3

As the last results these plots shows how no relation can be found. Independently one takes into account all the points or reduce it in small intervals, always these straight lines are present and don't let us to correlate both variables.

VI.2.2 SSC versus Turbidity

In this section a relation between suspended sediment concentration (SSC) and turbidity is trying to be found. The study is going to be divided in different cases: case 1 (erosion waves → beginning), case 2 (erosion wave → ending) and case 3 (accretion wave).

VI.2.2.1 Case 1

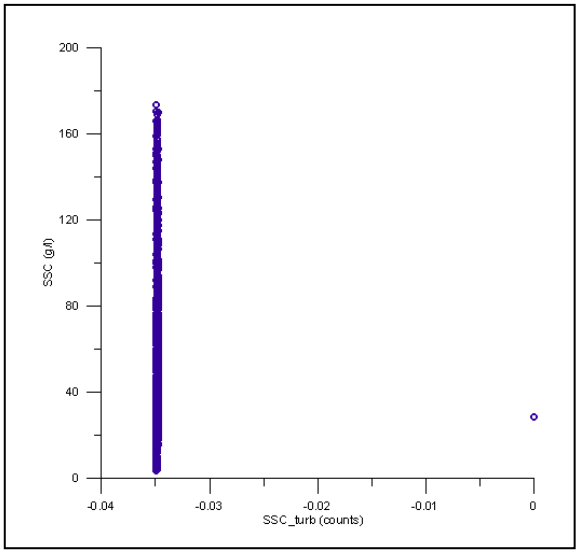

Figure 209: SSC from OBS versus SSC from BSI in case 1

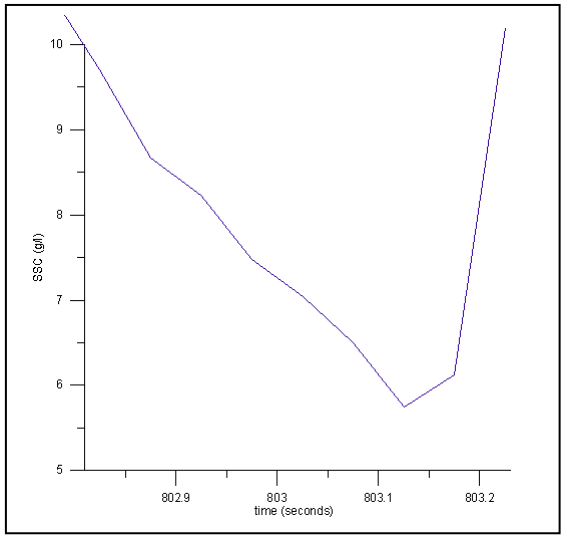

Figure 210: SSC from OBS, zoom in a time where SSC < 10 g/l. Case1

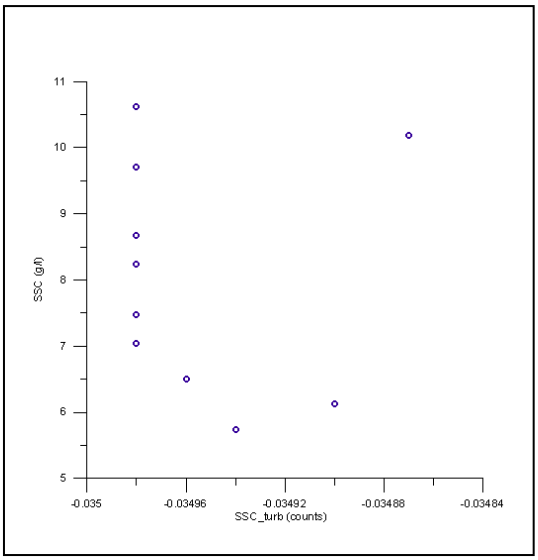

Figure 211: SSC from OBS versus SSC from BSI in case 1

As one can appreciate in these plots if one doesn't reduce the number of points one can not expect any relation between variables. In figure 210 we have reduced the number of data point until 10, therefore some relation can be expected even if this has a not too much higher determination coefficient.

VI.2.2.2 Case 2

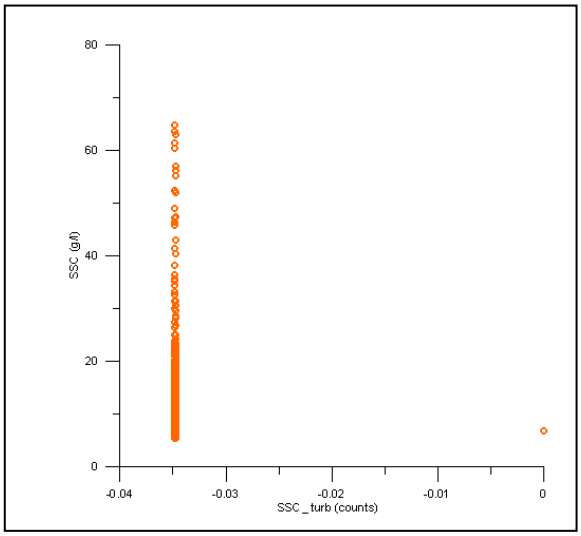

Figure 212: SSC from OBS versus SSC from BSI in case 2

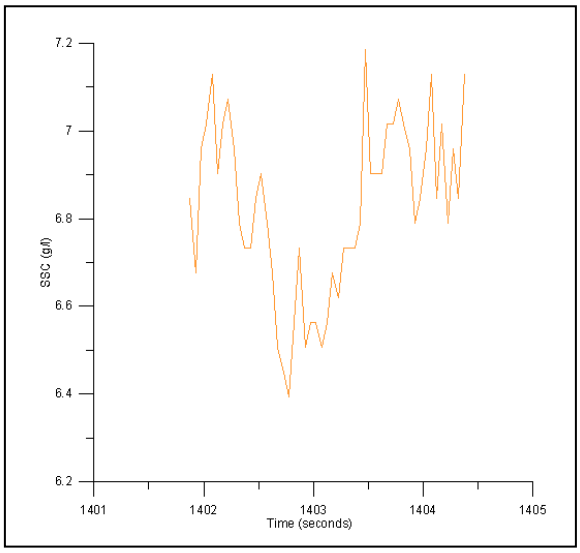

Figure 213: SSC from OBS, zoom in a time where SSC < 10 g/l. Case2

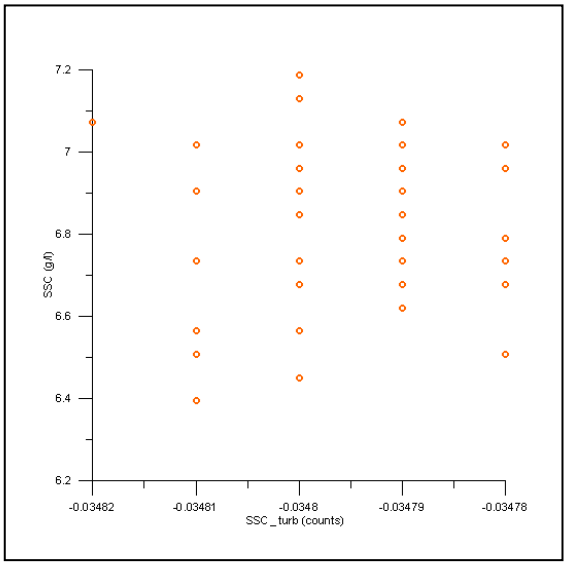

Figure 214: SSC from OBS versus SSC from BSI in case 2

In these plots one can appreciate how no relation can be found. Here, when concentration is downing, and also the number of points taken into account (51 points), straight separated lines are appearing and therefore no relation can be expected.

VI.2.2.3 Case 3

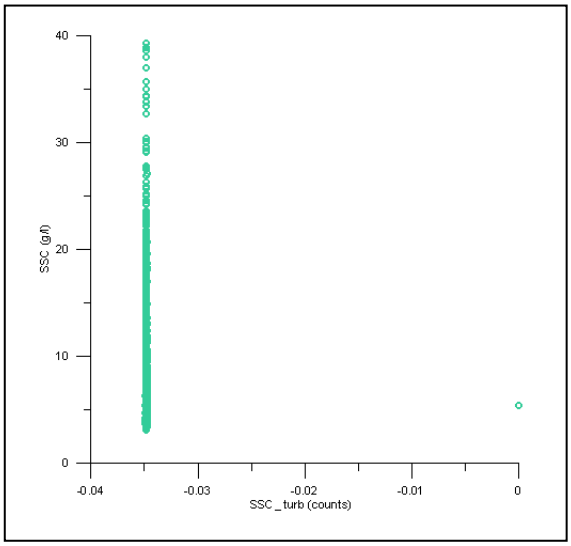

Figure 215: SSC from OBS versus SSC from BSI in case 3

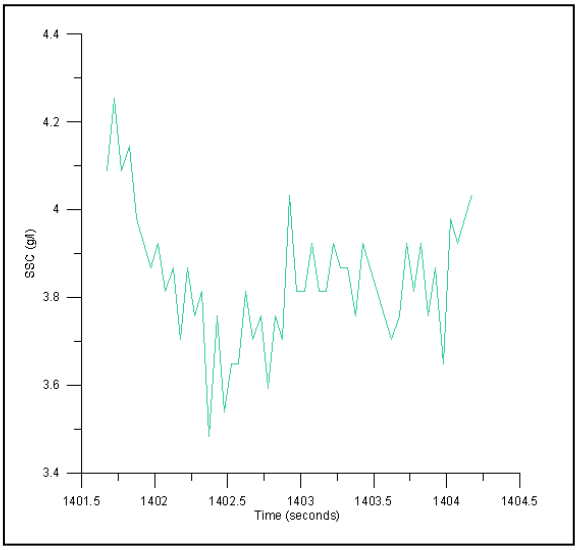

Figure 216: SSC from OBS, zoom in a time where SSC < 10 g/l. Case 3

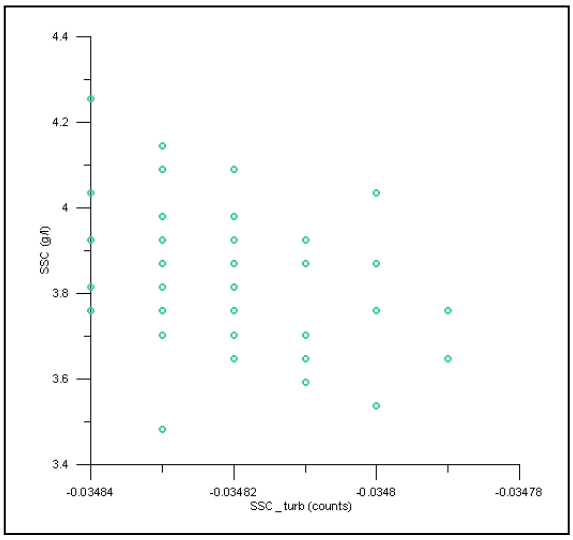

Figure 217: SSC from OBS versus SSC from BSI in case 3

As one can appreciate in figure 215 just one vertical line of points is present. Therefore when one plots a few points (51 data points) these lines are also present and one sees that no relation can be expected.

VI.3 Conclusions

In this section we have applied the guidelines of two different works. In one we have applied multivariate analysis and in the other we have worked with backscattered intensity and turbidity.

As one can appreciate from the results, no reliable relation between SSC and the variables used can be found.

First of all we have worked with SNR with a linear equation and the results that we got were that SSC calculated from SNR had the same pulsating structure as SNR; therefore no relation can be expected. Secondly we tried to add more variables to the multivariate analysis in order to smooth the data and get some reliable relation, but the result was very dependant from SNR and although we mix more variables than SNR the resultant function from SSC calculated still had dependence behaviour on SNR so no result could be found.

Next we tried to get a relation between SSC obtained from OBS and SSC calculated from backscattered intensity (BSI). When we did it, we found that SSC calculated from BSI had a behaviour strongly dependant on BSI. Therefore, another time, we get a pulsating structure where no relation could be found. The same was happening when we tried to find a relation between SSC and turbidity.

Furthermore, as many authors said, working with low concentration has to be separated from working with high concentration; therefore in sections VI.2.1 and VI.2.2 we are working separately with the different cases. As one can appreciate in these subsections BSI seems to adjust better than turbidity, although no reliable relation can be expected due to the vertical lines present in the figures.

In conclusion one can notice how the equations given by these authors are not working with our data. This can be because of the different environment in which we are working or/and due to the different volume sampling frequency of the ADV. Another point to take into account is that in order to measure the suspended sediment concentration we had used an OBS while they used other kind of devices.

VII. Conclusions

As some authors did before in their works, here we have tried to find some reliable way to measure suspended sediment concentration (SSC) from the signals of an ADV. The aim of this work has been in all moment to try to correlate directly or indirectly the outputs given from an ADV (signal to noise ratio (SNR), signal amplitude (SA) and correlation) with the outputs given by an OBS (suspended sediment concentration (g/l).

Through all the work we have been given some mathematical and statistical tools to apply to the data obtained by these devices. In that way we have seen how some direct methods like least squared method or running average are less effectives than the indirect ones (weighted least squared method and weighted running averaged method). Notice that the best fit was obtained with weighted running average least squared method with a determination coefficient of R^2= 0.25.

Moreover, some different analysis like multivariate analysis, intensity method or backscattered intensity and turbidity method, have also been carried out. It has to be noticed, but, that no reliable result has been obtained even if, as the authors of these methods said, we work with low suspended sediment concentrations (SSC below 10 g/l). These differences can be due to the different environment in which they work and to the different sampling frequency of the ADV.

Besides this and observing the results obtained one is able to notice that the better relations were obtained when we were working with case 1 where concentrations are above 10g/l in disagreement to that many authors expose in their works.

As a result of this work done and getting no reliable result we have applied to our data, and in the conditions fixed by the authors of several works, the equations those they approved as reliable approximations. In section VI we have tested our data according to Sebnem Elçi, Ramazan Aydn and Paul A. Work and Hubert Chanson, Maiko Takeuchi and Mark Trevethan. As they did, we tried to work in the more similar conditions we could, but not reliable result was achieved.

To sum up the non agreement obtained between ADV signals and OBS sensors can be explained through the fact that in all cases reflect high rates conditions due to the instantaneous comparations.

VIII. References

Agrawal, Y.C., Pottsmith, H.C., 1994. Laser diffraction particle sizing in STRESS. Continental Shelf Research 14 (10–11), 1101–1121.

Agrawal, Y.C., Pottsmith, H.C., 1996. "Laser instruments for particle sizing and settling velocity measurements in the coastal zone". Proc. Oceans – Conf. – 1996, Vol. I, IEEE, Piscataway, N.J., 1135-1142.

Agrawal, Y.C., Pottsmith, H.C., 2000. Instruments for particle size and settling velocity observations in sediment transport. Marine Geology 168, 89–114.

Baker, E.T. and Lavelle, J. (1984). "The effect of particle size on the light attenuation coefficient of natural suspensions". J. Geophys. Res. 89(C5), 8107-8203.

Bale, A.J., 1996. "In situ laser optical particle sizing". Journal of Sea Research 36 (1–2), 31–36.

Bale, A.J., Barrett, C.D., West, J.R., Oduyemi, K.O.K., 1989. "Use of in-situ laser diffraction particle sizing for particle transport studies in estuaries". In: McManus, J., Elliott, M. (Eds.), Developments in Estuarine and Coastal Study Techniques. Olsen and Olsen, Fredensborg, Denmark, pp.133–138.

Battisto, G.M., 2000. "Field Measurement of mixed grain size suspension in the nearshore under waves". M.S. Thesis, School of Marine Science, College of William and Mary, Gloucester Point, VA, 87pp.

Black, K.P. and Rosenberg, M.A. (1994). "Suspended sand measurements in a turbulent environment: Field comparison of optical and pump sampling techniques". Coastal Engineering, 24: 137-150.

Berke, B. and Racoczi, L. (1981). "Latest achievements in the development of nuclear suspended sediment gauges". Proc., Erosion and Sediment Transport Measurement (Symp.), International Association f Hydrological Sciences, Wallingford, U.K., 83-90.

Beuselinck, L., Govers, G., Poesen, J., 1999. "Assessment of micro-aggregation using laser diffractometry". Earth Surface Processes and Landforms 24 (1), 41–49.

Bhargava, D.S. and Mariam, D.W. (1991). "Light penetration depth, turbidity and reflectance related relationship and models". ISPRS J. Photogrammetry and Remote Sensing, Elsevier Science Publishers, Amsterdam, 46, 217-230.

Blanchard,B.J. and Leamer, R.W. (1973). "Spectral reflectance of water containing suspended sediment". Remote Sensing and Water Resour. Mgmt,., 17, 339-347.

Cáceres,I., Alsina, J.M. and Sánchez-Arcilla, A., 2009. "Mobile bed experiments focused to study the swash zone evolution". Journal of Coastal Research, SI 56 (Proceedings of the 10th International Coastal Symposium). Lisbon Portugal, ISBN.

Choubey, V.K. (1994). "The effect of properties of sediment type on the relationship between suspended sediment concentration and radiance". Hydro. Sci., Oxford, England, 39(5), 459-471.

Clifford, N.J., Richards, K. S., Brown, R.A. and Lane, S.N. (1995). "Laboratory and field assessment of an infrared turbidity probe and its response to particle size and variation in suspended sediment concentration". Hydrological Sciences. 40(6): 771-791.

Conner, C.S. and De Vlisser, A.M., 1992. "A laboratory investigation of particle size effects on an optical backscatterance sensor". Marine Geology, Amsterdam, 108, 151-159.

Crawford, A.M, and Hay, A.E. (1993). "Determining suspended sand size and concentration from multifrequency acoustic backscatter". J. Acoustic Soc. Of Am., 94(6), 3312-3324.

D & A Instruments, 1989. "Optical Backscatterance Turbidity Monitor". Instruction Manual Tech. Note 3, 2428, 39th Street, N.W., Washington, D.C., 2007, USA.

Dantec Dynamics: http://www.dantecdynamics.com/Default.aspx?ID=822&Printerfriendly=4

Deines, K.L., 1999. Backscatter estimation using broadband acoustic doppler current profilers. Oceans 99 MTS/IEEE Conference Proceedings. San Diego.

Downing, A, Thorne, P.D., and Vincent, C.E. (1995). "Backscattering from a suspension in the near field of a piston transducer". J.Acoustic Society of America, 97(3), 1614-1619.

Downing, J.P., Sternberg, R.W., Lister, C.R.B., 1981. "New instrumentation for the investigation of sediment suspension processes in the shallow marine environment". Marine Geology 42 (1981), pp. 19-34.

Downing, J.P, 1983. "An optical instrument for monitoring suspended particles in ocean and laboratory". In Oceans 1983, San Francisco, California, August 29-September 1, 1983, Proceedings: pp. 199-202.

Gray, J.R., 2003. U.S. Geological Survey suspended-sediment surrogate research, Part I: Call for a sediment monitoring instrument and analysis research program: Proceedings of the Virginia Water Research Conference, Virginia Tech, Blacksburg, October 8-10, 2003, 4 p. (in press).

Gray, J.R, and Glysson, G.D. 2003. "Proceedings of the Federal Interagency Sedimentation Workshop on Turbidity and Other Sediment Surrogates", April 30-May 2, 2002, Reno, Nevada: U.S. Geological Circular 1250, 136 p. (in press).

Gray, J. R., Gooding, D.J., Melis, T. S., Topping, D. J., and Rasmussen, P. P., 2003, U.S. Geological Survey suspended-sediment surrogate research, Part II: Optic technologies: Proceedings of the Virginia Water Research Conference, Virginia Tech, Blacksburg, October 8-10, 2003, 7 p. (in press).

Green, M.O. and Boon, J.D., III (1993). "The measurement of constituent concentrations in nonhomogeneous sediment suspensions using optical backscatter sensors". Marine Geology, Amsterdam, 110, 73-81.

Hanes, D.M. and Huntley, D.A., 1986. "Continuous measurements of suspended sand concentration in a wave dominated near shore environment". Continental Shelf Research, 6: 585-596.

Hay, A.E. and Bowen, A.J. (1994). "Coherences scales of wave – induced suspended sand concentrations fluctutions". Journal of Geophysical Research, 99(C6),12,749-12,765.

Hay, A.E. and Sheng, J. (1992). "Vertical profiles of suspended sand concentration and size from multifrequency acoustic backscatter". Journal of Geophysical Research. 97 (C10):15661-15677.

Hoitink, A.J.F. and Hoekstra, 2004. "Observations of suspended sediment from ADCP and OBS measurements in a mud-dominated environment". Coastal engineering 52 (2005), p. 103-118.

Hubert Chanson, Maiko Takeuchi and Mark Trevethan, 2007. "Using turbidity and acoustic backscatter intensity as surrogate measures of suspended sediment concentration in a small subtropical estuary". Journal of environmental management 88 (2008):1406-1416.

Instruction manual for OBS -1 & 3 (1991). D & A Instrument Co,. Port Townsend, Wash.

Interagency Comitee on Water Resources, Subcomitee on Sedimentation. (1963). "A study of metohds used in measurement and analysis of sediment loads in streams- Report No.14 Field particle and Equipment used in Sampling Susended sediment". Rep. No.14,St.Anthony Falls Hydraulic Laboratory, Minneapolis, Minn.

Jeffrey W. Gartner and John R. Gray (2002). "Summary of suspended sediment technologies considered at the interagency workshop on turbidity and other sediment surrogates". U.S. Geological Survey.

Kineke, G.C. and Sternberg, R.W. (1992). “Measurements of high concentration suspended sediments using the optical backscatterance sensor”. Marine Geology, Amsterdam, 108, 253-258.

Knight, J.C., Ball, D. and Jones, S.E. (1991). “Analytical inversion for laser diffraction spectrometry giving improved resolution and accuracy in size distribution”. Appl. Optics 30(33), 4795-4799.

Kostaschuk, R.A., and Church, M.A. (1993). “Macroturbulence generated by dunes: Fraser river, Canada”. Sedimentary Geology, 85, 25-37.

Kostaschuk, R.A., and Villard, P. (1996). “Flow sediment transport over large subaqueous dunes: Fraser river, Canada”. Sedimentology, 43, 849- 863.

Kraus, N.C., Lohrmann, A., and Cabrera, R. (1994). “New acoustic meter for measuring 3D laboratory flows”. J. Hydr. Engrg., ASCE, 120(3), 406-412.

Lapointe, M.F. (1992). “Burst like sediment suspension events in a sand bed river”. Earth surface process and landforms, 17, 253-270.

Lapointe, M.F. (1993). “Monitoring alluvial sand suspension by eddy correlation”. Earth surface process and landforms, 18, 157-175.

Lapointe, M.F. (1996). “Frequency spectra and intermittency of the turbulent suspension process in a sand-bed river”. Sedimentology, 43: 439-449.

Larsen, M. C., Alamo, C. F., Gray, J.R. and Fletcher, William, 2001. “Continuous automated sensing of Streamflow density as a surrogate for suspended sediment concentration sampling”. Proceedings of the 7th Federal Iteragency Sedimentation Conference, March 25-29, 2001, Reno, Nevada, pp III 127-134.

Law, D.J., Bale, A.J. and Jones, S.E. (1997). “Adaption of focused beam reflectance measurement to in-situ paticle sizing in esturies ans coastal waters“. Marine Geology, Amsterdam, 140(1-2), 47-59.

Lewis, A.J. and Rasmussen, T.C., 1999. “Determination of suspended sediment concentrations and particle size distributions using pressure measurements”. J. Environ. Qual., 28, pp.1490-1496.

Lewis, J. 1996. “Turbidity-controlled suspended sediment sampling for runoff-event loadEstimation”. Water Resources Research. 32(7): 2299-2310.

Lewis, J. & Eads, R.E. (2001). “Turbidity threshold sampling for suspended sediment load estimation. In: *Federal Interagency Sedimentation* (Proc. Seventh Conf., Reno, Nevada, USA, March 2001), III-110 to III-117”. Federal Interagency Project, Technical Committee of the Subcommittee on Sedimentation.

Lewis, J. & Eads, R.E. (2002). “Continuous Turbidity Monitoring In Streams of Northwestern California”. Turbidity and other sediments surrogates Workshops, April 30- May 2, 2002, Reno NV.

Lewis, Jack, 2002. Estimation of suspended sediment flux in streams using continuous turbidity and flow data coupled with laboratory concentrations. *In* Workshop on Turbidity and Other Sediment Surrogates, Apr 29-Mar 2, 2002, Reno, Nevada.

Lynch, J.F., Irish, J.D., Sherwood, C.R., Agrawal, Y.C., 1994. Determining suspended sediment particle size information from acoustical and optical backscatter measurements. Continental Shelf Research 14 (10–11), 1139–1164.

Lohrmann,A., Cabrera,R. (1994). “Acoustic Doppler velolcimeter (ADV) for laboratory use”. Proc. Symp. On Fundamentals and Advancements in Hydr. Measurements and Experimentation, C.A. Pugh, ed., ASCE, 351- 365.

Ludwig, K.A. and Hanes, D.M., 1990. “A laboratory evaluation of optical backscatterance suspended solids sensors exposed to sand- mud mixtures”. Marine Geology, 94: 173- 179.

McHenry, J.R. et al. (1967). “Performance of nuclear – sediment concentration geuges”. Proc., Isotopes in Hydrology SYmp., International Atomic Energy Agency, Vienna, 207-225.

McHenry, J.R., Coleman, N.L., Willis, A.C., Sansom, O.W., and Carrol, B.R. (1970). “Effect of concentration gradients on the performance of a nuclear sediment concentration gage”. Water Resour. Res., 6(2), 538-548.

Medwin, H., 1975. “Speed of sound in water: a simple equation for realistic parameters”. J. Acoust. Soc. Am. 56, 1318–1319.

Medwin, H., Clay, C.S., 1998. “Fundamentals of Acoustical Oceanography”. Academic Press.

Mikkelson, O.A., Pejrup, M., 2000. “In situ particle size spectra and density of particle aggregates in a dredging plume”. Marine Geology 170, 443–459.

Miller, K. S., and M. M. Rochwarger, 1972: “A covariance approach to spectral moment estimation”. *IEEE Trans. Inform. Theory,* IT- 18, 588-596.

Nortek,1997. “ADV Operation Manual”. Nortek AS, Bruksveien 17, 1390 Vollen, Norway, 33.

Novo, E.M.M, Hansom, J.D. and Curran, P.J. (1989). “The effect of Beijing geometry and wavelenghth on the relationship between reflectance data and suspended sediment concentration”. Int. J. Remote Sensing, Taylor & Francis Ltd., New York, 10(8), 1357-1372.

Padadopoulus,J. and Ziegler, C.A. (1966). “Radioisotope technique for monitoring sediment concentration in rivers and streams”. Proc., Radioisotope Instruments in Industry and Geophysics. International Atomic Energy Agency, Vienna, 381-394.

Phillips, J.M., Walling, D.E., 1995. “An assessment of the effect of sample Collection, storage and resuspensión on the representativeness of measurements of the effective particle size distribution of fluvial suspended sediment”. Water Research, 29(11), 298-2508.

Phillips, J.M., Walling, D.E., 1995. “Measurement in situ of the effective particle size characteristics of fluvial suspended sediment by means of a field- portable laser backscatter probe: Some preliminary results”. Marine Freshwater Research, 46, 349-357.

Phillips, J.M., Walling, D.E., 1998. Calibration of a Par-Tec 200 laser back-scatter probe for in situ sizing fluvial suspended sediment. Hydrological Processes 12 (2), 221–231.

Precht, E., Janssen, F. and Huettel, M., 2006. “Near- bottom performance of the Acoustic Doppler Velocimeter (ADV) – a comparative study”. Aquatic Ecology, 2006. 40: 481-492.

Rakcozi, L. (1973). “Critical review of current nuclear suspended sediment gauges”. Tech. Rep. Ser. No.145, Tracer Techniques in Sediment Transport, International Atomic Energy Agenct, Vienna.

Rijn, L.C. van (1986). “Manual sediment transport measurements”. Delft, The Netherlands: Delft Hydraulics Laboratory.

Riley, J.B. and Agrawal, Y.C. (1991). “Sampling and inversion of data in diffraction particle sizing”. Appl. Optics 30(33), 4800 – 4817.

Ritchtie, J.C. and Schiebe, F.R. (1986). “Monitoring suspeded sedimets with remote sensing techniques”. Proc., Workshop: Hydrologic Applications of Space Technol., International Association of Hydrological Sciences, Wallingford, U.K.

S.A. Hosseini, A.Shamsai, B. Ataie- Ashtiani, 2006. “Synchronous measurements of the velocity and concentration in low density turbidity currents using an Acoustic Doppler Velocimeter”. Flow Measurement and Instrumentation 17, 59-68.

Schat, J. (1997). “Multifrequency acoustic measurement of concentration and grain size of suspended sand in water”. J. Acoustic Soc. of Am., 101(1), 209-217.

Stuart,J. McLelland and Andrew, P.Nicholas, (2000). “A new method for evaluating errors in high- frequency ADV measurements”. Hydrological Process, 14, 351-366.

Swithenbank, J., Beer, J.M., Taylor, D.S., Abbot, D. and McCreath, G. C . (1976). “A laser diagnostic technique for the measurement of droplet and particle size distribution”. Proc., AIAA 14th Aerosp. Sci. Meeting, American Institute of Aeronautics and Astronautics, Reston, Va., 421-447.

Tazioli, G.S. (1981). “Nuclear techniques for measuring transport in natural streams- Examples from intrumented basins”. Proc., Erosion and Sediment transport measurement, International Association of Hydrological Sciences, Wallingford, U.K., 63-81.

Thevenot, M.M., Prickett,T.L., Kraus, N.C., 1992. “Tylers beach, Virginia, dredged material plume monitoring project 27 September to 4 October 1991”. Dredging research program Technical report DRP- 92-7, US Army Corps of Engineers, Washington, DC, 204 pp.

Thorne, P.D.,and Campbell, S.C. (1992). “Backscattering by a suspension of spheres”. J. Acoustic Soc. Of Am., 92(2), 978-986.

Thorne, P.D., Hardcastle, P.J., and Hogg, A. (1996). “Observations of near-bed suspended sediment turbulence structures using multifrequency acoustic backscattering”. From coherent flow structures in open channels. Edited by Ashworth, P.J., Bennett, S.J., Best J.L, and McLelland, S.J.

Thorne,P.D., Hardcastle, P.J., Flatt, D. and Humphery, J.D. (1994). “On the use of acoustics for measuring shallow water suspended sediment processes”. IEEE Journal of Oceanic Engineering. 19 (1): 48-57.

Thorne, P.D, Hardcastle, P.J., and Soulsby, R.L. (1993). “Analysis of acoustic measurements of suspended sediments”. J. Geophysical Res., 98 (C1), 899-910.

Thorne, P.D., Vincent, C.E., Hardcastle, P.J., Rehman,S., and Pearson, N. (1991). “Measuring suspended concentrations using acoustic backscatter devices”. Marine geology., Amsterdam, 98, 7-16.

Thorne, P.D., Waters, K.R., Brudner, T.J. (1995). “Acoustic measurements of scattering by objects of irregular shape”. Journal of Acoustic society af America. 97(1): 242-251.

Tony, L. Wahl, 2000. “Analyzing ADV Data using WinADV”. 2000 Joint Conference on Water Resources Engineering and Water Resources Planning & Management. July 30 – August 2, 2000 – Mineapolis, Minnesota.

Traykovski, P., Latter, R.J., Irish, J.D., 1999. A laboratory evaluation of the laser in situ scattering and transmissometry instrument using natural sediments. Marine Geology 159, 355–367.

Urick, R.J., 1975. “Principles of underwater sound”, (2nd ed.). McGraw Hill, New York, p.384.

V.I. Nikora, D.G. Goring. “Fluctuation if suspended sediment concentration and turbulent sediment fluxes an open channel flow”. J. Hydr. Eng. 128 (2002). p 214-224.

Vollgaris, G. and Trowbridge, J.H., 1997. “Evaluation of the Acoustic Doppler Velocimeter (ADV) for turbulence Measurements”. Journal of the Atmospheric and Oceanic technology, 1997. vol.15, pp. 272- 289.

Welch, N.H., and Allen, P.B. (1973). “Field calibration and evaluation of a nuclear sediement gage”. Water Resour. Res., 9(1), 154-158.

Witt, W. and Rothele, S. (1996). “Laser diffraction- unlimited?”. Part. & part. Sys. Charact., 13, 280-286.

Wren, D.G., Barkdoll, B.D., Kuhnle, R.A., and Derrow, R.W. (2000). “Field techniques os suspended sediment measurement”. Journal of Hydraulic Engineering. 126(2): 97-104.

Xu, J.P. (1997). “Converting near bottom OBS measurements into suspended sediment concentrations”. Geo- Marine Letters, 17, 154-161.

Zrnic DS, 1997. “Spectral moment estimates from correlated pulse pairs”. IEEE Transactions on Aerospace and Electronic Systems, AES-9: 151-165.